Identification and characterisation of the role of endozepine in apoptosis induced by ceramide.

Mervin Meyer

A thesis submitted in fulfilment of the requirements for the degree of Doctor Philosophiae in the Faculty of Science, University of the Western Cape.

Supervisor: Prof. D. Jasper G. Rees

June 2003

ABSTRACT.

Identification and characterisation of the role of endozepine in apoptosis induced by ceramide.

M. Meyer

PhD thesis, Department of Biotechnology, Faculty of Science, University of the Western Cape.

Apoptosis is a form of programmed cell death and is required for the normal development, tissue homeostasis and survival of organisms. The identification of mutations that can lead to alterations in cell death not only contributes to our understanding of this process, but it can also provide us with novel therapeutic targets to treat diseases such as cancer.

Defects in the regulation of apoptosis contribute to a number of human diseases, e.g. excessive down regulation of this process has been linked to the development of cancer while excessive up regulation causes autoimmune and neurodegenerative disorders such as Alzheimer's disease. Genes involved in the regulation of cell death present good opportunities as possible drug targets to treat these diseases. This

research describes the identification of a gene that may be involved in the regulation of cell death induced via the mitochondrial apoptotic pathway.

Promoter-trap retroviral insertional mutagenesis was used to randomly introduce mutations in pseudohaploid CHO22 cells. Retroviral mutagenesis was followed by selection for apoptosis resistant clones using C_2-ceramide. The viral integration sites in one of these mutants were characterised and led to the identification of a gene coding for an acyl-CoA binding protein, called endozepine.

This protein is capable of displacing benzodiazepines from the peripheral benzodiazepine receptor (PBR). The PBR forms part of the mitochondrial permeability transition pore (MPTP). Mitochondrial permeability transition has been demonstrated to play a key role in apoptosis. It has also been shown that ligands to the PBR induce mitochondrial permeability transition in isolated mitochondria by collapsing the inner mitochondrial transmembrane potential. This study demonstrates that endozepine may regulate apoptosis by acting as an endogenous ligand to PBR facilitating mitochondrial permeability transition in cells.

This research illustrated the use of promoter-trap mutagenesis to generate cell mutants that are resistant to apoptosis and revealed the involvement of endozepine in ceramide-induced apoptosis. This data support other studies that suggest that apoptosis may be regulated at the mitochondria and in particular through the

interaction of proteins or drugs with the MPTP. The findings of this study also lend support to previous reports, which suggested that endozepine might play a role in mitochondrial apoptotic pathway. The emerging role of the MPTP, its ligands and their role in apoptosis make these ligands attractive targets for future anti-cancer drug development.

June 2003

Keywords:

Apoptosis

Ceramide

Promoter-trap mutagenesis

Insertional mutagenesis

CHO22

Endozepine

Acyl-CoA binding proteins

Diazepam Binding Inhibitor

Mitochondrial Permeability Transition Pore

Peripheral Benzodiazepine Receptor

For my parents.

DECLARATION.

I declare that ***"Identification and characterisation of the role of endozepine in apoptosis induced by ceramide"*** is my own work that has not been submitted for any degree or examination in any other university and that all the sources I have used or quoted have been indicated and acknowledged by complete references.

Mervin Meyer June 2003

Signed:.....

TABLE OF CONTENTS: **PAGE**

CHAPTER 2: Materials and Methods.

CHAPTER 3: Generation of apoptosis-resistant mutants.

CHAPTER 6: The expression and purification of endozepine.

LIST OF TABLES.

LIST OF FIGURES.

ABBREVIATIONS.

AIDS	Acquired immune deficiency syndrome
ADP	Adenosine 5'-diphosphate
AIF	Apoptosis inducing factor
ANC	Adenine nucleotide carrier
Apaf-1	Apoptosis activating factor-1
ATP	Adenosine 5'-triphosphate
Bad	Bcl-x_L /Bcl-2-associated death promoter
Bax	Bcl-2 -associated x protein
Bcl-2	B cell leukaemia-2
Bid	BH3 Interacting Domain Death Agonist
BIR	Baculoviral inhibitory repeat
BLAST	Basic local alignment search tool
Bod	Bcl-2 -related ovarian death gene
Bok	Bcl-2 -related ovarian killer
bp	Base pair
BSA	Bovine serum albumin
CAD	Caspase-activated deoxyribonuclease
CAPK	Ceramide-activated kinase
CAPP	Ceramide-activated protein phosphatase
CARD	Caspase recruitment domain
Caspases	Cysteine aspartic acid-specific protease

CD	Cluster of differentiation
CED	Cell death defective
c-FLIP	Cellular-Fas-associated death domain-like ICE inhibitory protein
CHAPS	3-(3-Cholomidopropyl)-dimethyl-lammonlol-1-propanesulphonate
CHO	Chinese hamster ovary
CrmA	Cytokine response modifier A
DAG	Diacylglycerol
DAP	Death associated proteins
DAPI	4', 6'-Diamidino-2-phenylindole
dATP	deoxyadenosine triphosphate
Daxx	Fas death domain associated protein
DBI	Diazepam binding inhibitor
DcR	Decoy receptor
DD	Death domain
DED	Death effector domain
DIABLO	Direct IAP-binding protein with low pI
DISC	Death Inducing Signalling Complex
DMEM	Dulbecco's modified medium
DMSO	Dimethyl sulphoxide
DNA	Deoxyribonucleic acid
DR	Death receptor

DTT	Dithiothreitol
EDTA	Ethylene diamine tetra acetic acid
EGL-1	External germinal layer-1
EGTA	Ethyleneglycol-bis(β-aminoethyl ether)
ELP	Endozepine-like protein
FACS	Fluorescence activated cell sorter
FADD	Fas-associated death domain
Fas	Fibroblast-associated
FCS	Foetal calf serum
FLICE	FADD-like ICE FLIP Fas-associated death domain-like ICE inhibitory protein
FSC	Forward scatter
GABA	Gamma-aminobutyric acid
GFP	Green fluorescent protein
GST	Glutathione S-Transferase
HEPES	*N*- (2-Hydroxyethyl) piperazine'-(ethane sulphonic acid)
HIV	Human immunodeficiency virus
hrs	Hours
Hsp	Heat shock protein
IκB	Inhibitor of NF-κB
IAP	Inhibitors of apoptosis

ICAD	Inhibitor caspase-activated deoxyribonuclease IFN
	Interferon
ICE	Interleukin-1β converting enzyme
IEF	Isoelectric focusing
IKK	Inhibitor of κB kinase complex
IPTG	Isopropyl β-D-thiogalactopyranoside
JNK	Jun-N-terminal kinase
kb	Kilo base
kD	Kilo Dalton
l	Litre
LB	Luria Broth
LDH	Lactate dehydrogenase
LIT	Lymphocyte inhibitor of TRAIL
LTR	Long terminal repeat
MACH	MORT-associated CED-3 homologue
MALDI-PSD	Matrix-assisted laser desorption ionisation post-source decay
MEK	MAPK/ERK kinase
min	Minutes
MKK	Mitogen-activated protein kinase kinase
MoMLV	Moloney murine leukaemia virus
MOPS	4-Morpholine propanesulphonic acid
MPTP	Mitochondrial permeability transition pore

mV	Millivolts
Nedd	Neural precursor cell expressed, develòpmentally down regulated
NF-κB	Nuclear factor κB
NGF	Nerve growth factor
NIK	NF-κB-inducing kinase
NPD	Niemann-Pick disease
PAGE	Polyacrylamide gel electrophoresis
PARP	Poly (ADP-ribose) Polymerase
PBR	Peripheral benzodiazepine receptor
PBS	Phosphate buffer saline
PCR	Polymerase chain reaction
PK11195	1-(2-chlorophenyl-N-methyl-1-methylpropyl)-3-isoquinolinecarboxamide
PMSF	Phenylmethylsulphonyl fluoride
PP1	Protein phosphatase 1
PRAX-1	PBR associated protein-1
PVDF	Polyvinylidene difluoride
Ro5-4864	7-chloro-5- (4-chlorophenyl)-1, 3-dihydro-1-methyl-2H-1, 4-benzodiazepine-2-one
RAIDD	RIP associated ICH/CED-3 homologous protein with a death domain
RIP	Receptor interacting protein

RNA	Ribonucleic acid
S1P	Sphingosine-1-phosphate
SDS	Sodium dodecyl sulphate
Sec	Seconds
Smac	Second mitochondria-derived activator of caspases
SPHK	Sphingosine kinase
SSC	Side scatter
TEMED	*N*, *N*, *N'*, *N'*-Tetramethylethylenediamine
TNF	Tumour necrosis factor
TRADD	TNFR-associated death domain
TRAF	TNFR-associated factor
TRAIL	TNF-related apoptosis-inducing ligand
TRICK	TRAIL receptor inducer of cell killing
TRID	TRAIL receptor without an intracellular domain
TRUNDD	TRAIL receptor with a tDD
TWEAK	TNF-like and weak inducer of apoptosis
UV	Ultra violet
V	Volt
Vh	Volt hours
VDAC	Voltage-dependent-anion channel

ACKNOWLEDGEMENTS.

I wish to express my sincere gratitude to my supervisor, Prof. Jasper Rees for his guidance in carrying out this research. My thanks are also due to Drs Shadrack Moephuli, David Pugh, Bongani Ndimba and Mr Tumelo Seameco for helping me with reagents and methodology. I also wish to thank the staff and students in the Department of Biotechnology at the University of the Western Cape and in particular the members of the Rees lab for their assistance and friendship. I am also grateful to my family for their support and encouragement. Finally, I want to thank the Claude Harris Leon Foundation, the South African National Research Foundation and Cancer Association of South Africa for financial support.

CHAPTER 1: INTRODUCTION.

CHAPTER 1: INTRODUCTION.

1.1. Introduction to apoptosis.

The cycles of life and death form essential parts of many natural biological processes. It is estimated that almost 1 % of all cells in the human body are replaced every day. This is evident from the dynamic nature of tissues. There are many examples to illustrate this: red blood cells only have a life span of 120 days, while cells in the intestinal villus only live for a few days.

Death of cells within an organism may either be by accident or by design. Accidental death, also referred to as necrosis, can be the result of physical injury or disease. During necrosis, failing membrane pumps and consequent influx of water and sodium ions cause cells to swell and eventually lyse, releasing their cytoplasmic material with a resultant inflammatory response (Kroemer *et al.*, 1995). Apoptosis is a different form of cell death, first observed in liver hepatocytes. Individual hepatocytes died without any evidence of cell lysis or inflammatory response (Kerr *et al.*, 1972). The phenotypic characteristics of this form of cell death are distinct from necrosis. These characteristics include cell shrinkage, chromatin condensation, plasma membrane blebbing and the collapse of the cell into small intact membrane bound fragments (apoptotic bodies) that are removed by phagocytes. The engulfment of apoptotic bodies is triggered by changes in the membrane of apoptotic cells. These changes involve the externalisation of a phospholipid, phosphatidylserine, through the activation of an

enzyme called flippase (Fadok *et al.*, 1992; Williamson *et al.*, 2002). This type of cell death is referred to as apoptosis.

Apoptosis plays an active role in normal embryological development, morphogenesis and metamorphosis (Steller, 1995). In this context apoptosis can be viewed as a form of programmed cell death that performs a vital role in sculpting tissues, organs and organisms. Defects in the regulation of cell death contribute to a number of human diseases, e.g. excessive down regulation of this process has been linked to the development of cancer and viral infections, while excessive up regulation causes autoimmune disorders and neurodegenerative diseases such as Alzheimer's disease and ischaemic injury (e.g. stroke and myocardial infarction) (Iwahashi *et al.*, 1997; Benoist and Mathis, 1997). AIDS is another example of a disease that has been linked to increased apoptosis (Hellerstein and McCune, 1997; Tomei and Umanski, 2001).

Mutational analysis in the nematode worm, *Caenorhabditis elegans,* led to the identification three crucial components of the cell death pathway. Three gene products, CED-3, CED-4 and CED-9 (**c**ell **d**eath **d**efective) were implicated as having important roles in the regulation of cell death in *C. elegans* (Hengartner and Horvitz, 1994). CED-4 is able to form a complex with both CED-3 and CED-9. Subsequent studies revealed that the association of CED-3 and CED-4 leads to the induction of apoptosis. Normally, CED-4 is unable to form a complex with CED-3 because it is already associated with CED-9 at the mitochondrial membranes (Xue and Horvitz, 1997). This inhibitory effect of CED-9 is

neutralised by another protein, EGL-1 (external germinal layer-1), during apoptosis by promoting the dissociation of CED-4/CED-3 complex from CED-9 (Conradt and Horvitz, 1998; del Peso *et al.*, 2000). The mammalian homologue of CED-9 and EGL-1 is the Bcl-2 protein family (Hengartner and Horvitz, 1994; Vaux *et al.*, 1994; Adams and Cory, 1998) while CED-4 is homologous to Apaf-1 (Peter *et al.*, 1997; Zou *et al.*, 1997) and CED-3 is homologous to a family of mammalian cysteine proteases called caspases (Peter *et al.*, 1997).

There has been increasing evidence to support the idea that the basic molecular apoptosis mechanisms have been conserved during evolution among eukaryotes as diverse as plants, slime moulds, nematodes, insects and mammals (Vaux *et al.*, 1994; Aravind *et al.*, 1999). Vertebrates are found to have homologues of the *C. elegans* cell death genes (Ashkenazi and Dixit, 1998). CED-3 was found to be very similar to a protease involved in the processing of pro-IL-1β, interleukin-1β converting enzyme (ICE). Upon its discovery ICE defined a new class of cysteinyl proteases because it was distinguishable from other cysteine protease families based on structural organisation and the absolute requirement for an aspartic acid residue in the P1 position in the active site (Cerretti *et al.*, 1992; Thornberry *et al.*, 1992). Based on these characteristics, ICE was also called caspase-1 or **c**ysteine **asp**artic acid-specific prote**ase**-1 (Alnemri *et al.*, 1996). Caspases are central to the execution mechanisms of apoptosis and are responsible for many of the morphological changes observed in apoptotic cells.

Cell death in unicellular organisms seems not to involve caspases, although these proteases play a key role in apoptosis in multicellular organisms. However, there is growing evidence that some sort of programmed cell death does exist in unicellular organisms (Ameisen, 1996; Frohlich and Madeo, 2001) and maybe even in bacteria (Yarmolinsky, 1995; Koonin and Aravind, 2002).

There are two major apoptotic pathways: the "extrinsic" pathway initiated through cell surface receptors (tumour necrosis factor receptor-family) and the "intrinsic" pathway initiated via mitochondria (Reed, 1997). These pathways can be activated by a wide range of stimuli, which includes DNA damage, chemotherapeutic agents, serum starvation, ultraviolet radiation, the activation of tumour suppressor proteins (such as p53) and oncogenes (such as *c-Myc*). A multitude of gene products play key roles in the initiation and execution of apoptosis. The molecular components of these pathways can generally be classified as initiators, effector or executioners of apoptosis.

1.2. Caspases: the initiators or effectors of apoptosis.

Caspases were first implicated in apoptosis with the discovery of the *C. elegans* pro-apoptotic gene, CED-3. These enzymes are synthesised as inactive zymogens consisting of an N-terminal pro-domain, a large subunit and a small subunit (Nicholson, 1999). The residues that constitute the active site are conserved for all caspases (Figure 1.1). To date 14 mammalian caspases were identified (Cohen, 1997; Wolf *et al.*, 1999; Creagh and Martin, 2001). Only 11 of these enzymes i.e.

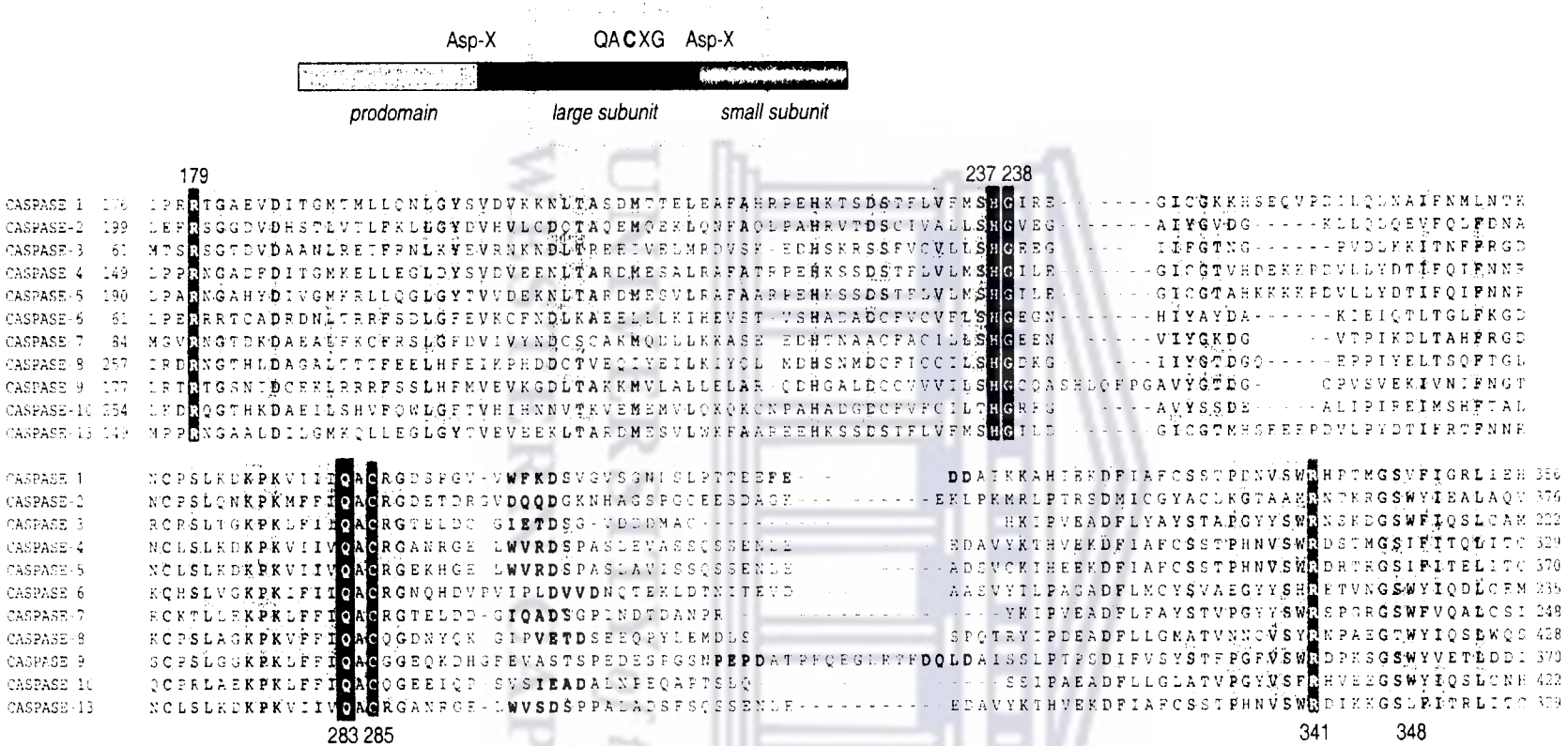

Figure 1.1. Sequence alignment of known caspases (taken from Nicholson, 1999). The sequence alignments shown represent most of the large subunit and part of the small subunit. The P1 Asp (red), the catalytic dyad (green) and the "oxyanion hole" (green) are indicated. The cleavage site for activation is indicated in yellow.

caspases-1 to -10 and caspase-14 have been identified in humans (Van de Craen *et al.*, 1998; Nicholson, 1999). Caspase-11 exists in the mouse only and human caspase-4 is believed to be the homologue of caspase-11 (Van de Craen *et al.*, 1997). Humans have lost the expression of caspase-12 due to several mutations in this gene (Fischer *et al.*, 2002). The active site for all caspases is a pentapeptide with the general structure: QACXG, where X is R, Q or G. The connection between caspases and apoptosis was made when it was discovered that there is extensive similarity between CED-3 and ICE (Yuan *et al.*, 1993). The precise biological functions of some of these enzymes are still not clear. Their role in apoptosis is to activate processes that will lead to the disassembly of cells. Most if not all of the morphological and biochemical changes observed in apoptotic cells are triggered by caspases. Based on their role in apoptosis, caspases can either be classified as initiator caspases (caspases that initiate disassembly in response to apoptotic stimuli) or effector caspases (caspases that function directly in the disassembly of the cell). Phylogenetic analysis categorises caspases into three subfamilies: (1) the ICE subfamily of cytokine processors (caspase-1, -4, -5, -11, -12, -13 and -14), (2) the CED-3/CPP32 subfamily of apoptotic executioners (caspase-3, -6 and -7) and the ICH-1/Nedd-2 subfamily of apoptosis initiators (caspase-2, -8, -9 and -10) (Nicholson, 1999). The classification of these enzymes is illustrated in Figure 1.2. These sub-families reflect differing substrate specificity, function and activation.

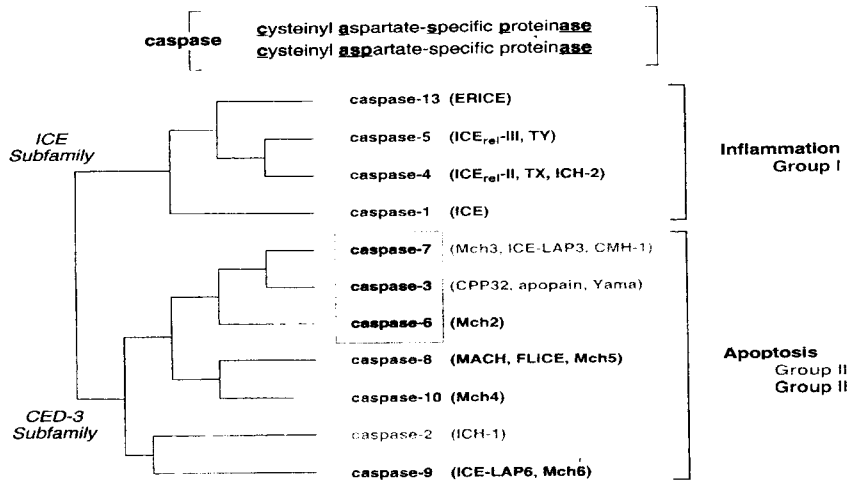

Figure 1.2. The classification of caspases into three subfamilies based on phylogenetic analysis (from Nicholson, 1999).

1.2.1. Activation and regulation of caspases.

Caspases are synthesised as inactive pro-enzymes, which are proteolytically processed to their active forms by initiator caspases. The pro-enzymes contain three domains: an N-terminal pro-domain (30 to 50 kD), a large subunit (~20 kD) and a small subunit (~10 kD) (Zimmermann *et al.*, 2001). The activation of pro-caspases involves cleavage at critical aspartate residues between these domains followed by the association of small and large subunits to form a heterodimer (illustrated in Figure 1.3). The binding of the substrate activates the catalysis of a cysteine protease mechanism, which involves a catalytic dyad composed of Cys^{285} and His^{237} plus an "oxyanion hole" composed of Gly^{238} and Cys^{285} (Figure 1.1; Nicholson, 1999).

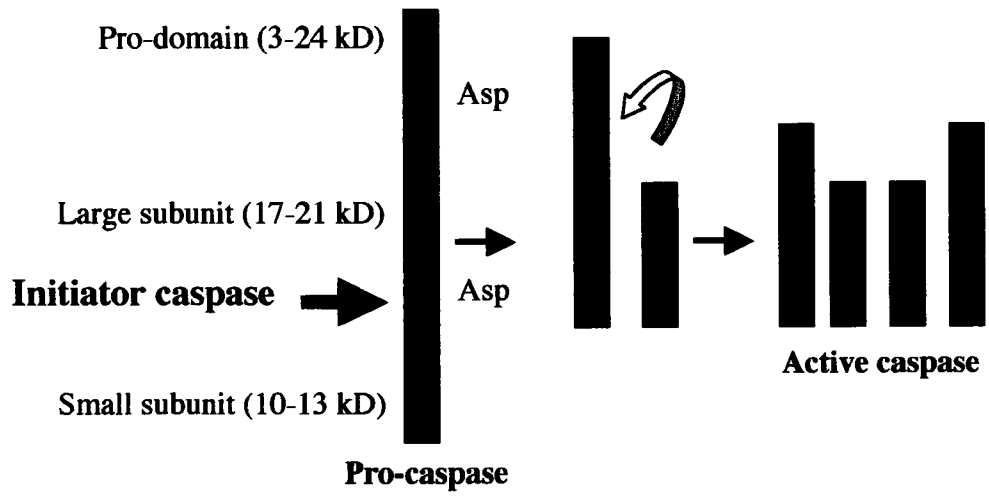

Figure 1.3. The activation of pro-caspases (from Zimmermann *et al.*, 2001).

The pro-domain for some caspases (caspase-3, -6, -7 and -14) range from small peptides to large domains (caspase-2, -8, -9 and -10) containing recognisable structural domains that play important roles in the regulation of caspases by acting as transducers of apoptotic signals (Nicholson, 1999). The pro-domain of caspase-8 and -10 contains a DED (death effector domain), which interacts via an adaptor molecule with the cytoplasmic tail of the CD95/TNFR1 receptors. The activation of initiator caspases is triggered through one of at least two structural domains [DED or CARD (caspase recruitment domain)] present in the caspase pro-domain. Pro-caspases are activated either through auto-activation (by themselves) or other non-caspase proteinases such as granzyme B. For example, strong evidence exists to suggest that caspase-8 auto-activates itself upon recruitment to the death receptor signalling complex. Once activated the active enzyme activates effector caspases-3 and -7. This cascade model of activation is one that is also employed by other complex proteolytic systems (coagulation for example) to

regulate enzyme activity. In some cases the binding of co-factors is essential for caspase activation. This in itself is a way to regulate the activation of caspases. In addition, the compartmentalisation of caspases and their co-factors is also a way of regulating caspase activity (Liu *et al.*, 1996). Caspase-9 is an example of a caspase that does not require proteolytic processing to be activated. It binds to Apaf-1 through its CARD domain. In this instance the co-factors (Apaf-1 and cytochrome c) are localised inside the mitochondria and in order to activate caspase-9 these factors first need to be released from the mitochondria.

Viruses have develop various strategies to block apoptosis in host cells following infection. Several viral caspase inhibitors have been identified: cytokine response modifier A (crmA), (Ray *et al.*, 1992), p35 (Clem *et al.*, 1991) and a family of IAP's proteins (reviewed in Section 1.3.2). CrmA, a protein from cowpox virus, is an inhibitor of caspases-1 and -8. CrmA blocks inflammation and apoptosis in the host. Genetic analysis of the Baculovirus genome led to the identification of p35, which inhibits caspases by substrate trapping of the active enzyme.

1.2.2. Molecular targets of caspases.

Caspases are central to apoptosis and, in their role as effectors, either de-activate proteins that protect living cells from apoptosis or activate proteins that promote apoptosis. Comparative 2-D gel analysis suggests that up to 200 proteins are targeted by caspases during apoptosis (Nicholson, 1999). Only about 70 of these caspase targets are known. The targets of caspases can be divided into classes

based on their function: (1) Activation of pro-caspases by active caspases to overcome the inhibitory effects of apoptosis inhibitors. (2) The inhibition of the anti-apoptotic Bcl-2 and Bcl-x_L proteins through cleavage by caspase-3 (Cheng *et al.*, 1997). (3) Activation of Bid through cleavage by caspase-8, which results in the translocation of tBid (truncated Bid) to the mitochondria and consequent release of cytochrome c (Li *et al.*, 1998). (4) The cleavage of ICAD/DFF45 by caspase-3 resulting in the translocation of CAD (caspase-activated deoxyribonuclease) to the nucleus with consequent degradation of the nuclear DNA (Sakahira *et al.*, 1998). (5) The activation of gelsolin and lamins through cleavage by caspase-3 and caspase-6, respectively, which promotes the apoptotic features in the nuclear and cytoplasmic membrane (Kothakota *et al.*, 1997). (6) The de-activation of the DNA repair enzyme, PARP (poly-ADP-ribose polymerase), through cleavage by caspase-3 (Takahashi *et al.*, 1996) and as a consequence the fragmented DNA cannot be repaired.

1.3. The Bcl-2 protein family: the regulators of apoptosis.

The Bcl-2 protein family plays key roles in the regulation of apoptosis through the activation or inhibition of factors required for apoptosis. These proteins act as integrators of death and survival signals received through signalling pathways that are activated by death receptors and transmitted through death effector proteins.

The Bcl-2 family is structurally conserved, sharing four protein domains: BH1, BH2, BH3 and BH4. Figure 1.4 shows a diagrammatic representation of these

A. The Bcl-2-like survival factors

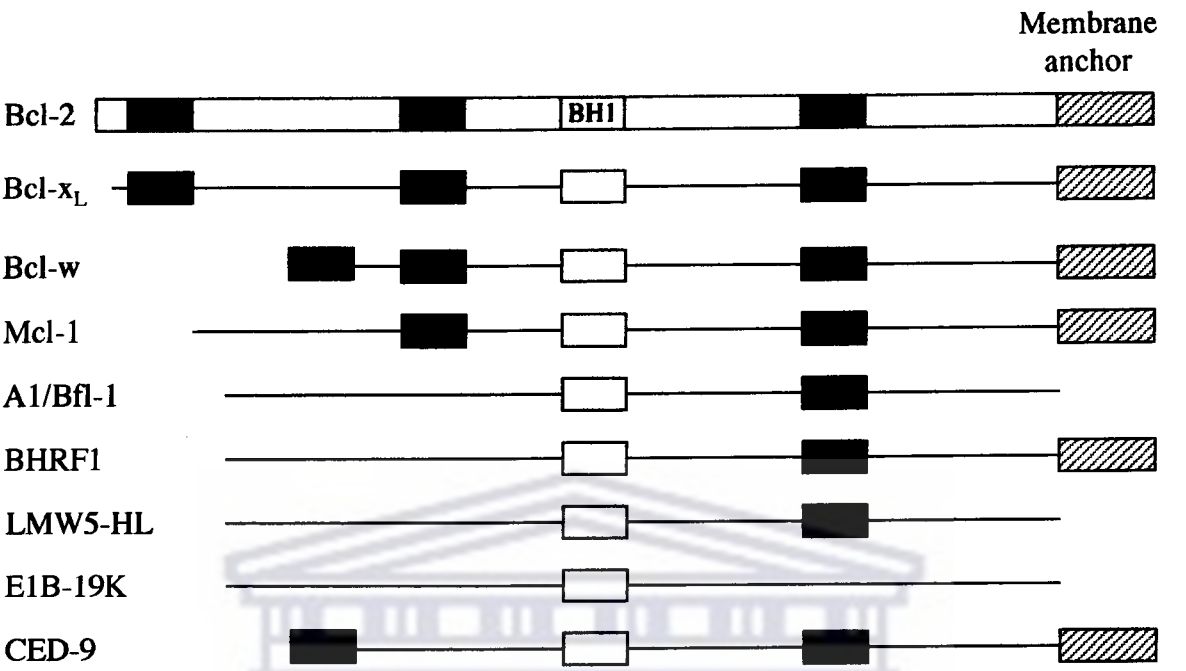

B. The Bax-like death factors

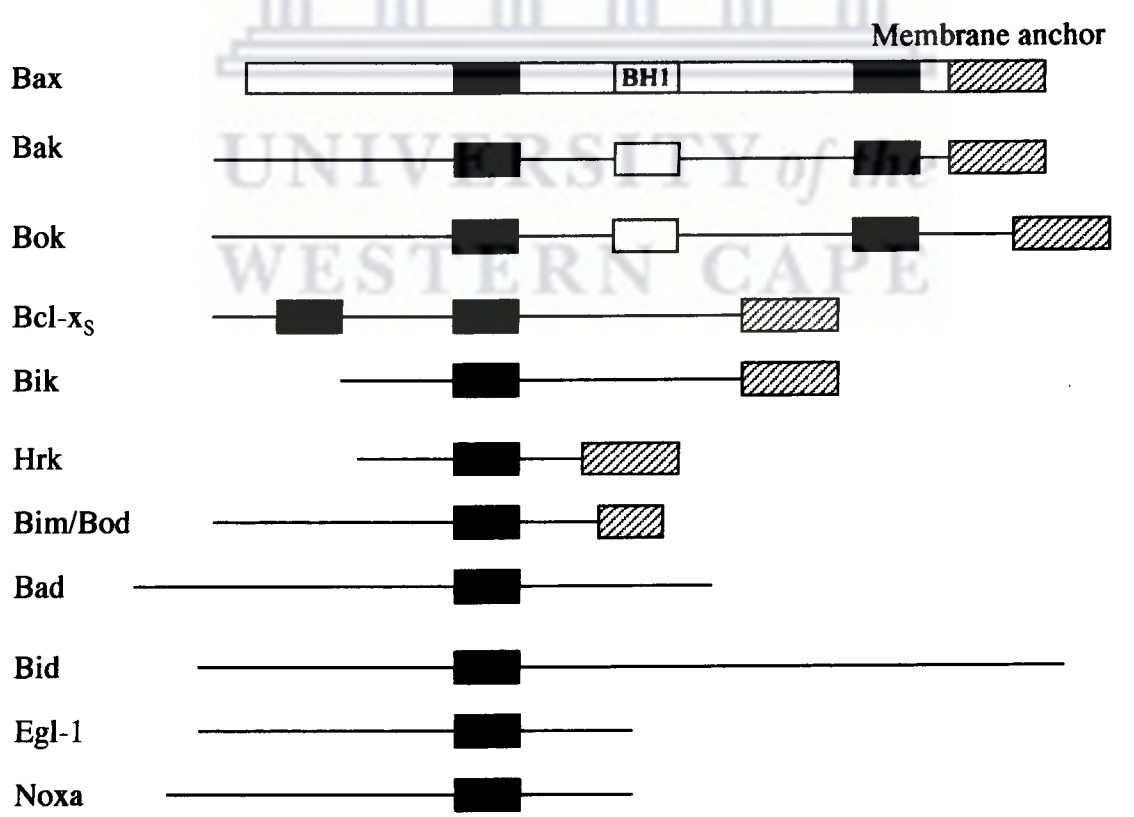

domains in the Bcl-2 protein family. This protein family can be divided into two groups based on their role in apoptosis and their structure. The one group of proteins includes the Bcl-2-like survival factors such as Bcl-2, Bcl-x_L, Bcl-w, Bfl-1, Mcl-1, A1, E1B19K, LMW5-HL and EBV BHRF1 while the other group include Bax-like death factors such as Bax, Bak, Bcl-x_S, Bad, Bid, Bik, Hrk, Bim and Bok (Sattler *et al.*, 1997; Borner, 2003). The BH1, BH2 and BH4 domains appear to be functionally important, while the BH3 domain is essential for pro-apoptotic function. *Bcl-2* was first identified as proto-oncogene acting as the target gene at the translocation site of the t (14; 18) chromosomal translocation breakpoint in the tumour cells of approximately 80 % of patients with human follicular B-cell lymphoma (reviewed in Strasser *et al.*, 1997). Functional studies demonstrated that *Bcl-2* inhibits apoptosis in lymphocytes (Vaux *et al.*, 1988; Massaia *et al.*, 1995). Another member of the *Bcl-2* gene family, the *Bcl-x* gene, encodes two polypeptides, which can be expressed through alternative splicing (Boise *et al.*, 1993). The longer transcript encodes a 28 kD protein, Bcl-x_L, which contains all four BH domains. The shorter transcript encodes an 18 kD protein, Bcl-x_S, which only contain the BH1 and BH2 domains. Bcl-x, like Bcl-2 acts as a death suppressor. Conversely, both Bax and Bak promote apoptosis. Both these proteins contain BH1, BH2 and BH3 domains. The cytotoxic effects of these proteins are dependent on the BH3 domain, which also mediates the dimerisation between Bax/Bak and Bcl-2, Bcl-x_L, E1B 19K, Bid or Bax/Bax or Bak/Bak (Sattler *et al.*, 1997). The "rheostat" model has been proposed to describe the function of the Bax/Bcl-2, where the relative ratios of Bax/Bax homodimers, Bax/Bcl-2 heterodimers and Bcl-2/Bcl-2 homodimers regulate apoptosis

(Kroemer, 1997). In this model an excess of Bax homodimers favours apoptosis, while an excess of Bax/Bcl-2 heterodimers inhibits apoptosis. Another group of pro-apoptotic Bcl-2 proteins, the so-called "BH3 only Bcl-2 family members" (Bad, Bik, Blk, Hrk, Bid, Bim, Noxa) also promote apoptosis (Zornig *et al.*, 2001). These proteins share the BH3 domain with the Bcl-2 protein family and EGL-1 of *C. elegans*, which allow these proteins to bind to anti-apoptotic Bcl-2 proteins and neutralise their functions.

The mechanism of function of the Bcl-2 protein family is still a very controversial issue. Currently there are three models describing Bcl-2 function. The first model describes Bcl-2 proteins as proteins that regulate the activation of caspases, a second model describes Bcl-2 proteins as ion channels and a third model describes suggests that these proteins act as inhibitors of cytochrome c release from mitochondria (reviewed in Zornig *et al.*, 2001). The model that proposes a role for the involvement of Bcl-2 in the activation of caspases stems from the observation that in *C. elegans* the binding of CED-4 to CED-3 induces ATP-dependent activation of CED-3. The activation of CED-3 can be blocked by CED-9, which is the homologue of Bcl-2 (Wu *et al.*, 1997). By comparison it is possible that Bcl-2 may block the activation of caspase-9 through the action of Apaf-1, which is the homologue of CED-4 (Chinnaiyan *et al.*, 1997). The view that Bcl-2 may function as a membrane channel stems from evidence that the three-dimensional structure of Bcl-x_L resembles the membrane insertion domain of diphtheria toxin (Muchmore *et al.*, 1996). Although ion channel activity has been detected for Bcl-2 and Bcl-x_L, evidence for the *in vivo* formation of such

channel structure is still lacking (Gross *et al.*, 1999). It was also demonstrated that Bax is able to interact with proteins in the mitochondrial membrane: the voltage-dependant-anion channel (VDAC), adenine nucleotide carrier (ANC) (Shimizu *et al.*, 2000a; Brenner *et al.*, 2000) These proteins form part of the mitochondrial permeability transition pore (MPTP) thought to be involved in the release of cytochrome c from the mitochondria during apoptosis (reviewed in Section 1.5.1). There is also evidence to suggest that the release of cytochrome c could be blocked by the BH4 domain-containing Bcl-2 family members, Bcl-2 and Bcl-x_L (Shimizu *et al.*, 2000b).

It is possible that the Bcl-2/x_L proteins functions through all three these mechanisms and that channel formation by these proteins facilitate the release of cytochrome c and that part of the protein is involved in the binding to Apaf-1 (Zornig *et al.*, 2001).

1.4. The cell surface receptor or "extrinsic" signalling pathways.

Cells constantly receive pro- and anti-apoptotic signals from their environment. Balances between these conflicting signals determine whether downstream effector targets (caspases, Bcl-2 proteins and other pro- or anti-apoptotic proteins) are activated and therefore also determine whether a cell lives or dies. One view is that a cell needs signals from surrounding cells in order to survive (Raff, 1992). In the absence of such signals a cell will activate apoptotic pathways. Mammals also developed an additional mechanism for the "instructive" activation of apoptosis.

It is especially in the immune system where this type of "instructive" signalling is used (Osborne *et al.*, 1996). Death receptors expressed on the surface of cells are capable of transmitting apoptotic signals across the cell membrane. Death receptors are CD95 (FAS or Apo1) (Smith, 1994; Nagata, 1997), TNFR1 (also called p55 or CD120a) (Smith, 1994; Nagata, 1997), CAR1 (Brojatsch *et al.*, 1996), DR3 (Apo3, TRAIL-R2, TRICK2) (Chinnaiyan *et al.*, 1996; Kitson *et al.*, 1996; Screaton *et al.*, 1997) DR4 (Pan *et al.*, 1997) and DR5 (MacFarlane *et al.*, 2003; Walczak *et al.*, 1997). Ligands to these receptors are synthesised as type II membrane proteins. These proteins share a 150 residue C-terminal extracellular domain that interacts with its respective receptor. These receptors belong to the tumour necrosis factor (TNF) receptor gene super family and are type I membrane proteins characterised by conserved extracellular cysteine rich domains. They transmit apoptotic signals through pathways constructed by the association of proteins containing homology domains of the same class (Wallach, 1997). Three homology domains described thus far include the DD, the DED and the CARD. All three these domains consist of a conserved sequence motif of about 90 amino acids that forms a six anti-parallel α-helical structure (Wolf *et al.*, 1999; Weber and Vincenz, 2001). Signals are transmitted from one protein to the next by interactions through these homologous domains. The DD is involved in the early stages of the signalling pathway; inducing oligomerisation of death receptors and in some cases the binding of these receptors to downstream DD-containing proteins (Chinnaiyan *et al.*, 1995). The DED and CARD domains play crucial roles in the recruitment of caspases inside the cell.

1.4.1. Signalling by CD95/Fas/Apo 1.

CD95 and its ligand CD95L play an important role in three types of apoptosis: (1) deletion of activated mature T cells when they become redundant; (2) killing of virus-infected or cancer cells by cytotoxic T lymphocytes and (3) killing of inflammatory cells at "immune privileged" sites such as the eye (Ashkenazi and Dixit, 1995). CD95 is expressed in activated lymphocytes and other tissues such as liver, heart and lung. Binding of CD95L to CD95 leads to the clustering of death domains in the receptor (Huang *et al.*, 1996). FADD (Fas-associated death domain or Mort1) is an adaptor protein, which contains both a death domain and a death effector domain (Chinnaiyan *et al.*, 1995). Following activation of CD95 this adaptor protein binds to the clustered death domains of the receptor. Figure 1.5 illustrates the CD95 signalling pathway.

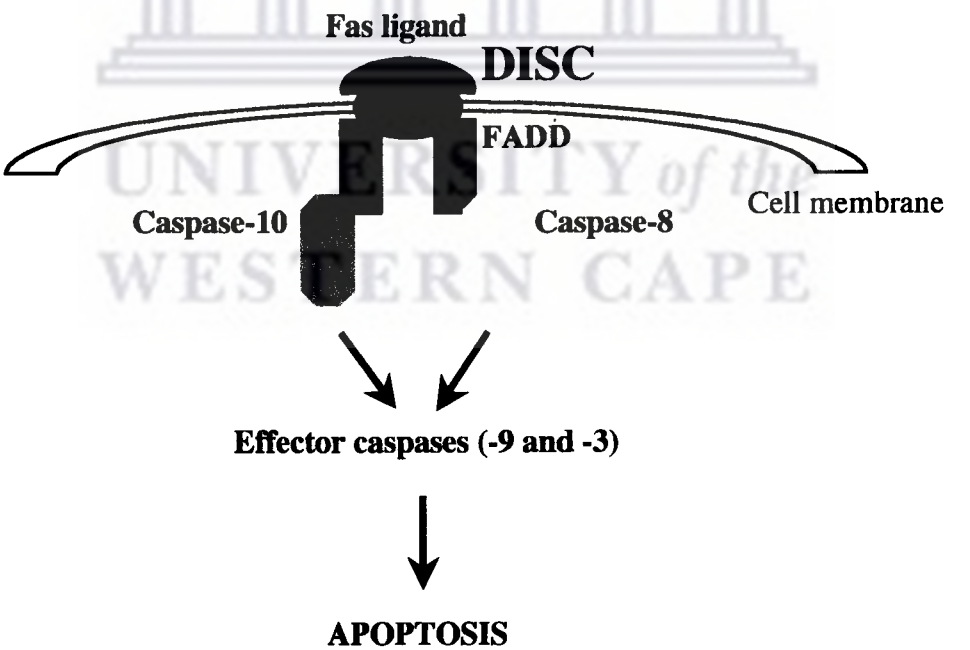

Figure 1.5. The Fas/CD95 signalling pathway.

FADD then binds the pro-domain of caspase-8 (FLICE or MACH), which leads to the oligomerisation of caspase-8 (Boldin *et al.,* 1996; Hahne *et al.,* 1996; Haung *et al.,* 1996; Strasser and Newton, 1999). The recruitment of pro-caspase-8 by FADD to the activated CD95 receptor leads to the formation of DISC (**D**eath **I**nducing **S**ignalling **C**omplex) (Kischkel *et al.,* 1995; Scheel-Toellner *et al.,* 2002). Once activated by FADD, caspase-8 can catalyse it's own activation through self-cleavage. Caspase-8 then activates downstream effector caspases such as caspases-9 and -3, which ultimately leads to the apoptosis.

The death domain of CD95 and TNFR1 can interact with a second protein called RIP (receptor interacting protein) (Stanger *et al.,* 1995) (illustrated in Figure 1.6). RIP is required for the CD95L/TNF-induced activation of the transcription factor NF-κB (Martinon *et al.*, 2000). The activation of NF-κB promotes anti-apoptotic signals. Hence, during apoptosis, activation of NF-κB is prevented by cleavage of RIP by activated caspase-8. Once recruited by CD95 or TNFR1, RIP interacts with a death adaptor protein called RAIDD (RIP associated ICH/CED-3 homologous protein with a death domain). The N-terminus of RAIDD is homologous to, and is capable of oligomerising with the pro-domain of caspase-2. A third CD95 binding-protein is Daxx. Daxx is able to bind CD95 but lacks a death domain. The over-expression of Daxx has been shown to activate JNK (c-Jun-N-terminal kinase), which potentiates CD95 induced apoptosis (Yang *et al.,* 1997). Hence, two CD95 apoptosis pathways have been proposed: one pathway is activated via FADD/caspase-8/-2 and another pathway is activated via Daxx/JNK (Zornig *et al.,* 2001; Wajant, 2002) (illustrated in Figure 1.6).

Both the CD95 and TNFR1 death signalling pathways can be regulated by proteins called FLIP's (Fas-associated death domain-like ICE inhibitory protein). Some viruses during infection produce FLIP's as a mechanism to protect themselves against apoptosis induced by the host cell (Thome *et al.*, 1997; Srinivasula *et al.*, 1997). A cellular homologue of the viral FLIP protein, c-FLIP was identified (Srinivasula *et al.*, 1997). c-FLIP contains two death domains and an inactive caspase-like domain. It is therefore able to bind CD95 or TNFR1 but unable to activate caspase-8 and therefore apoptosis is blocked.

1.4.2. Signalling by TNF receptors.

The cytokine TNF is a ligand for two receptors: TNFR1 and TNFR2. Activated macrophages and T cells, in response to infection, secrete TNF that binds to these receptors (Tartaglia and Goeddel, 1992). TNFR1 is able to induce apoptosis while TNFR2 appears to promote cell survival. However it has been demonstrated that over-expression of TNFR2 can induce cell death in some cell types (Grell *et al.*, 1999). Binding of TNF to TNFR1 activates the clustering of the death domains within the receptor (Smith *et al.*, 1994). Figure 1.6 illustrates the TNF signalling pathway. An adaptor protein called TRADD (TNFR-associated death domain) binds through its own death domain to the clustered death domains of the activated TNFR1 (Hsu *et al.*, 1995). This leads to the recruitment of two additional proteins: TRAF (TNFR-associated factor) and RIP to the receptor (Ting *et al.*, 1996). TRAF2, TRAF5, TRAF6 and RIP can activate NIK (NF-κB-inducing kinase), which in turn activates IKK (inhibitor of κB kinase complex) by

phosphorylation (Malinin *et al.*, 1997; Ye *et al.*, 1999). Activation of IKK leads to phosphorylation and consequent degradation of Inhibitor of κB, allowing NF-κB to move to the nucleus and activate transcription. TRAF2 and RIP can also activate c-Jun NH_2-terminal kinase (JNK) (Malinin *et al.*, 1997; Mercurio *et al.*, 1997). While the activation of FADD mediates apoptosis through the activation of caspase-8, the activation of JNK and NF-κB leads to the induction of pro-inflammatory and immunomodulatory genes. The pathway from TRAF2 and RIP to JNK involves a cascade of signalling events that includes MAP kinases, MAP/Erk kinase kinase-1 and JNK kinase and JNK (Liu *et al.*, 1996; Natoli *et al.*, 1997).

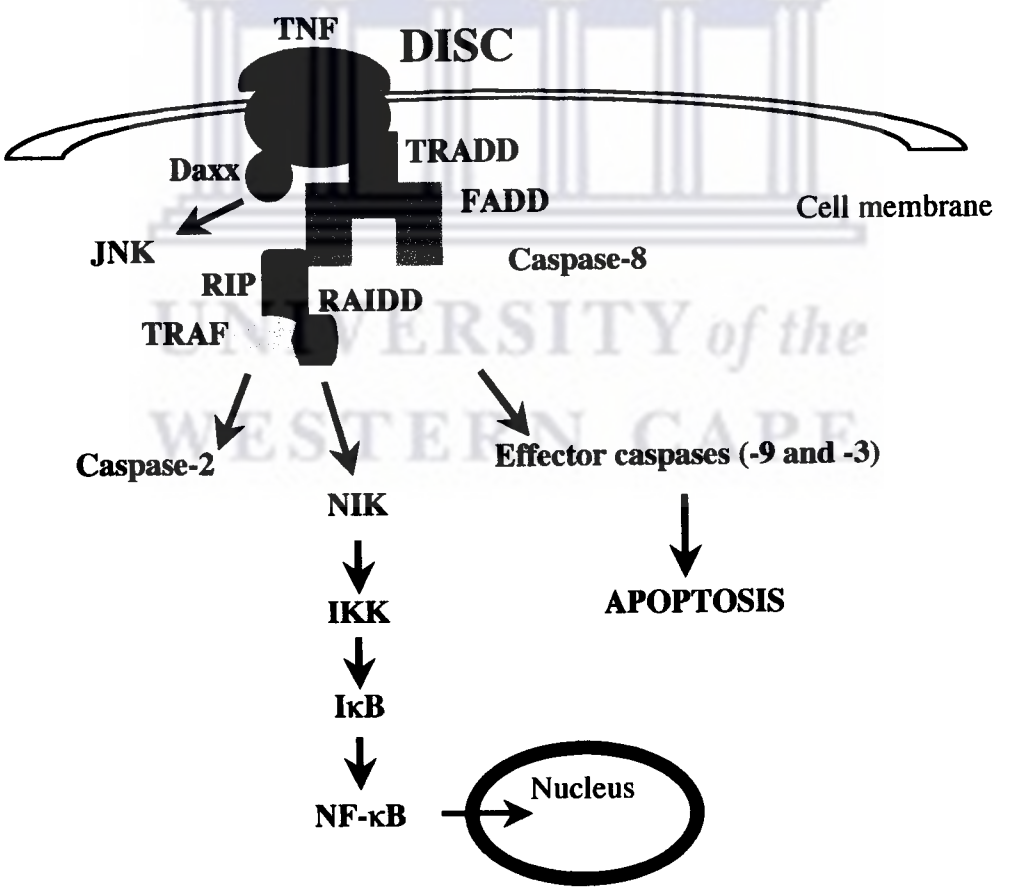

Figure 1.6. The TNF signalling pathway.

1.4.3. Signalling by DR3.

DR3 is mainly expressed on cells in the spleen, thymus, and peripheral blood. DR3 is activated by Apo3 ligand (Apo3L or TWEAK). DR3 shares sequence similarity with TNFR1 (Chinnaiyan *et al.*, 1996; Kitson *et al.*, 1996; Screaton *et al.*, 1997). Activation through DR3 resembles TNFR1 in that DR3 also activates the transcription factor NF-κB through TRADD, TRAF and RIP while apoptosis is activated through TRADD, FADD and caspase-8. Figure 1.7 illustrates the DR3 signalling pathway.

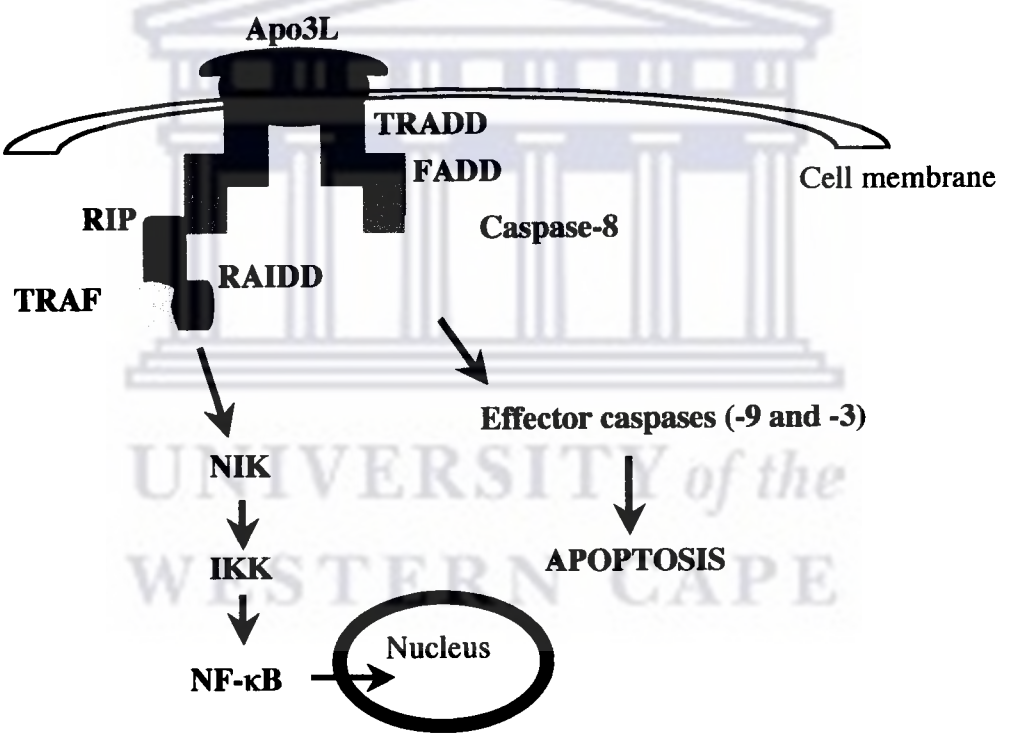

Figure 1.7. The DR3 signalling pathway.

Although the signalling through TNFR1 and DR3 is similar, there are differences in the expression of these ligands (TNF and Apo-3) and receptors (TNFR1 and DR3). TNF expression occurs mainly in activated macrophages and lymphocytes

(Tartaglia *et al.,* 1992), whereas Apo3L is expressed in many tissues (Chicheportiche *et al.,* 1997), conversely TNFR1 is expressed ubiquitously whereas DR3 are present mainly in the spleen, thymus and peripheral blood (Chinnaiyan *et al.,* 1996). This suggests that these two signalling pathways may have distinct biological functions.

1.4.4. Signalling by the TRAIL receptors.

TRAIL (or TNF-related apoptosis–inducing ligand, also called Apo2L) is a TNF–related ligand, which does not bind CD95 or TNFR1 (Gura, 1997; Ashkenazi and Dixit, 1998). Two pro-apoptotic TRAIL binding receptors DR4/TRAIL-R1 and DR5/TRAIL-R2/KILLER/TRICK-2 have been identified (Pan *et al.*, 1997; Sheridan *et al.*, 1997). DR4 and DR5 are expressed in several tissues, including spleen, lung and prostate. DR5 was identified as a member of the TNF receptor family by homology search following the discovery of DR4. These two receptors respectively share a 66% and 64% identity in their cysteine-rich and death domains. As is the case for the CD95 signalling pathway, these receptors contain a death domain that activates apoptosis through FADD and caspase-8 (Pitti *et al.,* 1996). Figure 1.8 illustrates the TRAIL signalling pathway. Although these receptors and ligands are widely expressed, normal cells appear to be less sensitive to apoptosis induced by TRAIL when compared to tumour cells. One possible explanation for this selective resistance can be attributed to the existence of decoy receptors. Decoy receptor 1 (DcR1/TRID/LIT/TRAIL-R3) and decoy receptor 2 (DcR2/TRUNDD) (Pan *et al.*, 1998) are unable to activate

apoptosis due to the absence of a functional death domain. It was speculated that the presence of these receptors in some cell types might prevent TRAIL from binding to DR4 and DR5 and hence protect these cells against apoptosis induced by TRAIL. It was expected that varying expression levels of the decoy receptors might account for the differential sensitivity of normal and transformed cells. However, several tumour cell lines have been demonstrated to express DR5 but show little or no expression of DcR1 (Sheridan *et al.*, 1997) and therefore there was no correlation between the expression levels of the decoy receptors and resistance to TRAIL-induced apoptosis (Walczak and Krammer, 2000). Recent studies suggests that the selective resistance may be due to other factors such as TRAIL-induced NF-κB activation or death inhibitors such as c-FLIP (MacFarlane, 2003).

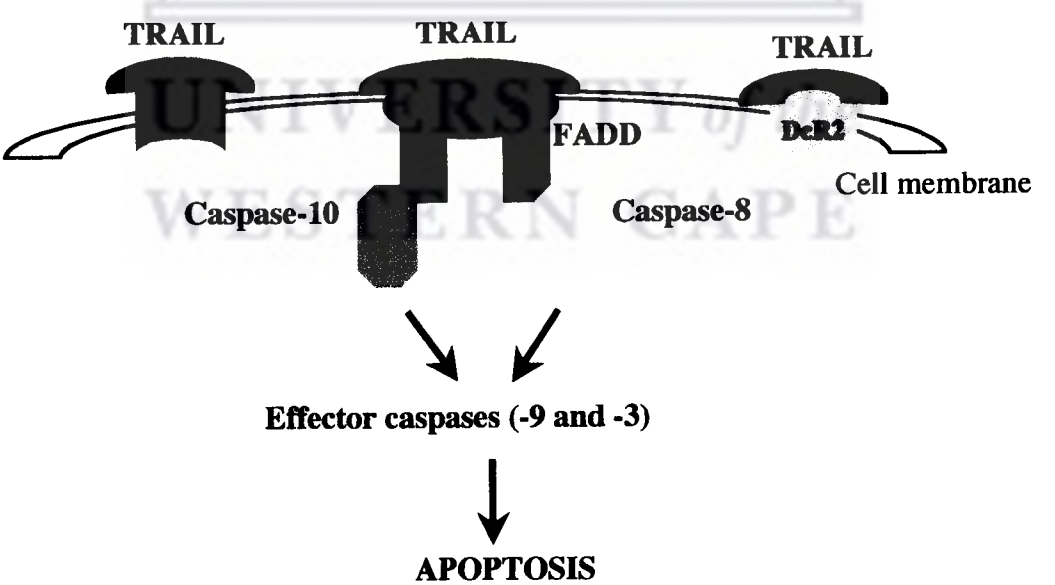

Figure 1.8. The TRAIL signalling pathway.

1.5. The mitochondrial or "intrinsic" signalling pathway.

Mitochondria are well known for their role in energy metabolism and Ca^{2+}-homeostasis. However, recent data also suggest that mitochondria play a central role in the regulation of apoptosis. An investigation into the activation of caspase-3 led to the discovery that the two mitochondrial proteins Apaf-1 (apoptosis activating factor-1) and cytochrome c are required for caspase-9 action (Liu *et al.*, 1996; Vaux, 1997; Reed, 1997; Slee *et al.,* 1999; Kroemer and Reed, 2000). Cytochrome c normally resides inside the intermembrane space between the outer and inner mitochondrial membrane. During apoptosis cytochrome c is released from the mitochondria along with pro-apoptotic proteins such as adenylate kinase-2, Smac/DIABLO, IAPs (inhibitor of apoptosis proteins) and AIF (apoptosis inducing factor).

Binding of CD95L in the CD95-mediated pathway (Section 1.4.1) leads to receptor aggregation and the recruitment of death adaptor molecules on the cytoplasmic side of the membrane. Figure 1.9 illustrates the signalling pathways induced by CD95. Pro-caspase-8 is activated and recruited to the DISC where it is activated and can cleave pro-caspase-3. This direct interaction between the extracellular CD95L and the intracellular apoptotic machinery only occurs in type I cells (Scaffidi *et al.,* 1998; Scaffidi *et al.*, 1999).

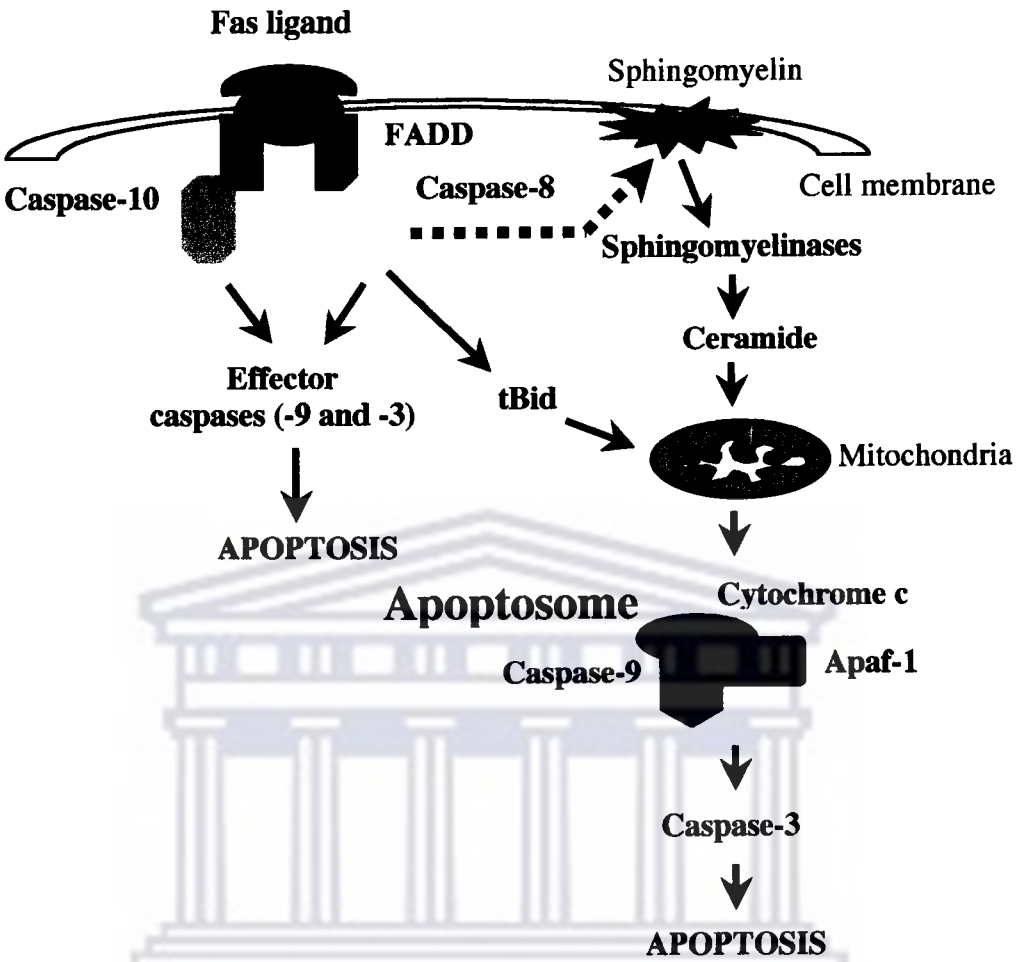

Figure 1.9. The "intrinsic" apoptotic pathway.

In type II cells, binding of the Fas ligand, CD95L, to CD95 leads to changes in the mitochondria that activate caspases. In type II cells the amount of active caspase-8 formed during the activation of apoptosis is much less than in type I cells (Scaffidi *et al.*, 1999). As with most inducers of apoptosis, the activation of apoptosis by CD95 coincides with the production of ceramide (Hannun, 1996; Mathias *et al.*, 1998). However, except for CD95-induced apoptosis there appears to be a significant lag-time in the production of ceramide with most other inducers of apoptosis. It has been proposed that this lag-time between the activation of

upstream (caspase-8) and downstream (caspase-3) proteases may be the result of the activation of events such as the activation of enzymes called sphingomyelinases that lead to the production of ceramide and the release of cytochrome c (Perry and Hannun, 1998). The activation of apoptosis through CD95 also results in the production of ceramide. In type I cells the activated caspase-8 targets mitochondria through cleavage of the BH3-only protein, Bid. Cleaved Bid (tBid) binds to Bax, leading to Bax oligomerisation and the release of cytochrome c from the mitochondria (Li *et al.*, 1998). Once released into the cytoplasm cytochrome c associates with Apaf-1, dATP or ATP and caspase-9 to form a multimeric complex, the apoptosome (Li *et al.*, 1997; Adams and Cory, 2002). This leads to the activation of caspase-9 (illustrated in Figure 1.10), which in turn activates caspase-3.

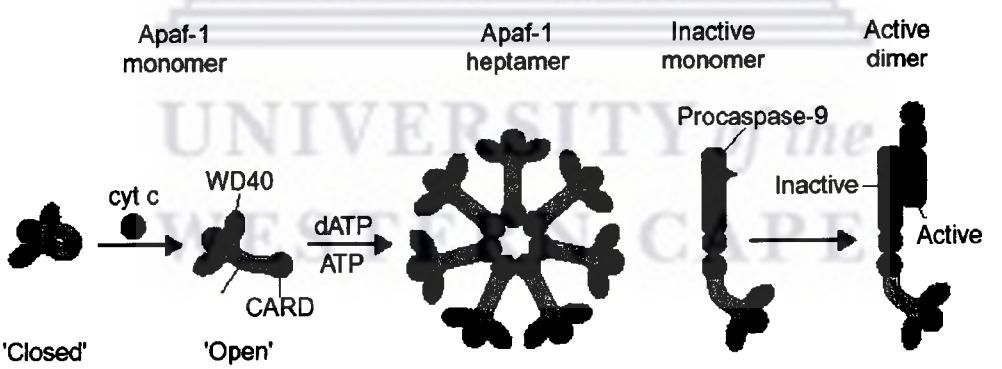

Figure 1.10. The activation of pro-caspase-9 through the formation of the apoptosome (from Adams and Cory, 2002).

Apaf-1 is the mammalian homologue of CED-4. The CED-4-like domain of Apaf-1 is flanked by a CARD motif on the N-terminus end and several WD-40 repeats

on the C-terminus end (Zou *et al.,* 1997; Slee *et al.,* 1999). The CARD domain of Apaf-1 interacts with the pro-domain of caspase-9 in the presence of cytochrome c and either dATP or ATP. The binding of cytochrome c and dATP/ATP converts Apaf-1 from a closed monomeric structure to an open conformer and then to a heptameric structure, which acts as a scaffold for pro-caspase-9 assembly (Figure 1.10). The binding of cytochrome c to the WD-40 repeats induces oligomerisation of Apaf-1, which leads to the activation of caspase-9 (Slee *et al.,* 1999). Normally the oligomerisation of Apaf-1 is blocked by the WD-40 repeats. This blockade is lifted once cytochrome c binds to the WD-40 repeats. The activation of caspase-9 leads to the activation of downstream effector caspases (caspase-2, -3, -7, -8 and -10).

Anti-apoptotic members of the Bcl-2 protein family such as Bcl-2 and Bcl-x_L can block the release of cytochrome c from the mitochondria. These anti-apoptotic proteins reside in the outer mitochondrial membrane. Bcl-2 and Bcl-x_L are the structural homologues of the *C. elegans* anti-apoptotic protein CED-9. These proteins might suppress apoptosis by either blocking cytochrome c release or binding to Apaf-1 preventing its activation by caspase-9. Alternatively, pro-apoptotic proteins such as Bax, Bak and Bik may promote apoptosis by displacing Apaf-1 from Bcl-2 and Bcl-x_L (Zornig *et al.*, 2001). The mechanism of interaction between Apaf-1 and caspase-9 appears to be similar to the CED-3/CED-4 interactions in *C. elegans.*

1.5.1. The release of cytochrome c from mitochondria during apoptosis.

It is estimated that 85-97% of the cells cytochrome c is located in the crystal lumen of the mitochondria while the rest is located inside the inter-membrane space. It is generally accepted that mitochondria play some role in apoptosis and that the release of cytochrome c into the cytoplasm is required. However, the mechanism for release of cytochrome c from the mitochondria is still an issue of much debate (Zimmermann *et al.*, 2001).

Several models have been proposed to describe the release of cytochrome c from mitochondria. However, none of these models is able to fully explain the mechanics of this process. The first model (Section 1.5.1.1) is based on the formation of the mitochondrial permeability transition pore (MPTP) in the mitochondrial membrane, which ultimately leads to disruption of mitochondrial function and lysis of the outer mitochondrial membrane with consequent release of cytochrome c (Petit *et al.*, 1996). The second model suggests that the Bcl-2 protein, Bax, forms a pore in the mitochondrial membrane (Muchmore *et al.*, 1996; Schlesinger *et al.*, 1997). A third model proposes that an interaction between Bax and VDAC may produce a pore large enough to facilitate cytochrome c release (Shimuzu *et al.*, 1999; Shimuzu *et al.*, 2000a).

1.5.1.1.The mitochondrial permeability transition pore (MPTP).

Mitochondrial permeability transition involves the opening of a pore (MPTP) in the inner membrane of the mitochondria. The opening of this pore ultimately

leads to the release of pro-apoptotic proteins from the mitochondria. The MPTP is a multi-protein complex formed at contact sites between the inner and outer mitochondrial membrane (Petit *et al.*, 1996). The MPTP normally participates in the regulation of matrix Ca^{2+}, pH, transmembrane potential and volume by acting as a Ca^{2+}, voltage, pH and redox-gated channel with several levels of conductance and almost no ion selectivity (Zoratti and Szabo, 1995; Ichas *et al.,* 1997). The open pore allows passage of solutes with a molecular mass of up to 1.5 kD. Opening of the MPTP allows the respiratory chain to generate a transmembrane electrochemical gradient ($\Delta\psi m$) that drives ATP synthesis. The $\Delta\psi m$ results from the pumping of protons from the inner membrane by the electron transport chain.

The structure and composition of this pore is still only partially defined. A total of six proteins have been identified to play a role in either the formation or regulation of the pore (illustrated in Figure 1.11) (Joseph-Liauzun *et al.,* 1998). These proteins include the 32 kD voltage-dependant-anion channel (VDAC), the 30 kD adenine nucleotide carrier (ANC), the 18 kD peripheral benzodiazepine receptor (PBR), the 240 kD PBR associated protein-1 (PRAX-1), the 20 kD cyclophilin D, hexokinase and creatine kinase. In addition, an unidentified 10 kD protein was found to associate with the PBR (Blahos, 1995). This highlights the fact that our understanding of the function and the structure of the MPTP may at this stage be incomplete.

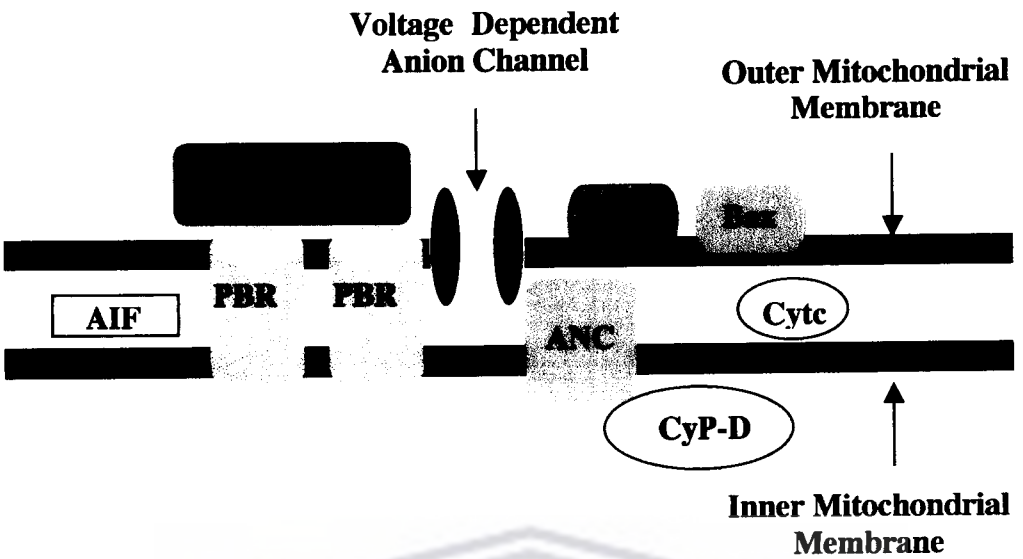

Figure 1.11. Diagrammatic representation of the mitochondrial permeability transition pore.

ANC is responsible for the export of ATP in exchange for ADP across the inner mitochondrial membrane (Halestrap *et al.*, 2002). The ANC operates as a gated pore that flips between two conformations: the c-state where the substrate-binding site faces the cytoplasmic side of the inner membrane and the m-state where it faces the matrix side. The proposed involvement of the ANC in MPTP opening stems from the observation that ligands (e.g. atractylate) to the c-state of the ANC can activate the opening of the MPTP pore (Halestrap and Davidson, 1990; Zoratti and Szabo, 1995). This led to the suggestion that the c-state conformation is susceptible to Ca^{2+}-induced deformation of the MPTP into an open-pore state while the m-state is not.

The immunosuppressive drug, cyclosporin A, was shown to inhibit the opening of the MPTP at sub-micromolar concentrations. The immunosuppressive effect of cyclosporin A involves its binding to a cytoplasmic protein called, cyclophilin A. (Crompton *et al.*, 1988). The cellular functions of cyclophilins are not known, but they most probably play a role in protein folding and/or inducing conformational changes in other proteins since cyclophilins exhibit peptidyl-prolyl cis-trans isomerase activity (Galat, 1993). Cyclophilin D (CyP-D) is a cyclosporin A-sensitive mitochondrial peptidyl-prolyl cis-trans isomerase that was shown to interact with ANC (Halestrap and Davidson, 1990). It is therefore possible that these proteins could induce conformational changes in membrane proteins that will lead to the opening of the MPTP.

The PBR forms a trimeric complex with VDAC and ANC in the outer mitochondrial membrane (McEnergy *et al.,* 1992). The VDAC forms a non-selective pore in the outer mitochondrial membrane that allows the passage of metabolites and ions. The open channel allows the passage of solutes (< 1 kD) by diffusion across the outer mitochondrial membrane. The VDAC localise at contact sites between the inner and outer mitochondrial membrane and can associate tightly with the inner membrane (Halestrap *et al.*, 2002). VDAC is an abundant protein in the outer mitochondrial membrane and constitutes up to 20 % of this membrane. VDAC can also bind hexokinase and creatine kinase. Hexokinase converts glucose to glucose-6-phosphate, which is an intermediate of the glycolytic pathway. Creatine kinase is involved in the production and export of phosphocreatine in the cytosol (Casellas *et al.*, 2002). Hexokinase and creatine

kinase associate with VDAC/ANC in such a way that most of the ATP generated by oxidative phosphorylation is channelled to these enzymes. PRAX-1 was identified by yeast two-hybrid screening and is presumed to interact with PBR in a 1:2 PRAX-1:PBR stoichiometry (Galiegue *et al.,* 1999). It is believed that the role of PRAX-1 may be to induce conformational changes in PBR to facilitate the binding of other proteins.

A number of events are triggered within mitochondria during apoptosis: (1) disruption of electron transport, oxidative phosphorylation and ATP production, (2) release of proteins that trigger activation of caspases and (3) alteration of cellular reduction-oxidation potential (Ashkenazi and Dixit, 1998). It is thought that these events are to be triggered by the collapse of the mitochondrial inner transmembrane potential ($\Delta\psi m$) which is indicative of the opening of the mitochondrial permeability transition pore. The opening of this channel leads to equilibration of ions between the matrix and inter-membrane space of the mitochondria. Consequently the H^+ gradient across the inner membrane is lost and ATP production stops. Unrestrained the loss of ATP production can lead to necrotic cell death. To ensure that cell death progress down an apoptotic rather than a necrotic pathway the MPTP must be closed again so that ATP levels would be maintained (Halestrap *et al.*, 2002). However, MPTP opening may also be involved in the activation of apoptosis through the release of cytochrome c and pro-apoptotic proteins from the mitochondria. The inner mitochondrial membrane possesses a larger surface area relative to the outer membrane because of its folded cristae. Therefore, matrix volume expansion will

eventually lead to rupture of the outer membrane, releasing caspase-activating proteins located within the inter-membrane space. Other proteins released from mitochondria include caspases (caspase-2, -3 and -9), caspase activators (cytochrome c) and AIF (apoptosis inducing factor). A number of apoptosis inducers which include TNF-α and growth factor withdrawal have been demonstrated to indirectly result in the opening of the mitochondrial permeability transition pore (Gottlieb, 2000; Kroemer and Reed, 2000). It is proposed that apoptosis inducers such as ceramide, oxidants and calcium-overload convert ANC from a protein that is specifically involved in the transport of adenine nucleotides into a non-specific pore. Binding of cyclophilin D to ANC may induce these conformational changes. It is known that high levels (> 1 μM) of cytoplasmic free calcium can induce such conformational changes in ANC. When calcium levels are low the binding of cyclophilin D can sensitise ANC to calcium. Matrix adenine nucleotides decrease the sensitivity of ANC to calcium by binding to ANC.

Most activators of MPTP opening require the accumulation of excessive amounts of calcium in the mitochondrial matrix. However, ligands to the PBR are able to induce MPTP even when calcium levels are low. The benzodiazepine derivatives, Ro5-4864, PK11195 and diazepam are ligands to PBR (Syapin and Skolnick, 1979; Le Fur *et al.*, 1983). Their role in regulating mitochondrial permeability transition is well documented: It has been demonstrated that these ligands could have both pro- and anti-apoptotic effects on cells. PK11195 have been shown to induce apoptosis in HL60 cells (Fennell *et al.*, 2001). PK11195 induced a collapse

of the inner mitochondrial membrane potential and mitochondrial swelling in HL60 human leukaemia cells. While PK11195 did not activate apoptosis in thymocytes, it enhanced the pro-apoptotic activity of UV radiation, etoposide, doxorubicin, dexamethasone and ceramide (Hirsch *et al.*, 1998). Over-expression of the anti-apoptotic gene Bcl-2 protects cell from the apoptotic effects of glucocorticoids and chemotherapeutic agents. However, treatment with PK11195 can abolish the inhibitory effects of Bcl-2 (Zamzami *et al.*, 1996). The anti-apoptotic activities of Ro5-4864 have been demonstrated in U937 and Jurkat cells. PK11195 has been shown to enhance the pro-apoptotic activity of TNF-α and inhibited the anti-apoptotic effects of Ro5-4864 (Xia *et al.*, 2000). The pro-apoptotic effect of tamoxifen on MCF-7 and BT-20 breast cancer cells has shown to be inhibited by treatment with PK11195 and Ro5-4864 (Strohmeier *et al.*, 2002). A recent study (Chelli *et al.*, 2001) demonstrated that the exposure of rat cardiac mitochondria to Ro5-4864, PK11195 or diazepam induced a cyclosporin A-sensitive swelling which is indicative of mitochondrial permeability transition. To further support the role of mitochondrial permeability transition in apoptosis this study also demonstrated that the supernatant of mitochondria that had undergone permeability transition was capable of inducing changes reminiscent of apoptosis in isolated cardiac nuclei. This demonstrated that pro-apoptotic proteins were released from the mitochondria during mitochondrial permeability transition.

Aberrant apoptosis signalling pathways have been linked to the development of various cancers. The expression of PBR is significantly up regulated in ovarian,

adenocarcinoma, hepatic and colonic carcinoma (Katz *et al.*, 1990; Venturini *et al.*, 1999). A recent study demonstrated that the resistance to CD95-induced apoptosis in four human tumour cells lines (T-cell Jurkat, neuroblastoma SHEP, osteosarcoma 143N2 and glioblastoma SNB79) can be reversed by R05-4864, PK11195 and diazepam (Decaudin *et al.*, 2002). This study also showed that cell death induced by these ligands could be associated with the release of cytochrome c and Smac/DIABLO from the mitochondria as well as the activation of caspase-3 and -9.

However, another study (Goldstein *et al.*, 2000) contradicts the MPTP model by showing that the release of cytochrome c precedes the drop in mitochondrial potential. This study confirms that mitochondrial depolarisation does occur during apoptosis; but that it is dependant on caspase activation and that it only occurs some time after cytochrome c has been released from the mitochondria.

1.5.1.2. Pore formation by Bax.

This model proposes that there is no damage to the outer mitochondrial membrane but that a pore is formed in this membrane that allows the passage of cytochrome c and other pro-apoptotic proteins. The NMR and X-ray structures of Bcl-x_L have demonstrated structural similarity of this protein to the pore forming bacterial toxin, diphtheria toxin (Muchmore *et al.*, 1996). Another member of the Bcl-2 protein family, Bax, was viewed as a good candidate as the protein that might be involved in the formation of such channels. It was demonstrated that in artificial

lipid membranes Bax oligomers were able to form large ion conductance channels (Schlesinger *et al.* 1997). The addition of Bax to isolated mitochondria triggers the release of cytochrome c. This mechanism does not involve mitochondrial swelling and cannot be blocked by permeability blockers. However, the size of cytochrome c is 11 kD and there is no evidence to suggest that Bax can form a multimeric structure big enough to accommodate such a large protein structure.

1.5.1.3. Bax opens VDAC.

This model proposes an interaction between Bax and VDAC that will lead to the formation of high-conductance channels. These channels are large enough to accommodate cytochrome c (Shimizu *et al.*, 1999). This can also be demonstrated in artificial membranes, however, evidence to support the existence these structures in mitochondria is still lacking.

In the absence of experimental evidence for the existence of channels described in the latter two models, the MPTP model appears to be the most likely explanation for the release of cytochrome c and other pro-apoptotic proteins from the mitochondria. This research will also provide more evidence in support of this model.

1.5.2. Proteins released from the mitochondria during apoptosis.

Permeabilisation of the outer mitochondrial membrane results in the release of soluble intermembrane pro-apoptotic proteins. These proteins include relatively small proteins such as cytochrome c (11 kD) and larger proteins such as adenylate kinase-2 (50 kD). Once released into the cytoplasm these proteins either activate apoptosis or amplify apoptosis by inhibiting anti-apoptotic proteins. These proteins and their functions are listed in Table 1.1.

Table 1.1. A summary of the proteins released from mitochondria during apoptosis.

Protein	Function	Reference
cytochrome c	Initiates caspase activation within the apoptosome	Liu *et al.*, 1996
adenylate kinase-2	Regulates cellular adenine and guanine nucleotide levels	Kohler *et al.*, 1999
Smac/Diablo	Binds to IAP (inhibitor of apoptosis protein) thereby disrupting the association of IAP with caspases and releasing the inhibitory effects of IAP	Ekert *et al.*, 2001; Yang *et al.*, 2000
Hsp 60, Hsp 10, caspase-2, -3 and -9	Function not clear, but it is proposed that the Hsp regulate the activation of the mitochondrial caspases, which when activated amplify the caspase cascade	Susin *et al.*, 1999a; Samali *et al.*, 1999; Krajewski *et al.*, 1999
AIF (apoptosis inducing factor)	Translocates to the nucleus during apoptosis to activate nucleosomal DNA fragmentation in a caspase-independent manner	Susin *et al.*, 1999b; Cande *et al.*, 2002
Endonuclease G	Induces caspase-independent nucleosomal DNA fragmentation	van Loo *et al.*, 2001
Endozepine/diazepam binding inhibitor	Unknown	Patterson *et al.*, 2000; van Loo *et al.*, 2002

The role of most of these proteins in apoptosis is well characterised, however although it has been reported that endozepine is also released from mitochondria during apoptosis, the role of this protein is not known. However, this research will demonstrate that reduced expression of this gene can be linked to a reduction in apoptosis.

1.6. The sphingomyelin signalling pathway.

The sphingolipid pathway is a signalling system conserved from yeast to human (Hannun, 1996; Ballou *et al.*, 1996). TNF-α, CD95, γ-interferon, interleukin–1, NGF (nerve growth factor), heat, radiation, dexamethasone, daunorubicin and vincristine are some of the factors demonstrated to activate this pathway (Hannun, 1996; Ballou *et al.*, 1996). The precise mechanism of activation of this pathway is not known but it is proposed that the DD of the adaptor proteins TRADD and FADD/MORT as well as caspase-8 might be involved in the activation of enzymes called sphingomyelinases, which catalyse the synthesis of ceramide. This stems from findings that suggested that defective sphingomyelin pathways maybe responsible for resistance to TNF-induced apoptosis in MCF7 breast cancer cells (Cai *et al.*, 1997). Ceramide, an sphingolipid derived second messenger molecule, is central to this pathway. Ceramides (N-acetylsphingosines) constitute the hydrophobic backbone of more complex sphingolipids such as sphingomyelin, cerebrosides and gangliosides. They can be synthesised either by the hydrolysis of sphingomyelin by sphingomyelinases, or by *de novo* synthesis by ceramide synthase. Both CD95 and TNFR1 have been shown to activate

sphingomyelinases (Cifone *et al.*, 1994). Ceramide is thought to play a role in cellular responses such as cell cycle arrest, cell differentiation and apoptosis (Spiegel and Merrill, 1996; Kolesnick and Hannun, 1999; Hannun and Luberto, 2000).

1.6.1. Sphingomyelinases.

Several isoforms of sphingomyelinases have been identified. These enzymes are differentiated based on their pH optima and sub-cellular localisation. The acid sphingomyelinases have been localised to structures such as the lysozymes and the caveolae (sphingomyelin rich plasma membrane microdomains) and have a pH optimum of about 4.5. This enzyme is synthesised as an inactive 75 kD precursor, which is processed into a 72 kD form and then to 70 kD and 57 kD forms. In response to cytokine stimulation, cells secrete the 70 kD and 57 kD forms. The precise role of the secreted forms of the acid sphingomyelinases is not clear. Deficiency of this enzyme leads to a lysosomal disorder, Niemann-Pick disease (NPD) (Otterbach and Stoffel, 1995). Alkaline sphingomyelinase activity has been demonstrated in the intestinal mucosa and the bile. One isoform of the neutral sphingomyelinases is a membrane bound, Mg^{2+}-dependent enzyme. Another isoform appears to be a cation independent cytosolic enzyme. The role of the acid sphingomyelinase in apoptosis is still a very controversial issue. However, acid sphingomyelinases have been implicated in the mechanism of action in apoptosis triggered by CD95L, irradiation or anthracyclines (Segui *et al.*, 2000). Most of these findings are based on the resistance of the NPD cell line

MS1418. However, other studies demonstrated that the thymocytes and T and B lymphocytes of acid sphingomyelinase-deficient mice was susceptible to apoptosis induced by CD95L which was accompanied by an increase in ceramide levels, suggesting that the acid sphingomyelinase is not required for apoptosis signalling (Segui *et al.*, 2000). The role of the neutral sphingomyelinases in apoptosis is well studied. NPD and normal lymphoid cells treated with daunorubicin demonstrated a ~30 % increase in cellular ceramide levels which was accompanied a ~30 % increase in neutral sphingomyelinase activity (Segui *et al.*, 2000).

1.6.2. *De novo* ceramide synthesis.

The endoplasmic reticulum is the site for the *de novo* synthesis of ceramide (illustrated in Figure 1.12). Condensation of serine and palmitoyl CoA, catalysed by the enzyme serine palmitoyl transferase, generates the formation of ketosphinganine (Perry and Hannun, 1998). Ketosphinganine reductase reduces the ketone group on ketosphinganine to yield sphinganine. N-acetylation of sphinganine by dihydroceramide synthase produces dihydroceramide. Finally ceramide is produced by the introduction of a double bond by the enzyme dihydroceramide desaturase.

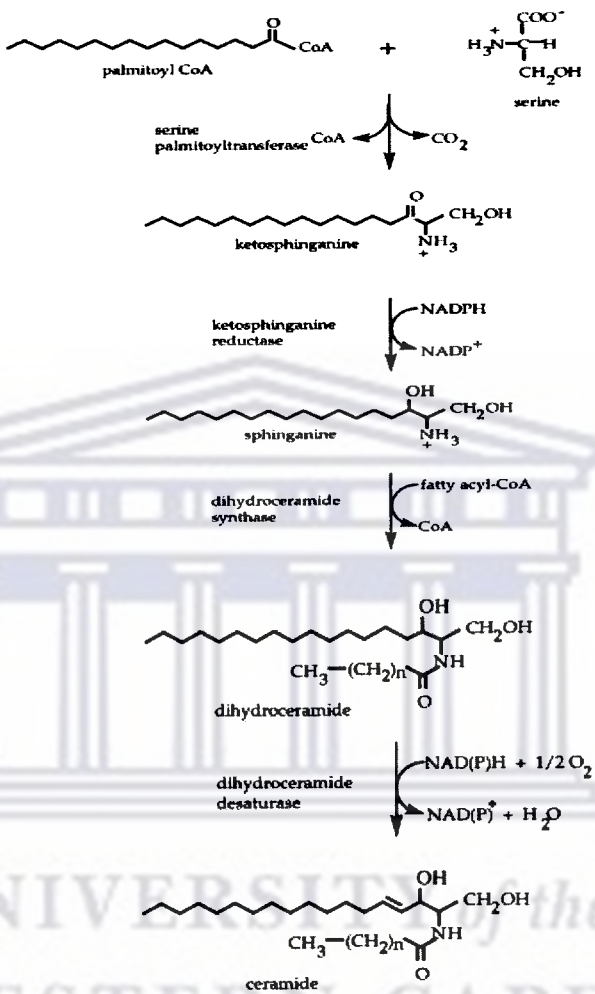

Figure 1.12. The synthesis of ceramide (from Perry and Hannun, 1998).

1.6.3. Ceramide metabolism.

Ceramide serves as a precursor for the synthesis of more complex sphingolipids and glycolipids in the Golgi apparatus (illustrated in Figure 1.13). Sphingomyelin synthase catalyses the transfer of phosphorylcholine groups from phosphatidylcholine to ceramide, resulting in the formation of sphingomyelin and diacylglycerol (DAG). Sphingomyelin synthase activity has been demonstrated in the endoplasmic reticulum, the Golgi apparatus and the plasma membrane.

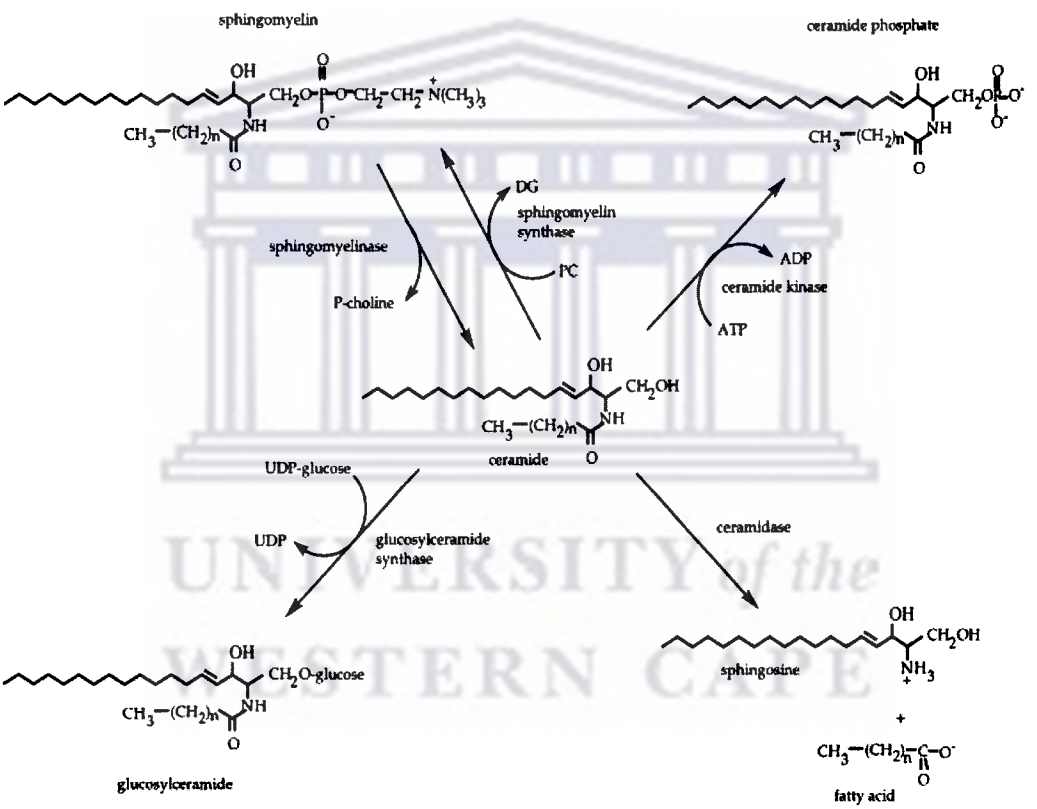

Figure 1.13. The catabolism of ceramide (from Perry and Hannun, 1998).

Ceramidases hydrolyse ceramide to generate free fatty acid and a sphingosine. Sphingosine can be re-incorporated into the synthesis of ceramide by ceramide synthase or it can be phosphorylated to sphingosine-1-phosphate (S1P) by

sphingosine kinase (SPHK) (Olivera and Spiegel, 2001). S1P is a potent mitogen and can reverse the apoptotic effects of ceramide. Three types of mammalian ceramidases have been identified. These enzymes are classified based on their pH optima and sub-cellular localisation. These enzymes also differ in terms of their substrate preference. Acid ceramidases are located in the lysozymes and mostly target long chain ceramides (Koch *et al.*, 1996). A mutation in this enzyme, results in the sphingolipid storage disorder called Farbers disease. Neutral/alkaline ceramidases are located in the lysozymes and preferentially use long chain ceramides (Tani *et al.*, 2000). Alkaline ceramidases hydrolyse phytoceramides and are found in the Golgi apparatus and the endoplasmic reticulum (Mao *et al.*, 2001). Phytoceramide is a constituent of major complex sphingolipids in lower organisms such as *S. cerevisiae*. Phytoceramides have also been identified in a variety of mammalian tissues and organs. The precise role of some ceramidases is still unknown, but it is proposed that ceramidases catalyse the breakdown of ceramide and may therefore play a role in balancing the opposing cellular signalling pathways activated by ceramide/sphingosine and S1P.

Ceramide also serve as a precursor for the synthesis of gangliosides. Gangliosides are mostly localised in the plasma membrane (76 %) and smaller portion are located in the mitochondria and endoplasmic reticulum (10 %) (Tomassini and Testi, 2002). Gangliosides are synthesised in the endoplasmic reticulum through the action of glycosyl transferases. The synthesis of gangliosides starts with the synthesis of glucoceramide by the action of the enzyme UDP-glucose glucosyltransferase. Glucoceramide is transferred to the endoplasmic reticulum

where it is converted to lactosylceramide by the addition of a galactose unit catalysed by galactosyl transferase. The stepwise addition of sugar groups to lactosylceramide leads to the synthesis of gangliosides (GM3, GD3 and GT3 (Maccioni *et al.*, 1999). There is also evidence to suggest that GD3 ganglioside activates the mitochondrial apoptotic pathway by the inducing mitochondrial permeability transition. GD3 was able to induce swelling in isolated mitochondria. This effect could be blocked by mitochondrial permeability transition inhibitors such as cyclosporin A, ADP and $MgCl_2$ (Petronilli *et al.*, 1994).

1.6.4. The role of ceramide in apoptosis.

Most of the evidence suggesting a role for ceramide in apoptosis comes from studies that show that changes in endogenous ceramide levels occur during the induction of apoptosis. Many inducers of apoptosis (e.g. Fas-ligands, ultraviolet radiation, growth factor withdrawal and chemotherapeutic agents) also induce the accumulation of ceramide in cells (Hannun, 1996; Mathias *et al.*, 1998). Furthermore, the addition of cell permeable analogues of ceramide (e.g. C_2-ceramide) to the culture medium induces apoptosis in cells in tissue culture (Obeid *et al.*, 1993; Jarvis *et al.*, 1994; Cifone *et al.*, 1994). Changes in endogenous levels of ceramide appear to precede the onset of the execution of apoptosis. Other studies demonstrated that the modulation of enzymes involved in ceramide synthesis affects the susceptibility of cells to apoptosis. Fumonisin B1 is an inhibitor of ceramide synthase. Treatment of cells with Fumonisin B1 blocks

ceramide synthesis and renders cells resistant to apoptosis induced by various stimuli (Bose *et al.*, 1995; Liao *et al.*, 1999; Lehtonen *et al.*, 1999; Xu *et al.*, 1998). Treatment of tumour cells with B13, a ceramidase inhibitor, leads to an increase in endogenous ceramide levels in these cells (Selzner *et al.*, 2001). This sensitises the cells to apoptosis. Knockout mice that lack acid sphingomyelinases are resistant to ionising radiation (Santana *et al.*, 1996). It has been demonstrated that ionising radiation induces marked increase in the production of ceramide in the lung tissue of wild type C3H/HeJ mice. This rise in ceramide levels was accompanied by a significant increase in apoptosis in this tissue. In contrast sphingomyelinase-deficient mice do not exhibit significant pulmonary apoptosis or increase in ceramide levels in response to ionising radiation. The over-expression of bacterial sphingomyelinase in mammalian cells leads to an increase in endogenous ceramide levels and consequent induction of apoptosis (Zhang *et al.*, 1997). It is also known that cells isolated from Niemann-Pick patients demonstrate resistance to apoptosis induced by γ-radiation and chemotherapy (Santana *et al.*, 1996), which could probably linked to aberrant ceramide metabolism.

The primary intracellular targets of ceramide are phosphatases and kinases. At this stage there is no direct link between ceramide and known apoptotic proteins. Ceramide-activated protein phosphatase (CAPP), a member of the 2A class of protein phosphatases (PP2A) has been identified as a target of ceramide (Dobrowsky and Hannun, 1992). PP2A has been shown to mediate ceramide-induced growth arrest in yeast (Fishbein *et al.*, 1993). This was confirmed with

knockout studies in yeast, which demonstrated that yeast which lack PP2A are resistant to ceramide-induced growth arrest. This enzyme has also been demonstrated to catalyse the dephosphorylation of protein kinase C-α with the consequent dephosphorylation and inactivation of Bcl-2. Protein phosphatase 1 (PP1) is also a possible target of ceramide. Inhibitors of both PP2A and PP1 are able to inhibit ceramide–induced caspase activation. PP2A has been reported to activate the transcription factor c-Jun (Reyes *et al.*, 1996), while both PP2A and PP1 can dephosphorylate the retinoblastoma gene product. The protein kinase, ceramide-activated kinase (CAPK) is also a target for ceramide (Mathias *et al.*, 1991). CAPK phosphorylates and Raf-1, which in turn phosphorylates and activates MEK leading to the activation of the MAP kinase cascade. However, it is still unclear how the above mentioned factors interact to induce/regulate apoptosis induced by ceramide or whether other as yet unidentified targets of ceramide play a more central role in ceramide induced apoptosis.

1.7. Genetic approaches used to identify genes involved in apoptosis.

1.7.1. Developmental genetic analysis.

Apoptosis is regulated by the expression of a multitude of proteins. A number of genetic approaches based on mutational analysis screens have shown to be powerful methods to study and identify novel genes involved in the regulation of apoptosis.

Genetic studies using the invertebrate models *C. elegans* and *Drosophila melanogaster* have been instrumental in identifying such genes. The development of the nematode worm *C. elegans* is very well characterised. During the development of these organisms, 131 cells out of a total of 1090 cells die by programmed cell death (Ellis *et al.*, 1991). Such detailed knowledge of the development of *C. elegans* which was possible because the animals are transparent and individual cells could be studied, provided researchers with a genetic model that could be used to study precisely how these cells die. Using mutational analysis screens three essential apoptosis genes; *CED-3*, *CED-4* and *CED-9* were discovered (Hengartner and Horvitz, 1994). This led to the identification of large gene families in mammals, representing homologues to the *C. elegans* genes. The *C. elegans* gene *EGL-1* is another example of a gene isolated from the invertebrate model that led to the identification of mammalian homologue, *Bcl-2* (Gross *et al.*, 1999). As a model system *D. melanogaster* offers the same advantages as *C. elegans* and has equally been useful in the identification of apoptosis genes such as Reaper, Grim and Hid, although no mammalian homologues of these genes have been identified yet (Verhagen and Vaux, 2002). The N-termini of these proteins interact with IAP and promote apoptosis by antagonising the IAP inhibition of caspases. The observation that mammalian IAPs can interact with Reaper, Grim and Hid suggest that mammalian IAP antagonists may exist.

A number of approaches have been used in addition to genetic screens in order to identify genes involved in apoptosis. These approaches included DNA microarray

technology, yeast two-hybrid technology, gene knockout technology and anti-sense technology.

1.7.2. DNA microarray technology.

DNA microarray is a technique that allows the researcher to study differential gene expression. Since induction of apoptosis requires up or down regulation of certain gene products this technique has been useful in the identification of genes that are differentially expressed during apoptosis. This technique relies on the principle of nucleic acid hybridisation (Watson *et al.*, 1998). For differential gene expression studies, cDNA "probes" (known sequences) are immobilised onto a solid support. "Targets" are made from RNA transcripts through reverse transcription, giving a mixture of cDNAs. During the reverse transcription process, a fluorescent dye is incorporated into the cDNA. Differential gene expression studies require that the cDNAs for the samples to be compared (e.g. untreated control versus the treated sample) be labelled with two different dyes with non-overlapping spectra. A mixture of the two fluorescent target populations is then hybridised to the immobilised cDNA "probes". Determining the ratio of fluorescence intensities of the two dyes after hybridisation is used to compare gene expression patterns. Microarrays have been used extensively comparing normal and malignant cells/tissue to identify genes that are differentially expressed (Frohme *et al.*, 2000). It also proved useful in the study of gene expression profiles in cultured cells during the activation of apoptosis signalling pathways (Alam and Gorska, 2001).

1.7.3. Yeast two-hybrid technology.

Another technique that has proved to be a useful tool for the identification of genes involved in apoptosis is the yeast two-hybrid system. Two-hybrid systems have been used to probe the interactions between two proteins (Chien *et al.*, 1991; Fields and Song, 1989). In this method one of the proteins is fused to a DNA-binding domain (the bait) while other the protein is fused to a transcriptional activation domain (the prey). Both fusion proteins are expressed in two different haploid yeast strains of opposite mating type (MATa and MATa). The two strains are mated and if the two proteins interact transcription of a reporter gene (e.g. gal-1-lacZ - the beta-galactosidase gene) is activated. A number of novel apoptotic proteins (e.g. Bok, Bad and Bod) belonging to Bcl-2 protein family have been identified using two-hybrid systems. The role of the p53 tumour suppressor gene in the induction of either cell growth arrest or apoptosis is well documented. The functions of a number of p53-related genes, such as p51/p63 and p73, have also been studied using yeast two-hybrid technology (Ikawa *et al.*, 1999). Yeast two-hybrid assays between p51 and p53, between p51 and p73, and between p51 and oncoproteins showed although both p51 and p53 proteins were induced in response to DNA-damaging treatment with UV and actinomycin D, that p51 is functionally rather distant from p53. A limitation of this technique is that it is not really a functional approach to gene discovery and that the demonstration of interaction between two proteins does not necessarily mean that these two proteins also interact under normal physiological conditions inside a cell. The genome of an organism is represented by the complete set of genes and the proteome represents all the proteins that can be synthesised using the genome as a

blueprint. The proteome can therefore be considered as the protein complement of the genome. However, it is more complicated than the genome because a single gene can be translated into several proteins by mechanisms such as alternative splicing. Thus, the set of proteins present in a cell can vary from one cell type to another and from one moment to the next due to changing physiological conditions. In view of these complications and the complexity of the networks in biochemical pathways, yeast two-hybrid technology should be regarded as the starting point for the analysis of protein-protein interactions and should therefore be used in combination with other techniques.

1.7.4. Gene knockout technology.

Gene knockout studies in mice and cultured cells have also been used successfully to either identify genes involved in apoptosis or to study their role in this process. It is especially the caspase knockout studies in mice that provided valuable information about the role these proteases play during apoptosis. Mouse model systems have the advantage over *C. elegans* and *D. melanogaster* model systems in that these organisms are genetically more closely related to humans making them better systems to study human physiology. For example, caspase-1 knockout mice demonstrated that this caspase is involved in the CD95 signalling pathway. These mice were able to develop normally with no abnormalities but thymocytes from these animals showed resistance to CD95-induced apoptosis. Mice lacking caspase-3 demonstrated marked developmental difficulties. These animals were smaller than the wild types and did not survive longer than three weeks after birth.

The thymocytes of the caspase-3 knockout mice did not express any abnormality in the CD95 signalling pathway but did show gross defects in the development of the central nervous system. A limitation of mouse knockout technology is that several mouse models can have phenotypes that are quite different from their human counterparts. The p53 knockout is a good example. The role of this gene in apoptosis has been well characterised and it has also implicated in as many as half of all human cancers. However, p53 knockout mice develop a different spectrum of tumours than humans do. In particular, mice develop lymphomas and sarcomas, whereas humans tend to develop epithelial cell-derived cancers. The mutant phenotypes are to some extent dependent on the strain background and the use of knockout mice as models of human disease is somewhat limited by these phenotypic differences.

1.7.5. Antisense technology.

Several strategies have been developed to knock out genes in cultured cell lines and these techniques were also used to generate knockout mice. Some of these techniques involve the use of anti-sense RNAs, ribozymes and retroviruses. Antisense technology is the process in which a synthetic antisense strand (3' to 5') targets and hybridises to a specific sense strand (5' to 3') (Helene and Toulme, 1990). The sense strand is the mRNA of a gene of interest and hybridisation of the antisense strand leads to loss of expression of the gene of interest. A DNA antisense molecule must be approximately seventeen bases in order to function, and approximately thirteen bases for an RNA molecule. RNA antisense strands

can be either catalytic, or non catalytic. Catalytic antisense strands, also called ribozymes, can cleave the RNA molecule at specific sequences, while a non-catalytic RNA antisense strand blocks further RNA processing. The exact mechanism of antisense strand knockouts has not been determined. A cell will recognize the double helix hybrid as foreign to the cell and proceed to degrade the mRNA molecule and thus prevent the expression of the protein of interest. The current hypotheses include blocking RNA splicing, accelerating degradation of the RNA molecule, preventing introns from being spliced out of the hnRNA, impeding the exportation of mRNA into the cytoplasm, hindering translation, and the triplex formation in DNA. Recent evidence suggests that antisense RNA may act by forming a double-stranded RNA with its mRNA target, the double-stranded RNA being a target for degradation, is cleaved every 21 to 23 nucleotides (Zamore *et al.*, 2000).

A variation on this technology is the technical knockout method (TKO) (Kimchi, 1998). This technique involves the random inactivation of genes expression by targeting RNA followed by the selection of mutants that have required resistance to apoptosis. Gene targeting was performed by a random transfection with antisense cDNA libraries and producing a large spectrum of antisense RNAs. The principle of this method is based on the fact that antisense RNA mediated inactivation of a pro-apoptotic gene will confer a growth advantage to such mutants when exposed to a cytokine that induces apoptosis. This technique was used successfully to identify five novel genes that mediate IFN-γ-induced apoptosis. A cDNA expression library was prepared from cells treated with IFN-γ.

HeLa cells were then transfected with this library and transfectants resistant to IFN-γ-induced apoptosis were selected. Characterisation of these transfectants led to the identification of novel pro-apoptotic protein family called death associated protein kinases (DAPk). DAPk is a calcium/calmodulin-regulated Ser/Thr kinase that promotes apoptosis by the phosphorylation of myosin light chain resulting in membrane blebbing and participates in apoptosis induced by INF-γ, TNF-α, TGF-β and detachment from extracellular matrix (Deiss and Kimchi, 1991; Cohen *et al.*, 1997). The DAPk also contains a DD at the 3' end, which shares homology with other DD-containing proteins such as the TNF receptor, Fas/APO-1 receptor, DR3-5, FADD/MORT-1, RIP, and TRADD (Darnell *et al.*, 1994). The overexpresssion of the wild type DAPk in HeLa cells reduced the viability of the cells. In contrast the transfections with catalytically inactive kinase resulted in loss of the death inducing activity, which suggested that the induction of apoptosis is dependent on the kinase activity (Cohen *et al.*, 1997). Genes that promote apoptosis may be lost or down regulated in tumours as is the case with the tumour suppressor gene *p53*. It was demonstrated that the mRNA and protein expression levels of DAPk was below detectable levels in 70 % of B-cell lymphoma and leukaemia cell lines and in 30 % of cell lines derived from bladder carcinomas, breast carcinomas and renal cell carcinoma (Kissil *et al.*, 1997). In contrast DAPk mRNA is expressed in human and murine tissues (Kimchi, 1998). Four additional kinases that share significant homology with that catalytic domain of DAPk have also been identified. These include ZIP (D1k)-kinase, DRP-1, DRAK1 and DRAK2 (Inbal *et al.*, 2000). ZIP (D1k)-kinase and DRP-1 is closely related to DAPk showing approximately 80 % identity to the catalytic domain of

DAPk, while DRAK1 and DRAK2 are more distant DAPk-related proteins (Shohat *et al.* 2002). These proteins differ considerably in their extracatalytic domain and cellular localisation, with ZIP (D1k)-kinase, DRAK1 and DRAK2 located in the nucleus and also do not require calcium/calmodulin for activation. DRP-1 is a cytoplasmic protein and contains a calcium/calmodulin-regulatory domain similar to DAPk (Inbal *et al.*, 200; Shani *et al.*, 2001).

The success of antisense technology is based on reduced production of a protein of interest. However, there are a number of complications with this technology. Firstly there is the problem with getting antisense molecules into cells without the cell degrading the molecules even before they have started to reduce the expression of the protein of interest. Secondly, target specificity is a major drawback in the use of antisense to knock out genes. Antisense strategies rely on the binding of a 17 base pair antisense molecule, through Watson-Crick base paring, to the mRNA of a single gene. To achieve this sort of accuracy inside a cell is very rare. To knock out a single gene, the 17 base pair molecule should be able to recognise and bind to a target with a 17 base pair match. A single mismatch can lead to the undesired degradation of bystander mRNAs and consequently affect the expression of genes other than the target. Although the mechanism of antisense technology is not fully understood yet, there is evidence to suggest that to achieve degradation of DNA/RNA hybrid molecules, only 4 to 6 bases are required. It has also been demonstrated that antisense molecules have a high affinity for proteins and therefore accessibility to the target mRNA can also pose another obstacle. Target recognition by ribozymes also depends on Watson-

Crick base paring and therefore the same limitations apply to the use of ribozymes to knock out genes.

An improvement on this technology is RNAi (RNA interference), which refers to the introduction of homologous double stranded RNA (dsRNA) to specifically target a gene's product resulting in either reduced expression or loss of expression. RNAi was first observed in *C. elegans* as a response to dsRNA that resulted in sequence-specific gene silencing (Fire *et al.*, 1998). In this technique dsRNA rather than single-stranded antisense RNA is used as the interfering agent. The use of RNAi appears to be more specific than single-stranded antisense RNA and it requires only a few dsRNA molecules per cell to be effective. The mechanism of RNAi is still not well understood but it is suggested that the primary interference effects are post-transcriptional. It was observed that only dsRNA targeting exon sequences was effective and that dsRNA targeting promoter and intron sequences could not produce an RNAi effect (Fire *et al.* 1998; Montgomery *et al.*, 1998). The DNA sequence of targeted genes appears to be unaltered, initiation and elongation of transcription appears to be unaffected and nascent transcripts can be detected but are apparently degraded before leaving the nucleus which suggests that the mature message is the most likely target of RNA-mediated interference. RNAi provide a simple but powerful technique for the identification of genes that can be associated with specific phenotypes and has been useful in the identification of genes involved in apoptosis: Using RNAi technology seven additional cell death-related nucleases (crn genes) have been identified from *C. elegans* (Parrish and Xue, 2003). This technology also led to

the identification of a Parkin-like ubiquitin ligase (Parc) that acts as a cytoplasmic anchor protein for p53-associated protein complexes (Nikolaev *et al.*, 2003). The tumour suppressor function of p53 is dependent on its translocation to the nucleus. Parc regulates p53-induced apoptosis through the formation of a complex with p53, thus preventing it from translocating from the cytoplasm to the nucleus and hence apoptosis is blocked. RNAi reduction of Parc expression in neuroblastoma cells demonstrated that the mutants are more sensitive to apoptosis (Nikolaev *et al.*, 2003).

1.8. The use of retroviruses as insertional mutagens.

Retroviruses are RNA viruses; i.e. they contain an RNA genome that replicates through a DNA intermediate. These viruses are able to attach to host cells with the aid of cell surface receptors that are recognised by viral envelope proteins and they enter their host through receptor-mediated endocytosis (Varmus, 1988).

The retrovirus life cycle includes reverse transcription of the viral genome into DNA, integration of the viral DNA into the host chromosome and the utilisation of the host mechanisms for the expression of the viral genes. During synthesis of viral DNA, the sequences near the ends of the viral RNA (U3 and U5) are duplicated to generate long terminal repeats (LTRs). The LTRs include promoter/enhancer regions and sequences involved with integration. The viral genome contains at least three genes: gag (coding for core proteins), pol (coding for reverse transcriptase) and env (coding for the viral envelope protein). In

addition, there are sequences required for packaging the viral DNA (psi) and RNA splice sites in the *env* gene. Figure 1.14 illustrates a diagrammatic representation of the viral gene structure.

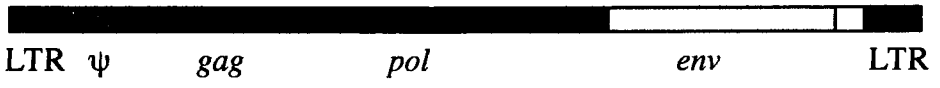

Figure 1.14. The genomic structure of retroviruses.

Since the life cycle of the retrovirus involves integration of viral DNA into different sites on the host chromosome, they can act as insertion mutagens. The insertion of viral DNA can affect the expression of nearby host genes. Retroviruses are known to cause cancers by transforming cells when the retrovirus inserts close to tumour suppressor or proto-oncogenes. Retroviral promoters in the LTR can down regulate the expression of tumour suppressor genes or up regulate proto-oncogenes leading to the development of cancer. The α1-collagen I gene is an example of a gene that was inactivated by viral insertion. (Schnieke *et al*, 1983). This characteristic of retroviruses has been exploited to develop viral vectors, which can be used to introduce mutations in cultured cells. Most of these viral vectors are based on the Moloney murine leukaemia virus (MoMLV). All the nonessential viral genes have been removed and replaced by a transgene, which normally carries a selectable marker gene such as neomycin or β-galactosidase, which allowed for the selection of transformed cells. The only DNA sequences that are required so that the virus maintains its capacity to act as an insertional mutagen are the 5' and 3' LTRs and the packaging sequences.

The use of retroviruses as insertion mutagens in mammalian cultured cells and as probes in the molecular cloning of mutant genes requires that proviral insertion be nearly random, that the mutant phenotypes be recognised easily and that the insertion-induced mutations occur at a higher rate than spontaneous mutations (King *et al.*, 1985). The biological and genetic behaviour of retroviruses make them attractive tools for use as insertional mutagens to isolate genes responsible for phenotypes in mammalian cells. However, retroviral insertional mutagenesis is very inefficient, as evidenced by the fact that between 5×10^6 and 10^8 integration events are required to disrupt single copy cellular genes (Varmus *et al.*, 1981; Frankel *et al.*, 1985; King *et al.*, 1985). These difficulties may be attributed to the size of the genome and are further complicated by the diploid nature of the genome.

A number of strategies have been used to increase the efficiency of retroviral insertional mutagenesis. Retroviral vectors were developed that confer selectable phenotypes when the virus integrates into expressed genes. The Moloney murine leukaemia derived virus, tkneoU3hygro, is a promoter-trap retroviral vector developed for this purpose (von Melchner and Ruley, 1989). It contains a neomycin resistance (*tk*-neo) gene expressed from the Herpes simplex viral thymidine kinase (*tk*) promoter in place of the retroviral *gag/pol* genes and a promoterless bacterial antibiotic resistance gene, hygromycin B phosphotransferase ($Hygro^R$), inserted into the U3 region of a replication defective Moloney murine leukaemia virus (illustrated in Figure 1.15).

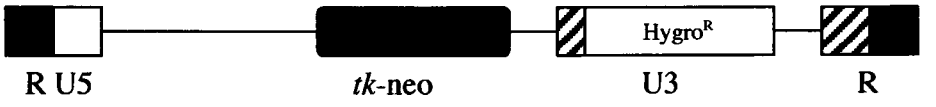

Figure 1.15. The structure of the Moloney murine leukaemia virus (MoMLV), tkneoU3hygro.

The *tk*-neo gene acts as a selectable marker for retroviral insertion, while the Hygro^R gene acts as selectable marker. The *tk-neo* gene constitutively expressed following retroviral insertion, while the Hygro^R gene can only be expressed if retroviral insertion is downstream of a host promoter. This greatly improved the efficiency of insertional mutagenesis and reduced the number of required integration events needed to disrupt single copy genes from the order of 10^6 to 10^4 (Chang *et al.*, 1993). In this study the gene encoding the enzyme UDP-GlcNAc: α-3-D-mannoside β-1, 2-N-acetylglucosaminyl transferase I, was disrupted by retroviral insertion. CHO cells lacking this enzyme are still viable and since these cells lose the expression of this gene spontaneously at a frequency of 10^5, it also suggest that it is functionally hemizygous (Stanley, 1981; Stanley and Chaney, 1985). These mutants were selected on media containing wheat germ agglutinin. This study demonstrated that ~1×10^5 events (equivalent to the number of genes in the mammalian genome) are required to disrupt the expression of a single copy gene (Chang *et al.*, 1993).

The use of Chinese hamster ovary (CHO) cells as targets for mutagenesis also increased the efficiency of retroviral insertional mutagenesis. These cells are

functionally hemizygous at a number of genetic loci (Siminovitch, 1985). CHO cell lines have been developed for use in retroviral mutagenesis. CHO22 is a clone of CHO that expresses the murine ecotropic retroviral receptor. This clone has been isolated by co-transfection with a murine ecotropic retroviral receptor (Albritton *et al.*, 1989) using pSV2*gpt* as the selectable marker (Hubbard *et al.*, 1994). These cells are susceptible to infection by the Moloney murine leukaemia virus because they express murine ecotropic retroviral receptor. These cells were used in a study (Hubbard *et al.*, 1994), which demonstrated that retroviral insertional mutagenesis could be used to generate CHO mutants which were resistant wheat germ agglutinin and express a phenotype not previously observed in mutants which resulted from spontaneous mutations. Sequence analysis of four such mutants revealed retroviral insertion into four distinct positions spanning a 796 bp region of the CHO genome conferred resistance to wheat germ agglutinin. This implied that a single gene could be targeted. This study also illustrated that the use of gene trap retroviruses together with pseudohaploid CHO cells could potentially provide a model system for the isolation of genes involved in various biochemical pathways.

The Moloney murine leukaemia virus, tkneoU3hygro was also used for the isolation of mutants resistant to cytotoxic T lymphocyte (CTL) killing (George, 1995). The Major Histocompatibility Complex (MHC) Class I restricted $CD8^+$ CTLs play a key role in the immune response to viral infections. In this study the CHO clone, Y10 which was derived from CHO22, was used as a target cell line for mutagenesis using the tkneoU3hygro retrovirus. Y10 was generated by

transfection with plasmids expressing leader minus influenza haemagglutinin (L-HA) and MHC class I K^K genes. The consequence of this was that Y10 cells expressing these two genes were shown to be susceptible to CTL killing and thus provided a model system for the identification of genes involved in antigen presentation and processing and T cell induced apoptosis, since mutagenesis of these genes would result in resistance to CTL killing. This led to the identification of a novel protein, DWNN (**D**omain **W**ith **N**o **N**ame), which is thought to play a role in apoptosis (Skepu, Ndabambi, Seameco, Pretorius, George, Pugh, Rees; unpublished data). This research demonstrated that promoter-trap mutagenesis could be used to select for mutants that are resistant to apoptosis.

1.9. The aims of this research.

Apoptosis is executed and regulated by the expression of a multitude of genes. Functional genetic approaches have proven to be extremely powerful methods to study and identify the genes involved in apoptosis. The objective of this study was to randomly inactivate genes in CHO22 cells using insertional mutagenesis and to then select for mutants that were resistant to apoptosis induced by chemical agents (such as ceramide) known to induce apoptosis in CHO22 cells. Characterisation of such mutants would either reiterate the involvement of known apoptotic genes or lead to the identification of novel apoptotic genes or implicate the involvement of known genes (i.e. genes not previously linked to apoptosis) in apoptosis. There is strong evidence to suggest that aberrant regulation of apoptosis can be linked to the development of cancer. The generation of well-characterised mutants that are

resistant to apoptosis can potentially provide useful tools to study the action and efficiency of known or novel drugs directed against cancer. The identification of such genes would also provide novel targets for drug development to treat diseases such as cancer.

CHAPTER 2: MATERIALS AND METHODS.

2.15. Amplification of DNA by PCR.

2.16. Inverse PCR amplification of DNA.

2.17. Gel electrophoresis of DNA.

2.17.1. Agarose gel electrophoresis.

2.17.2. Acrylamide gel electrophoresis.

2.18. Purification of DNA fragments.

2.18.1. Agarose gels.

2.18.2. Polyacrylamide gels.

2.19. Cloning PCR fragments into pGEM®-T easy.

2.20. Colony PCR.

2.21. Sequence analysis.

2.22. Isolation of mitochondria from cultured cells.

2.23. Isolation of proteins from cultured cells.

2.24. SDS-polyacrylamide gel electrophoresis (SDS-PAGE).

2.24.1. One-dimensional SDS-PAGE.

2.24.2. Two-dimensional (2-D) SDS-PAGE.

2.25. The expression and purification of recombinant GST fusion proteins.

2.25.1. Screening for the expression and solubility of fusion proteins.

2.25.2. Large-scale expression of fusion proteins.

2.25.3. Purification of fusion proteins.

2.26. The generation of polyclonal anti-rabbit antibodies.

2.27. Affinity purification of antibodies.

2.28. Western blotting.

2.29. Apoptosis assays.

2.29.1. Screening the effects of DMSO on CHO22 cells.

2.29.2. The screening of C_2-ceramide and camptothecin as inducers of apoptosis.

2.29.3. DNA fragmentation assay.

2.29.4. LDH release assay.

2.29.5. APOPercentage™ assay.

2.29.6. Caspase-3 assay.

2.29.7. Mitochondrial depolarisation assay.

2.30. Fluorescence microscopy.

2.31. Primers used.

CHAPTER 2: MATERIALS AND METHODS.

2.1. General chemicals and enzymes.

40 % 19:1 Acrylamide:bis-acrylamide	Biorad
40 % 37.5:1 Acrylamide:bis-acrylamide	Biorad
Agarose	Promega
Ammonium persulphate	Merck
Ampicillin	Roche
Bacteriological agar	Merck
Boric acid	Merck
Bovine serum albumin	Roche
Bromophenol blue	Sigma
Buffer saturated phenol	Invitrogen
Camptothecin	Roche
CHAPS (3-[3-cholamidopropyl]-dimethyl-lammonlol-1-propanesulphonate)	Amersham Pharmacia
Chloroform	BDH
Coomassie Brilliant Blue R 250	Sigma
Crystal violet	Sigma
DAPI (4', 6'-diamidino-2-phenylindole)	Sigma
DMSO (Dimethyl sulphoxide)	Sigma
Donkey anti-rabbit IgG-Rhodamine	Santa Cruz Biotechnology
DTT (Dithiothreitol)	Roche

EDTA (Ethylene diamine tetra acetic acid)	Merck
EGTA ethylene glycol-bis (β-aminoethyl ether)	
- N, N, N', N'-tetra acetic acid	Sigma
Ethanol	BDH
Ethidium bromide	Promega
G-418 (neomycin sulphate)	ICN Biochemicals
Glacial acetic acid	Merck
Glucose	BDH
Glutathione	Sigma
Glycine	BDH
HEPES (*N*-[2-hydroxyethyl] piperazine-*N*'-	
[ethane sulphonic acid])	Sigma
Hydrochloric acid	Merck
IPTG (Isopropyl β-D-thiogalactopyranoside)	Promega
JC-1 (5, 5', 6, 6'-tetrachloro-1, 1', 3, 3',-	
Tetra ethylbenzimidazolocarbocyanine iodide)	Molecular Probes
Methanol	Merck
MOPS (4-Morpholine propanesulphonic acid)	Roche
N-Acetyl-D-sphingosine (C_2-ceramide)	Sigma
Paraformaldehyde	Sigma
Pharmalyte ™ 3-10	Amersham Pharmacia
PMSF (phenylmethylsulphonyl fluoride)	Roche
Ponceau S	Sigma
Premixed Protein markers	Roche

Proteinase K	Roche
PVDF (Polyvinylidene difluoride)membrane	Amersham Pharmacia
SDS (Sodium dodecyl sulphate)	Promega
Sodium azide	Roche
Sodium hydroxide	Merck
TEMED (*N*, *N*, *N'*, *N'*-Tetra methylethylene-diamine)	Promega
Tris (Tris[hydroxymethyl] aminoethane)	BDH
Triton X-100 (iso-octylphenoxypoly-ethoxyethanol)	Roche
Tryptone	Merck
Tween 20 (Polyoxyethylene [20] sorbitan)	Merck
Urea	Amersham Pharmacia
Xylene cyanol	BDH
Yeast extract	Merck

The chemicals used were of AnalaR or equivalent grade. Restriction endonucleases were supplied by New England Biolabs or Roche Diagnostics. T4 DNA ligase was obtained from Promega. *Taq* DNA polymerase was obtained from Takara Biotechnology.

Biochemical Assay kits used:

1). LDH (lactate dehydrogenase) release assay or Cytotoxicity Detection Kit (Roche).

2). APOPercentage™ Apoptosis assay (Biocolor Ltd)

3). Active Caspase-3 FITC Mab Apoptosis Kit (BD Biosciences).

2.2. General stock solutions and buffers.

10× TAE: 0.4 M Tris-acetate and 0.01 M EDTA, pH 8.

10× TBE: 0.9 M Tris, 0.89 M boric acid and 25 mM EDTA, pH 8.3. This stock solution was diluted 10 fold for the electrophoresis of agarose and polyacrylamide gels.

4× Stacking gel Buffer: 0.5 M Tris-HCl, pH 6.8.

5× SDS Electrophoresis Buffer: 25 mM Tris, 0.1 % SDS and 250 mM glycine, pH 8.3.

5× Sequencing Buffer: 1 M Tris-HCl and 25 mM $MgCl_2$. This buffer was stored at –20 °C and used at 2.5× concentrate when needed.

6× Glycerol BPB Gel-loading Buffer: 30 % glycerol, 0.25 % Bromophenol blue and 0.25 % Xylene cyanol.

8× Separating gel Buffer: 3 M Tris-HCl, pH 8.8. This buffer was stored at 4 °C.

Agarose Sealing Solution: 0.5 % agarose and 0.002 % bromophenol blue in 1× SDS Electrophoresis Buffer.

Ammonium persulphate: A 10 % stock solution was prepared in deionised water. This solution was stored at 4 °C.

Ampicillin: A 50 mg/ml stock solution was prepared in deionised water. This solution was filter sterilised using a 0.22 micron filter and stored at – 20 °C.

Bradford dye: 100 mg Coomassie Brilliant Blue G 250, 50 % concentrated phosphoric acid and 25 % ethanol. This solution was kept at 4 °C. The Bradford dye was diluted 5 times in deionised water before use.

C_2-ceramide Stock Solution: A 120 mM stock solution was prepared in DMSO. The stock solution was used to prepare a working stock solution at 1 mM in complete Ham's F12 medium. This solution was aliquoted and stored at – 20 °C.

Camptothecin Stock Solution: A 10 mg/ml stock solution was prepared in DMSO. This solution was stored at – 20 °C.

Coomassie Staining Solution: 0.25 g Coomassie Brilliant Blue R 250, 45 % methanol and 5 % acetic acid.

Destain Solution: 30 % methanol and 10 % acetic acid.

Digestion Buffer: 100 mM NaCl, 10 mM Tris-HCl; pH 8, 25 mM EDTA; pH 8, and 0.5 % SDS. Proteinase K (to a final concentration of 0.1 mg/ml) was added just before use.

DNA Elution Buffer: 0.5 M ammonium acetate, 10 mM magnesium acetate and 1 mM EDTA (pH 8 with NaOH). Stored covered in the dark at room temperature.

DTT: A 1 M stock solution was prepared in 0.0 1M Sodium acetate, pH 5.2. This solution was sterilised by filtration, aliquoted and stored at – 20 °C.

GTE: 50 mM Glucose, 50 mM Tris-HCl and 10 mM EDTA, pH 8.0.

IPTG: A 1 M stock solution was prepared in deionised water. The solution was sterilised by filtration; divided into aliquots and stored at – 20 °C.

JC-1 Stock Solution: A 5 mg/ml stock solution was prepared in DMSO.

L Agar: 10 g/l Tryptone, 5 g/l Yeast extract, 5 g/l NaCl and 14 g/l Bacteriological agar.

L Broth: 10 g/l Tryptone, 5 g/l Yeast extract and 5 g/l NaCl.

Lysis Buffer: PBS containing 1 % Triton X-100.

Lysis Solution: 200 mM NaOH and 1 % SDS.

Mitochondrial Isolation Buffer: 220 mM mannitol, 68 mM sucrose, 10 mM KCl, 1 mM EGTA, 1 mM EDTA, 0.1 % BSA, 0.01 mM DTT, 0.1 mM PMSF and 10 mM HEPES-KOH, pH 7.4.

Mitochondrial Resuspension Buffer: 200 mM mannitol, 50 mM sucrose, 10 mM succinate, 0.1 % BSA, 5 mM potassium phosphate and 10 mM HEPES-KOH, pH 7.4.

MitoTracker Green FM Stock Solution: A 1 mM stock solution was prepared in DMSO.

Neutralisation Solution: 3 M potassium acetate, pH 5.

Paraformaldehyde Fixative: 16 g paraformaldehyde was dissolved in 80 ml deionised water by stirring at 70 °C (in fume cupboard). One drop of 2 M NaOH was added. The solution was cooled down to room temperature and the volume adjusted to 100 ml with deionised water. This solution was filter sterilised through a 0.45 micron filter and a 100 ml 2× PBS added. The paraformaldehyde solution was aliquoted and stored at – 20 °C.

PBS: 137 mM NaCl, 2.7 mM KCl, 8 mM Na_2HPO_4 and 1.5 mM KH_2PO_4, pH 7.4.

Phenol:chloroform:isoamyl alcohol: 25 parts Tris-saturated phenol, 24 parts chloroform and 1 part isoamyl alcohol.

PMSF: A 10 mM stock solution was prepared in isopropanol. The solution was aliquoted and stored at – 20 °C.

Protein Elution Buffer: 10 mM glutathione and 50 mM Tris-HCl, pH 8.0.

Rehydration Stock Solution: 8 M Urea, 4 % CHAPS, 2% Pharmalyte™ 3-10 and 0.002 % bromophenol blue.

RNAse (DNase free): A 20 mg/ml stock solution was prepared in a buffer containing 0.1 M sodium acetate and 0.3 mM EDTA (pH 4.8, with acetic acid). This solution was boiled for 15 min and cooled quickly by placing it in ice water, dispensed into aliquots and stored at – 20 °C.

SDS Equilibration Buffer: 6 M urea, 30 % glycerol, 2 % SDS, 0.002 % bromophenol blue and 50 mM Tris-HCl, pH 8.8,

TBS: 20 mM Tris-HCl and 150 mM NaCl, pH 7.4.

TBS-MT: 5 % Low fat dried milk powder and 0.1 % Tween 20 in TBS.

TBS-T: 0.1 % Tween 20 in TBS.

TE: 10 mM Tris-HCl and 1 mM EDTA, pH 7.4.

Tfb1 Buffer: 30 mM Potassium acetate, 50 mM $MnCl_2$, 0.1 M KCl, 6.7 mM $CaCl_2$ and 15 % glycerol (v/v).

Tfb2 Buffer: 9 mM MOPS, 50 mM $CaCl_2$, 10 mM KCl and 15 % glycerol (v/v).

Transfer Buffer: 25 mM Tris, 192 mM glycine and 20 % methanol.

TTE: TE buffer, containing 1 % Triton X-100.

Turks reagent: 0.02 g of crystal violet and 7.2 % glacial acetic acid.

TYM Broth: 20 g/l Tryptone, 5 g/l Yeast extract, 3.5 g/l NaCl and 2 g/ $MgCl_2$.

2.3. Tissue culture media.

The following tissue culture medium and supplements were supplied by Invitrogen: Dulbecco's modified medium (DMEM), nutrient mixture Ham's F12, 100× penicillin-streptomycin, Foetal calf serum (FCS), G418-sulphate, 50× HAT (680 μg/ml hypoxanthine, 9 μg/ml aminopterin, 195 μg/ml thymidine).

Additional supplements were obtained from the following sources:

Mycophenolic acid (Sigma) - made up as a 100× stock by dissolving 25 mg/ml in 0.1 M NaOH. If some mycophenolic acid failed to dissolve 1 M NaOH was added drop-wise. Stock solution was stored at – 20 °C.

Sodium xanthine (Sigma) - made up as a 20× stock-solution by dissolving 2.8 g/l in deionised water with heating slowly to 37 °C. Stock solution was stored at – 20 °C.

Puromycin dihydrochloride (ICN Pharmaceuticals) - diluted in distilled water to a concentration of 1.2 mg/ml and used as 100× stock solution. Stock solution was stored at – 20 °C.

Polybrene (Sigma) - made to a concentration of 0.8 mg/ml with PBS, filter sterilised and used as 100× stock.

Hygromycin B (Roche Diagnostics) - used at 0.6 mM concentration by adding it directly to the growth medium.

2.4. Cell culture.

The cell lines used were as follows: CHO22 and Ψ8tkneoU3hygro. CHO22 is a clone of CHO, which was derived from CHO-K1. The Moloney murine leukaemia virus (MoMuLV) murine ecotropic receptor was previously cloned into an expression vector, pJET (Albritton *et al.*, 1989). CHO22 was isolated by co-transfection of CHO-K1 with pJET and pSV2gp*t* (Hubbard *et al.*, 1994). Clones expressing the xanthine-guanine phosphoribosyltransferase were selected in a *gpt* selective medium. The resistant clones were tested for the expression of the murine ecotropic retroviral receptor. CHO22 was isolated as one of the clones expressing this receptor. The media used to culture the cell lines are shown in Table 2.1.

Table 2.1. Cell lines used in this thesis.

Species	Cell Line	Medium	Serum	Supplements
Mouse	ψ8tkneoU3hygro	DMEM	10 % FCS	None
Hamster	CHO22	Ham's F12	5 % FCS	*gpt* selection-25 mg/ml Mycophenolic acid, 0.143 mg/ml sodium xanthine, 1× HAT

Complete Ham's F12 = Ham's F12 + L-glutamine + penicillin-streptomycin + 5 % FCS.

Complete DMEM = DMEM + L-glutamine + penicillin-streptomycin + 10 % FCS.

Both these cell lines are adherent and were maintained in an incubator at 37 °C in an atmosphere of 5 % CO_2. Cells were removed for passage using 0.125 % trypsin (Invitrogen). Cell counts were performed by diluting the cell suspension two fold with a solution of Turks reagent and then viewed and counted under a Nikon inverted light microscope using a Neubauer haemocytometer cell counting chamber.

Freezing of cells was carried out, as required, when cells approached confluency. Cells were washed with PBS and then incubated for 10 min with 5 ml 0.125 % trypsin. Trypsinisation was stopped by the addition of 1 ml complete Ham's F12 medium and the cells were recovered by centrifugation for 2 min at 200× *g* in a bench-top centrifuge The cell pellet was re-suspended in a solution of 90 % FCS and 10 % DMSO, dispensed into 1 ml aliquots in cryo-vials prior to freezing at –150 °C.

2.5. Sub-cloning of cells using cloning rings.

Cells were seeded at low cell density (1000, 100, 10 cells/flask) in 75 cm^2 flasks. Cells were cultured until colonies were visible on the bottom of the flask. The positions of the clones were marked on the flask. The growth medium was removed and the cells washed with sterile PBS. The top of the flask was removed using a hot wire. Sterile ceramic cloning rings were positioned over the clones and fixed to the bottom of the flask using sterile vacuum grease. The cells isolated by the cloning ring were removed using 100 µl of 0.125 % trypsin. The cells were

transferred to a 96 well tissue culture plate and cultured in Ham's F12 until confluent. The cells were sub-cultured into a 24 well tissue culture plate and then transferred to a 25 cm^2 tissue culture flask. Stocks of these cell lines were prepared and stored at –150 °C.

2.6. Promoter-trap mutagenesis using MoMLV tkneoU3hygro retrovirus .

2.6.1. Harvesting of MoMLV tkneoU3hygro retrovirus.

The retroviral producer cells, Ψ8tkneoU3hygro, were seeded in 75 cm^2 flasks and maintained in the complete DMEM growth medium, described in Table 2.1. To harvest the secreted virus, the growth medium was removed when the flask reached a 50 % confluence and replaced with 25 ml complete DMEM. The cells were cultured for a further 48 hrs at 37 °C in an atmosphere of 5 % CO_2. The retrovirus-containing medium was removed and the retroviral particles recovered by filtering the supernatant through a 0.45 micron sterile filter to remove any dead cells. Polybrene was added to the retroviral stock to a final concentration of 8 μg/ml and this mixture was either used immediately as an infectious retroviral stock or stored at –150 °C after freezing it rapidly in liquid nitrogen.

2.6.2. Promoter-trap mutagenesis.

CHO22 cells were maintained in *gpt* selective medium (Table 2.1) for two weeks before being infected with the retrovirus. The flow diagram in Figure 2.1 shows the general scheme of promoter-trap mutagenesis.

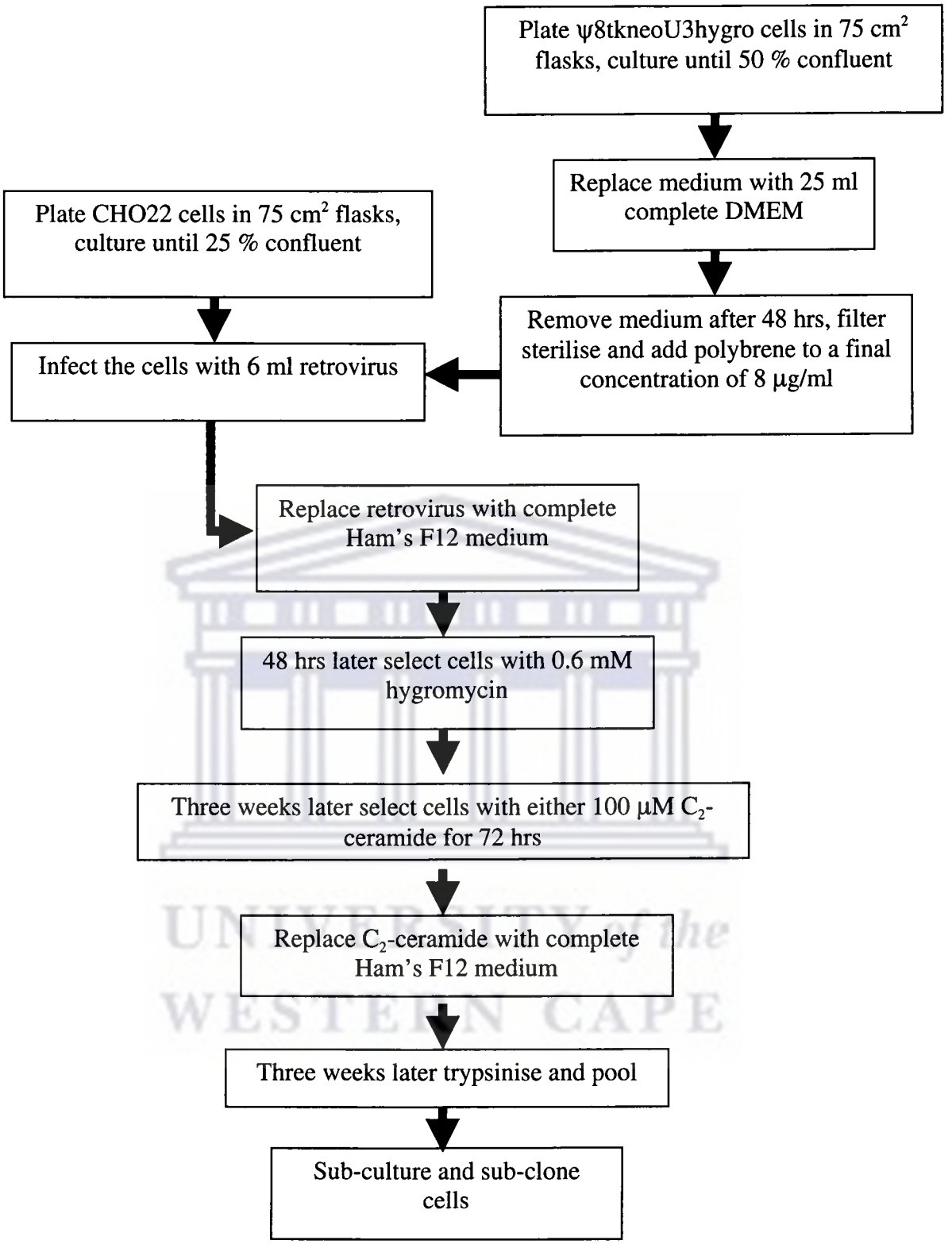

Figure 2.1. Schematic representation of promoter-trap mutagenesis of CHO22 cell using C_2-ceramide.

CHO22 cells were plated and cultured in 75 cm^2 tissue culture flasks until a cell density of 2×10^6 cells (~25 % confluent) was reached. Some of these flasks represented control experiments to test the efficiency of the promoter-trapping. These controls included combinations of +/– retrovirus, +/– hygromycin B and +/– C_2-ceramide.

The media in the + retrovirus flasks were replaced with 6 ml retroviral stock. The cells were cultured for a further 6 hrs. After 6 hrs the medium containing the virus was removed and replaced with fresh medium. The cells were cultured for a further 48 hrs followed by a selection in 0.6 mM hygromycin. After three weeks the cells were selected with 100 mM C_2-ceramide for 72 hrs. After 72 hrs the C_2-ceramide was replaced with fresh media and cultured for a further three weeks with regular media changes. After three weeks the cells were removed by trypsinisation, sub-cultured and sub-cloned as described in Section 2.5.

2.7. Isolation of genomic DNA from tissue culture cells.

Cells were cultured in 25 cm^2 tissue culture flasks until confluent. Cells were washed with ice-cold PBS and 1 ml Digestion Buffer was added. The flasks were incubated overnight with gentle shaking at 37 °C. The cell suspension was removed and an equal volume of phenol:chloroform:isoamyl alcohol was added and the samples were mixed briefly before centrifugation at 10 000× *g* for 5 min in a microfuge. The aqueous (top) layer was transferred to a new tube and the DNA precipitated by the addition of half volume of 7.5 M ammonium acetate and

two volumes of 100 % ethanol. The DNA was recovered by centrifugation at 10 000× *g* for 10 min. The DNA pellet was washed with 200 µl 70 % ethanol, and again centrifuged at 1 700× *g* for 5 min. The ethanol was removed and the pellet was air-dried. The DNA was re-suspended in TE buffer.

2.8. Bacterial strains used.

(1). *Escherichia coli* MC1061:

F$^-$, *ara*D139, (*ara leu*) 7697, Δ*lac*x74, *gal*U$^-$, *gal*K$^-$, *hs*$^-$, *hsm*$^+$, *str*A.

(2). *E. coli* BL21 Star™ pLys (DE3) (Stratagene):

F$^-$ *omp T hsdS*$_B$(*r*$_B^-$*m*$_B^-$) *gal dcm rne131* (DE3)

2.9. Bacterial cultures.

Escherichia coli MC1061 was used to produce plasmid DNA, while *E. coli* BL21 Star™ pLys (DE3) was used to express recombinant fusion proteins. *E. coli* was grown in L Broth and on L Agar plates with or without ampicillin. When required ampicillin was added to L broth and L Agar plates to a final concentration of 100 µg/ml. All cultures were grown at 37 °C.

Glycerol stocks were prepared directly from overnight cultures, grown under selectable conditions, by dilution of the culture with an equal volume of 80 % sterile glycerol. These were then stored at – 70 °C.

2.10. Preparation of *E. coli* competent cells for transformation.

The desired bacterial strain (from a glycerol stock) was used to streak an L Agar plate (L Agar contained 10 mM $MgCl_2$). A single colony from this plate was used to inoculate 20 ml TYM Broth. The culture was incubated at 37° C, until an optical density (OD) of 0.2 at 550 nm was reached. This culture was then added to 100 ml fresh TYM Broth and incubated at 37 °C until an optical density of 0.2 at 550 nm was reached. The culture was transferred into a 2 l flask, 400 ml TYM Broth was added and the culture was incubated at 37 °C until the optical density at 550 nm was between 0.4 and 0.6. The culture was cooled rapidly in ice water and centrifuged at 6 000× *g* for 10 min at 4 °C in a Beckman J2-21 centrifuge. The supernatant was discarded and the cell pellet re-suspended 250 ml ice-cold Tfb1 Buffer. After 30 min the cell suspension was centrifuged at 6 000× *g* for 10 min at 4 °C. The pellet was gently re-suspended in 50 ml Tfb2 Buffer, dispensed in 300 µl aliquots and then rapidly frozen using liquid nitrogen. These aliquots were stored at – 70 °C.

For transformations, the competent cells were thawed on ice and 100 µl of the cells were added to the DNA. The mixture was incubated on ice for 20 min. The cells were heat-shocked at 42 °C for 45 sec and incubated on ice for 5 min. After 5 min, 900 µl pre-warmed L Broth was added and the tubes were incubated at 37 °C. After 30 min, 50 µl of the culture was plated on L Agar plates containing 100 µg/ml ampicillin and incubated at 37 °C.

2.11. Preparation of plasmid DNA.

2.11.1. Small-scale preparation of plasmid DNA.

A single colony of a transformed *E. coli* was used to inoculate 40 ml L Broth containing 100 µg/ml ampicillin and this was cultured overnight at 37 °C. This culture was then centrifuged for 10 min at 6 000× *g* at 4 °C in a Beckman J2-21 centrifuge. The supernatant was discarded and the cell pellet was re-suspended in 300 µl GTE, containing 100 µg/ml RNase A. The cell suspension was transferred to a 1.5 ml tube and incubated on ice for 5 min. To this cell suspension 300 µl Lysis Solution was added followed by careful mixing by inversion. After 5 min incubation on ice 300 µl Neutralisation Solution was added, the solution was mixed by inversion and centrifuged for 10 min in a microfuge at 10 000× *g*. After centrifugation 600 µl of the supernatant was transferred into a 1.5 ml tube and 450 µl isopropanol was added. The samples were mixed by vortexing and placed at – 20 °C for 30 min. The samples were centrifuged for 20 min at 10 000× *g* in a microfuge. The supernatant was discarded and the pellet was re-suspended in 500 µl TE. An equal volume of phenol:chloroform:isoamyl alcohol was added and the tubes were centrifuged for 5 min at 10 000× *g*. The supernatant was transferred to a new tube and 0.1 volumes of 3 M sodium acetate and 2.5 volumes of ethanol was added. The samples were incubated at – 20 °C for 30 min. The DNA was recovered by centrifugation for 10 min at 10 000× *g*. The supernatant was removed and the pellet was washed with 70 % ethanol. The plasmid DNA was recovered again by centrifugation for 5 min 10 000× *g*. The pellet was air-dried and re-suspended in 50 µl TE. The DNA was quantified by measuring the

optical density at 260 nm in a spectrophotometer (one OD_{260} unit of double stranded DNA equals 50 ng/µl).

2.11.2. Large-scale preparation of plasmid DNA.

A 5 ml overnight culture of the appropriate *E. coli* was used to inoculate 500 ml L Broth containing 100 µg/ml ampicillin. The culture was grown overnight at 37 °C. The culture was centrifuged in a Beckman J2-21 centrifuge for 10 min at 6 000× *g*. The supernatant was discarded and the cell pellet was re-suspended in 15 ml GTE containing 100 µg/ml RNase A. The cell suspension was incubated on ice for 5 min. To this cell suspension 15 ml Lysis Solution was added, followed by careful mixing by inversion. After 5 min incubation, 15 ml of Neutralisation Solution was added, the solution was mixed by inversion and centrifuged for 20 min at 10 000× *g*, in a Beckman J2-21 centrifuge. The supernatant was filtered through Miracloth™ (Calbiochem). The volume of the supernatant was determined and 0.6 volumes of isopropanol were added. The solution was mixed thoroughly before incubating it at – 20 °C for 30 min. The nucleic acids were precipitated by centrifugation at 10 000× *g* for 20 min. The supernatant was discarded and the pellet was dissolved in 500 µl TE. The samples were transferred to 2 ml tubes and 500 µl phenol:chloroform:isoamyl alcohol was added. The samples were briefly mixed and centrifuged at 10 000× *g* in a microfuge for 5 min. The aqueous (top) phase was removed and transferred to a new 1.5 ml tube. The phenol extraction was repeated one more time. After the second extraction, the DNA was precipitated by the addition of 0.1 volume of 3 M

sodium acetate (pH 5 with glacial acetic acid) and 2.5 volumes of ethanol. After incubating the samples for 30 min at – 20 °C, the DNA was recovered by centrifugation for 10 min at 10 000× *g* in a microfuge. The supernatant was discarded and the pellet was washed with 70 % ethanol. The plasmid DNA was recovered by centrifugation for 5 min. The pellet was air-dried and re-suspended in 500 µl TE.

2.12. Cloning vectors.

2.12.1. pGEM®-T Easy.

The pGEM®-T Easy Vector System (Promega) is suited for direct cloning of PCR fragments. This cloning strategy makes use of the terminal extendase activity of *Taq* polymerase which adds an extra base (usually an adenosine) on the 3' end of PCR products (Clark, 1988). The pGEM®-T Easy Vector, as supplied for cloning by the manufacturer, contains single 3'-T overhangs at the insertion site, and is able to accommodate the ligation of PCR fragments (Figure 2.2).

2.12.2. pGEX-6P-2.

The Glutathione S-Transferase (GST) gene fusion system (Amersham Pharmacia) is a protein expression system, which can be used for the expression, purification and detection of recombinant fusion proteins produced in *E. coli*. This system is designed for the inducible, high-level intracellular expression of genes or gene fragments as fusions with *Schistosoma japonicum* GST (Smith and Johnson,

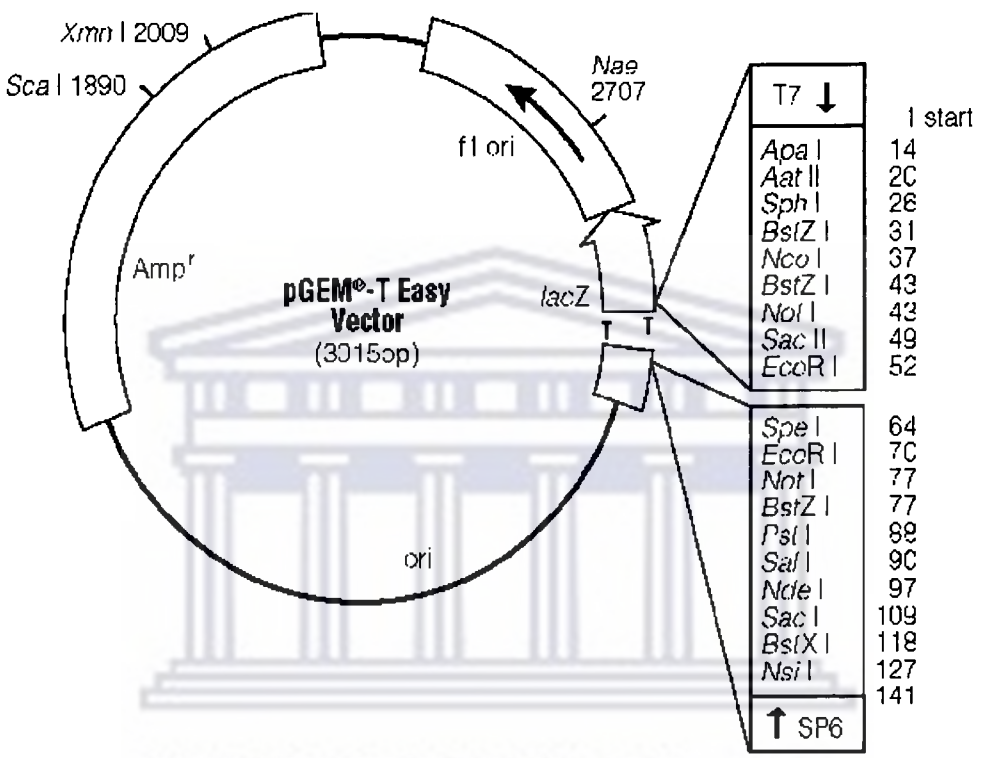

Figure 2.2. A circular map of the pGEM®-T Easy Vector System. Also indicated in this figure is the multiple cloning site and the T-overhangs.

1988). The GST domain acts as an affinity tag that allows for the purification of the fusion protein by affinity chromatography using glutathione agarose (Sigma). A number of glutathione S-transferase fusion vectors have been developed. One such vector is pGEX-6P-2 (Figure 2.3).

Separation of the protein of interest from GST can be achieved by using a site-specific protease whose recognition sequence is located upstream of the multiple cloning site, i.e. between the GST domain and the protein of interest. In the case of pGEX-6P-2 this protease is PreScission™ Protease (Amersham Pharmacia). This protease is a genetically engineered fusion protein consisting of human rhinovirus 3C protease and GST. This enzyme specifically cleaves between the Gln and Gly residues of the recognition sequence of Leu-Glu-Val-Leu-Phe-Gln/Gly-Pro (Cordingley *et al.*, 1990).

2.13. Restriction enzyme digestion of DNA.

Restriction enzymes were used according to manufacturer's instructions. In general 1 μg of DNA was digested with 1 Unit of enzyme in the appropriate buffer and temperature. Restriction enzymes were inactivated by either heating the reaction mixture at 70 °C for 10 min, or by phenol/chloroform extraction if the enzyme is heat stable.

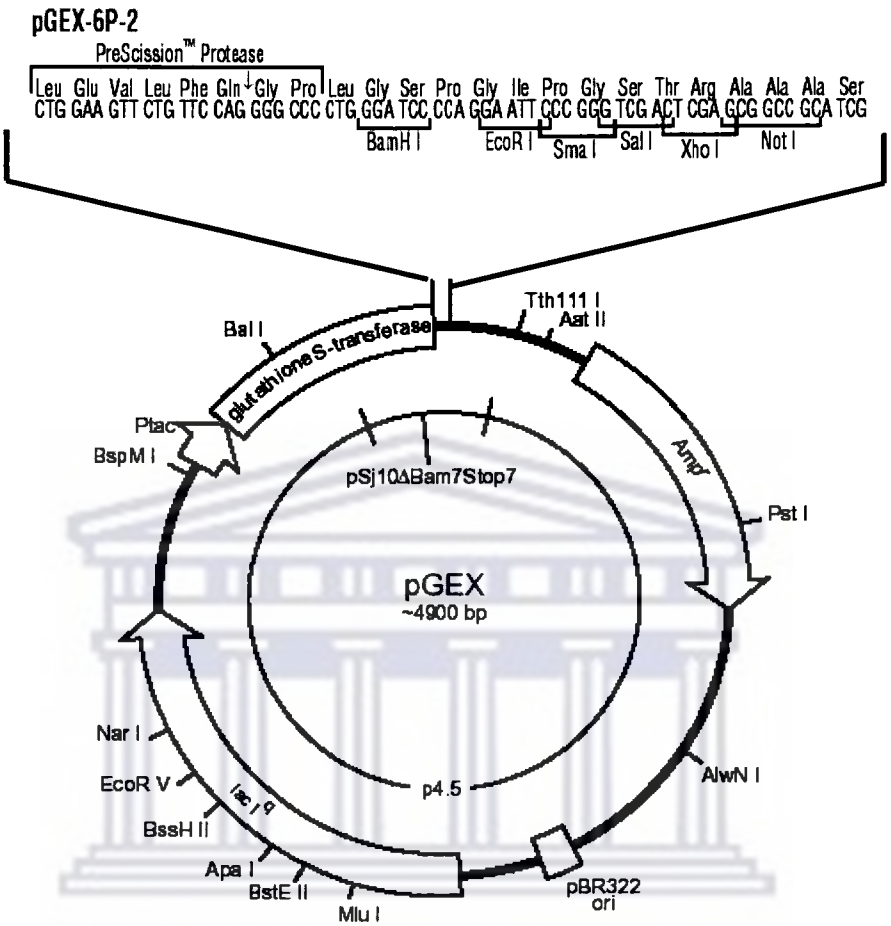

Figure 2.3. A circular map of the pGEX -6P-2 expression vector. This map shows the GST (Glutathione S-transferase) domain next to the multiple cloning site and the position of the PreScission™ Protease cleavage site between the GST domain and the multiple cloning site.

2.14. Ligation of DNA.

Ligation reactions were set up according to the manufacturer's instructions. Reactions were performed in 1× ligase buffer (30 mM Tris-HCl, pH 7.8, 10 mM $MgCl_2$, 10 mM DTT and 1 mM ATP) using T4 DNA ligase (Promega). Ligations were performed according to the manufacturer's instructions. The enzyme was heat inactivated by incubation 70 °C for 10 min.

2.15. Amplification of DNA by PCR.

PCR reactions were performed in 1× reaction buffer according to the manufacturers instructions. The enzyme *Taq* polymerase (Takara Biotechnology) was used at 0.2 Units per reaction. The primers were present at 1 pmol and between 1 and 10 ng of DNA template was used in each reaction. In general the $MgCl_2$ concentration was 1.5 mM, otherwise the optimal $MgCl_2$ concentration was determined by titration.

2.16. Inverse PCR amplification of DNA.

A restriction map of the tkneoU3hygro retrovirus was generated using DNA Strider 1.2 software. This map was used to identify cleavage sites and design primers for inverse PCR that will allow amplification of DNA fragments that will permit the identification of hamster genomic sequences flanking the tkneoU3hygro retrovirus. The restriction enzyme Tsp 509 I was chosen to digest the genomic DNA. Figure 2.4 shows the positioning of the Tsp 509 I restriction sites and the PCR primers in the tkneoU3hygro retroviral sequence.

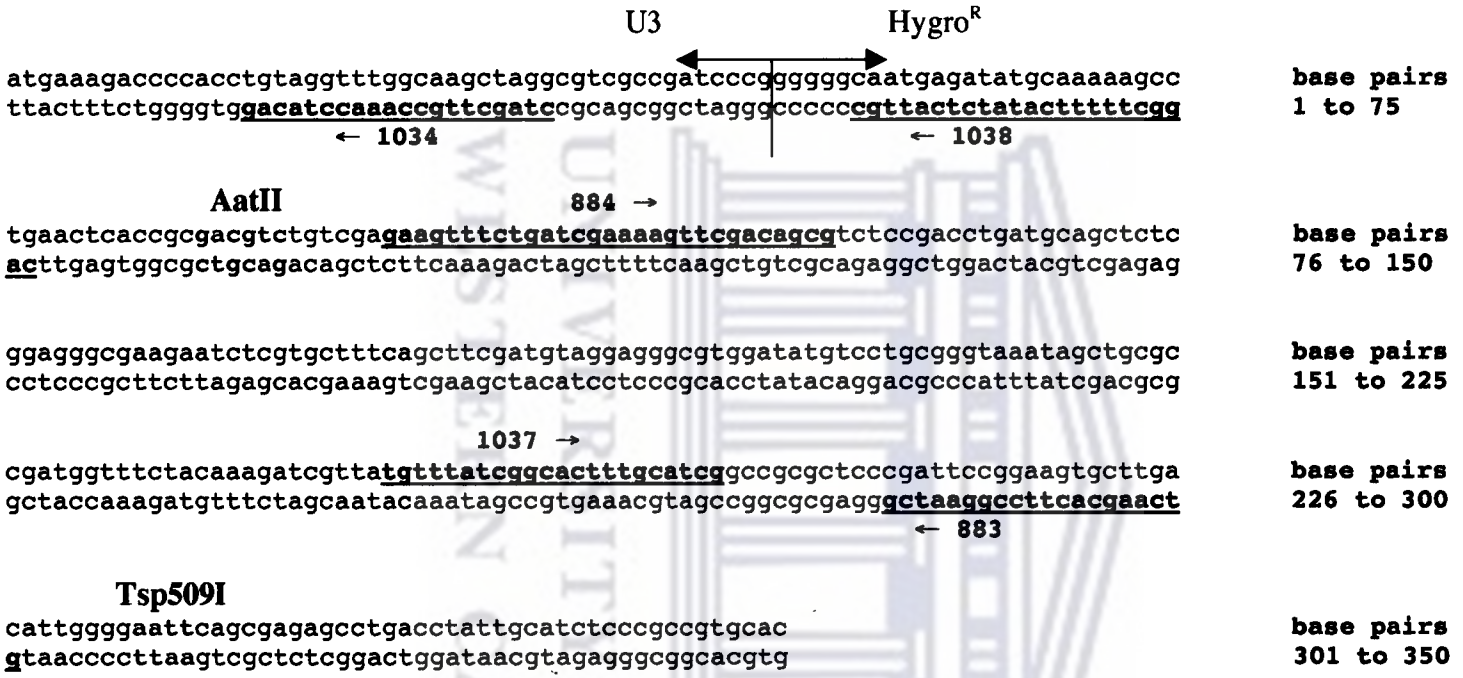

Figure 2.4. The first 350 base pairs of the 5' LTR of the retrovirus, tkneoU3hygro. The positions of the restriction enzymes Aat II and Tsp 509 I are indicated in red. The positions of the PCR primers for the inverse PCR are underlined and indicated in bold. The boundary between the U3 region of the retrovirus and the hygromycin resistance gene ($Hygro^R$) is also indicated.

Genomic DNA was isolated from cultured cells as described in Section 2.7. Figure 2.5 shows a detailed schematic diagram of the inverse PCR strategy. The genomic DNA was digested for 5 hrs at 65 °C with the restriction enzyme Tsp 509 I. The DNA was then analysed for complete digestion on an agarose gel. The digested DNA was purified by phenol-chloroform extraction. The DNA was quantified and a series of ligation reactions containing DNA concentrations that will favour the ligation of fragments varying in size between 200 and 500 base pairs were set up. The re-ligated DNA was then linearised by digestion with the restriction enzyme, Aat II at 37 °C for 2 hrs. Figure 2.4 shows that the positioning of this restriction site between the PCR primer sites in the tkneoU3hygro retroviral sequence. The enzyme, Aat II, was heat-inactivated and the DNA was recovered by ethanol precipitation. The products of these reactions were used as templates for inverse PCR. PCR reactions were performed as described in Section 2.15, using the primer pair 1039 and 1038. The PCR cycling conditions were as follows: 95 °C – 2 min, followed by; 94 °C – 30 sec, 65 °C – 30 sec, 72 °C – 1 min, repeated for 35 cycles; followed by 72 °C – 10 min. The products of this PCR were electrophoresed on an agarose gel.

A second round PCR reaction was performed using the nested primer pairs 1034/1037. In the second round PCR, 1 µl of the first round PCR product was used as template DNA. The PCR cycling conditions were: 95 °C – 2 min, followed by; 94 °C – 30 sec, 67 °C – 30 sec, 72 °C – 1 min, repeated for 35 cycles; followed by 72 °C – 10 min. The products of the second round PCR reaction were electrophoresed on a 5 % polyacrylamide gel and PCR fragments of

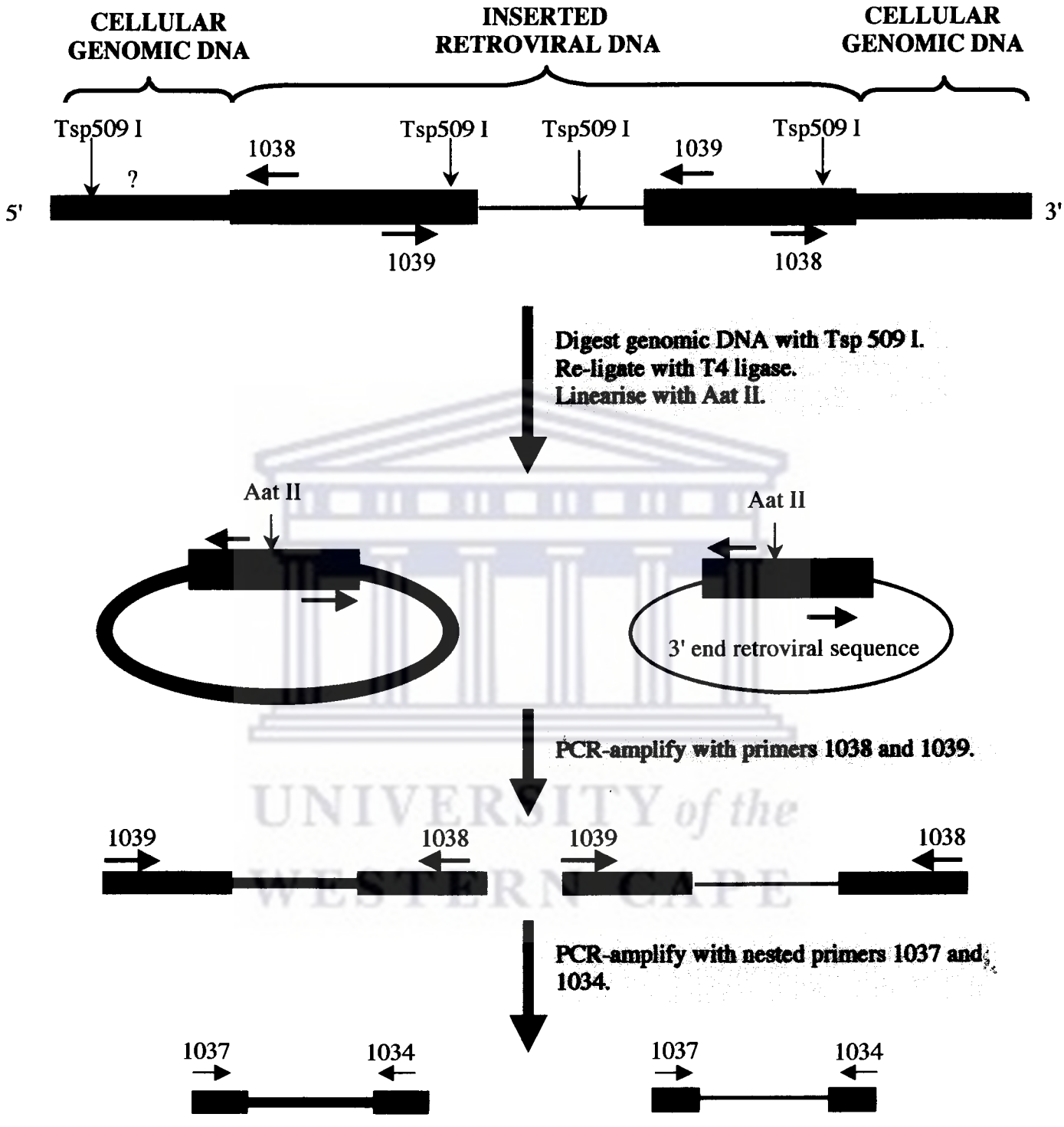

Figure 2.5. A schematic representation of the inverse PCR protocol.

interest were purified from the gel as described in Section 2.18.2. The DNA was quantified, and sequenced (as described in Section 2.21) using primer 1037.

2.17. Gel electrophoresis of DNA.

2.17.1. Agarose gel electrophoresis.

DNA was size fractionated by electrophoresis on agarose gels containing 0.5 μg/ml ethidium bromide. The concentration of agarose varied 0.8 % to 2 %. The DNA sample was diluted with 6× Glycerol BPB Gel-loading Buffer before electrophoresis on gels. The DNA was electrophoresed at 10 V/cm in either 1× TBE or 1× TAE electrophoresis buffer. After electrophoresis the DNA was visualised on an UV trans-illuminator. Gel images were recorded with a UVP (Ultra Violet Products) image capture system.

2.17.2. Acrylamide gel electrophoresis.

Denaturing electrophoresis was performed on 6 % polyacrylamide gels. The components of the gels were as follows: 7 M urea, 1× TBE or TAE, 6 % 19:1 acrylamide:bis-acrylamide. To initiate polymerisation, 0.5 % ammonium persulphate and 0.1 % TEMED were added. Electrophoresis was performed in 1× TBE or TAE running buffer at 5 V/cm until the bromophenol blue dye reached the bottom of the gel. After electrophoresis the gel was stained for 30 min in 1× TBE or TAE buffer containing 0.5 μg/ml ethidium bromide. The gel was de-

stained in 1× TBE or TAE buffer for 1 hr before visualisation on an UV trans-illuminator. Gel images were recorded as described above.

2.18. Purification of DNA fragments.

2.18.1. Agarose gels.

The DNA was electrophoresed on a 0.8 % agarose gel in TAE buffer (Section 2.17.1). The DNA was visualised using a long wavelength (360 nm) UV lamp. The DNA fragment of interest was cut out from the gel and the gel slice was macerated. The agarose was weighed and an equal volume of phenol was added. The sample was mixed by vortexing and placed at – 70 °C for 15 min. It was allowed to thaw and centrifuged for 10 min at 10 000× *g* in a microfuge. The upper aqueous layer was removed and the DNA precipitated by the addition of 0.1 volumes of 3 M sodium acetate and 2.5 volumes of ethanol. The samples were incubated at – 20 °C for 30 min. The DNA was recovered by centrifugation for 10 min at 10 000× *g* in a microfuge. The supernatant was discarded and the pellet was washed with 70 % ethanol. The pellet was air-dried and re-suspended in 1× TE.

2.18.2. Polyacrylamide gels.

The DNA was electrophoresed on either 6 % or 12 % polyacrylamide gels in TAE buffer. After destaining, the DNA was visualised using a long wavelength (360 nm) UV lamp. The DNA fragment of interest was cut out from the gel and

the gel fragment was macerated. The gel was weighed, covered with 2 volumes of DNA Elution Buffer and incubated overnight at 37 °C (while shaking). The gel pieces were removed from the solution by centrifugation. The supernatant was transferred to a new 1.5 ml tube and the DNA was precipitated by the addition of 0.1 volumes 3 M Sodium acetate and 2.5 volumes ethanol. The samples were incubated at – 20 °C for 1 hr. The DNA was recovered by centrifugation at 10 000× *g* for 10 min. The DNA pellet was washed twice with 70 % ethanol. The pellet was dried and dissolved in 1× TE buffer.

2.19. Cloning PCR fragments into pGEM®-T Easy.

PCR fragments were cloned using the pGEM®-T Easy Vector System (Promega). Following the PCR, a fraction of the PCR product was checked on an agarose gel. The PCR product was quantified and the appropriate concentration of the PCR product required in the ligation reaction was determined using the following equation:

$$\frac{\text{ng of vector} \times \text{kb size of insert}}{\text{kb size of vector}} \times \text{insert:vector molar ratio} = \text{ng of insert}$$

Molar ratios from 3:1 to 1:3 (insert:vector) were used to calculate the amount of PCR product that should be added to the ligation reactions. The following table describes how the ligations reactions were set up.

Table 2.2. Experimental set up of ligation reactions for cloning PCR fragments into pGEM®-T Easy Vector.

	Standard reaction	Positive Control	Negative Control
2× Rapid Ligation Buffer	5 µl	5 µl	5 µl
pGEM®-T Easy Vector (1 ng/µl)	1 µl	1 µl	1 µl
PCR product	X µl	-	-
Control insert	-	2 µl	-
T4 DNA ligase (1 Unit/µl)	1 µl	1 µl	1 µl
Deionised water to final volume of	10 µl	10 µl	10 µl

The ligation reactions were briefly mixed and incubated at 22 °C for 3 hrs. After ligation, 100 µl of competent cells were added to the ligation mix and the transformations were done as previously described (Section 2.10).

2.20. Colony PCR.

E. coli colonies were screened for the presence of the insert by colony PCR. Following transformations the colonies to be screened were removed from the plate and re-suspended in 5 µl sterile deionised water. PCR reactions were performed as described in Section 2.15, using 10 pmol of the M13 reverse and M13 forward primers. For each of the colonies 1 µl of the cell suspension was added to 49 µl of the PCR reaction mix. A negative control which substituted the 1 µl bacterial cell suspension with 1 µl of water was also performed. The cycling PCR conditions were as follows: 95 °C – 2 min, followed by; 94 °C – 30 sec,

60 °C – 30 sec, 72 °C – 1 min, repeated for 30 cycles; followed by 72 °C – 10 min. The products of the colony PCR were analysed by electrophoresis on an agarose gel.

2.21. Sequence analysis.

Sequencing reactions were performed using the DNA Sequencing Kit, BigDye™ Terminator v3.0 Cycle Sequencing Ready Reaction (Applied Biosystems). The PCR sequencing reactions were performed in a 10 µl final volume containing 3.2 pmol of the sequencing primer, 2 µl Terminator Ready Reaction mix (Applied Biosystems) and 2 µl 2.5× Sequencing Buffer. For plasmid DNA templates 500 ng of DNA was added, while the DNA concentration for PCR fragments was dependent on the size of the PCR fragment (Table 2.3).

Table 2.3. The amount of PCR template DNA used in sequencing reactions.

Size of PCR fragment	Amount of DNA added
100 – 200 bp	1 – 3 ng
200 – 500 bp	3 – 10 ng
500 – 100 bp	5 – 20 ng
1000 – 2000 bp	10 – 40 ng
> 2000 bp	40 – 100 ng

The cycle conditions were as follows: 96 °C – 30 sec, 60 °C – 4 min, repeated for 25 cycles. Following the PCR sequencing reactions the DNA was precipitated by adding 16 µl deionised water and 30 µl absolute ethanol. The samples were

incubated at 25 °C for 30 min. The DNA was recovered by centrifugation at 10 000× *g* for 20 min in a microfuge. The supernatant was removed and the pellet was washed in 250 µl 70 % ethanol. The DNA was again recovered by centrifugation at 10 000× *g* for 15 min. After a second wash, the pellet was air-dried and re-dissolved in 15 µl Template Suppressor Buffer (Applied Biosystems). The samples were heat-denatured by incubation at 95 °C for 2 min before the samples were analysed on an ABI 310 PRISM™ Genetic Analyzer (Applied Biosystems). Data was collected using ABI 310 PRISM™ Collection Software (Applied Biosystems) and the analysis was done using Sequence Analysis 3.3 Software (Applied Biosystems).

2.22. Isolation of mitochondria from cultured cells.

Cells were cultured in 25 cm^2 flasks until confluent. The cells were removed by trypsinisation (Section 2.4). Cells were recovered by centrifugation for 5 min at 200× *g* and washed with 5 ml complete Ham's F12 medium. The cells were recovered again by centrifugation for 2 min at 200× *g* and washed twice in 5 ml ice-cold PBS. The cells were re-suspended in 300 µl Mitochondrial Isolation Buffer. The cells were lysed on ice in a glass homogeniser (with a type B pestle). The lysate was centrifuged for 20 min at 800× *g* in a microfuge at 4 °C. The supernatant was centrifuged again at 800× *g* in a microfuge at 4 °C for 20 min. The supernatant was removed and centrifuged at 10 000× *g* in a microfuge at 4 °C for 20 min. The pellet containing the mitochondria was re-suspended in 200 µl ice-cold Mitochondrial Resuspension Buffer.

2.23. Isolation of proteins from cultured cells.

Cells were removed by trypsinisation and recovered by centrifugation for 5 min at 200× *g*. The cells were then washed twice with 5 ml ice cold PBS. The cell pellet was re-suspended in 200 µl PBS containing 1 % Triton X-100. The cells were lysed by three freeze/thaw cycles by placing the samples at – 70 °C for 10 min and thawing the samples at 37 °C for 5 min. After lysis an equal volume of 1× Reducing Loading Buffer was added to the sample. This sample was either stored at – 70 °C or boiled for 3 min and centrifuged for 5 min at 10 000× *g* in a microfuge before electrophoresis on a SDS-PAGE gel.

2.24. SDS-polyacrylamide gel electrophoresis (SDS-PAGE).

2.24.1. One-dimensional SDS-PAGE.

Proteins were separated on SDS-PAGE gels, according to Laemmli's method (Laemmli, 1970). Gels were made from a 40 % of pre-mix acrylamide: bisacrylamide (37.5:1) (Biorad). The separating gel consisted of 12 to 16 % acrylamide: bisacrylamide (37.5:1), 0.375 M Tris-HCl, pH 8.8, 0.1 % SDS, 0.5 %, ammonium persulphate and 0.1 % TEMED. The stacking gel consisted of 4 % acrylamide: bisacrylamide (37.5:1), 0.125 M Tris-HCl, pH 6.8, 0.1 % SDS, 0.5 % ammonium persulphate and 0.1 % TEMED. The samples were mixed with an equal volume of 2× Sample Buffer, boiled for 3 min, centrifuged for 10 min at 10 000× *g*, and electrophoresed in 1× SDS Electrophoresis Buffer (25 mM Tris, 192 mM glycine, 0.1 % SDS, pH 8.3) at 100 V (constant voltage) for 30 min using a Hoefer Mighty Small II Gel electrophoresis system (Amersham

Pharmacia). The voltage was increased to 150 V (constant voltage) when the bromophenol blue dye front reached the separating gel. Electrophoresis was stopped when the bromophenol blue dye front reached the bottom of the gel. The gel was incubated in Coomassie Staining Solution for 30 min and then incubated overnight in Destain Solution.

2.24.2. Two-dimensional (2-D) SDS-PAGE.

Proteins were isolated from tissue culture cells as described in Section 2.23. The protein concentrations were determined using the Bradford assay. A 60 µg aliquot of each protein sample was precipitated by adding three volumes of acetone and incubating the samples at – 20 °C for 30 min. The samples were centrifuged for 10 min at 10 000× *g* in a microfuge. The protein pellets were washed twice with ice-cold 80 % acetone. The pellets were allowed to dry before 100 µl Rehydration Stock Solution was added. A DTT stock solution (6.5 M) was prepared in Rehydration Stock Solution and 2.5 µl of this DTT/Rehydration Stock Solution was added to the protein sample. To this mixture 2.5 µl Pharmalyte™ 3-10 (Amersham Pharmacia), was also added. The proteins were solubilised by vortexing and then centrifuged at 10 000× *g* for 2 min in a microfuge. The supernatants, containing the soluble proteins were loaded into an Immobiline DryStrip Reswelling Tray (Amersham Pharmacia). IPG strips (7 cm Non-linear, pH 3-10) (Amersham Pharmacia) were positioned over the protein samples. Each IPG strip was overlaid with 3 ml DryStrip Cover Fluid (Amersham Pharmacia). The IPG strips were allowed to rehydrate overnight (16 hrs) at 25 °C. After

rehydration the strips were washed with deionised water and the excess water removed on damp Wattmann 3MM paper. The first-dimension isoelectric focusing was performed using a Multiphor II system (Amersham Pharmacia). The electrophoresis protocol is summarised in Table 2.4.

Table 2.4. The electrophoresis protocol for isoelectric focusing using 7 cm Non-linear Immobiline DryStrips, pH 3-10.

Phase	Voltage (V)	Current (mA)	Time
1	200	1	1 min
2	1000	1	1 hr
3	2000	1	1 hr
4	2500	1	1.5 hr

Total volt hours = 6 950 vh

The IPG strips were incubated in SDS Equilibration Buffer for 30 min after the first-dimension isoelectric focusing. For the second-dimension electrophoresis, a SDS-PAGE gel was prepared and cast as described in Section 2.24.1. However the separating gel was not overlaid with a stacking gel as described. The IPG strips were placed on top of the separating gel. The protein molecular weight marker was loaded onto a 0.5 cm^2 strip of Wattmann 3MM paper, which was dried and then placed next to the IPG strip on top of the stacking gel. The IPG strip was then sealed on the stacking gel with Agarose Sealing Solution. The gel was electrophoresed in 1× SDS Electrophoresis Buffer at 50 V (constant voltage) using a Hoefer Mighty Small II Gel electrophoresis system (Amersham

Pharmacia). When the bromophenol blue dye front reached the separating gel the voltage was increased to 100 V (constant voltage). Electrophoresis was stopped when the dye front reached the end of the gel. The gel was used for Western blotting as described in Section 2.28 or incubated in Coomassie Staining Solution for 30 min and then incubated overnight in Destaining Solution. The gels were photographed using a UVP image capture system.

2.25. The expression and purification of recombinant GST fusion proteins.

2.25.1. Screening for the expression and solubility of fusion proteins.

E. coli bacterial cells were screened for the expression of recombinant GST fusion proteins by inoculating 5 ml aliquots of L Broth (containing 100 µg/ml ampicillin) with these colonies and growing the culture overnight at 37 °C. The following day a 1 ml aliquot (representing the un-induced sample) was removed and the cells were harvested by centrifugation at 10 000× *g* for 2 min in a microfuge. The supernatants were removed and the cells were stored at – 20 °C. The remaining 4 ml culture was used to screen for the expression of the protein of interest by adding IPTG to a final concentration of 0.1 mM. The culture was incubated for a further 4 hrs at 37 °C. After 4 hrs another 1 ml aliquot (representing the induced sample) was removed and the cells were recovered centrifugation at 10 000× *g* for 2 min in a microfuge. Both the un-induced and induced cell pellets were re-dissolved in 50 µl Lysis Buffer. The cells were lysed by repeated freeze/thaw cycles, by placing the samples at – 70 °C for 10 min and thawing the samples at 37 °C for 5 min. Following lysis, 50 µl 2× Sample Buffer was added to the

samples. The samples were boiled for 3 min and centrifuged for 5 min at 10 000× *g* for 5 min in a microfuge before electrophoresis on a SDS-PAGE gel.

2.25.2. Large-scale expression of fusion proteins.

The glycerol stock of a clone that was found by expression screening to express the protein of interest was used to streak an agar plate (containing 100 µg/ml ampicillin). A single fresh colony was used to inoculate 100 ml of L Broth (containing 100 µg/ml ampicillin). This culture was grown overnight at 37 °C. The following day 1000 ml L Broth was inoculated with the 100 ml overnight culture and grown at 37 °C, until the OD_{600} was approximately 0.6. Expression was induced by the addition of IPTG to a final concentration of 0.1 mM. The culture was incubated for a further 4 hrs at 37 °C, before the cells were recovered by centrifugation for 10 min at 6 000× *g* in a J2-21 Beckman centrifuge. The cell pellet was re-suspended in 20 ml Lysis Buffer. The cells were lysed through successive freeze/thaw cycles by placing the samples at – 70 °C for 10 min and thawing the samples at 37 °C for 5 min. The bacterial lysate was centrifuged for 30 min in a J2-21 Beckman centrifuge at 10 000× *g*, at 4 °C. The supernatant containing the soluble protein was removed; PMSF (to a final concentration of 1 mM) and sodium azide (to a final concentration of 0.02 %) was added to the sample before it was stored at 4°C until further use. A fraction of the lysate was analysed for the expression of recombinant protein on a SDS PAGE gel.

2.25.3. Purification of fusion proteins.

A glutathione agarose column was prepared according to the manufacturer's instructions (Amersham Pharmacia). The column was equilibrated with three column-volumes of PBS. The bacterial lysate was added onto the column and the flow-through was collected. A fraction of the column flow-through was analysed on a SDS PAGE gel. The column was washed twice with three column-volumes of PBS. The protein was eluted with 3 column-volumes of Protein Elution Buffer. DTT (1 mM) and 10 Units of PreScission™ Protease (Amersham Pharmacia) were added to the column eluate. The eluate was then dialysed overnight at 4 °C in a buffer containing 50 mM Tris-HCl, 150 mM NaCl, 10 mM EDTA and 1 mM DTT, pH 7.0. The sample was analysed on a SDS-PAGE gel to check for complete cleavage. The next step was to remove GST from the cleaved protein. The cleaved sample was added onto a pre-equilibrated glutathione agarose column. The flow-through contained the recombinant protein and the eluate contained GST.

2.26. The generation of polyclonal anti-rabbit antibodies.

Polyclonal antibodies against recombinant protein were generated at Department of Biochemistry, University of Stellenbosch. The purified recombinant protein was used to generate antibodies in rabbits, according to Bellstedt's method (Bellstedt *et al.*, 1987). Pre-immune serum was collected on Day 0 before immunisation and a bleed serum was collected on Day 28 after the animals were immunised with the protein.

2.27. Affinity purification of antibodies.

The recombinant protein was electrophoresed on a SDS-PAGE gel (Section 2.24.1). The protein was transferred unto a PVDF-P membrane (Amersham Pharmacia) using a Mini Protean II™ system (Biorad) (Section 2.28). Transfer was performed at 4 °C, 35 V (constant voltage) overnight in pre-cooled transfer buffer. After transfer the membrane was stained with Ponceau S (Sigma) to verify protein transfer. The region of the membrane representing recombinant protein was cut out from the membrane. The membrane-strip was incubated for 1 hr in TBSMT. The serum (1 ml) was then incubated for 3 hrs with the membrane-strip while shaking slowly. The serum was removed and the membrane-strip was washed once with TBST and three times with TBS. The purified antibody was eluted from the strip by incubation in 500 µl of 200 mM glycine-HCl and 1 mM EDTA, pH 2.5. The pH of the antibody-eluate was adjusted to pH 7 by the addition of 100 mM Tris, pH 8. The membrane-strip was washed in TBS, dried and stored at – 20 °C for future use.

2.28. Western blotting.

Protein samples were electrophoresed on 1-D or 2-D SDS PAGE gels as described in Section 2.24. The proteins were transferred unto a PVDF-P membrane (Amersham Pharmacia) using a Mini Protean II™ system (Biorad). Before transfer the membrane was pre-wetted in methanol for a few seconds, washed in deionised water for 5 min and equilibrated in Transfer Buffer for 10 min. The SDS PAGE gels were also equilibrated in Transfer Buffer for 10 min.

Transfer was performed at 4 °C, 35 V (constant voltage) overnight in pre-cooled Transfer Buffer. After transfer the membranes were stained with Ponceau S (Sigma) to check for protein transfer. The membranes were incubated in TBSMT for 2 hrs. The purified primary antibody was diluted 1:10 000 in TBSMT and the membranes were incubated in the primary antibody (polyclonal anti-rabbit anti-mouse endozepine) for 1 hr. The membrane was washed three times for 10 min in TBSMT. The secondary antibody, anti-rabbit Ig horseradish peroxidase (Amersham Pharmacia) was diluted (1:20 000) in TBSMT and the membranes were incubated in this antibody for 30 min. The membrane was washed three times for 10 min in TBSMT. This was followed by three more washes with TBST. Detection was performed using the ECL+plus Western Blotting Detection System (Amersham Pharmacia).

2.29. Apoptosis assays.

2.29.1. Screening the effects of DMSO on CHO22 cells.

CHO22 cells, cultured in complete Ham's F12 media, were plated in 25 cm^2 tissue culture flasks at a cell density of 2.5×10^4 cells per flask. After 24 hrs the medium was removed and the cells were washed with PBS. Fresh Ham's F12 media, containing DMSO, was added. The final concentration of DMSO in these flasks varied between 0 and 5 %. The cells were cultured in this media for a period of 72 hrs while being monitored for morphological changes using a Nikon inverted light microscope. Photographs of the cells were taken after 72 hrs using a 20× objective.

2.29.2. The screening of C_2-ceramide and camptothecin as inducers of apoptosis.

CHO22 cells were cultured in complete Ham's F12 medium. The cells were removed by trypsinisation and plated in 25 cm^2 tissue culture flasks at a cell density of 2.5×10^4 cells per flask. After 24 hrs the media was removed, the cells were washed with PBS, and fresh media containing either N-Acetyl-D-sphingosine/C_2-ceramide or camptothecin was added. The final concentration of C_2-ceramide varied between 0 and 100 μM, while the concentration of camptothecin varied between 0 and 6 μg/ml. In addition to the negative control (no C_2-ceramide or camptothecin added), a second control (cells treated with 0.01 % DMSO) was set up, as DMSO was the solvent used to dissolve both C_2-ceramide and camptothecin. The cells were exposed for 24 hrs to the C_2-ceramide-, camptothecin- or DMSO-conditioned media, during which time the cells were monitored for morphological changes and photographs were taken. At this time point the cells were harvested and assayed for DNA fragmentation as described in Section 2.29.3.

2.29.3. DNA fragmentation analysis.

Cells were cultured in 25 cm^2 tissue culture flasks and treated with the optimised conditions with either C_2-ceramide or camptothecin. The cells were harvested from the flasks and transferred into 1.5 ml tubes. The cell pellet was re-suspended in 0.5 ml TTE, to which 0.1 ml ice-cold 5 M NaCl and 0.7 ml ice-cold isopropanol was added. The samples were mixed and placed at – 20 °C for 16 hrs

to precipitate the DNA. The samples were centrifuged at 10 000× *g* for 10 min in a microfuge, at 4 °C. The pellets were washed once with 0.5 ml 70 % ethanol and centrifuged at 10 000× *g* for 10 min, at 4 °C. The supernatants were removed and the pellets were dried. The pellets were re-dissolved in 30 µl TE and analysed by electrophoresis on 2 % agarose gels.

2.29.4. LDH release assay.

This assay was performed using the LDH (lactate dehydrogenase) release assay or Cytotoxicity Detection Kit (Roche). The cells were plated in a 96-well tissue culture plate at a cell density of 0.25×10^5 cells/ml. The plate was incubated for 37 °C. After 24 hrs the medium was removed and 100 µl medium containing C_2-ceramide was added to the wells. The concentrations of the C_2-ceramide ranged from 20 to 100 µM. Triplicate wells were set up for each concentration. Two controls were also included: the low control (representing the spontaneous LDH release, 100 µl medium was added to each well) and the high control (representing the maximum LDH release, 100 µl medium containing 2 % Triton X-100 was added to each well). The plate was again incubated at 37 °C. After 24 hrs the plate was centrifuged at 250× *g* for 10 min and 80 µl of the supernatant was removed from each well and transferred to an optically clear 96-well flat bottom micro titre plate. To determine the LDH activity in these supernatants 80 µl of the Dye/Catalyst reaction mixture (as described in the manufacturer's manual) was added each well and the plate was incubated for 20 min at 25 °C. During this incubation period the plate was protected from light. The

absorbance's of the samples were measured as described in the manufacturer's manual.

To determine the percentage cell death, the average absorbance was calculated for the set of triplicates and the resulting values were substituted in the following equation:

$$\text{Percentage cell death} = \frac{\text{experimental value} - \text{low control}}{\text{high control} - \text{low control}}$$

The results were plotted on bar graph with percentage cell death on the Y-axis and the concentration of C_2-ceramide on the X-axis.

2.29.5. APOPercentage ™ assay.

This assay was performed using the APOPercentage™ Apoptosis assay (Biocolor Ltd., Patent: GB 2356929). Cells were plated and cultured in 96 well tissue culture plates as described in Section 2.29.4. The concentrations of C_2-ceramide used, varied between 0 and 100 µM. Triplicate wells were set up for each concentration. The cells were treated for 2 hrs. Thereafter the cells were gently washed with PBS. The PBS was replaced with 100 µl of APOPercentage™ dye (as described in manufacturer's manual) and the cells were incubated at 37 °C. After 1 hr staining the cells were washed twice with 100 µl PBS to remove residual dye. The cells were visually inspected using a Nikon inverted light microscope. Photographs were taken using the 20× objective. The dye trapped

inside the cells was released by the addition of 100 µl Dye Release Agent (as described in manufacturer's manual) and incubating the plate for 10 min at 25 °C. The cell bound dye recovered into solution was quantified as described in the manufacturer's manual. The results were plotted on a bar graph with absorbance on the Y-axis and the concentration of C_2-ceramide on the X-axis.

2.29.6. Caspase-3 assay.

This assay was performed using the Active Caspase-3 FITC Mab Apoptosis Kit (BD Biosciences). Cells were plated in 6-well tissue culture plates at a cell density of 2.5×10^4 cells per well and cultured for 24 hrs. The cells were treated with 60 µM C_2-ceramide. After 24 hrs the cells were washed with PBS, 500 µl trypsin (0.125 %) was added and the cells were incubated at 37 °C for 2 min until the cells started to detach (but not allowing the cells to become completely detached) and re-suspended in solution. The cells were removed by washing using 1 ml ice-cold PBS. The cells were recovered by centrifugation at 200× *g* for 2 min and the pellet was re-suspended in 500 µl Cytofix/Cytoperm™ Solution (as described in the manufacturer's manual). The cell suspension was incubated on ice for 20 min. The cells were again recovered by centrifugation and washed twice with 500 µl Perm/Wash™ Buffer. Each cell pellet was re-suspended in 100 µl Perm/Wash™ Buffer, and 20 µl anti-active caspase-3 FITC monoclonal antibody (BD Biosciences) was added. The cells were incubated at room temperature for 30 min and then washed once with 1 ml Perm/Wash™ Buffer. The cells were harvested by centrifugation for 2 min at 200× *g* and re-suspended in 500 µl Perm/Wash™

buffer and analysed by flow cytometry. Forward Scatter (FSC) and Side Scatter (SSC) were used to differentiate normal and apoptotic cells from cell debris. The cell fluorescence was measured by flow cytometry using the FL1 channels on a FACSan (Becton Dickinson) instrument. A minimum of 10 000 cells per sample were acquired and analysed using CELLQuest PRO software (BD Biosciences).

2.29.7. Mitochondrial depolarisation assay.

Cells were plated in 6-well tissue culture plates at a cell density of 2.5×10^4 cells per well and cultured for 24 hrs. The cells were treated for different time intervals (0 min, 2 hrs, 3 hrs and 6 hrs) with 60 µM C_2-ceramide. After treatment the cells were washed with PBS, 500 µl trypsin (0.125 %) was added and the cells were incubated for 2 min at 37 °C. Cells were removed by vigorous washing using PBS. The cells were then recovered by centrifugation and re-suspended in 1 ml Ham's F12 medium containing 10 µg/ml JC-1 dye. The cell suspension was mixed and incubated for 15 min at room temperature in the dark and analysed by FACS. Forward Scatter (FSC) and Side Scatter (SSC) were used to differentiate normal and apoptotic cells from cellular debris. The cell fluorescence was measured by flow cytometry using both the FL1 and FL2 channels on a FACScan (Becton Dickinson) instrument. A minimum of 10 000 cells per sample were acquired and analysed using CELLQuest PRO software.

2.30. Fluorescence microscopy.

Cells were cultured on sterile cover slips. For analysis the cells were washed twice with PBS, fixed in Paraformaldehyde Fixative for 15 min and rinsed three times with 2 ml PBS. This was followed by a 2 min permeabilisation by incubation with 2 ml PBS containing 0.1 % Triton X-100. The cover slips were washed twice with 2 ml PBS and then incubated for 30 min in PBS-BSA (PBS, containing 0.5 % BSA). The primary antibody (polyclonal anti-rabbit anti-mouse endozepine) was diluted (1:10 000) in PBS-BSA. 50 µl of the diluted primary antibody was placed on top of the cover slips (cells facing up) and incubated for 60 min, followed by two 5 min washes with PBS. The secondary antibody (donkey anti-rabbit IgG-Rhodamine, Santa Cruz Biotechnology) was diluted 1:100 in PBS-BSA. 50 µl of the diluted secondary antibody was placed on top of the cover slips and incubated for 60 min, followed by two 5 min washes with PBS. DAPI was diluted 1:1000 in PBS-BSA and 50 µl of the diluted DAPI was placed on top of the cover slips. The cover slips were washed twice in PBS before being mounted on microscope slides and viewed using a Zeiss Axioplan fluorescence microscope. Images were captured using a Spot RT Digital camera.

2.31. Primers used.

Primers were synthesised using a PCR-Mate EP™ Model 391 DNA Synthesiser (Applied Biosystems). Primers were synthesised at a 0.2 mM scale on the appropriate synthesis column as prescribed by the manufacturer. The primers were eluted from the column by manual deprotection and cleavage

(manufacturer's manual). The quality of the primers was verified by electrophoresis on 12 % polyacrylamide gels as described in Section 2.17.2. Quantification of primers was performed by measuring the optical density at 260 nm in a spectrophotometer (one OD_{260} unit of single stranded DNA equals 33 ng/ µl).

Table 2.5. Primer sequences.

Primer	Sequence	Reference
00-94	5' CAT GCT AGA TCT ATG AGC CAA GTG G 3'	Figure 6.1
00-95	5' GAA GAC CTC GAG TTA GCA TGG CTC 3'	Figure 6.1
1034	5' CTA GCT TGC CAA ACC TAC AG 3'	Figure 2.4
1038	5' GGC TTT TTC ATA TCT CAT TGC 3'	Figure 2.4
1037	5' TGT TTA TCG GCA CTT TGC ATC GG 3'	Figure 2.4
883	5' GTC AAGCAC TTC CGG AAT CG 3'	Figure 2.4
884	5' GAA GTT TCT GAT CGA AAA GTT CGA CAG CG 3'	Figure 2.4
M13 F	5' GTT TTC CCA GTC ACG ACG TTG TA 3'	
M13 R	5' TTG TGA GCG GAT AAC AAT TTC 3'	

CHAPTER 3: GENERATION OF APOPTOSIS-RESISTANT MUTANTS.

3.1. Introduction.

3.2. An investigation into the effects of DMSO on CHO22 cells in culture.

3.3. Screening C_2-ceramide as an inducer of apoptosis in CHO22 cells.

3.4. Screening camptothecin as an inducer of apoptosis in CHO22 cells.

3.5. Optimisation of C_2-ceramide and camptothecin-induced apoptosis.

3.6. Promoter-trap mutagenesis of CHO22 cells.

3.7. Summary.

CHAPTER 3: GENERATION OF APOPTOSIS-RESISTANT MUTANTS.

3.1. Introduction.

Apoptosis can be induced by various stimuli. Inducers of apoptosis include physiological factors such as Fas-ligands, neurotransmitters, growth factor withdrawal, loss of matrix attachment; damage related inducers such as heat shock, viral infection, bacterial toxins; therapy-associated agents such as cisplatin, vincristine, bleomycin, doxorubicin, staurosporine and toxins such as ethanol (Thompson, 1995).

Ceramide and camptothecin are described in the literature as chemical compounds that will induce apoptosis in cultured cells. Ceramide is a sphingosine-based lipid, acting as a second messenger-signalling molecule and is also known to regulate cellular differentiation, proliferation and apoptosis (Obeid *et al.*, 1993). Ceramide can be synthesised either by ceramide synthase, which is located in the endoplasmic reticulum and mitochondria, or by the hydrolysis of sphingomyelin in cell membranes by sphingomyelinase. Sphingomyelin hydrolysis and the generation of ceramide have been linked to the regulation of cellular differentiation (Hannun and Bell, 1989).

N-Acetyl-D-sphingosine or C_2-ceramide (Sigma) is a cell permeable synthetic analogue of ceramide. It has been demonstrated that C_2-ceramide induces apoptosis in U937 monoblastic leukaemia cells in culture (Obeid *et al.*, 1993) This study also showed that C_2-dihydroceramide was unable to induce apoptosis in cells. This suggested a critical role for the sphingolipid double bond in C_2-ceramide and that the action of ceramide was dependent on the interaction of this molecule with specific cellular targets. Various other studies have shown that C_2-ceramide was able to induce the typical morphological changes observed when cells undergo apoptosis. The use of synthetic analogues of ceramide has been instrumental in gaining further insights into the role of endogenous ceramide during apoptosis. It has been demonstrated that the use of C_2-ceramide to induce apoptosis in certain cell types (Jurkatt and HL60) is associated with increased caspase activity (Tepper *et al.*, 1997; Smyth *et al.*, 1996). Another study has shown that the activation of caspase-3 and subsequent PARP cleavage when AK-5 tumour cells are treated with C_2-ceramide (Anjum *et al.*, 1998). However, the cell death induced in B-chronic lymphocytic leukaemia (B-CLL) cells occurred in the absence of increased caspase activity. This demonstrated that the induction of apoptosis could be cell type specific (Mengubas *et al.*, 1999). All this evidence prompted an investigation into the use of C_2-ceramide to induce apoptosis in CHO22 cells.

Camptothecin, a compound isolated from the plant *Camptotheca acuminata*, has shown significant activity against a broad range of tumours (Liu *et al.*, 2000). It is

known that the anti-tumour activity of camptothecin can be linked to its ability to bind the enzyme, DNA topoisomerase I. DNA topoisomerase I catalyses the relaxation of super coiled DNA through the cleavage of double stranded DNA and the formation of a phosphotyrosyl bond between the cleaved DNA and the active site tyrosine on the enzyme (Fiorani and Bjornsti, 2000). Camptothecin inhibits the activity of topoisomerase I by blocking the re-ligation of the DNA strands after cleavage. Camptothecin reversibly stabilizes the covalent topoisomerase I/DNA intermediate by preventing DNA re-ligation, which results in the accumulation of these complexes. Potential collisions between these topoisomerase I/DNA complexes and advancing replication forks during the S-phase of the cell cycle contribute to the toxicity of camptothecin by increasing DNA damage, which activates stress-associated signalling pathways that may ultimately induce apoptosis. Camptothecin (Roche) has been used extensively to induce apoptosis in cultured cells. This has been demonstrated with leukaemia cells (HL60 and P388), which undergo apoptosis when treated with the camptothecin (Dassonneville *et al.*, 2000). This study shows that cells treated with camptothecin display internucleosomal degradation of genomic DNA, cleavage of PARP and morphological changes consistent with apoptosis.

The first objective of this section of the study was to identify suitable chemical reagents that could be used to induce apoptosis in CHO22 cells in culture. Once suitable chemical inducers of apoptosis were identified, the next step was identify the optimal selection conditions to generate somatic cell mutants by retroviral promoter-

trap mutagenesis and to select for mutants that were resistant to apoptosis induced by these substances.

3.2. An investigation into the effects of DMSO on CHO22 cells in culture.

DMSO (dimethyl sulphoxide) has been widely used as a solvent, as a surfactant and as a stabiliser in long-term cell culture and as a cryoprotectant in preserving cells in freeze-thaw processes (Lin *et al.*, 1995). DMSO has been documented to affect cell proliferation and differentiation (Lampugnani *et al.*, 1987). It has also been shown that DMSO can be used as a reversible G1 arresting agent for the synchronisation of Raji Burkitt's lymphoma cells which ultimately can lead to the induction of apoptosis (Lin *et al.*, 1995). This effect was observed when cells were exposed to DMSO concentrations ranging from 1 to 2 %. At higher concentrations it was observed that DMSO is capable of inducing apoptosis in cultured cells. DMSO was used in this research as a solvent for both C_2-ceramide and camptothecin. To eliminate any potentially conflicting results due to the presence of this solvent, a series of experiments aimed at investigating the effects of DMSO on CHO22 were undertaken.

CHO22 cells were plated and treated with DMSO as described in Section 2.29.1. Figure 3.1 shows the morphological effects (changes in cell density and cell shape) exerted by DMSO on CHO22 cells after a 72 hr treatment with DMSO concentrations varying between 0.1 and 5 %. Figure 3.1-**A** represents the untreated control, which

shows that the cell density was decreasing in relation to Figure 3.1-**B**, -**C** and -**D**. Figure 3.1-**A** also show that the cells were beginning to show signs of cell shrinkage after 72 hrs. These effects on the untreated control cells can be ascribed to depletion of the growth medium since the medium was not replaced during the 72 hr duration of the experiment. Figures 3.1-**B**, -**C** and -**D** represent cells treated with 0.1, 0.5 and 3 % DMSO, respectively. The cell density in these flasks is clearly much higher than that observed in Figures 3.1-**A** (the untreated control). In addition, the cells treated with these concentrations of DMSO appear to be healthier (i.e. did not show signs of cell shrinkage) compared to the untreated control. At concentrations higher than 3 %, DMSO induces massive cell detachment, which is evident in Figure 3.1-**F** (cells treated with 5 % DMSO). These results confirms previous reports that cells treated with DMSO concentrations below 2 %, protects cells from cell death and that higher concentrations may induce cell death through apoptosis. These results further suggests that a DMSO concentration below 0.1 % will be an appropriate concentration to use in an experiment that aims to investigate the apoptotic effects of substances (such as C_2-ceramide and camptothecin) on CHO22 cells.

3.3. Screening C_2-ceramide as an inducer of apoptosis in CHO22 cells.

CHO22 cells were plated in 25 cm^2 tissue culture flasks and treated with C_2-ceramide as described in Section 2.29.2. Figure 3.2 demonstrates the morphological effects exerted by C_2-ceramide. Figure 3.2-**A** represents the untreated control, while **B**

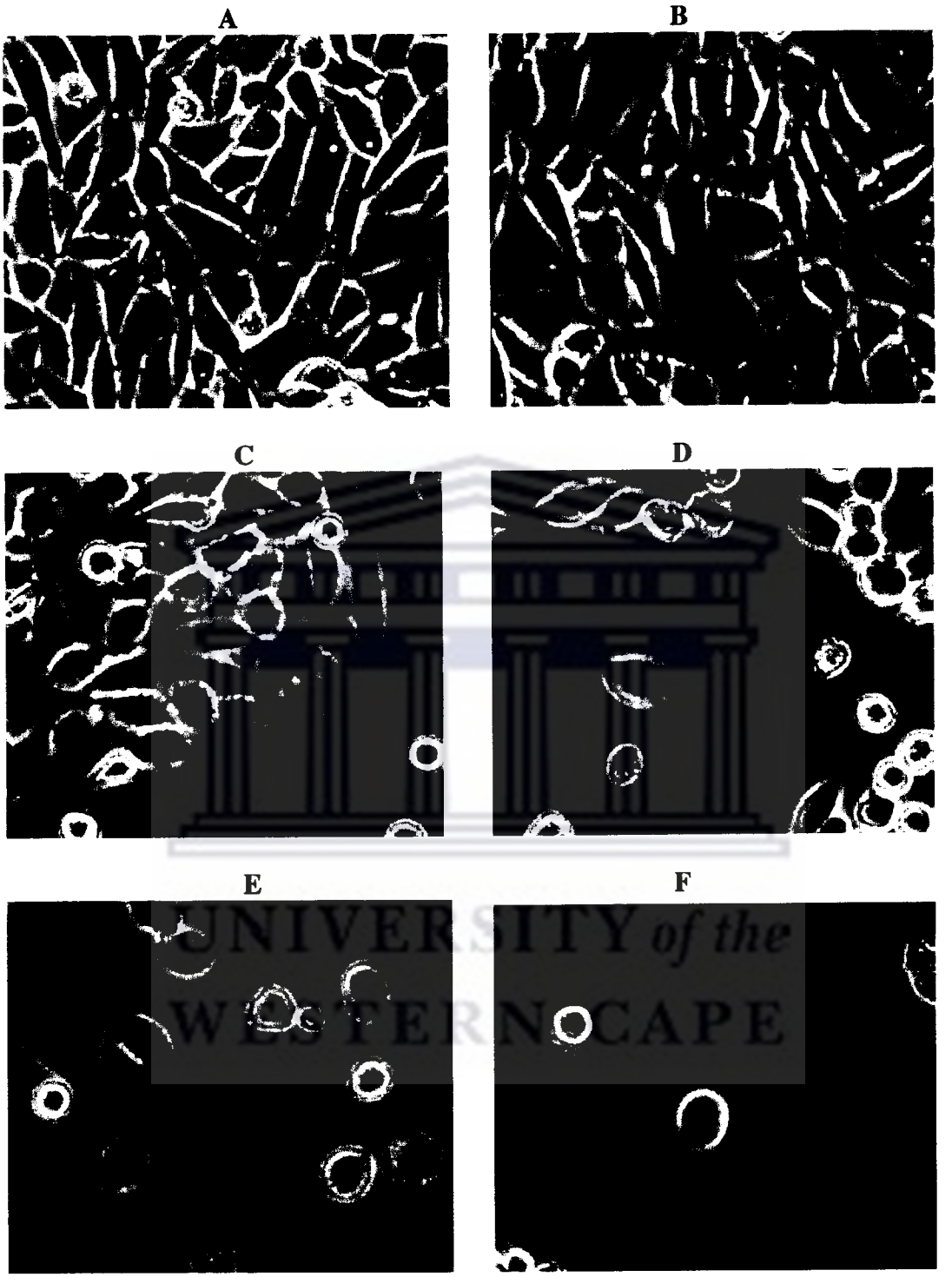

represents cells treated with 0.1 % DMSO for 24 hrs. Both these flasks show the same cell density, suggesting that 0.1 % DMSO does not adversely affect cell growth. Figures 3.2-**C**, -**D**, -**E** and -**F** represent cells treated with 40 μM, 60 μM, 80 μM and 100 μM C_2-ceramide, respectively. These flasks show a decrease in cell density, which is inversely proportional to an increase in the C_2-ceramide concentration. In addition, these cells also express phenotypic characteristics (cell shrinkage, membrane blebbing and cell detachment) that can be associated with apoptosis.

To confirm whether the effects observed in the cells treated with C_2-ceramide were the consequence of apoptosis; the cells were harvested by trypsinisation, the DNA isolated and assayed for DNA fragmentation as described (Section 2.29.3). Figure 3.3 illustrates the results the DNA fragmentation assay. Lane-**B** and -**C** represents DNA isolated from the untreated control and cells treated with 0.1 % DMSO, respectively. The DNA isolated from these cells appears as a single high molecular weight intact fragment on the gel, which suggests the absence of DNA degradation, which also means that these cells did not undergo apoptosis. Lanes-**D**, -**E**, -**F** and -**G** represents DNA isolated from cells treated with 40 μM, 60 μM, 80 μM and 100 μM C_2-ceramide, respectively. The DNA isolated from these cells show evidence of DNA fragmentation into a 200 bp ladder, which is a hallmark of apoptosis. This result demonstrates that C_2-ceramide is able to induce apoptosis in CHO22 cells treated for 24 hrs with concentrations varying between 60 μM and 100 μM. It also shows that DMSO does not induce apoptosis at a concentration of 0.1 %.

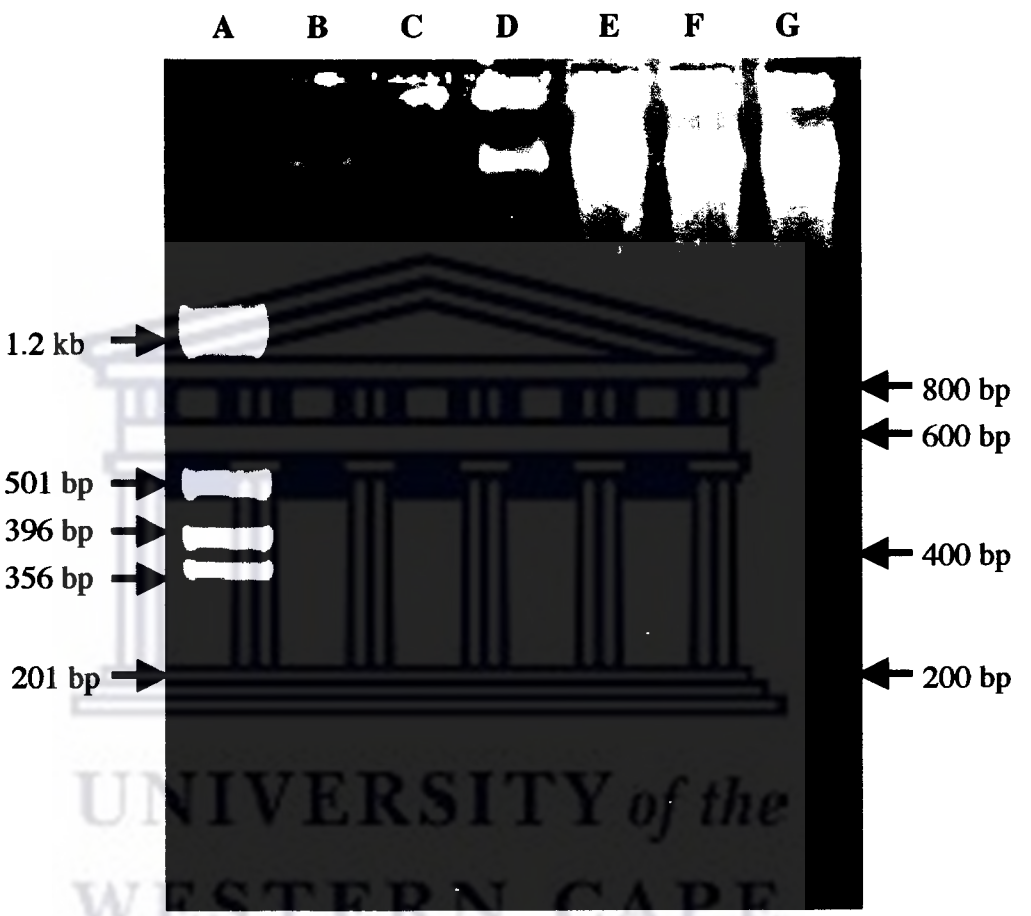

3.4. Screening camptothecin as an inducer of apoptosis in CHO22 cells.

CHO22 cells were plated as described in Section 2.29.2. The cells were treated with camptothecin for 24 hrs. The concentrations of camptothecin varied between 0 and 6 μg/ml. The cells were monitored for morphological changes and photographs were taken 24 hrs after treatment.

Figure 3.4 shows the morphological effects exerted by camptothecin on CHO22 cells. Figure 3.4-**B** represents the untreated control. Figures 3.4 -**C**, -**D**, -**E** and -**F** represent the cells treated with 1 μg/ml, 2 μg/ml, 4 μg/ml and 6 μg/ml camptothecin, respectively. Cells treated with camptothecin showed similar morphological features (cell shrinkage, membrane blebbing and cell detachment) and decrease in cell density with increasing camptothecin concentration, as was observed in CHO22 cells treated with C_2-ceramide.

After 24 hr treatment with camptothecin the cells were harvested by trypsinisation, the DNA isolated and assayed for DNA fragmentation (Section 2.29.3). Figure 3.5 shows the results of the DNA fragmentation assay. Lane-**B** shows DNA isolated from the untreated control cells, which appeared as a high molecular weight intact fragment. Lanes-**C**, -**D**, -**E** and -**F** show DNA isolated from cells treated for 24 hrs with camptothecin concentrations varying between 1 μg/ml and 6 μg/ml. This result demonstrates that camptothecin is able to induce apoptosis in CHO22 cells treated for 24 hrs with concentrations varying between 1 μg/ml and 6 μg/ml.

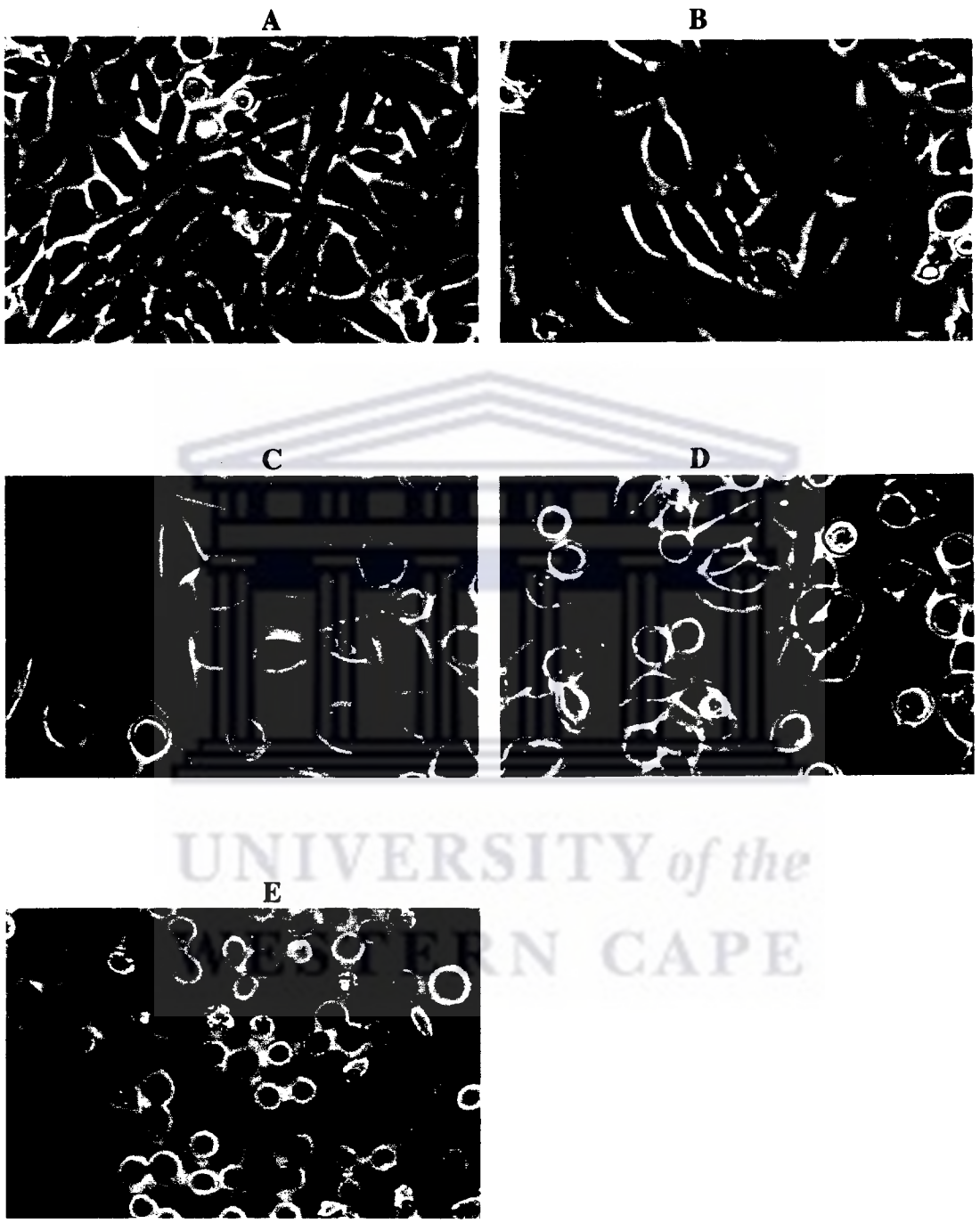

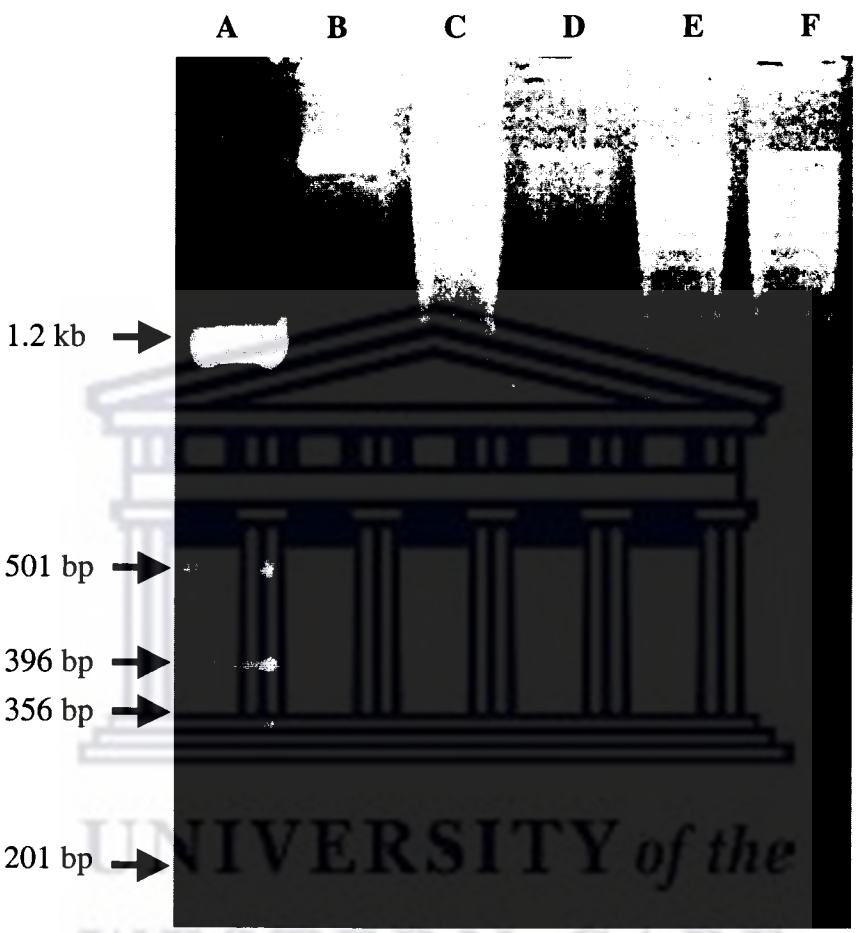

3.5. Optimisation of C_2-ceramide- and camptothecin-induced apoptosis.

The aim of these experiments was to identify the optimal exposure time to C_2-ceramide and camptothecin required to achieve 100 % killing of CHO22 cells. Since the strategy was to use these chemicals to isolate promoter-trap mutants that are resistant to apoptosis, it was important to verify that any cell clone that survived the selection process was a resistant clone resulting from promoter-trapping and not a false positive resulting from insufficient treatment of the cells.

CHO22 cells were seeded in 25 cm^2 tissue culture flasks as described in Section 2.29.2. The cells were treated with 100 μM C_2-ceramide for different time intervals. These time intervals varied between 0 and 96 hrs. In a separate experiment, cells were seeded and treated with 5 μg/ml camptothecin for the same time intervals. After treatment the supernatant was removed, the cells were washed with PBS and fresh media was added to the flasks. The cells were cultured for a further two weeks, changing the media every third day. During this time the cells were monitored for recovery (data not shown). This experiment demonstrated that a 72 hr treatment with 100 μM C_2-ceramide or a 24 hr treatment with 5 μg/ml camptothecin is sufficient to achieve 100 % killing and that these conditions and inducers would be suitable to select for apoptosis resistant mutants. Exposure times less than 72 hrs to 100 μM C_2-ceramide or 24 hrs to 5 μg/ml camptothecin was not adequate to ensure 100 % killing, as some cells were able to recover from such treatments (data not shown). Although this data show that camptothecin can be used in this selection system it was

not used in the promoter-trapping mutagenesis of CHO22 cells to identify genes involved in apoptosis.

3.6. Promoter-trap mutagenesis of CHO22 cells.

CHO22 cells were mutagenised using the promoter-trap retrovirus, tkneoU3hygro, as described in Section 2.6.2. Flask 1 is the untreated control. The cells in Flask 2 were treated with 0.6 mM hygromycin B. This flask represents a control testing for background resistance in CHO22 cells to hygromycin B. Cells in Flask 3 were treated with for 72 hrs with 100 μM C_2-ceramide. These controls tested for background resistance to C_2-ceramide under these selection conditions. These results confirm previous data (Section 3.5), which illustrated that these selection conditions were sufficient to achieve 100 % cell death in CHO22 cells.

Cells in Flask 4 were infected with the retrovirus and maintained in Ham's F12 for the duration of the experiment. This control tested the effect of the 6 hr retroviral infection on the cells. The similarity in cell density between this flask and the untreated control (Flask 1) at the end of the experiment suggests that the retroviral infection did adversely affect the growth of the cells.

Cells in Flask 5 were selected with G418 (neomycin) after retroviral infection. The retrovirus contains a neomycin resistance gene that is under the control of a

thymidine kinase promoter (Section 1.8). This gene is constitutively expressed upon viral integration into the host genome and (unlike the promoterless hygromycin B resistance gene) the expression of this gene does not require integration downstream of a host promoter. Hence this control gives an indication of the total number of retroviral integration events into the target cells.

Flask 6 is the experimental flask in which the apoptosis resistant clones were generated. After retroviral infection the cells were selected with 0.6 mM hygromycin B. Resistance to hygromycin B is dependent on the expression of the hygromycin B resistance gene, which in turn is dependent on retroviral integration downstream of a cellular promoter. Hence, selection with hygromycin B will result in the death of cells which were either not infected with the retrovirus or cells which were infected but where retroviral integration did not occur downstream of a host promoter. Selecting the virus-infected cells with hygromycin B produced about 300 colonies (representing the promoter-trap events). These colonies were then selected with C_2-ceramide (Flask 6). Cells that survived this selection process were promoter-trap mutants, which had lost the expression of a gene that is required for the activation of apoptosis by these compounds. After three weeks 5 resistant colonies were generated in Flasks 6. To eliminate the possibility that these 5 colonies resulted from clone scatter and to ensure that each colony is a distinct clone, the cells from Flasks 6 were pooled and sub-cloned as described in Section 2.5. The sub-clones generated from Flask 6 were designated cerR1, cerR2 and cerR3. As a pilot experiment this demonstrated the

feasibility of using this technology to generate cell mutants that are resistant to apoptosis induced by C_2-ceramide.

Table 3.1 Summary of the results for promoter-trap mutagenesis.

Flask	Retrovirus (R)	Hygromycin B (H) or G418 (G)	C_2-ceramide (C_2)	No. of cell colonies
1	-R	-H/-G	- C_2	> 2.5×10^6
2	-R	+H	-C_2	0
3	-R	-H/-G	+C_2	0
4	+R	-H/-G	- C_2	> 2.5×10^6
5	+R	+G	- C_2	~3×10^4
6	+R	+H	+C_2	~5

3.7. Summary.

The investigation into the effects of DMSO on CHO22 cells demonstrated some of the protective effects of DMSO at concentrations varying between 0.1 and 3 %. Cells treated with these concentrations of DMSO were able to endure the effects of serum deprivation better than the untreated control cells. DMSO concentrations higher than 3 % induced morphological changes such as cell shrinkage, membrane blebbing, growth-inhibition and cell detachment in CHO22 cells. All these features are hallmarks of apoptosis. The DNA fragmentation assay showed that DMSO is not able to induce apoptosis at a concentration of 0.1 % and therefore when used at these

concentrations as a solvent, DMSO should not interfere with or enhance the ability of the tested compound (C_2-ceramide and camptothecin) to induce apoptosis.

C_2-ceramide and camptothecin both induce apoptosis in CHO22 cells. Treatment of CHO22 cells for 72 hrs with C_2-ceramide concentrations varying between 40 μM and 100 μM, or for 24 hrs with camptothecin concentrations varying between 1 μg/ml and 6 μg/ml, were able to induce morphological changes (cell shrinkage, membrane blebbing, growth inhibition and cell detachment) and biochemical features (DNA fragmentation) in CHO22 cells which can be linked to apoptosis.

The aim of this study was to use C_2-ceramide and camptothecin to select for promoter-trap mutants of CHO22 cells that were resistant to apoptosis. It therefore follows that the selection conditions (exposure time and concentration) should be sufficiently stringent to ensure that the clones that survive the selection process are resistant to apoptosis due to retroviral promoter-trapping and not due to inadequate selection. This will eliminate the possibility of false positive apoptosis resistant clones (this could also be considered as background resistance). Optimisation of the selection conditions for the use of C_2-ceramide or camptothecin as inducers of apoptosis for the purpose of selecting promoter-trapped mutants that are resistant to apoptosis induced by either of these compounds, showed that a 24 hr selection with 100 μM C_2-ceramide or a 72 hr selection with 5 μg/ml camptothecin was sufficient to achieve 100 % killing. Following promoter-trap mutagenesis using the tkneoU3hygro

retrovirus, these selection conditions were used to isolate three apoptosis resistant cell lines. Three of these cell lines: cerR1, cerR2 and cerR3 were generated by selection with C_2-ceramide.

The control experiments (Flasks 2, and 3) for promoter-trap mutagenesis using the tkneoU3hygro retrovirus demonstrated the following: a) 100 % killing of CHO22 cells selected with 0.6 mM hygromycin B (Table 3.1-Flask 2), b) 100 % killing of CHO22 cells selected for 72 hrs with 100 μM C_2-ceramide (Table 3.1-Flask 3). This suggests that there is no background resistance of CHO22 cells to hygromycin B or C_2-ceramide.

The control experiments (Table 3.1-Flasks 1 and 4) demonstrated that a 6 hr infection with the tkneoU3hygro retrovirus did not affect the growth rate or survival of CHO22 cells since the number of colonies in both the infected and un-infected flasks, were the same.

The control experiment (Table 3.1-Flask 5) represents the G418 or neomycin resistance control. The cells in this flask were infected with the tkneoU3hygro retrovirus and then selected for the expression of the neomycin resistance gene that is under the control of an internal thymidine kinase promoter (Figure 1.15). A total of ~3×10^4 colonies, which also represents the total number of target cells infected by the retrovirus, survived this selection.

The cells in the experimental flask (Table 3.1-Flasks 6) were first selected for the expression of the promoterless U3 marker gene, hygromycin B phosphotransferase. Since this gene does not have a promoter it can only be expressed if retroviral integration occurred downstream of a host cellular promoter. It therefore follows that cell clones surviving selection with hygromycin B would represent promoter-trap retroviral integrations. Previous reports using the tkneoU3hygro retroviral vector (Chang *et al.*, 1993; Hubbard *et al.*, 1993; George, 1995) indicated selection for the promoterless U3 marker gene, hygromycin B phosphotransferase, generates fewer resistant colonies than selections for the internal neomycin resistance gene: about 100 times more neomycin-resistant colonies were generated than hygromycin B-resistant colonies. A similar pattern was observed in this study. This implies that the selection of Flasks 6 with hygromycin B would have resulted in ~300 hygromycin B resistant colonies since the selection for neomycin resistance generated ~3×10^4 colonies. Given that 2×10^6 cells were infected and ~3×10^4 neomycin resistance colonies were generated suggests that the multiplicity of infection was 0.01. This is significantly lower compared to a previous study (George, 1995), which reported a multiplicity of infection of 0.6. This means that the retroviral titre for the current study was significantly lower.

If it is assumed that the size of the hamster genome is 3×10^9 bp and that 1 in 100 retroviral integration events leads to hygromycin B resistance, it would imply that there is 3×10^7 target sites in the genome. It is estimated that the human genome

contains about 3×10^4 genes and this figure would probably also apply to the hamster genome. This would imply that a study that aims to screen all possible gene targets in the genome would have to generate a library of hygromycin B resistance colonies in the excess of 3×10^4 colonies to ensure that each gene in the genome is targeted at least once. In this study a total of ~300 hygromycin B resistance colonies were generated and screened for resistance to C_2-ceramide induced apoptosis. A library of ~300 hygromycin B resistance colonies represent only 1% of the genome and is therefore not sufficient to account for all the possible target sites in the hamster genome. It therefore follows that the gene(s) that would be identified from a library of ~300 hygromycin B resistance colonies would most probably not represent all the possible genes that could be involved in C_2-ceramide induced apoptosis. It should also be noted that clone scatter could potentially also affect the number of resistant clones generated in these selections. It is for this reason that colonies that appeared after selection for resistance to apoptosis were sub-cloned.

CHAPTER 4: ANALYSING RESISTANCE OF cerR1 TO APOPTOSIS INDUCED BY C_2-CERAMIDE.

4.1. Introduction.

4.2. APOPercentage™ assay.

4.3. LDH release assay.

4.4. Caspase-3 assay.

4.5. Summary.

CHAPTER 4: ANALYSING RESISTANCE OF cerR1 TO APOPTOSIS INDUCED BY C_2-CERAMIDE.

4.1. Introduction.

The objective of this section of the work was to investigate the resistance of the ceramide-resistant CHO22 derived cell line, cerR1, to apoptosis induced by C_2-ceramide. A range of biochemical assays were used to detect and quantify the induction of apoptosis in the mutant cerR1 compared to the parental CHO22 cell line. The activation of a particular apoptotic pathway is dependent on the reagent used to activate apoptosis, its concentration and to some extent also on the cell type. It is for this reason that assays that detects different morphological and biochemical changes in cells during apoptosis were used to examine the resistance of cerR1 to apoptosis.

4.2. APOPercentage™ Apoptosis assay.

The APOPercentage™ Apoptosis assay (Biocolor, Ltd.) is a colorimetric assay system that can be used to detect and quantify apoptosis (Patent: GB 2356929). The APOPercentage™ apoptosis assay detects apoptosis during the mid-phase stage of apoptosis, which coincides with the externalisation of phosphotidylserine (Fadok *et al.*, 1992). When cells undergo apoptosis, a so-called "flip-flop" mechanism results in the translocation of phosphatidylserine from the inner to the outer membrane surface (Fadok *et al.*, 1992). The APOPercentage™ apoptosis

assay exploits this mechanism to label apoptotic cells and have been used in previous studies to detect and quantify apoptosis (Joyce *et al.*, 2001; Kisseleva *et al.*, 2002). The principle of this assay is based on a purple-red dye, the disodium salt of 3, 4, 5, 6, -tetrachloro-2', 4', 5', 7'-tetraiodofluorescein, which is trapped inside cells during the translocation of phosphatidylserine. Apoptotic cells can be identified due to their purple-red stain and has this been used to quantify apoptosis. Treating the cells with a lysis buffer will release the trapped dye from the labelled cells, which can be quantified by reading the absorbance at 550 nm. There is a direct relationship between the number of apoptotic cells and the amount of dye released from the cells (Patent: GB 2356929).

CHO22 and cerR1 cells were plated in a 96-well tissue culture plate. The cells were treated with C_2-ceramide concentrations varying between 0 and 100 μM. After 2 hr treatment the cells were stained with APOPercentage™ dye as described in Section 2.29.5. Figure 4.1 shows the untreated control (**A**) and cells treated for 24 hrs with 100 μM C_2-ceramide (**B**). Apoptotic cells retain the APOPercentage™ dye and stain pink as is illustrated by Figure 4.1-**B**. The cell bound dye recovered into solution and was quantified using a microplate colorimeter as described in the manufacturer's manual. The results were plotted on a bar graph with absorbance on the Y-axis and the concentration of C_2-ceramide on the X-axis (Figure 4.2). The untreated control demonstrates a background absorbance of 0.035. This background will therefore also be present in the treated samples (40 to 100 μM C_2-ceramide). Figure 4.2 demonstrates that the mutant cell line, cerR1, is more resistant to C_2-ceramide-induced apoptosis

A

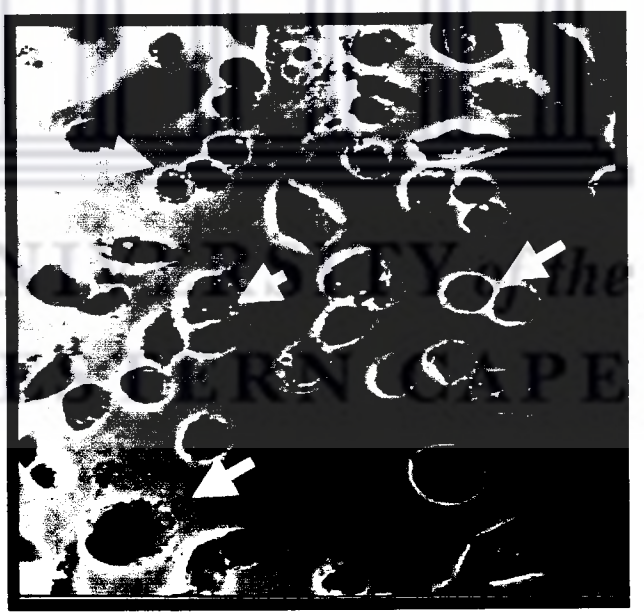

B

compared to the parental cell line, CHO22. Since the absorbances were lower for the cerR1 cells it means that less dye was released from the cerR1 cells and therefore less cells stained positive for apoptosis.

4.3. LDH release assay.

The LDH release assay or Cytotoxicity Detection Kit (Roche) is also a colorimetric assay system that can used to detect and quantify apoptosis. In contrast to the APOPercentage™ Apoptosis assay, the LDH assay detects the final stages of apoptosis. This assay does not differentiate between apoptosis and toxic cell death or necrosis. The LDH release assay determines cell death as a consequence of membrane damage. Cells undergoing apoptosis under *in vitro* conditions eventually undergo secondary necrosis leading to lysis of the cell, releasing its cytoplasmic enzymes. This is a late apoptotic event and therefore the LDH release assay can be used to quantify cell death at the final stages of apoptosis.

Lactate dehydrogenase (LDH) is one of the enzymes released from cells when this occurs. The test principle of the LDH release assay or Cytotoxicity Detection Kit is based on the cleavage of a yellow tetrazolium salt (2-[4-iodophenyl]-3-[4-nitrophenyl]-5-phenyltetrazolium chloride) in the presence of LDH to produce a red formazan salt. This reaction is catalysed by a two-step reaction that first requires LDH to convert lactate to pyruvate through the reduction of NAD^+ to NADH and H^+. In the second step of the reaction, diaphorase catalyses the

transfer of H/H^+ from $NADH/H^+$ to the tetrazolium salt leading to the formation of the red formazan salt as described in the manufacturer's manual. The amount of the red salt produced in this reaction is dependent on the LDH activity and the LDH activity is dependent on the number of cells lysed or damaged during apoptosis (Szekeres *et al.*, 1981). Thus by measuring LDH activity it is possible to indirectly quantify cell death.

CHO22 and cerR1 cells were treated as described in Section 2.29.4. The percentage cell death was determined and the results were plotted on a bar graph with percentage cell death on the Y-axis and the concentration of C_2-ceramide on the X-axis (Figure 4.3). Figure 4.3 demonstrates that the mutant cell line, cerR1, is less susceptible to cell death induced by C_2-ceramide than the parental cell line, CHO22. The extent of cell death in the ceR1 cell line is on average almost 50 % lower at all of the C_2-ceramide concentrations tested.

4.4. Caspase-3 assay.

Caspase-3 is a member of the caspase family of cysteine proteases demonstrated to play key roles during apoptosis (reviewed in Section 1.2). It is especially caspase-3 that plays a central role during apoptosis. Caspases are produced as inactive pro-enzymes that are proteolytically activated by cleavage. Polyclonal antibodies that preferentially recognise the active (cleaved) form of caspase-3 have been used to detect and quantify apoptosis (Belloc *et al.*, 2000).

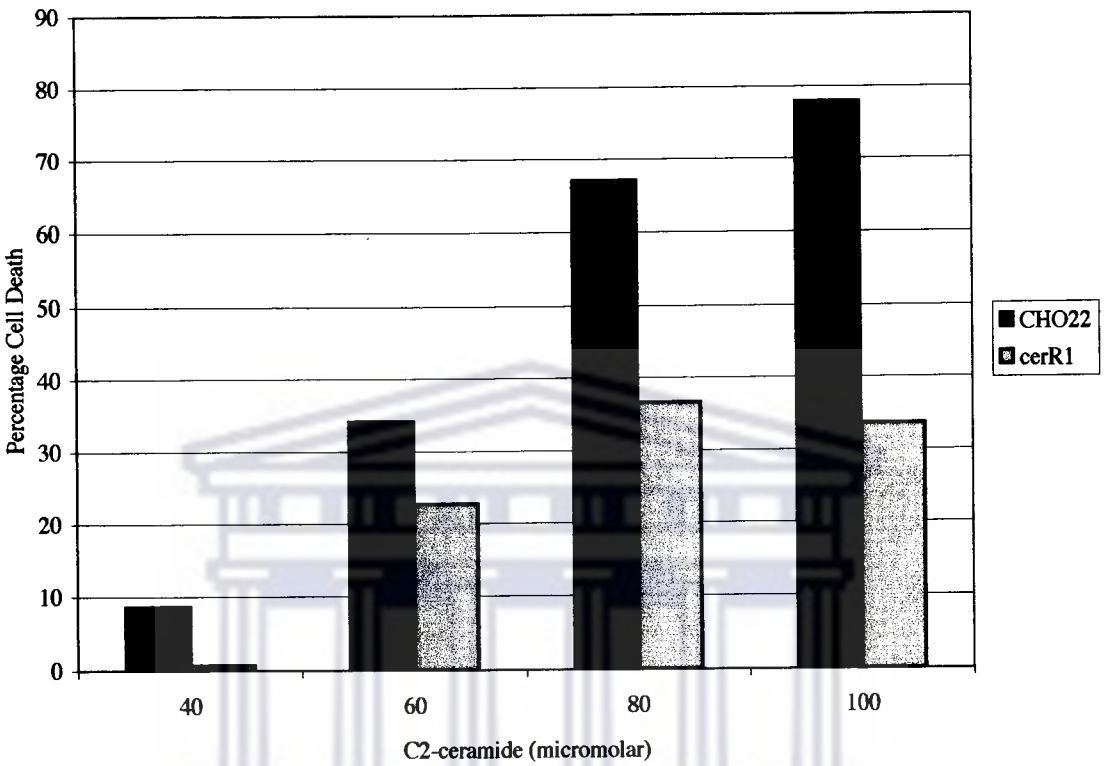

Figure 4.3. The LDH release assay demonstrating resistance of cerR1 to apoptosis induced by C_2-ceramide. Cells were treated for 24 hrs with increasing concentrations (40, 60, 80,and 100 μM) of C_2-ceramide. Cell death was calculated based on the amount of LDH released during a 24 hrs period after C_2-ceramide-treatment.

The Active Caspase-3 FITC Mab Apoptosis Kit (BD Biosciences) is an assay that measures caspase-3 activation by flow cytometric analysis. This system uses a polyclonal anti-active caspase-3 antibody that is conjugated with fluorescein isothiocyanate (FITC) (Belloc *et al.*, 2000). Caspases are synthesised as inactive pro-enzymes that are proteolytically activated by cleavage during apoptosis. Activated caspase-3 consists of a heterodimer of 17 kD and 12 kD subunits derived from a 32 kD proenzyme. The polyclonal anti-active caspase-3 antibody specifically recognises the active (cleaved) fragment of caspase-3. Since the antibody is fluorescently labelled with fluorescein isothiocyanate it is detectable by conventional flow cytometer FL1 channels.

CHO22 and cerR1 cells were treated as described in Section 2.29.6. The cells were stained with a FITC-conjugated polyclonal active caspase-3 antibody and analysed on a FACScan (Becton Dickinson) instrument. Forward Scatter (FSC) and Side Scatter (SSC) were used to differentiate normal and apoptotic cells from cell debris. The cell fluorescence was measured by flow cytometry using the FL1 channels. A minimum of 10 000 events per sample were acquired and analysed using CELLQuest PRO software (BD Biosciences) (Figure 4.4). Figure 4.4-**A** and –**B** show the caspase-3 activity in the untreated controls for CHO22 and cerR1. Less than 0.5 % of the untreated cells demonstrate the presence of active caspase-3. Figure 4.4-**C** and –**D** shows the caspase-3 activity in cells treated for 24 hrs with 60 μM C_2-ceramide. Only 4.15 % of the mutant cerR1 cells treated with C_2-ceramide stain positive for active caspase-3, compared to 22.22 % for the wild-

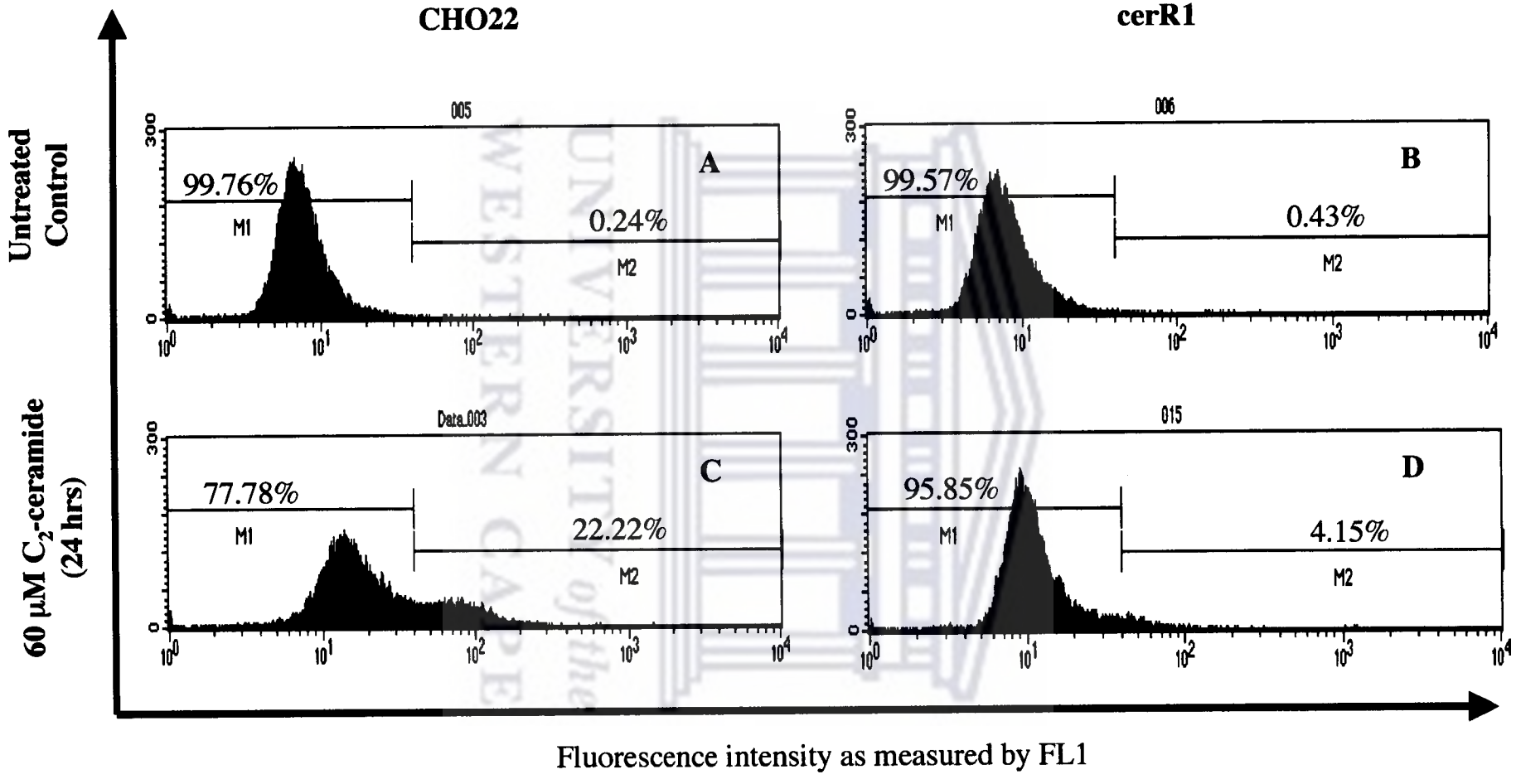

type CHO22 cells. This suggests reduced activation of caspase-3 in cerR1 after 24 hrs treatment with C_2-ceramide.

4.5. Summary.

In Section 3.3 it was demonstrated that CHO22 cells are susceptible to apoptosis induced by C_2-ceramide. Since cerR1 was derived from CHO22 it is expected that the phenotypic characteristics of these two cell lines should be alike. However cerR1 was derived from CHO22 by promoter-trap retroviral mutagenesis with the aim of generating mutants that are resistant to apoptosis induced by C_2-ceramide. Promoter-trap mutagenesis will alter the genetic composition of cerR1 and this will ultimately also be reflected in the phenotypic characteristics of this mutant cell line when compared to the parental cell line. The phenotypic characteristic that was of interest in this study was susceptibility to apoptosis. Chapter 4 aims to compare the susceptibility of the mutant cell line, cerR1 to that of its parental cell line (CHO22) to apoptosis.

The APOPercentage™ and the LDH release assays can be used to detect and quantify apoptosis. These two assays detect apoptosis at different stages of the apoptotic pathway. While the APOPercentage™ assay detects the early stages of apoptosis, the LDH release assay detects the final stages of apoptosis. Both the APOPercentage™ (Figure 4.2) and the LDH release assay (Figure 4.3) demonstrated that cerR1 is less susceptible to cell death induced by C_2-ceramide than the parental CHO22 cell line. The LDH release assay shows that the number

of cells that died as a consequence of C_2-ceramide treatment is almost 50 % lower in the mutant cell line, cerR1. This is comparable to the results obtained for the APOPercentage™ assay, even though the background for the APOPercentage™ assay was much higher compared to the LDH release assay.

The conditions for the selection of C_2-ceramide-resistant mutants were 100 μM C_2-ceramide for 72 hrs (Sections 3.5 and 3.6). The LDH release assay demonstrates a ~80 % killing of CHO22 cells treated for 24 hrs with 100 μM C_2-ceramide (Figure 4.3) which confirms that the stringency of the selection conditions were sufficient to ensure that no false positive or background resistant clones were generated during the selection for ceramide-resistant promoter-trap mutants. Figure 4.3 also shows a ~35 % killing of the cerR1 cells treated for 24 hrs with 100 μM C_2-ceramide. This result validates the feasibility of selecting for and isolating the ceramide-resistant mutant cerR1. Figure 4.4 demonstrates that the caspase-3 activity in cerR1 cells treated for 24 hrs with 60 μM C_2-ceramide is 4 times lower than for the parental cells, CHO22.

These results show that cerR1 is still susceptible to apoptosis induced by C_2-ceramide but in comparison to its parental cell line, cerR1 is more resistant to apoptosis. This embodies a phenotypic difference between cerR1 and CHO22, which can only be ascribed to genetic alterations in the mutant due to promoter-trap mutagenesis. The mutation(s) in cerR1 did not result in a complete blockage of the apoptotic pathway(s) induced by C_2-ceramide, but resulted in a reduced or delayed apoptotic response in cerR1. This is not an unexpected result since it is

well known that the activation of apoptosis does not necessarily occur through a single pathway, i.e. a single apoptotic trigger (such as C_2-ceramide) can activate numerous (or overlapping) apoptotic pathways. The mutagenesis of a single component of one of these pathways may result in the blockage of this pathway, leaving the other signalling pathways intact and functional. This scenario may result in reduced sensitivity to apoptosis rather than a total resistance to apoptosis and offers a possible explanation for the resistance of cerR1 to apoptosis induced by C_2-ceramide.

CHAPTER 5: CHARACTERISATION OF cerR1 CLONES BY INVERSE PCR AND SEQUENCE ANALYSIS.

CHAPTER 5: CHARACTERISATION OF cerR1 CLONES BY INVERSE PCR AND SEQUENCE ANALYSIS.

5.1. Introduction.

The aim of this section of the study was to characterise the mutations in cerR1, cerR2 and cerR3 sub-clones by inverse PCR. Inverse polymerase chain reaction is an extension of the conventional polymerase chain reaction that allows the amplification of unknown DNA sequences flanked by known sequences (Saiki, *et al.*, 1985). This technique has proven useful in the recovering of genomic sequences flanking viral and transposable element insertions. Another application of this technique was to amplify genomic DNA flanking integrated ecotropic proviruses in the mouse (Erlich, 1989). In the work described here inverse PCR was used to identify DNA sequence (unknown hamster genome sequence) flanking the insertion site of the promoter-trap mutagenesis retrovirus (known sequence), tkneoU3hygro.

5.2. Inverse PCR.

The first step of inverse PCR is to identify suitable restriction enzymes that will digest the genomic DNA into linear products containing the known sequence (tkneoU3hygro retroviral sequence) juxtaposed to the unknown sequence (genomic DNA) (Figure 5.1). These enzymes should digest the unknown sequence approximately 50 to 1000 bp from the junction between the known and unknown sequence. The products generated by the restriction enzymes should

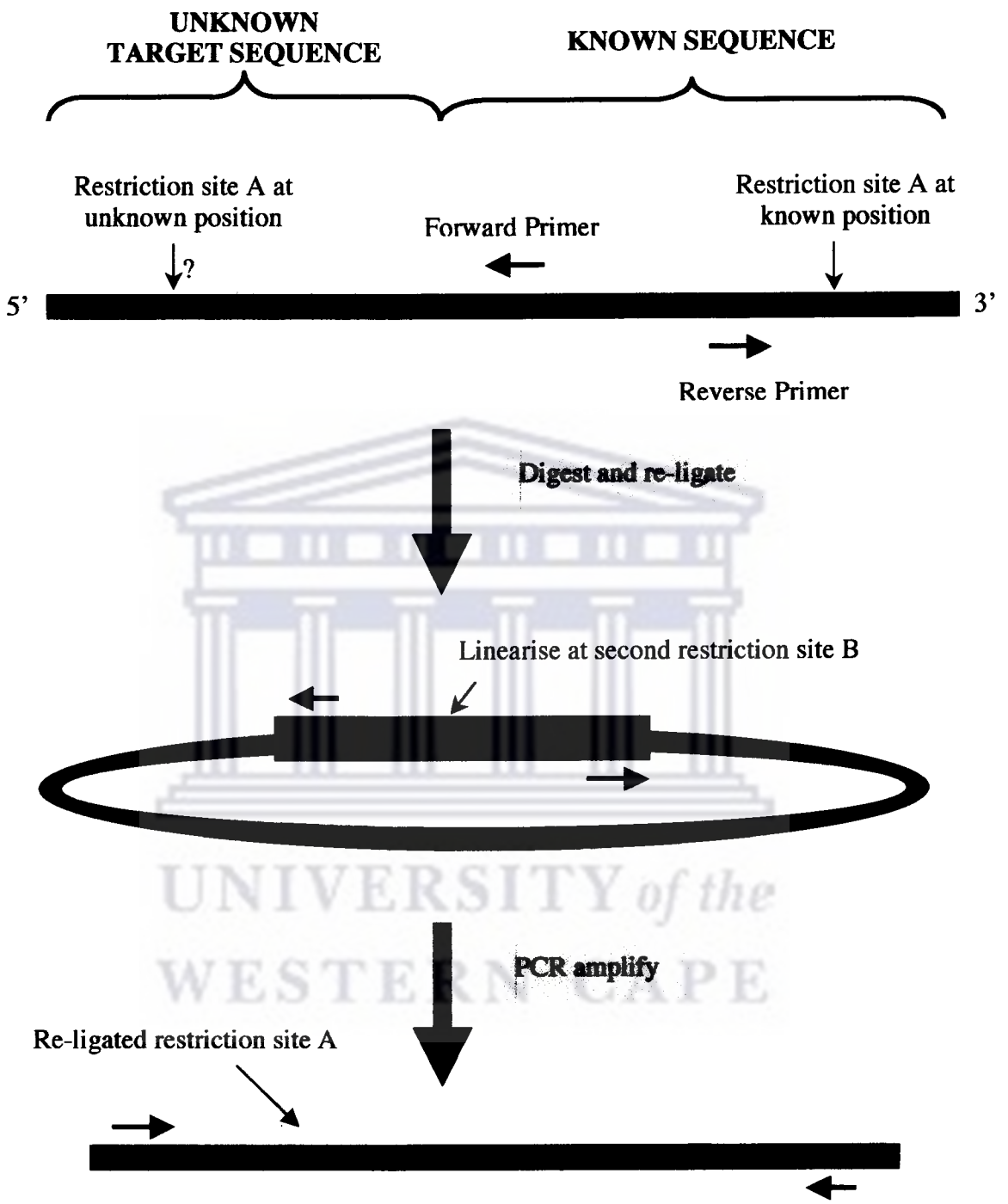

Figure 5.1. Identification of unknown sequences flanking known sequence using the inverse PCR strategy.

contain unknown sequence of adequate length so as to make it possible to identify this unknown sequence with database searches. This implies that the restriction enzyme should digest the DNA at a high frequency. Enzymes with four to six-base pair recognition sites would fulfil this criteria.

The next step is to re-ligate these linear fragments using T4-DNA ligase to generate DNA circles. It is this re-ligated DNA that is used as templates in PCR reactions. The re-ligation of these linear fragments is a crucial step in inverse PCR. There are two possible outcomes during re-ligation: the linear fragments containing cohesive ends either self-ligate to form circles or the fragments concatenate into multimeric structures (Collins and Weissman, 1998). The success of inverse PCR is dependent on the formation of these self-ligated circles rather than multimeric structures. The theoretical basis of ligation of linear polymeric molecules and DNA fragments has been experimentally tested in previous studies (Grosveld *et al.*, 1981). Considering the behaviour of a polymer in solution consisting of a series of segments of length b, joined by freely movable joints, and of total length l, then it would be possible to calculate a parameter j, that is the effective concentration of one end of a long polymer in the neighbourhood of the other using the following equation (Grosveld *et al.*, 1981):

$$j = \left[\frac{3}{2\pi lb}\right]^{3/2} \text{ Ends per ml}$$

A simplification of this equation, which is also applicable to the ligation of DNA fragments is as follow (Steinmetz *et al.*, 1982):

$$j = \frac{63.4}{(\text{kb})^{1/2}} \quad \mu\text{g per ml,}$$

where kb is the length of a DNA fragment in kilo bases. This implies that if the concentration of the DNA in a ligation reaction equals *j*, then theoretically 50 % of product of this reaction should be self-ligated circles. If the ligation is carried out at a DNA concentration, *i*, that is less than *j* the formation of circles will be favoured and therefore more that 50 % of the ligated product should be self-ligated circles. The fraction of self-ligated circles can be predicted theoretically by the following equation (Carroll *et al.*, 1984):

$$\%\ \text{self-ligated circles} = \frac{j}{i+j} \times 100$$

When digesting genomic DNA the target sequences are unknown and therefore the restriction sites and fragment lengths generated by digestion cannot be predicted. However, applying these equations it is possible to predict the DNA concentrations and set up ligation reactions that will favour the re-ligation of a linear DNA fragment of particular size and this can significantly increase the success of the inverse PCR.

PCR amplification of circular DNA can also pose a problem due to the physical constraints amplifying highly coiled circular DNA. This problem can be solved by digesting the self-ligated DNA circles with an enzyme that cuts inside the known DNA sequence, between the primer sites, thus linearising the circular DNA and making PCR amplification easier (Figure 5.1). However this strategy will only be successful if there are no other restriction sites for this enzyme inside the unknown DNA sequences flanking the known sequence.

Figure 2.5 illustrates how the inverse strategy was used in this study to identify the hamster genomic DNA sequences flanking the integrated promoter-trap retrovirus. The strategy involved the isolation of genomic DNA from the mutant cell lines, which was then digested with the Tsp509 I restriction enzyme to generate fragments that contained part of the known sequence (tkneoU3hygro retroviral sequence) juxtaposed to the unknown sequence (genomic DNA). The digested DNA was re-ligated at concentrations that will favour the re-ligation of DNA fragments of between 200 and 500 base pairs. These concentrations were determined by the equations described above. The re-ligated DNA was first linearised using the Aat II enzyme before it was used as a template in PCR reactions.

5.2.1. Characterisation of cerR1, cerR2 and cerR3 using inverse PCR.

Genomic DNA was isolated from cerR1, cerR2 and cerR3 as described in Section 2.7. The genomic DNA was digested with Tsp 509 I as described in Section 2.16.

The digested DNA was electrophoresed on an agarose gel to verify complete digestion. Figure 5.2 shows the quality of the genomic DNA isolations and digestions. Lanes-**B**, **-D** and **-F** shows the undigested DNA isolated from cerR1, cerR2 and cerR3. Indicated in these lanes is the presence of a high molecular weight fragment representing the undigested genomic DNA and two smaller fragments representing RNA. As expected the RNA appears to be degraded since no RNAse inhibitors were used in the isolation of the genomic DNA. Lanes-**C**, **-E** and **-G** shows genomic DNA digested with Tsp 509 I, which appear to be completely digested.

Inverse PCR reactions were performed as described in, Section 2.16. The products of the first round inverse PCR reaction were electrophoresed on an agarose gel. Figure 5.3 shows the results of this PCR. Lane-**B** represents the negative control (no DNA added), while lanes-**C**, **-D** and **-E** represents inverse PCR products generated for cell lines cerR1, cerR2 and cerR3, respectively. For each of these cell lines four inverse PCR products were generated. The sizes of these products vary between 350 bp and 1 000 bp. The size distribution of the four inverse PCR products was identical for the four cell lines suggesting the cerR1, cerR2 and cerR3 originate from the same clone. It is expected that inverse PCR should produce two inverse PCR products (Section 2.16). However, inverse PCR on cerR1, cerR2 and cerR3 produced three additional PCR products, which could be the consequence of multiple retroviral integration into the hamster genomic DNA during promoter-trapping or the additional inverse PCR products could have been produced by the formation of multimeric structures during re-ligation of the Tsp

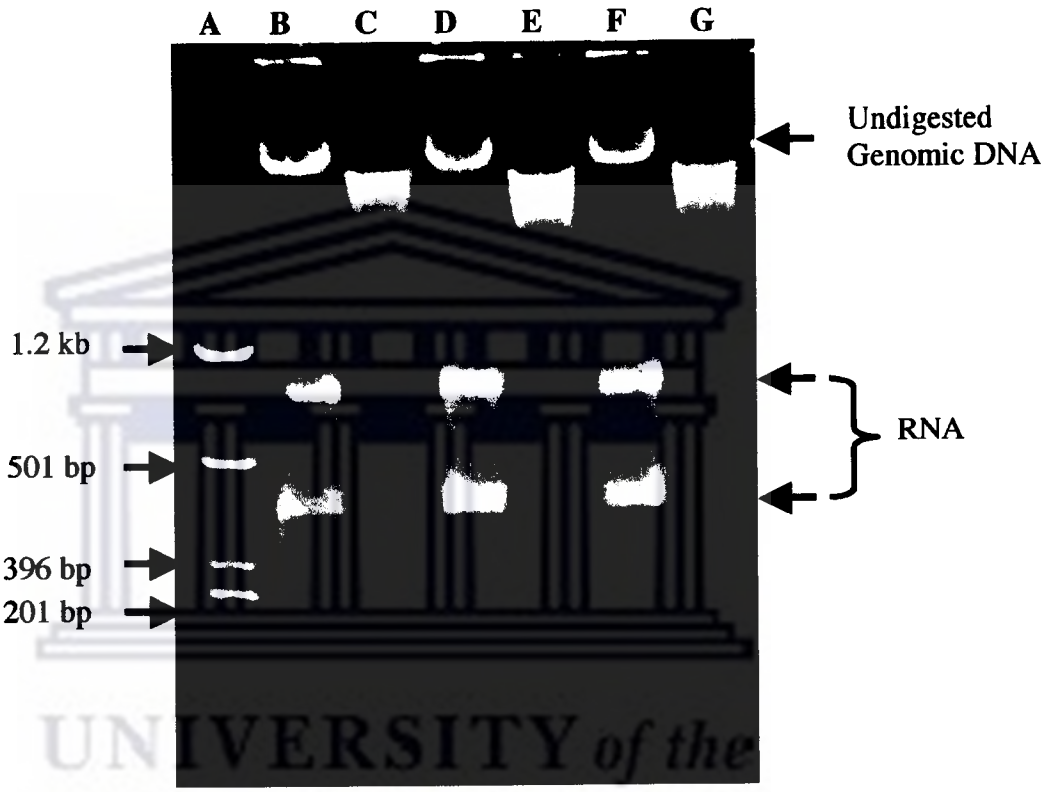

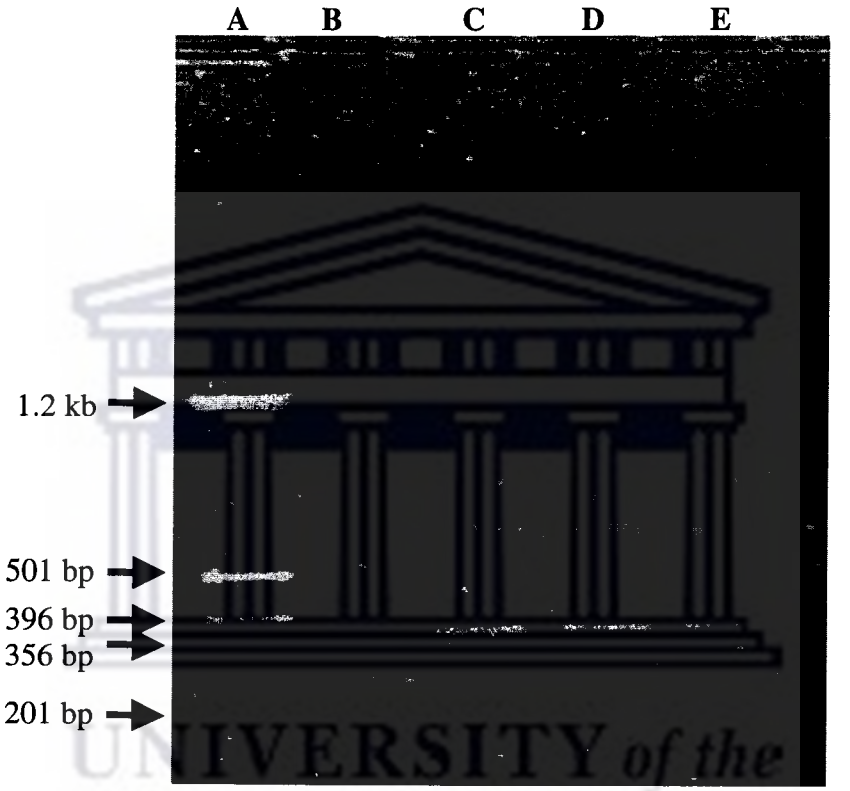

509 I digested genomic DNA. Sequence analysis of these inverse PCR products was undertaken to shed more light on this question.

5.2.2. Sequence analysis of cerR1.

A second round PCR reaction was performed for cerR1 and cerR2 as described in Section 2.16. The products of the second round inverse PCR were electrophoresed on a 5 % polyacrylamide gel. Figure 5.4 shows the results of this PCR. Lane-**D** represents the negative control (no DNA was added), lane-**B** inverse PCR on cerR1 and lane-**C** inverse PCR on cerR2. The second round inverse PCR also produced five inverse PCR products, similar to the first round PCR. However the sizes of these inverse PCR products are expected to be smaller than in the first round PCR since nested PCR primers were used. This is not very well reflected in a comparison of Figures 5.3 and 5.4. However, this could be ascribed to variation in DNA mobility since Figure 5.3 is an agarose gel while Figure 5.4 is an acrylamide gel. Re-amplification of the first round inverse PCR products also significantly increased the amount of product generated. These inverse PCR products were designated F1, F2, F3, F4 and F5 (Figure 5.4). The size of the F5 inverse PCR product corresponds to the expected size (260 bp) for the 3' end retroviral sequence and therefore it is expected that the other four inverse PCR products (F1, F2, F3 and F4) were produced from the 5' end of the virus and consequently these sequences should also contain genomic hamster DNA sequence (Figure 2.6). The inverse PCR products: F1, F2, F3 and F4 were isolated from the polyacrylamide gel using the procedure described in Section 2.18.2. The

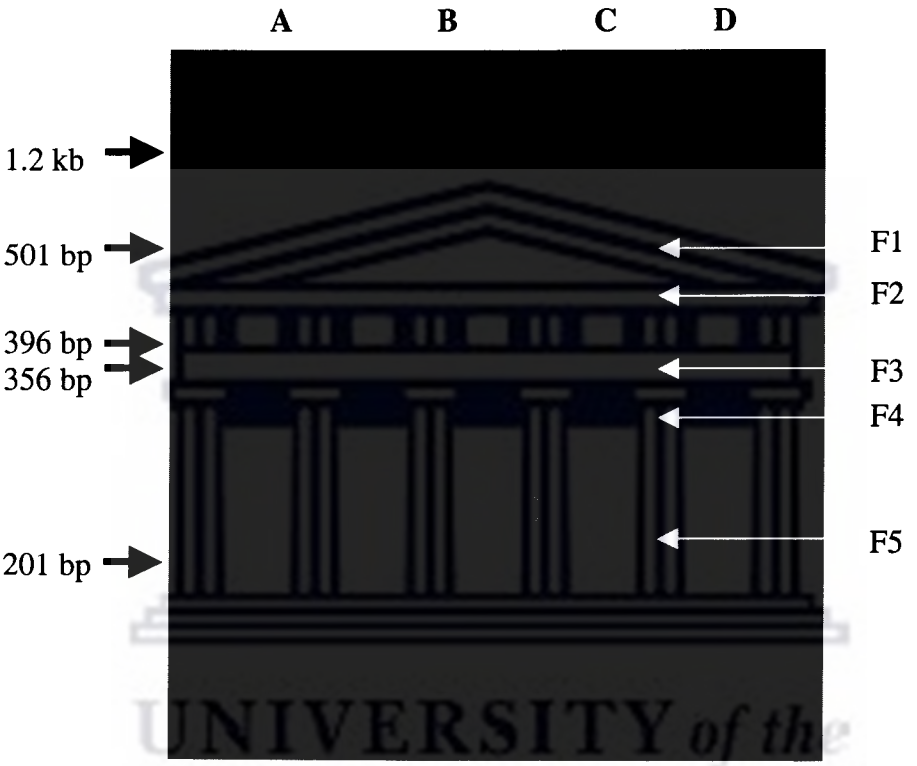

isolated DNA was sequenced directly using primer 1037 as described in Section 2.21. Figure 5.5 shows sequence data generated for the F1 inverse PCR product as an example of the quality of the sequence data generated for the four inverse PCR products.

5.2.3. BLAST analysis of the sequences generated for cerR1.

It is expected that the sequences generated for inverse PCR products F1, F2, F3 and F4 should include a region representing the known sequence (tkneoU3hygro retroviral sequence) next to the unknown sequence (hamster genomic DNA) (Figure 5.1). Since Tsp 509 I was used to digest the genomic DNA it is also expected that this restriction site should be present in the sequence at the junction between the known and unknown sequences. Primer 1037 is positioned inside the hygromycin resistance gene sequence about 50 bp from the first Tsp 509 I site in the 5' LTR of the retrovirus (Figure 2.5). The 5' ends of the inverse PCR products should therefore all contain a region that matches the 5' end of the tkneoU3hygro retroviral DNA sequence. The sequences generated for F1, F2, F3 and F4 were analysed using BLAST® (Basic Local Alignment Search Tool) (Altschul *et al.*, 1990). BLAST analysis was done using the "non-redundant" database, which includes all GenBank, RefSeq, Nucleotide, EMB, DDB and PDB sequences. Figure 5.6 shows the sequences generated for the four inverse PCR products. Also indicated (in colour code) are the regions representing the retroviral DNA sequence (blue), the hamster genomic DNA sequence (green) and the Tsp 509 I restriction site (red). The sequences of all four inverse PCR products show the

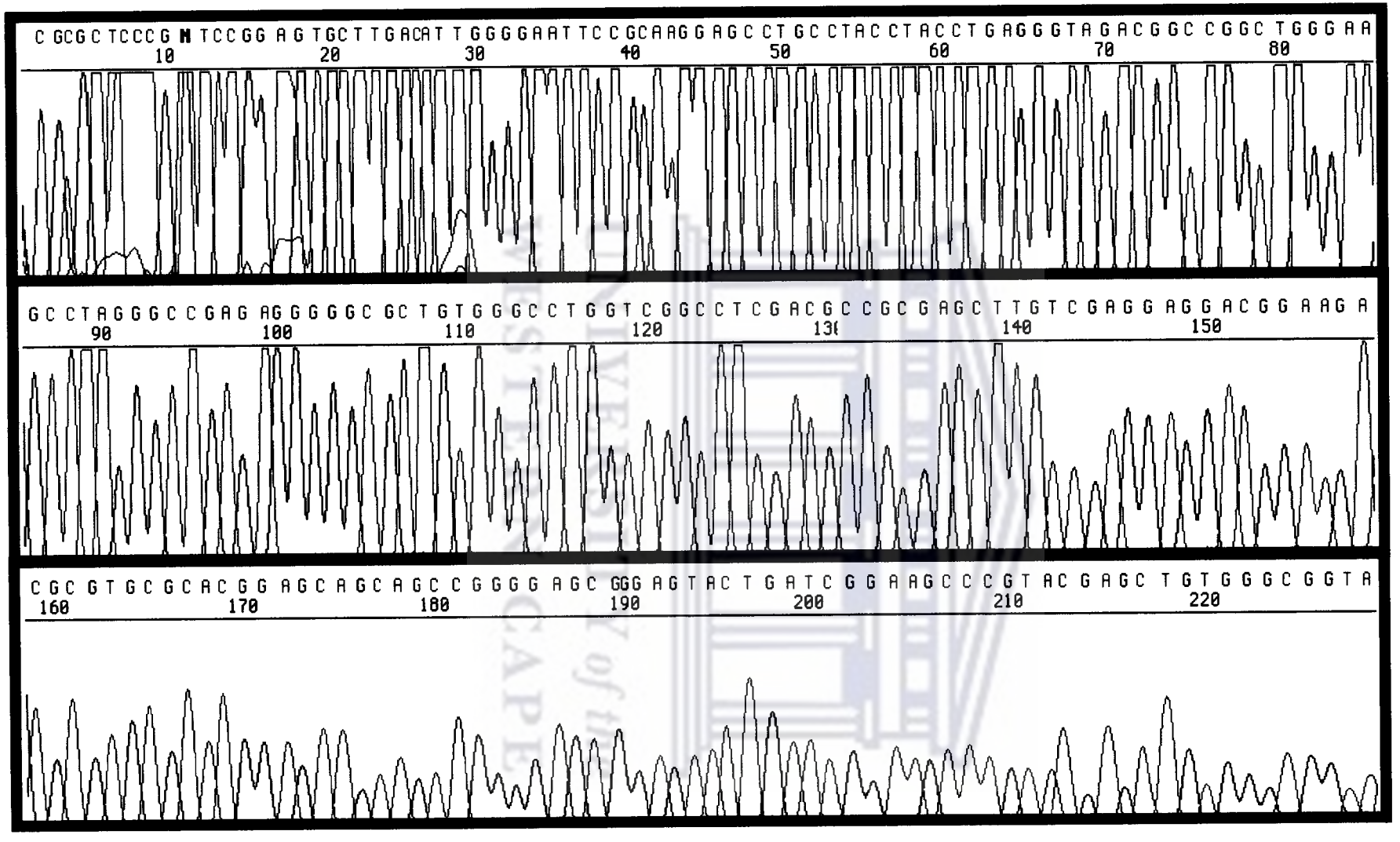

Figure 5.5. Sequence data generated for the F1 inverse PCR product.

presence of retroviral DNA sequence at the 5' end. Next to the retroviral sequence is a Tsp 509 I restriction site. The genomic DNA was digested with Tsp 509 I and then re-ligated (Figure 2.5), therefore it is anticipated that the Tsp 509 I restriction site should be present in the inverse PCR product. The sequence downstream (3' end) of the Tsp 509 I site represents the hamster genomic DNA. Figure 2.5 suggests that both the 5' and 3' ends of the inverse PCR fragment should contain retroviral DNA sequence. However, it is only the F4 and F3 inverse PCR products that show the presence of retroviral DNA sequence on the 3' end of the PCR product (downstream of the hamster genomic sequence) (Figure 5.6). This can be ascribed to the limitation of sequence analysis since only 400 bp can be read in one direction and the fact that the inverse PCR products were only sequenced in one direction. The F4 and F3 PCR products are respectively ~240 bp and ~300 bp, long, which make it possible to sequence across the hamster genomic sequence into the retroviral DNA sequence at the 3' end. The other two PCR products, F2 and F1 are ~480 bp and ~550 bp, respectively, which means that the retroviral DNA sequence on the 3' ends of these inverse PCR products can only be revealed by sequencing in a 3' to 5' direction.

Table 5.1 shows a summary of the BLAST results for the F1, F2, F3 and F4 PCR products. Indicated in this table are the most significant matches, their Score bits and E-values. The alignments produced for PCR products F1 and F2 are shown in Figures 5.7 and 5.8, respectively.

F1 Sequence:

CGCGCTCCCGNTCCGGAGTGCTTGACATTGGGG**AATTC**CGCAAGGAGCCTGCCTACCTACCTGAGGGTAGACGGCCGGCTGGGAAGCCTAGG
GCCGAGAGGGGGCGCTGTGGGCCTGGTCGGCCTCGACGCCGCGAGCTTGTCGAGGAGGACGGAAGACGCGTGCGCACGGAGCAGCAGCCGG
GGAGCGGGAGTACTGATCGGAAGCCCGTACGAGCTGTGGGCGGTACCTGTGACGCGCCTGTGGCGCCGCCCTTTGTGCCGTGGCGGGGGCAC
CGCGTTCGCGGCCTCGGAGTGGGAGGGGCGGTCCAGCCCGGCCGCCAGCTTCGCCGCCATGGACCTAGGTGGGTTCGCGTTTTCCTACTCCGG
CCTGGTGTCGGGCCGTGTCCGGAGAGCCCTCAGGGTGGCCCGAGCCCTGTGCTCTCCATGGCGCTCTCCGAACCGACTTTGAAGCCGGGGTCT
GAGAGTTTTAGGACCGGGCCGGAGCCGCTCAGCCTCAGCCGCCTGGGTGCTTTCTCACT

F2 Sequence:

GCGCGCTCCCGNTCCGGAGTGCTTGACATTGGGG**AATT**CCAGAAAGTATTACCGAACTGGCTGTGTGGTTCTAAATCACAGGGGGAAGGGTG
GGGAGGCAGCTGGCGCCCCACTTAAAGGTCACAGAATATTATTTCTACTTTAGTATCCAGAATCCAAGTAGAAATAAAGGAGAAGGTTAAGA
TCCAAGTTCACTTTCACAAAAGAAACTGAGGGCAGGGAGCCACGGAGTTCTCTGAGACTCACTTGCTTGCAGGAGAGTGCAAACCTCACTGG
CTGACATTTCACGAGCACTACTGAACACAAGACACAAGCAACAACAAAGGTAGCCACACATCACATAGAGGCAGGGGATGTCCAGTTCAGTG
GGTGGAAATCCTACCTCATGGACCTCTGGGAACAGTGCAGATGTAAGGAGTTAAATGGAAGACCCCAGACCGGTTGAAAGACCCCCCTGTCG
TTTCG

F3 Sequence:

GCGCGCTCCCGATTCCGGAGTGCTTGACATTGGGG**AATT**CAANNTTAAACTCATCACTTTAGTGACTCACACGAGCTCGTCATGCTTTTGCCT
GGCCTCTATGCCAGGGCACGCCTATCACACGAGCAGGCTGGGACCACACAGGATGAGCACACAGCACGACCATGTACTTGAAATCCCGTTGT
GCACTGGGACCATGATCTACACAATGAGTCCCATAGTACTCACTACAGGATCAGGAGCTGGGTCTACTAAGAGATGATGATGGATTGCGTCC
ATTATCAGAGGGAGTTCTTGAACGACCCCGCCTGACCGTTTGGGAGCTAGGGCAAGCTAGG

F4 Sequence:

TNCGGCTCCGNTCCGGAGTGCTTGAATTGGGG**AATT**GCATCCCATGATGGCTCACACTCATGCACGCACGCACACTTTAATGGTTTACTCTAT
TTTATTTGCATGGGTGTTTTGCCATACAAACGTCTGTGCACCATGTGATGGGGTGCCCACAGAGGCCAGAAGAGGGCATCTGATCCTCGGAAC
AACAGAGCATTGTTGCTCTCAATGTCGGTGCTTGAGAACTGAACTTGGGTCTTCTGGATTGAAAGACCCCACCTGTAGGTTTGGCAAGCTAGG
A

Figure 5.6. DNA sequences generated for F1, F2, F3 and F4 inverse PCR products. The tkneoU3hygro retroviral DNA sequence is indicated in blue, the Tsp 509 I restriction site in red and the hamster genomic DNA sequence in green.

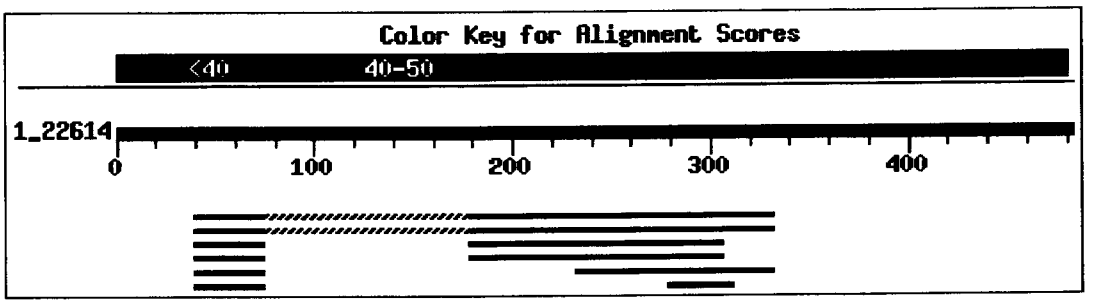

Sequences producing significant alignments:	Score (bits)	E Value	
gi|8777853|gb|AF229807.1|AF229807 Mus musculus endozepine-l...	180	1e-42	L
gi|21665918|emb|AL591129.24| Mouse DNA sequence from clone ...	180	1e-42	
gi|25057089|ref|XM_203450.1| Mus musculus gem (nuclear orga...	161	1e-36	L
gi|23622550|ref|XM_137731.2| Mus musculus similar to Compon...	161	1e-36	
gi|26087678|dbj|AK040188.1| Mus musculus 0 day neonate thym...	107	2e-20	
gi|28913568|gb|BC048474.1| Mus musculus, diazepam binding i...	56	5e-05	
gi|10946591|ref|NM_021294.1| Mus musculus diazepam binding ...	56	5e-05	L U
gi|12839678|dbj|AK006528.1| Mus musculus adult male testis ...	56	5e-05	L U
gi|1911855|gb|S83465.1|S83465 endozepine-like peptide [mice...	56	5e-05	L
gi|24418207|gb|AC087392.10| Homo sapiens chromosome 17, clo...	52	8e-04	

☐ >gi|8777853|gb|AF229807.1|AF229807 L Mus musculus endozepine-like protein gene, complete cds
Length = 2416

Score = 180 bits (91), Expect = 1e-42
Identities = 140/155 (90%), Gaps = 1/155 (0%)
Strand = Plus / Minus

```
Query: 179 gctgtgggcggtacctgtgacgcgcctgtggcgccgccctttgtgccgtggcgggggcac 238
           |||||||||||  |||||||||||||||| ||||||||||||||||||||||| |||||
Sbjct: 681 gctgtgggcggagcctgtgacgcgcctgtagcgccgccctttgtgccgtggcgcgggcaa 622

Query: 239 cgcgttcgcggcctcggagtgggaggggcggtccagcccggccgccagcttcgccgccat 298
           ||||||||||||| ||| | |||||||||||| ||||| ||||||||| ||||||||||
Sbjct: 621 cgcgttcgcggccttggactaggaggggcggtctagccc-gccgccagcgtcgccgccat 563

Query: 299 ggacctaggtgggttcgcgttttcctactccggcc 333
           |||||||||||||||| |  || ||||||||||||
Sbjct: 562 ggacctaggtgggttcccacttccctactccggcc 528
```

Score = 56.0 bits (28), Expect = 5e-05
Identities = 35/36 (97%), Gaps = 1/36 (2%)
Strand = Plus / Minus

```
Query: 40  ggctgggaagcctagggccgagaggggcgctgtgg 75
           |||||||||||||||| ||||||||||||||||||
Sbjct: 812 ggctgggaagcctagg-ccgagaggggcgctgtgg 778
```

☐ >gi|25057089|ref|XM_203450.1| L Mus musculus gem (nuclear organelle) associated protein 4 (Gemin4), mRNA
Length = 3539

Score = 161 bits (81), Expect = 1e-36
Identities = 118/129 (91%), Gaps = 1/129 (0%)
Strand = Plus / Plus

```
Query: 179 gctgtgggcggtacctgtgacgcgcctgtggcgccgccctttgtgccgtggcgggggcac 238
           |||||||||||  |||||||||||||||| ||||||||||||||||||||||| |||||
Sbjct: 61  gctgtgggcggagcctgtgacgcgcctgtagcgccgccctttgtgccgtggcgcgggcaa 120

Query: 239 cgcgttcgcggcctcggagtgggaggggcggtccagcccggccgccagcttcgccgccat 298
           ||||||||||||| ||| | |||||||||||| ||||| ||||||||| ||||||||||
Sbjct: 121 cgcgttcgcggccttggactaggaggggcggtctagccc-gccgccagcgtcgccgccat 179

Query: 299 ggacctagg 307
           |||||||||
Sbjct: 180 ggacctagg 188
```

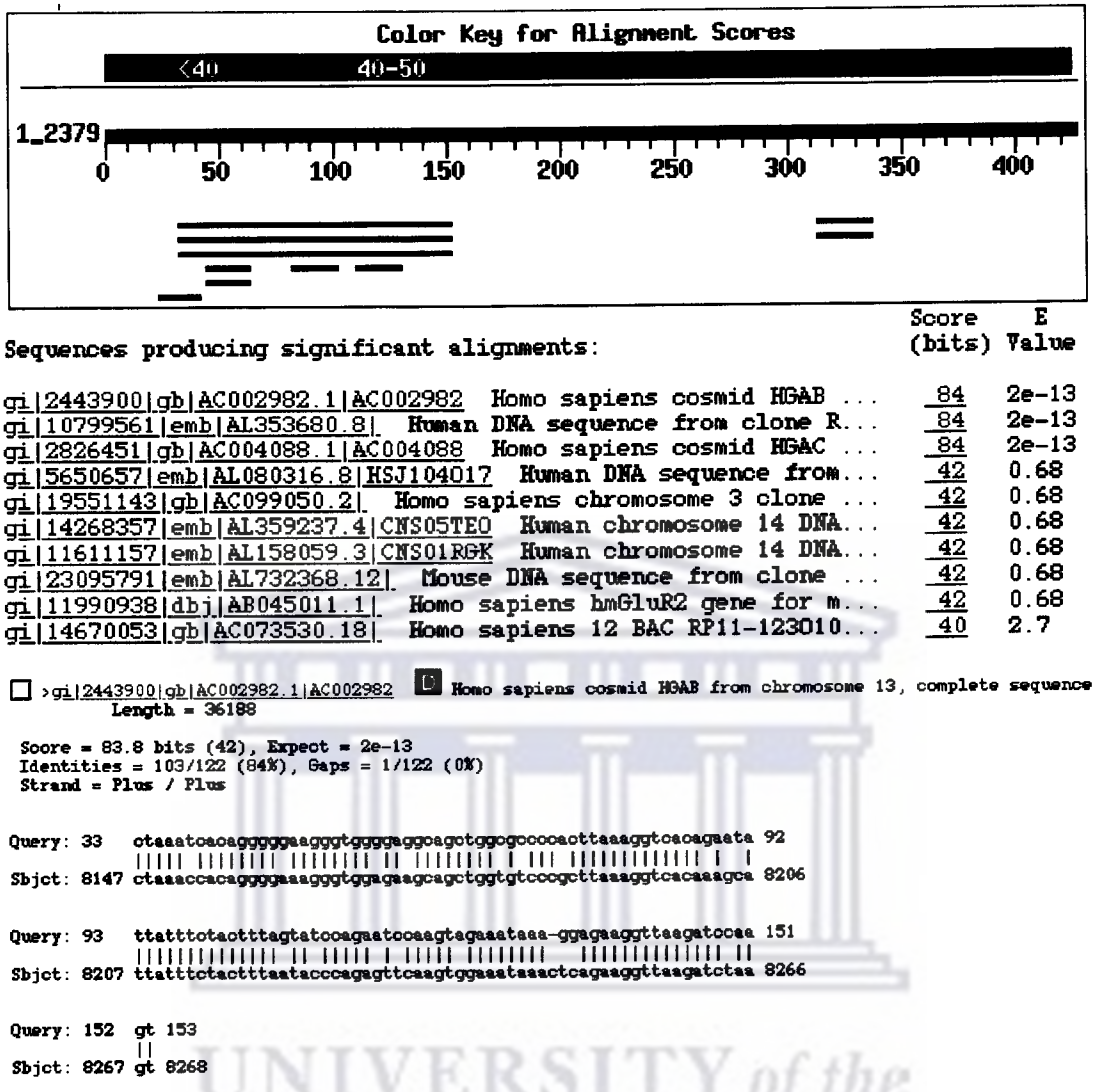

Figure 5.8. BLAST result generated for the sequence generated for the F2 inverse PCR product. Only the ten best matches are shown. The sequence alignment for the best match (*Homo sapiens* cosmid HGAB from chromosome 13) is also shown.

Table 5.1. Summary of the BLAST analysis of the sequences generated for the four inverse PCR products.

PCR product	Most significant match	Score bits	E-Value
F1	*Mus musculus* endozepine like protein Gemin4	180 161	1e-42 1e-36
F2	*Homo sapiens* cosmid HGAB from chromosome 13	83	1e-13
F3	*Homo sapiens* BAC clone RP11-20F1	38	2.9
F4	Mouse DNA sequence from clone RP23-108D12 on chromosome 2	66	2e-08

The additional PCR products could be the result of partial digestion of the genomic DNA. In this instance it would be assumed that F4 is the smallest PCR product that can be produced by digestion with Tsp 509 I and that failure to digest at the first, second or third Tsp 509 I sites will produce the F3, F2 and F1 inverse PCR products, respectively. The complete sequence for the two smallest PCR products: F4 and F3 have been obtained and did not show any overlap, which would eliminate the possibility that the F3 inverse PCR product is an extension of F4. Conversely the 3' end sequence for the larger inverse PCR products: F1 and F2 are not known. However the possibility that these inverse PCR products could be the result of partial digestion can also be eliminated since only ~50 bp of the 3' end sequence is unknown. As the known F1 and F2 sequences do not overlap with the smaller inverse PCR products and the fact that the smaller PCR products are much larger than 50 bp, it is therefore not possible for the F1 and F2 PCR products to be the result of partial digestion. Therefore these results rather suggest

that the additional PCR products produced in the inverse PCR, are the result of multiple retroviral integration and not the result of the formation of multimeric structures or partial digestion, since all four PCR products are distinct and do not overlap with each other. It therefore also suggests that four retroviruses were inserted into cerR1. Although the calculated multiplicity of infection for promoter-trapping was 0.01 (Section 3.7), it does not guarantee single retroviral insertion. This further suggests that one or more candidate gene(s) was knocked out by promoter-trapping resulting in resistance to apoptosis.

The F2 and F4 inverse PCR products matched regions of the human chromosome 13 and the mouse chromosome 2, respectively (Table 5.1). Based on E-Values these matches appear to be significant, however, no gene sequence has been assigned in these regions yet. The F3 inverse PCR product did not produce any significant match. These results eliminated F2, F3 and F4 as retroviral insertions that could have resulted resistance to apoptosis. The F1 inverse PCR product produced significant matches against two genes: the *Mus musculus* endozepine and Gemin4 (Table 5.1). These results are based on alignments produced by recent (2003) searches of sequence databases. Earlier (1999) screens of sequence databases did not match Gemin4 as a possible candidate gene and hence endozepine was pursued as the only candidate gene identified from the F1 retroviral insertion that may have resulted in resistance to apoptosis. The identification of nucleic acid or protein sequences by screening sequence databases has until recently been a common problem in molecular biology, due to the fact that the databases were incomplete. The consequence of this was that our

perspective of the genome of many organisms was an early and incomplete view of the genome. To some extent this still remains a problem even today because of incomplete or erroneous annotation of sequences. The complete sequencing of the genomes of several viruses, bacteria and higher organisms led to a revolutionary change in the identification and cloning of genes. These factors can be coined as the reasons for the earlier exclusion of Gemin4 as a possible candidate gene, although recent BLAST analysis provides strong evidence that Gemin4 is a candidate gene.

5.2.4. Genomic structure of the F1-retroviral insertion.

BLAST analysis for this inverse PCR product suggested that retroviral insertion occurred in between two genes: Gemin4 and endozepine. Figure 5.9-**A** illustrates the positioning of the retrovirus into the hamster genomic DNA between Gemin4 and endozepine. The orientation of the retrovirus suggests that the Gemin4 gene has been promoter-trapped and that retroviral insertion has occurred into the 5' untranslated regions of both genes. BLAST analysis of the F1 retroviral insertion match base pairs 61 to 188 and base pairs 528 to 812 of the Gemin4 and endozepine gene sequences, respectively (Figure 5.9-**B**). Although the integration into the endozepine gene was not a promoter-trap event, this retroviral insertion could have affected the expression of this gene as it occurred into the 5' untranslated region of the gene. This data strongly suggests that the gene Gemin4 has been promoter-trapped and that the promoter of this gene is driving the expression of the promoterless retroviral hygromycin resistance gene and may

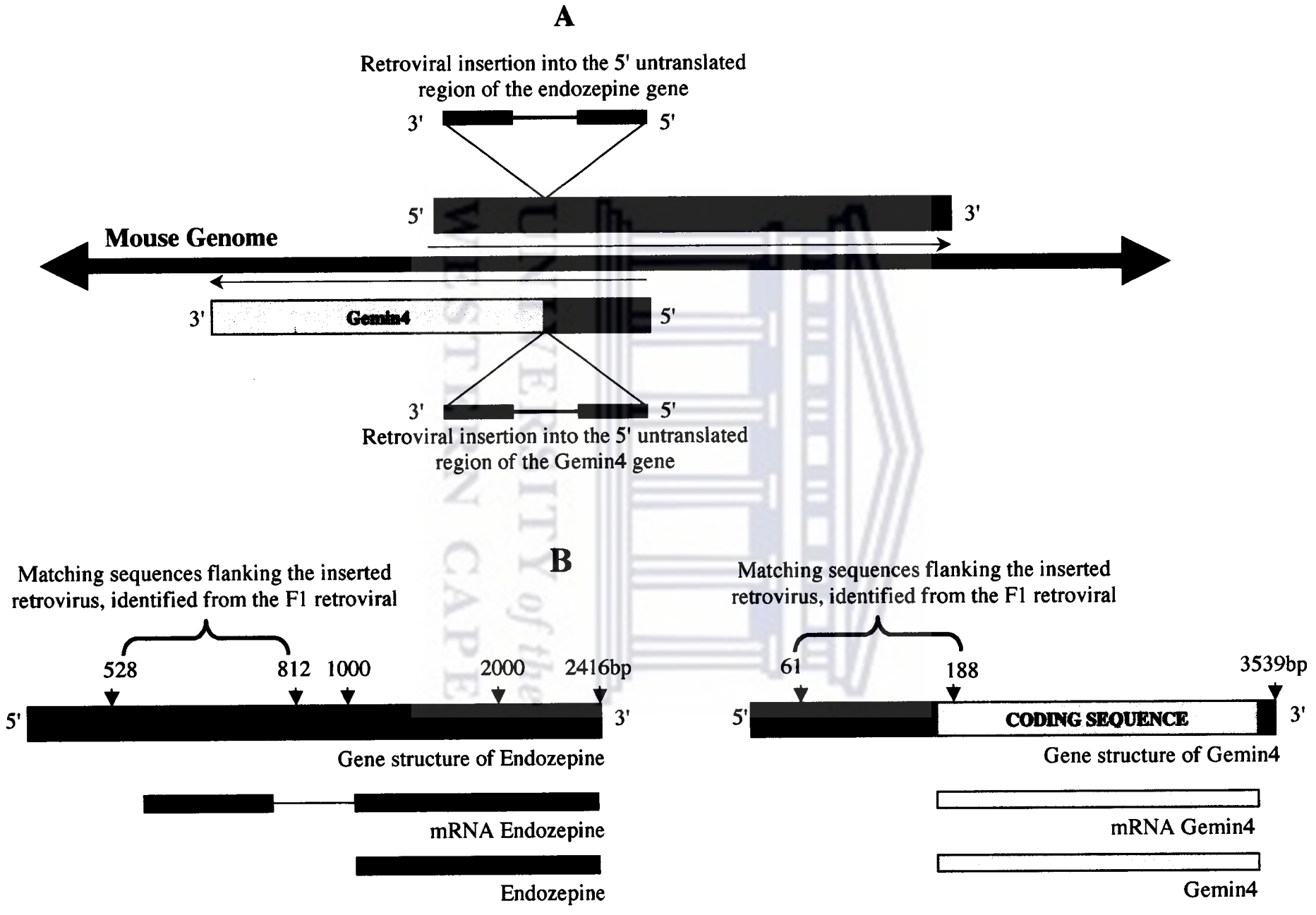

have been knocked out. However since Gemin4 was not pursued as a candidate gene, this study did not confirm if this is the case.

5.3. Endozepine as a candidate pro-apoptotic gene.

Endozepine-like protein (ELP) or diazepam binding inhibitor (DBI) is a 10 kD protein first isolated from rat brain tissue due to its ability to displace diazepam from benzodiazepine receptors (Guidotti *et al.*, 1983). Henceforth endozepine-like protein or diazepam binding inhibitor will only be referred to as endozepine. Endozepine consists of 87 amino acids and shares 54 % identity with acyl-CoA binding protein (ACBP) at amino acid level (Pusch *et al.*, 1996). Both these proteins are able to bind thiol esters of long fatty acids and coenzyme A.

5.3.1. Biological functions of acyl-CoA binding protein/endozepine.

Acyl-CoA binding protein is an 86-103 residue protein family. The ACBP family can be subdivided into at least five groups of ACBP based on sequence alignment. These subgroups include: 1-ACBP, t-ACBP, b-ACBP, m1-ACBP and m2-ACBP or membrane-associated ACBP (also called the endozepine-related protein) (Kragelund *et al.*, 1999). Figure 5.10 shows the sequence alignment of published ACBP sequences from various organisms including mouse, rat, worm, bovine, frog and human. The phylogenetic tree in Figure 5.11 demonstrates how the different subgroups cluster together based on sequence similarity. The first subgroup, 1-ACBP, contains no cysteines and is 86-92 residues long. The second

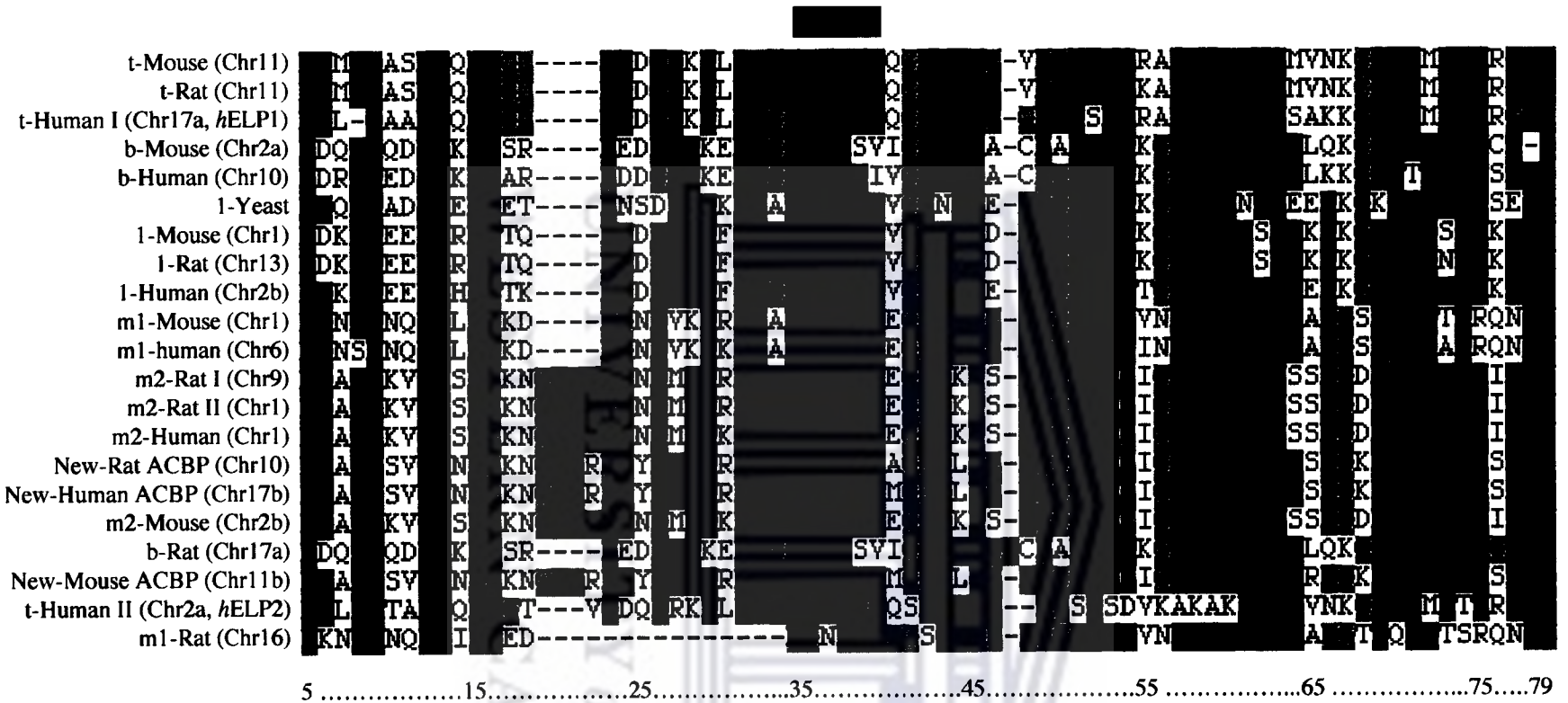

Figure 5.10. The sequence alignments of published acyl-CoA binding protein sequences from rat, mouse and human. Also indicated is the chromosome number (Chr) where the genes are located. Alignments were done against residues Phe5 to Ileu79 of the t-mouse protein sequence, using ClustalX (Thompson *et al.*, 1997) . The alignments also included the predicted protein sequences for a new subgroup of acyl-CoA binding proteins. The black box at the top of the alignment indicates the acyl-CoA binding domain (YKQAT).

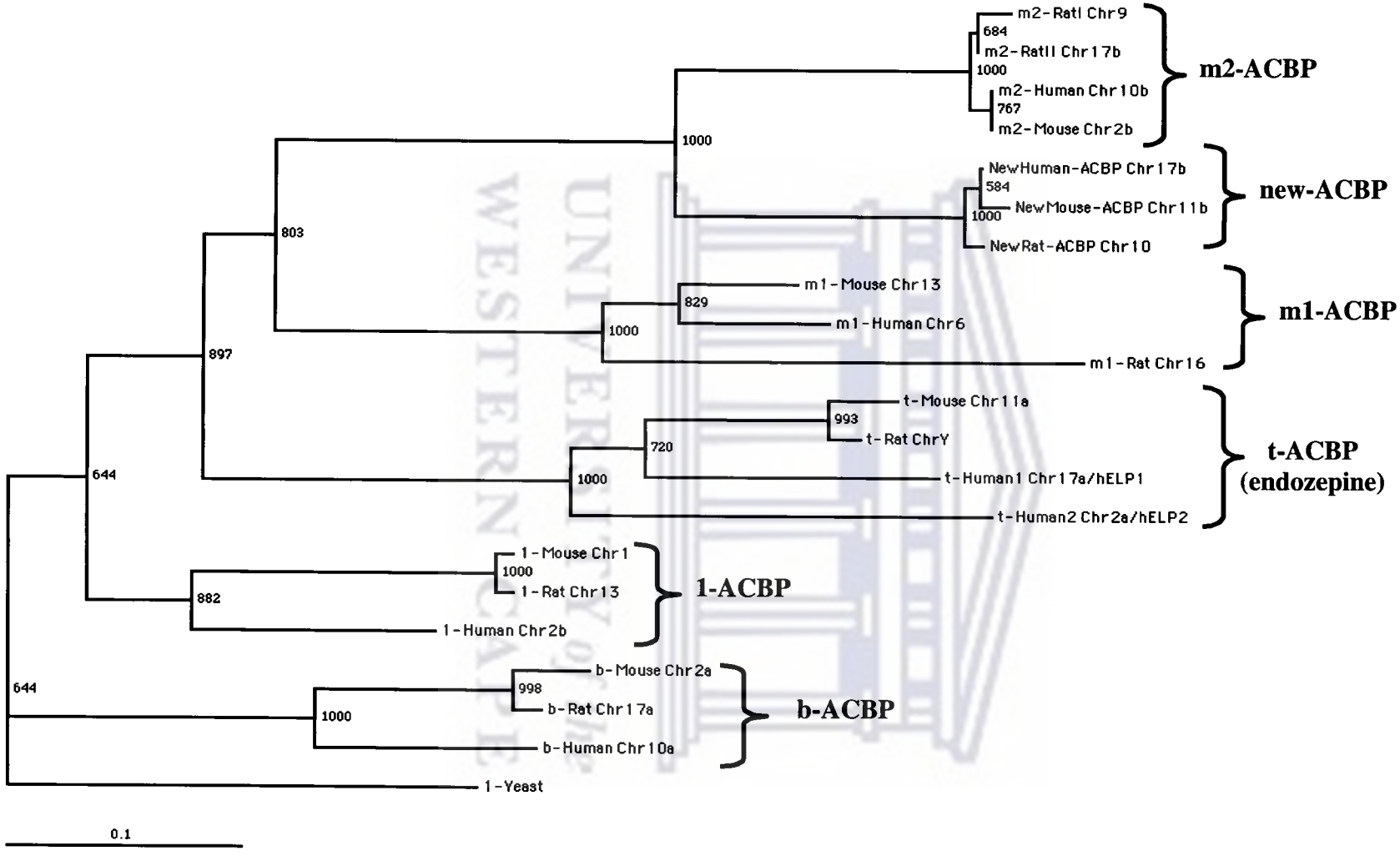

group, t-ACBP or endozepine, is primarily expressed in the testes. Proteins belonging to this subgroup contain three cysteines. A third subgroup, b-ACBP, is a brain specific isoform, which contains a single cysteine. The m1-ACBP and the m2-ACBP subgroups can be up to ~530 residues. The acyl-CoA binding motif, YKQAT is conserved in all the subgroups. With the exception of t-ACBP, all ACBP are structurally and functionally different from other lipid-binding proteins. Fatty-acid binding proteins have a so-called β-barrel structure and bind a broad spectrum of fatty-acids. In contrast ACBP has a four α-helical structure and specifically binds acyl-CoA esters (Kragelund *et al.*, 1999).

The biological functions of these proteins are not entirely known. Acyl-CoA binding proteins are multifunctional. A number of cellular functions have been ascribed to this protein family. It has been suggested that these proteins are involved in the regulation of biological processes such as acyl-CoA metabolism, steroidogenesis, insulin secretion and GABA/benzodiazepine receptor modulation. Acyl-CoA esters have been implicated in cell signalling processes and are important intermediates in fatty acid metabolism (Rasmussen *et al.*, 1993).

Disruption of the *1-ACBP* gene in *Saccharomyces cerevisiae* dramatically altered acyl-CoA metabolism (Gaigg *et al.*, 2001). These mutants demonstrated slow growth rates and the relative amount of C18:0 acyl-CoA esters was increased 3.5 fold while the amount of C26:0 acyl-CoA esters was dramatically reduced. This was accompanied by reduced sphingolipid synthesis and increased levels of

inositol-phosphoceramide, mannose-inositol-phosphoceramide and lysophospholipids in the plasma membrane of these mutants. In addition these mutants showed morphological defects which included the accumulation of differently sized vesicles, multi-layer plasma membrane domains and autophagosomes. This strongly suggested that yeast 1-ACBP was not required for general glycerolipid synthesis and that it plays an important role in transport-mediated lipid synthesis and membrane trafficking (Gaigg *et al.*, 2001).

A recent study (Faergeman and Knudsen, 2002) suggested that knocking down the expression of 1-ACBP in human cell lines by small interference RNA (siRNA) leads to growth arrest and cell death. In an effort to determine the mode of cell death the cells were analysed for DNA fragmentation. No DNA fragmentation was observed, leading to the suggestion that 1-ACBP-silenced cells died via necrosis and not apoptosis (Faergeman and Knudsen, 2002). However, it should also be noted that apoptosis can occur in the absence of DNA fragmentation or that DNA can be fragmented into larger (50 kb) fragments, which are only detectable by pulse-field gel electrophoresis. However, since DNA fragmentation is a late apoptotic event the cells in this study were also analysed for PARP cleavage, which is an early apoptotic event. It was found that PARP was cleaved in 1-ACBP-silenced cells, which led to the conclusion that 1-ACBP gene silencing resulted in the activation of early apoptotic events but that the cells did not have the capability to complete the apoptotic pathway. The intracellular concentration of acyl-CoA esters is dependent on 1-ACBP and acyl-CoA thioesterases. *S. cerevisiae* does not express cytosolic acyl-CoA hydrolases

(Faergeman and Knudsen, 1997) which may explain why a 1-ACBP knockout is lethal for mammalian but not for yeast cells. These studies suggest that 1-ACBP plays a role in essential biological functions, which may include lipid metabolism and that loss of this gene is lethal to an organism. The proposed structural differences (Kragelund *et al.*, 1999) and variant expression patterns of members of the ACBP protein family (reviewed in Section 5.3.2) suggests that these proteins may be functionally different. This implies that although 1-ACBP has been shown to be essential for survival, other members of the ACBP protein family may have other biological functions.

It has been demonstrated that acyl-CoA binding protein /endozepine can interact with two different types of receptors. In the central nervous system this protein interacts with the benzodiazepine recognition site that is associated with the gamma-amino butyric acid (GABA) receptor in neuronal tissue, where it functions as a negative modulator of this receptor (Costa and Guidotti, 1991). Acyl-CoA binding protein (most probably b-ACBP) has also been described as a neuropeptide and has been implicated in anxiety in the regulation of corticotrophin-releasing hormone secretion. Proteolytic cleavage sites in this protein generate several biologically active peptides such as triakonta-tetraneuropeptide and octadecaneuropeptide (Ferrero *et al.*, 1984; Slobodyansky *et al.*, 1989). It has been demonstrated that intra-cerebroventricular administration of these peptides could alter behavioural patterns in mice (de Mateos-Verchere *et al.*, 2001). Since most of these activities of ACBP have been identified in brain tissue it can be assumed that it is the b-ACBP subgroup that fulfil these functions.

Previous studies demonstrated that acyl-CoA binding protein/endozepine has the ability to displace benzodiazepine derivatives (e.g. PK11195, diazepam, Ro5-4864) from the central peripheral benzodiazepine receptor (Guidotti *et al.*, 1983; Costa *et al.*, 1983). In peripheral tissues acyl-CoA binding protein/endozepine was shown to interact with a second class of benzodiazepine receptors located on outer mitochondrial membranes. Benzodiazepine receptors located in peripheral tissues form part of the mitochondrial permeability transition pore (Section 1.3.3), a structure that has already been implicated in the activation or regulation of apoptosis. Since endozepine and ACBP share the conserved acyl-CoA binding domains, it is possible that these proteins may also share some of their biological functions (reviewed in Section 5.3.3).

5.3.2. The expression patterns of acyl-CoA binding protein and endozepine.

The basic ACBP isoform, 1-ACBP is expressed in almost every tissue in all eukaryotic species tested. It is speculated that this isoform is most likely the ancestor of the other specialised isoforms. The expression levels of 1-ACBP vary considerably between cell types and in response to changing metabolic conditions and the expression patterns of this isoform appear to correlate with increased lipogenesis. Cell types with a high level of 1-ACBP expression include hepatocytes, steroidogenic cells, and adipocytes (Helledie *et al.*, 2002).

Endozepine shares a 60 % identity with 1-ACBP but differs from 1-ACBP since endozepine is highly expressed in male germ cells of the testes (Pusch *et al.*,

1996). Low levels of endozepine expression were also detected in other tissues such as the ovary. It has been demonstrated that the expression of endozepine starts during spermatid elongation in post meiotic stages of male germ cell development (Pusch *et al.*, 1999). Immunocytochemistry demonstrated that the majority of endozepine was located at the middle piece of the spermatozoon tail, which is enriched with mitochondria. It was proposed that the expression of endozepine in spermatozoa reflects the usage of fatty acids as the primary energy source in spermatozoa and that endozepine therefore plays a role in spermatid metabolism (Kolmer *et al.*, 1997). Mice lacking endozepine expression, lacks spermatogenic stages later than round spermatids, which suggested a possible role in spermatid development (Valentin *et al.*, 2000).

Acyl-CoA binding protein is expressed ubiquitously in species ranging from yeasts, plants, worms, and insects to vertebrates. Endozepine is expressed in the testes of a wide range of mammals including rodents, carnivores and ruminants. However, it has recently been suggested that the endozepine gene has been progressively inactivated through primate evolution with no detectable protein in humans (Ivell *et al.*, 2000). This study reports that both Northern and Western blot analysis failed to detect the expression of endozepine in human tissues. Using RT-PCR it was possible to amplify a human endozepine transcript from human testicular mRNA. By probing a human testicular cDNA library, several full-length cDNA clones were identified. Sequence analysis of these transcripts (h*ELP1* = 1 692 bp and h*ELP2* = 2 677) led to the identification of two closely related genes (Ivell *et al.*, 2000). The h*ELP1* transcript includes a + frameshift after amino acid

25, while h*ELP2* includes a + frameshift after amino acid 8. These mutations resulted in new open reading frames and consequently the *ELP1* transcript encodes for a 66-residue protein and the *ELP2* transcript encodes 91-residue protein. The tyrosine in the acyl-CoA binding motif, YKQAT, has been substituted with cysteine. Cloning and analysis of endozepine cDNA sequences from other primates (marmoset monkey, cynomolgus macaque, chimpanzee, orangutan and gorilla suggest that the expression of endozepine has progressively been inactivated through primate evolution (Ivell *et al.*, 2000). Except for gorilla for which three PCR products were generated, a single gene product was obtained for all the primate species. No frameshift mutations were detected in marmoset monkey and cynomolgus macaque sequences. However the chimpanzee and gorilla sequences also contained the same frameshifts observed in the human h*ELP1* and h*ELP2* sequences. The detection of these sequences by RT-PCR and their presence in cDNA libraries suggest that these genes transcribed. However Northern blot analysis failed to detect the expression of these genes in humans, which strongly suggest that humans have lost the expression of the endozepine gene.

In humans the h*ELP2* gene is located on chromosome 2 and the h*ELP1* gene is located on chromosome 17. Figure 5.11 show that these two genes cluster together with the t-ACBP subgroup from rat, mouse and bovine. Analysis of the mouse genome, places the Gemin4/endozepine gene sequences on chromosome 11. Comparative analysis of gene synteny between mouse and human suggest that the human homologue of the mouse endozepine gene is indeed the gene on

chromosome 17, since the gene chronology for these two genes (endozepine and Gemin4) is the same for both species. It is not clear at this point why a gene that is so highly conserved in other species and which appear to play a crucial role in spermatid metabolism and development should no longer be active in humans. The structural homology between endozepine and other ACBP suggest functional similarities between these proteins. It is therefore possible that the other isoforms of ACBP could take over the functions of endozepine in humans. However, the very specific expression pattern of endozepine could also suggest that this protein may have distinct functions. A screen of the human genome database for other closely related endozepine proteins confirmed a previous report (Ivell *et al.*, 2000) that there is no functional homologue of endozepine in humans. Table 5.2 represents a summary of this database screen. The genes encoding human 1-ACBP, b-ACBP and m-ACBP (indicated in red) were identified on chromosomes 2, 10 and 6, respectively. Nine pseudo-genes were also identified on chromosomes 2, 5, 6, 8, 11, 15, 16 and 17. In addition this screen also led to the identification of a new ACBP subgroup. These proteins are closely related to the m2-ACBP subgroup but is significantly distant from m2-ACBP to form a distinct cluster as is illustrated in the phylogenetic tree (Figure 5.11). A screen of the rat and mouse genomes shows that this gene is also present in these organisms. Thus, although this gene is expressed in humans it is most probably not a substitute for t-ACBP (endozepine).

Table 5.2. A description of the BLAST hits generated for the screen of the human genome for acyl-CoA binding proteins.

Chromosome	Number of hits	Map element	ACBP-Subgroup	Transcript
2	3	NT 022135	1-ACBP	Active gene
2	1	NT 022184	ψ-t-ACBP (h*ELP2*)	Frameshifted
5	1	NT 006713	ψ-1-ACBP	Frameshifted
6	3	NT 034880	m1-ACBP	Active gene
6	2	NT 007299	ψ-1-ACBP	Frameshifted
8	1	NT 015280	ψ-1-ACBP	Frameshifted
10	2	NT 008705	m2-ACBP	Active gene
10	2	NT 077569	b-ACBP	Active gene
11	1	NT 028310	ψ-b-ACBP	Frameshifted
15	1	NT 010194	ψ-b-ACBP	Frameshifted
16	1	NT 010552	ψ-1-ACBP	Frameshifted
16	1	NT 010393	ψ-b-ACBP	Frameshifted
17	3	NT 035414	ψ-t-ACBP (h*ELP1*)	Frameshifted
17	2	NT 010748	New-ACBP	Active gene

5.3.3. A role for endozepine in the mitochondrial apoptotic pathway.

The peripheral benzodiazepine receptor and its ligands have been implicated in the activation or regulation of apoptosis through mitochondrial permeability transition. It is well documented that ligands to the PBR such as PK11195, Ro5-4864 and diazepam can induce mitochondrial depolarisation and consequent swelling of isolated mitochondria. There is also ample evidence to suggest that mitochondrial depolarisation may lead to the release of pro-apoptotic proteins from the mitochondria (reviewed in Section 1.5.1). Two independent studies recently demonstrated that endozepine is among the proteins released from the mitochondria during the opening of the MPTP. In one of these studies atractyloside was used to induce MPTP opening in isolated mouse liver mitochondria (Patterson *et al.*, 2000). The composition of the protein mixture released from the mitochondria was investigated using liquid chromatography coupled to tandem mass spectrometry (LC-MS/MS). A number of the proteins identified were known to be either directly or indirectly involved in apoptosis. This study also found endozepine to be amongst these proteins released from the mitochondria. A second study (Van Loo *et al.*, 2002) used cleaved Bid to induce MPTP opening in isolated mitochondria. The identity of the proteins released from the mitochondria was determined by proteomic matrix-assisted laser desorption ionisation post-source decay (MALDI-PSD). Amongst the proteins released from the mitochondria were cytochrome c, Smac/DIABLO and endozepine. Taken together these data point to a possible role for endozepine in the mitochondrial apoptotic pathway.

Gemin4 on the other hand is a nuclear protein, which localises in structures called gems as part of a multi-protein complex, which also include the survival of motor neuron (SMN) protein. The SMN complex associates with snRNP and plays a role in spliceosomal snRNP assembly. The functions of this protein complex appear to be impaired in patients with the neurodegenerative disease spinal muscular atrophy (Charroux *et al.*, 2000). Based on what is known about this gene, it does have any apparent role to play in apoptosis. However this does not mean that Gemin4 is not a candidate apoptotic gene, since it is expected that this study will also lead to the identification of novel pro-apoptotic genes. For reasons explained in Section 5.2.3 Gemin4 was excluded as a possible candidate gene and endozepine was pursued for further analysis.

5.4. Summary.

Characterisation of cerR1, cerR2 and cerR3 by inverse PCR demonstrated that these cell lines originated from the same clone, since the PCR fingerprint for these three cell lines were identical. All three cell lines generated five PCR products which varied in size between 250 bp and 1 000 bp. It is expected that inverse PCR should produce two products for a single retroviral insertion. This PCR produced three additional products, which raised the possibility that the extra products could be the consequence of either the formation of multimeric structures during ligation or partial digestion of the genomic DNA or that multiple retroviral insertion has occurred.

The smallest product (F5, 250 bp) although not sequenced, corresponded to the expected size for the 3' end retroviral sequence. This sequence is not expected to contain any host genomic sequence. The other four products demonstrated the presence of retroviral sequence at the 5' end. Except for the 5' end (derived from the retroviral vector), there was no overlap between these sequences, suggesting that the additional products produced by inverse PCR was as a result of multiple retroviral integration and not due to the formation of multimers in the ligation reaction or partial digestion with Tsp 509 I. This also meant that there could be four possible mutations. The possibility of the F2, F3 and F4 retroviral insertions as mutations, which could have resulted in resistance to apoptosis, was eliminated by sequence analysis, as these sequences did not match any sequence in the database with high significance. On the other hand the F1 retroviral insertion emerged as a stronger candidate as a mutation that may have affected the apoptotic machinery of the cerR1 clone. However, the F1 retroviral insertion is into a region between two genes: Gemin4 and endozepine. This implies that the retroviral insertion could have affected the expression of both these genes and therefore both these genes can be considered as candidate genes.

It was demonstrated in two independent studies that endozepine is amongst the pro-apoptotic proteins released from mitochondria during apoptosis. Endozepine is an endogenous ligand to the peripheral benzodiazepine receptor, which also forms part of the mitochondrial permeability transition pore. Several studies have demonstrated the role of peripheral benzodiazepine receptor ligands in the regulation of apoptosis. Endozepine may facilitate mitochondrial permeability

transition during apoptosis. Retroviral insertion into the 5' untranslated region of this gene, although it is not a promoter-trap, may have affected the expression of this gene in the mutant cerR1. Reduced expression of endozepine may have affected mitochondrial permeability transition resulting in resistance to apoptosis. Therefore the research undertaken in this project was designed to evaluate the role of endozepine in apoptosis induced by ceramide.

CHAPTER 6: THE EXPRESSION AND PURIFICATION OF ENDOZEPINE.

CHAPTER 6: THE EXPRESSION AND PURIFICATION OF ENDOZEPINE.

6.1. Introduction.

Sequence analysis of the F4 inverse PCR product suggested that retroviral insertion occurred into a gene that showed significant homology to the mouse endozepine gene sequence. Retroviral integration into this gene could have affected the expression of this gene. Western blot analysis can be used to shed more light on the expression of this gene in the mutant cerR1 cells. Western blot analysis required the production of antibodies and therefore the aim of this section of the work was to express recombinant mouse endozepine for the purpose of generating antibodies in rabbits, which could cross-react with hamster endozepine and be used in subsequent analysis of cerR1.

6.2. Cloning of endozepine into pGEX-6P-2.

6.2.1. PCR amplification of mouse endozepine gene sequence.

PCR primers were designed based on the mouse endozepine gene-sequence (Accession number, AF229807). The forward primer was designed to include a Bgl II restriction site while the reverse primer contained an Xho I restriction site as well as an additional stop codon (Figure 6.1). The inclusion of these restriction sites into the primers allowed sub-cloning of the PCR fragment generated by these primers into pGEX-6P-2. Genomic DNA isolated from mouse embryonic stem

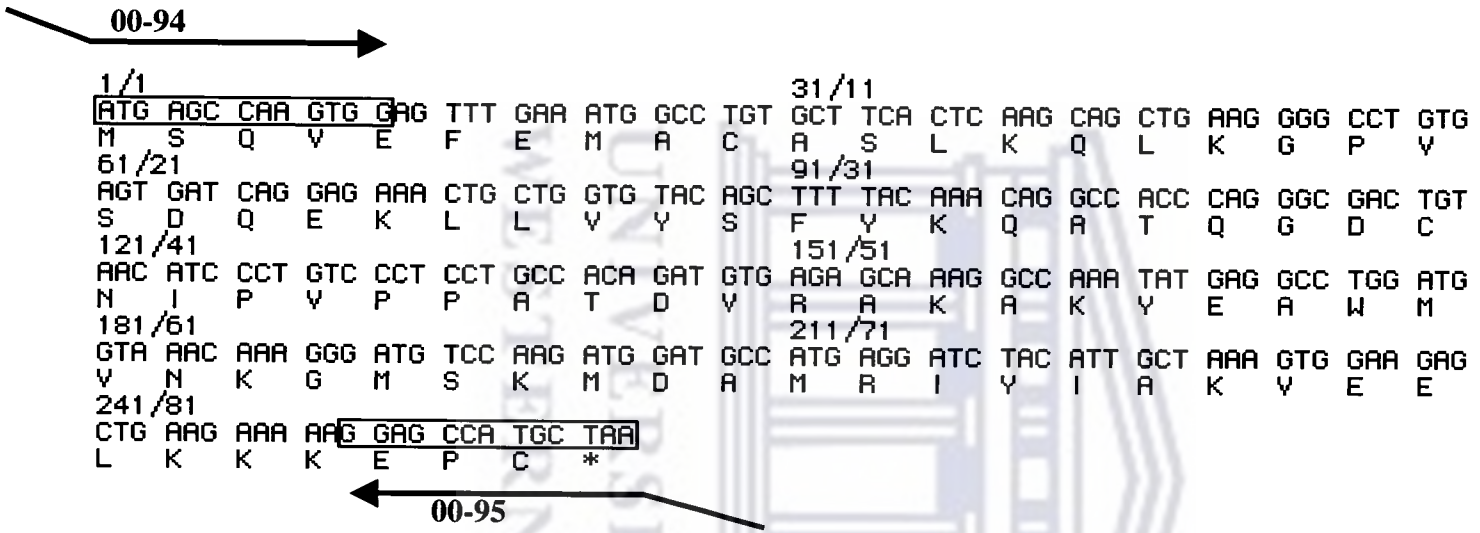

Figure 6.1. The cDNA gene sequence of mouse endozepine. The positions of the forward primer (00-94) and the reverse primer (00-95) are also indicated. The sequences for these primers were as follow:

00-94: 5'CAT GCT **AGA TCT** ATG AGC CAA GTG G 3'

00-95: 5' GAA GAC **CTC GAG** TTA GCA TGG CTC 3'

The Bgl II site in GFP-forward and Xho I site in 00-94 is indicated in bold with the stop codon in 00-95 being underlined.

cells was used as template for the PCR amplification of mouse endozepine. This PCR generated a fragment of 260 bp (Figure 6.2).

6.2.2. Cloning of mouse endozepine gene sequence into pGEM®-T Easy.

The mouse endozepine PCR fragment (Section 6.2.1) was cloned into pGEM®-T Easy (Section 2.19). Colony PCR was used to screen for positive clones (Section 2.20). Figure 6.3 shows the results of the colony PCR. The PCR for all of the colonies screened generated a fragment of about 510 bp, suggesting that all the colonies screened were positive. Large-scale plasmid isolation was prepared from one of these clones (Section 2.11.2). The plasmid DNA was digested with Bgl II and Xho I and analysed by electrophoresis on an agarose gel (Figure 6.4) which confirms the presence of a ~260 bp insert. The plasmid DNA was also sequenced with M13 forward and M13 reverse primers (Section 2.21). The insert sequence generated by sequence analysis was compared with the mouse endozepine cDNA sequence to check for possible mutations, which might have been introduced by *Taq* polymerase. Figure 6.5 shows the alignment between the mouse endozepine cDNA sequence and the insert sequence, which demonstrates that there is 100 % identity between the two sequences, confirming that the insert cloned into pGEM®-T Easy is the gene for mouse endozepine and that there are no mutations in the sequence.

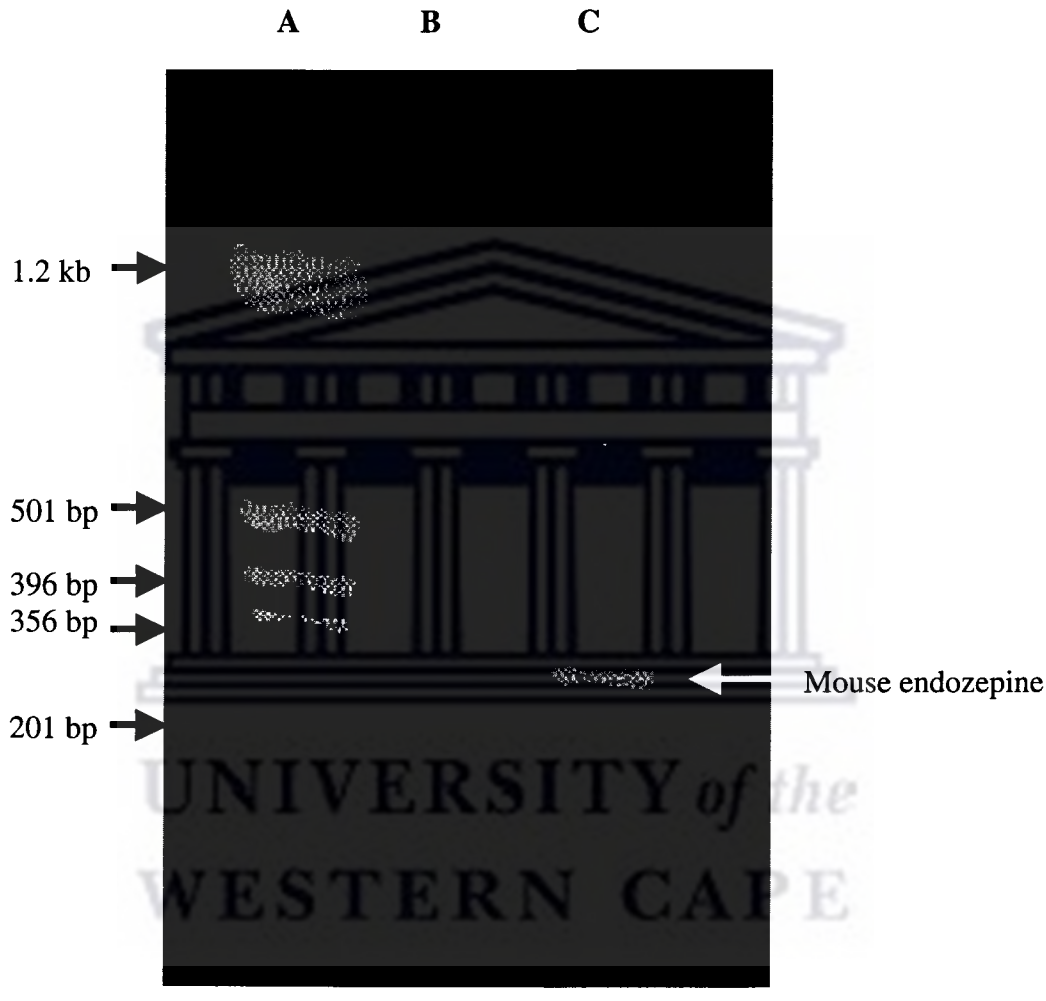

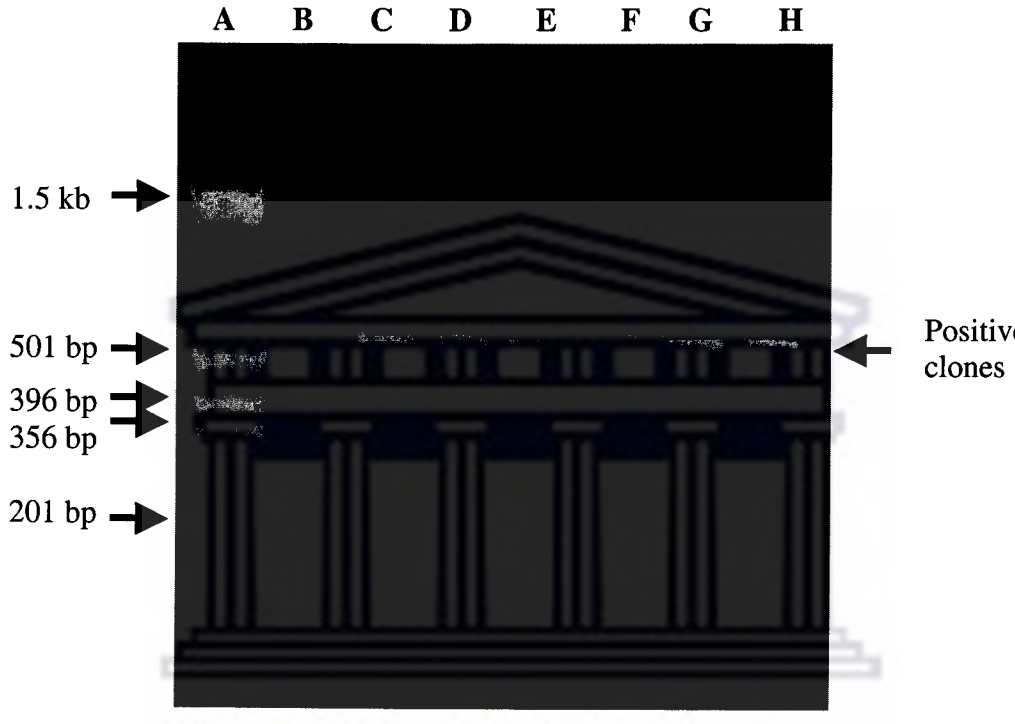

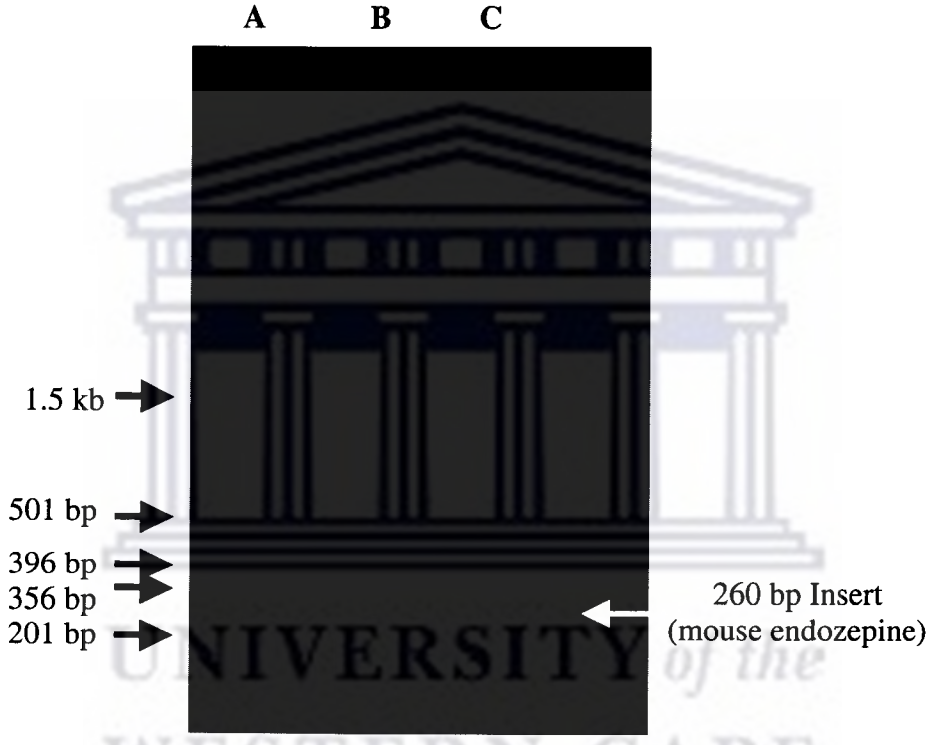

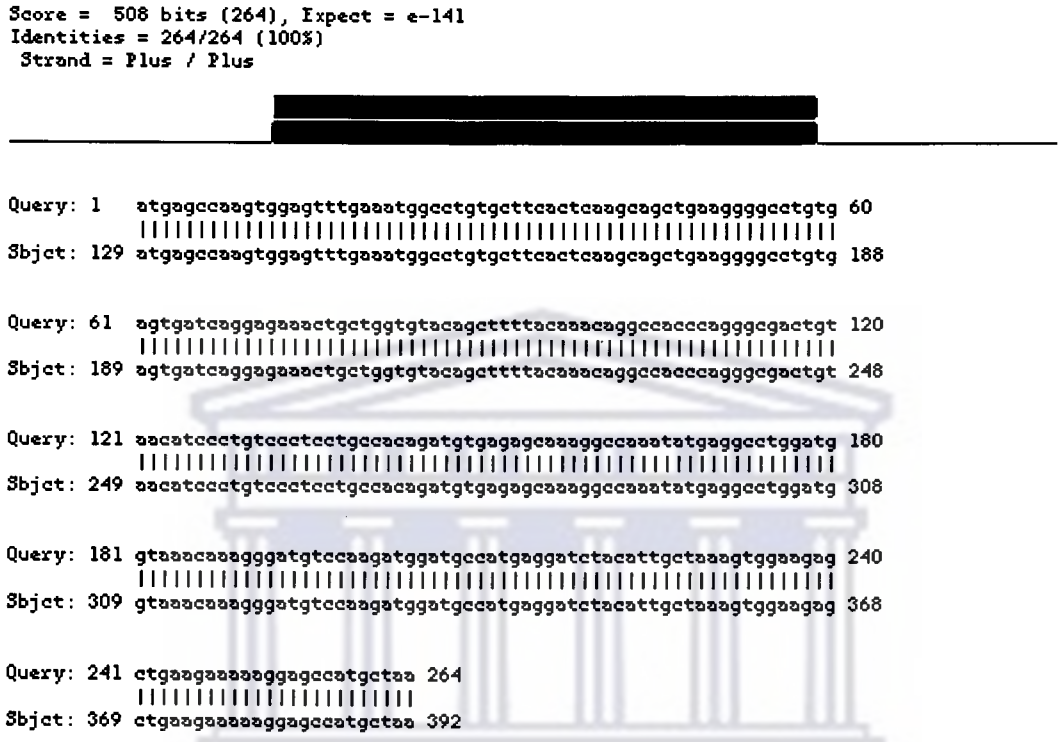

Figure 6.5. Sequence alignment between mouse endozepine coding sequence (Query) and the insert sequence (Subject) of a pGEM/mouse endozepine clone, using BLAST Pair wise alignment.

6.2.3. Sub-cloning of mouse endozepine gene sequence into pGEX-6P-2.

The fragment released from the pGEM/endozepine clone after digestion with Bgl II and Xho I was purified (Section 2.18.1) after agarose gel electrophoresis cloned into the BamH I and Xho I site of the GST fusion vector pGEX-6P-2 (Amersham Pharmacia) (Section 2.12.2). Figure 6.6 shows a diagrammatic representation of this construct. This plasmid DNA was transformed into competent *E. coli* BL21 Star™ pLys (DE3) cells as described in Section 2.10.

6.3. Expression and purification of endozepine.

6.3.1. Screening for the expression and solubility of endozepine.

The transformants were screened for the expression of recombinant GST-mouse endozepine protein as described in Section 2.25.1. Figure 6.7 shows the total bacterial protein lysates for three clones that were screened. Lanes-**B**, -**D** and -**F** represents the un-induced protein lysates, while lanes-**C**, -**E** and -**G** represent the bacterial lysates after protein expression was induced by the addition of 0.1 mM IPTG. The induced samples demonstrate the presence of a 37 kD protein. The size of this protein corresponds to the expected size of the GST/endozepine fusion protein (GST = 27 kD, endozepine = 10 kD).

6.3.2. Large-scale expression of endozepine.

A clone that was shown by expression screening to express GST/Endozepine fusion-protein was used for large-scale expression of endozepine as described in

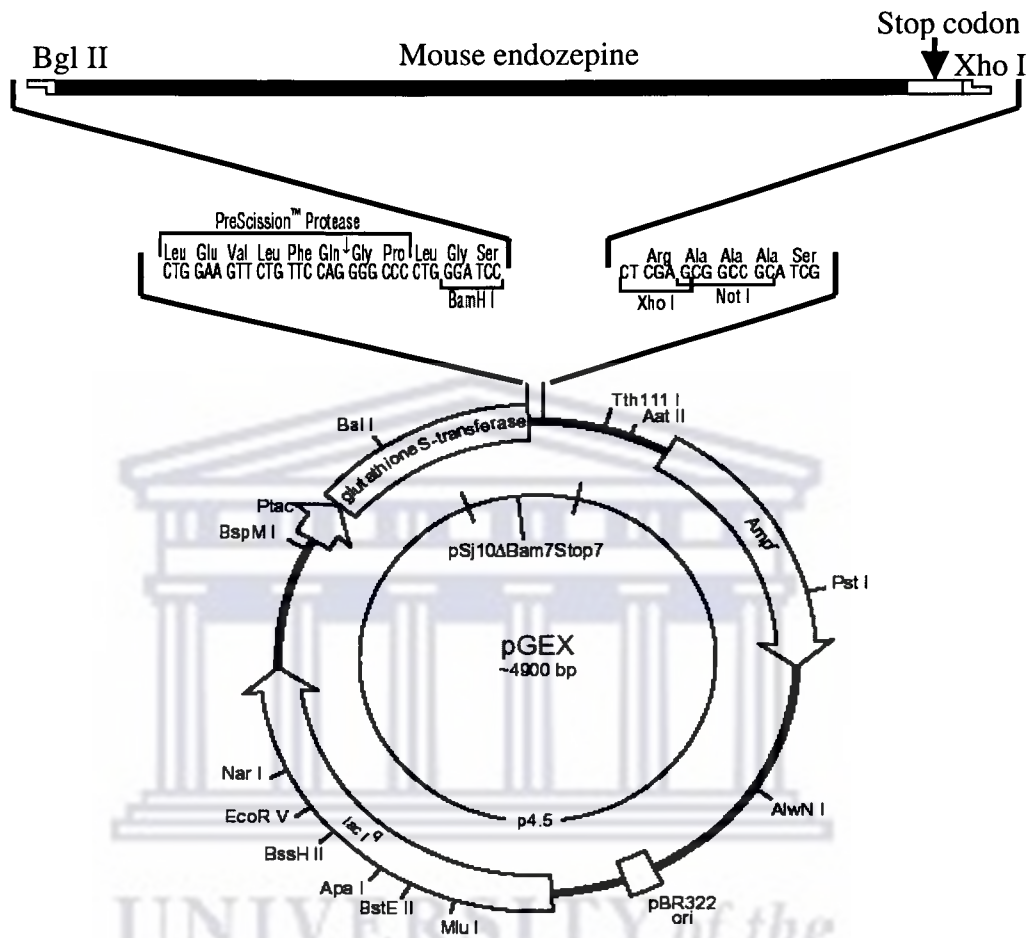

Figure 6.6. A diagrammatic representation of the pGEX-6P-2/mouse endozepine construct. Illustrated in this diagram is how the Bgl II/Xho I digested mouse endozepine fragment was cloned into the BamH I and Xho I sites of pGEX-6P-2.

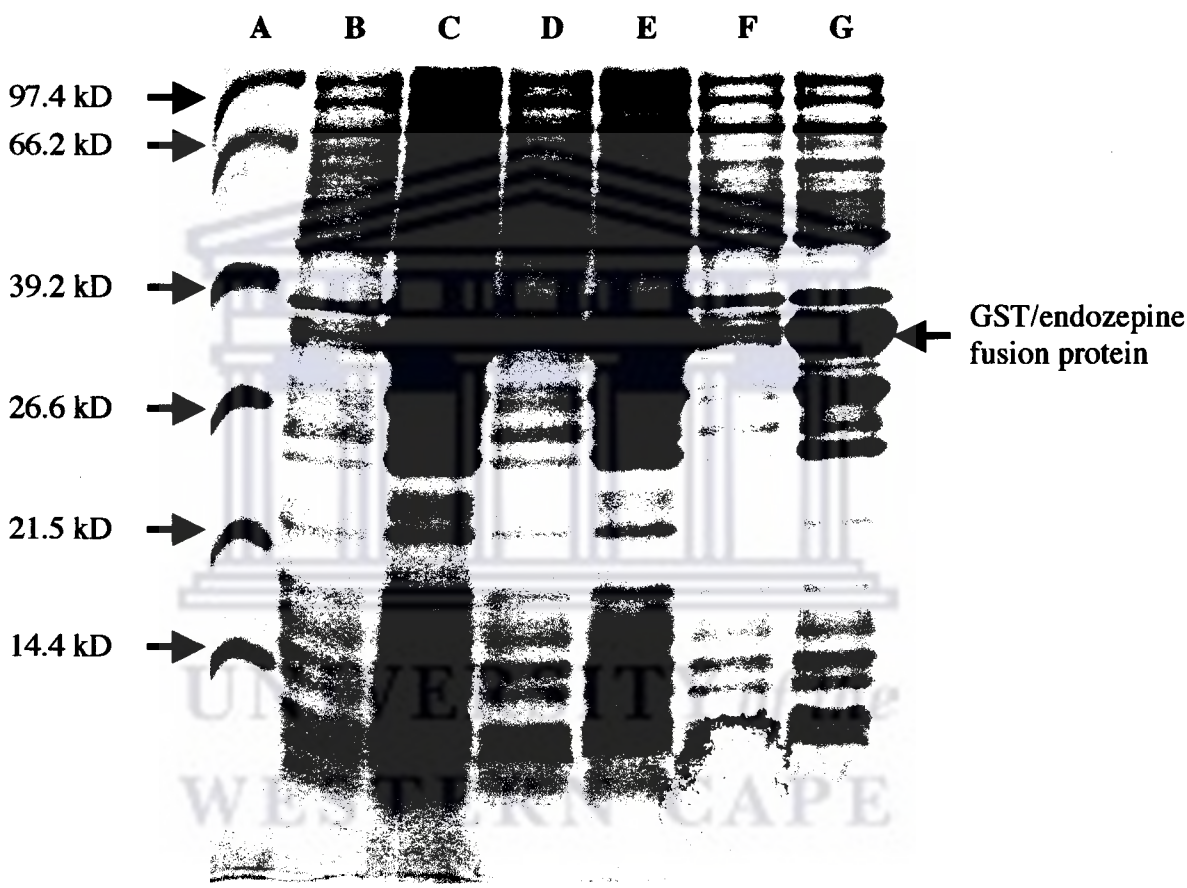

Section 2.25.2. After induction, a fraction of the lysate was analysed for the expression of recombinant endozepine on a SDS PAGE gel (Figure 6.8). The induced bacterial lysate (Figure 6.8, Lane-**B**) shows the expression of two proteins. One of these proteins (37 kD) represents the GST/Endozepine fusion protein, while the smaller protein (30 kD) could be a bacterial stress protein that is co-expressed with GST/Endozepine in large scale cultures, although not in the small scale cultures used for the initial screening of protein expression (Figure 6.7).

6.3.3. Purification of endozepine.

The GST/endozepine fusion protein was purified on glutathione agarose (Section 2.25.3). The fusion protein was eluted from the column and cleaved with PreScission™ Protease (Section 2.25.3). The cleaved protein was further purified by affinity chromatography on glutathione agarose. Figure 6.8 also shows the various steps of purification. The column flow-through (Lane-**C**) demonstrates that the 37 kD GST/Endozepine fusion protein remained bound to the column, while the 30 kD bacterial protein that was co-expressed with the recombinant fusion protein passed through the column. The column eluate (lane-**D**) shows the presence of a single protein of about 37 kD representing the recombinant GST/Endozepine fusion protein. The cleaved fusion protein (lane-**E**) shows the presence of two proteins: a 27 kD protein representing the GST domain and a 10 kD protein representing recombinant mouse endozepine. These two proteins were separated on by affinity chromatography on glutathione agarose. Figure 6.8,

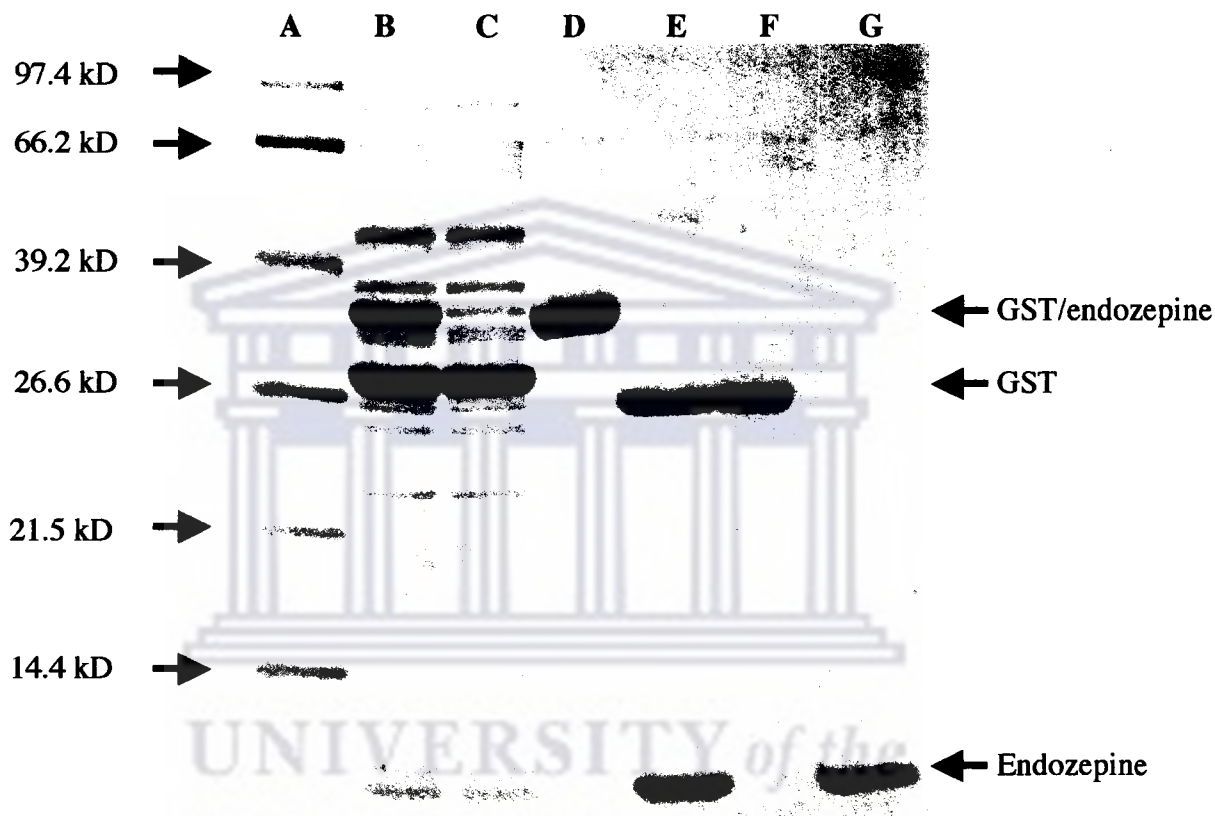

lane-**F** represents the eluate, GST and lane-**G** represents the flow-through, recombinant mouse endozepine.

6.4. The generation and screening the polyclonal anti-rabbit anti-mouse endozepine antibody for specificity.

The purified recombinant mouse endozepine was used to generate anti-rabbit anti-mouse endozepine antibody in rabbits (Section 2.26). Purified recombinant mouse endozepine was electrophoresed on a 16 % SDS PAGE gel. The proteins were transferred unto a PVDF-P membrane (Section 2.27). After transfer the membrane was stained with Ponceau S (Sigma) to verify protein transfer. The membrane was cut into 8 strips, each one of the strips representing a lane containing the recombinant mouse endozepine. The primary antibodies (both the Day 0 and Day 28 sera) collected from 4 rabbits were diluted (1:20 000) in TBSMT and used to detect the presence of recombinant mouse endozepine protein by Western Blot analysis (Section 2.28).

Figure 6.9 shows the results of this Western blot. The anti-sera collected from the rabbits 28 days after immunisation detected a 10 kD protein, which represents recombinant mouse endozepine protein (Figure 6.9, lanes-**A**, -**D**, -**F** and -**H**). The pre-immune sera collected before immunisation did not detect the recombinant mouse endozepine protein (Figure 6.9, lanes -**B**, -**E**, -**G** and -**I**). These results demonstrate that the antibody raised in these rabbits can be used to detect endozepine in a Western blot and that the rabbit pre-immune sera do not cross-

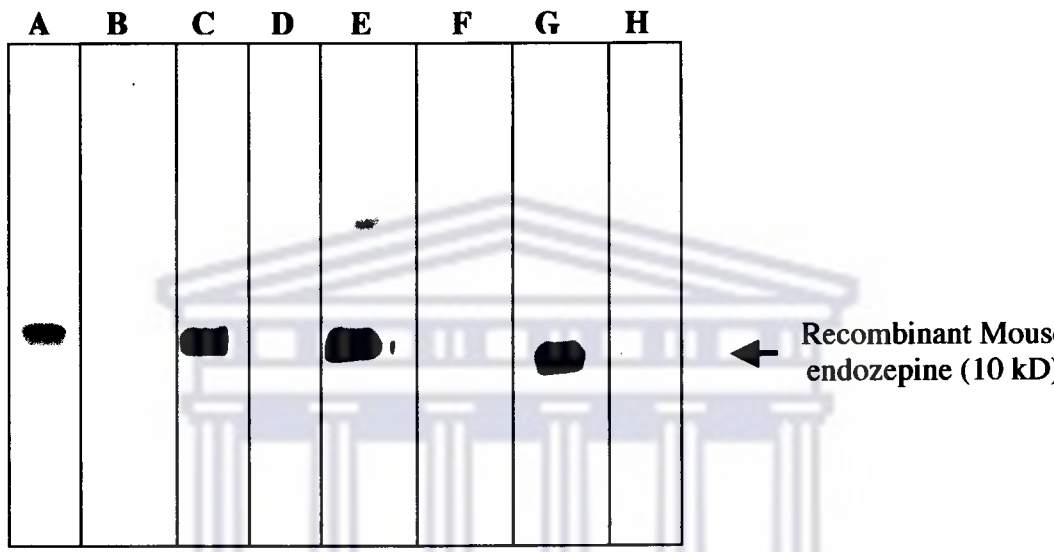

Figure 6.9. Western blot, screening anti-sera collected from four rabbits for the detection of recombinant mouse endozepine. Lanes-**A**, **-D**, -**F** and **-H** show the screening of anti-sera collected from rabbits 1, 2, 3 and 4, respectively. Lanes-**B**, -**E**, -**G** and -**I** show the screening of the pre-immune sera collected from rabbits 1, 2, 3 and 4.

react with recombinant mouse endozepine. Although cross-reactivity with other ACBP subtypes has not been tested it is not expected that there should be any cross-reactivity since there is only a 54 % identity between members of the ACBP protein family.

6.5. Summary.

PCR amplification of the gene sequence of mouse endozepine using mouse embryonic DNA as template, generated a 260 bp fragment, which was sub-cloned into pGEM®-T Easy vector. The identity of the insert was confirmed by colony PCR, restriction digestion and sequence analysis. This insert from the pGEM®-T Easy clone was then cloned into pGEX-6P-2. This clone was used to express recombinant mouse endozepine-like protein in *E. coli*. The addition of IPTG induced the expression of a 37 kD GST fusion protein which was purified by affinity chromatography. Cleavage with PreScission™ Protease cleaved the fusion protein into a 27 kD GST domain and the 10 kD mouse endozepine. The expression of this protein was scaled up, and the purified protein was used to generate polyclonal antibodies in rabbits. Screening the antibody reactivity with recombinant mouse endozepine demonstrated that rabbit pre-immune sera do not cross react with endozepine and that the polyclonal anti-rabbit anti-mouse endozepine antibody could be used to detect endozepine expression. Since an antibody dilution factor of 1:20 000 was able to detect recombinant endozepine suggest that the sensitivity and quality of this antibody is excellent.

CHAPTER 7: CHARACTERISATION OF THE EXPRESSION OF ENDOZEPINE AND ITS ROLE IN MITOCHONDRIAL DEPOLARISATION.

7.1. Introduction.

7.2. Screening cerR1 for differential protein expression using 2-D gel electrophoresis.

7.3. Characterisation of the expression of endozepine by Western blot analysis.

7.4. The sub-cellular localisation of endozepine by immunofluorescence.

7.5. Analysis of mitochondrial membrane potential changes using JC-1.

7.6. Summary.

CHAPTER 7: CHARACTERISATION OF THE EXPRESSION OF ENDOZEPINE AND ITS ROLE IN MITOCHONDRIAL DEPOLARISATION.

7.1. Introduction.

Two-dimensional (2-D) gel electrophoresis is considered as a method with the highest resolution for the separation of complex protein mixtures such as those present in eukaryotic cells (O'Farrell, 1975; Gorg *et al.*, 2000) and is often used to study differential protein expression. Proteins are separated based on two characteristics: in the first dimension step, isoelectric focusing (IEF), proteins are separated on the basis of their isoelectric points (pI) and the second dimension step, SDS-polyacrylamide gel electrophoresis, are separated on the basis of their molecular weight. Several thousand different proteins are expressed at any one time in a particular cell and 2-D gel electrophoresis makes it possible to resolve these proteins. Comparison of 2-D gels can reveal changes in expression of proteins due to mutations or changes under environmental conditions. Comparing normal and mutated samples it is possible to identify proteins for which the expression levels change.

This technique was used in this section of the work to compare the CHO22 cell line with the mutant cerR1 cell line for the presence of differentially expressed proteins. cerR1 was derived from CHO22 and therefore it is expected that there should be significant similarity between these two cell lines in terms of their

protein expression profiles. However, cerR1 also displays a phenotype (resistance to C_2-ceramide induced apoptosis) that is not present in CHO22. Inverse PCR and sequence analysis data already suggested that endozepine may be differentially expressed (i.e. cerR1 may have lost the expression of this gene) between these two cell lines and therefore this section also aimed at characterising the expression of endozepine in cerR1 and CHO22 cells by Western blot analysis. The two selectable marker genes: neomycin resistance (*tk*-neo) and hygromycin B phosphotransferase ($Hygro^R$) also represent differentially expressed genes. These two genes are expected to be present in the mutant cerR1 while it should be absent from the parental cell line CHO22. Although this study did not investigate the expression of Gemin4 it is possible that the expression of this gene could have been affected by promoter-trapping.

7.2. Screening cerR1 for differential protein expression using 2-D gel electrophoresis.

CHO22 and cerR1 cells were cultured in 25 cm^2 tissue culture flasks until confluent. The cellular proteins were isolated from the tissue culture cells as described in Section 2.23. The protein concentrations were determined using the Bradford assay and a 60 µg aliquot of each protein sample was analysed by 2D-gel electrophoresis (Section 2.24.2). The two gels were stained with Coomassie Brilliant Blue and photographed (Section 2.24.2).

Figure 7.1 shows a comparison between the total protein expression profiles of CHO22 (**A**) and cerR1 (**B**) cells. These gels illustrate that the protein expression profiles for these two cell lines are very similar for most of the cellular proteins and that the protein loading levels are the same. The gels also demonstrate that the expression of two ~20 kD proteins (indicated by the arrows in Figure 7.1) is significantly up regulated in the mutant cerR1 cell line compared to CHO22. However, these gels failed to demonstrate the differential expression of endozepine. This can most probably attributed to the low resolution of these gels. Consequently Western lot analysis was used to investigate the expression of endozepine in cerR1.

7.3. Characterisation of the expression of endozepine by Western blot analysis.

Attempts to detect endozepine by Western blot analysis in total cell lysates of both CHO22 and cerR1 were unsuccessful. The polyclonal anti-endozepine antibodies detected two proteins above 26 kD (data not shown) while the expected size for endozepine is 10 kD. Previous studies suggested that endozepine is localised in the mitochondria (Casellas *et al.*, 2002) and that the expression of this protein is not very high in tissue other than the testes. In an attempt to enrich the protein samples for endozepine, sub-cellular fractionation was performed as described in Section 2.22 and only the mitochondrial fractions were used to investigate the expression of endozepine in CHO22 and cerR1 cells. Mitochondrial proteins were isolated by incubating the mitochondria in 300 µl

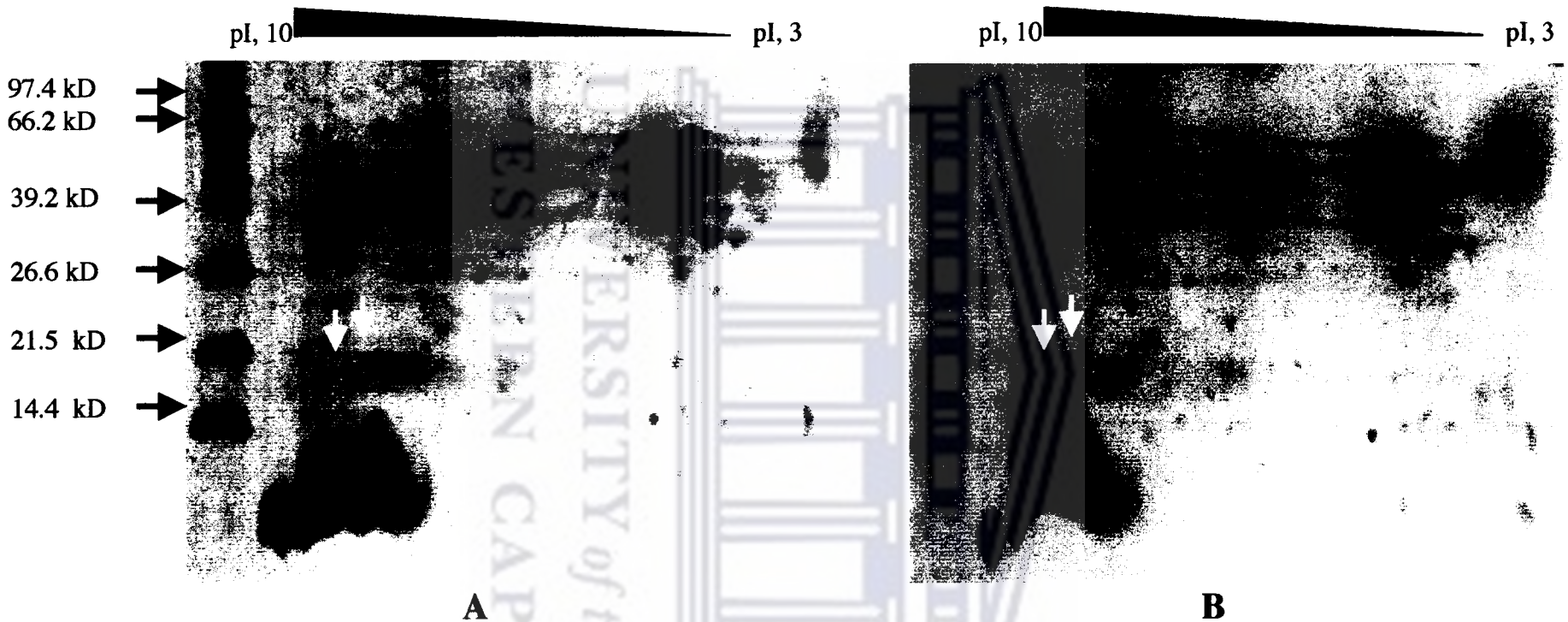

Figure 7.1. A comparison of the 2-D protein expression profile of CHO22 and cerR1 cell lines. **A** and **B** show 2-D gels of total cellular protein isolated from CHO22 and cerR1 cells, respectively. The arrows point to two proteins that are significantly up regulated in the mutant cerR1 cell line when compared to the parental CHO22 cell line.

Lysis Buffer for 20 min. To increase the specificity of the antibody it was first affinity purified as described in Section 2.26.

The purified polyclonal anti-endozepine antibody detected four proteins (sizes ranging from ~8 kD to ~20 kD) in the mitochondrial fraction with one-dimensional SDS-PAGE. Among these proteins was a 10 kD protein which could possibly represent endozepine. This result suggested cross-reactivity of the anti-endozepine antibody with other proteins (possibly acyl-CoA binding proteins). Two-dimensional protein electrophoresis separates proteins not only based on size but also pI. This increases the resolution of the proteins and the probability of detecting and differentiating a single protein from other related proteins.

The protein concentrations of the mitochondrial samples from CHO22 and cerR1 were determined using the Bradford assay and the protein samples were electrophoresed on 2-D SDS PAGE (Section 2.24.2). The proteins were transferred unto a PVDF-P membrane and screened by Western blot analysis using the polyclonal anti-rabbit anti-mouse endozepine antibody (Section 2.28).

Figure 7.2 shows the results of this Western blot, which detected a 10 kD protein with a pI close to 9. This corresponds to the expected size and pI of endozepine. The Western blot also demonstrates that the expression level of endozepine is about 90 % lower in cerR1 compared to CHO22.

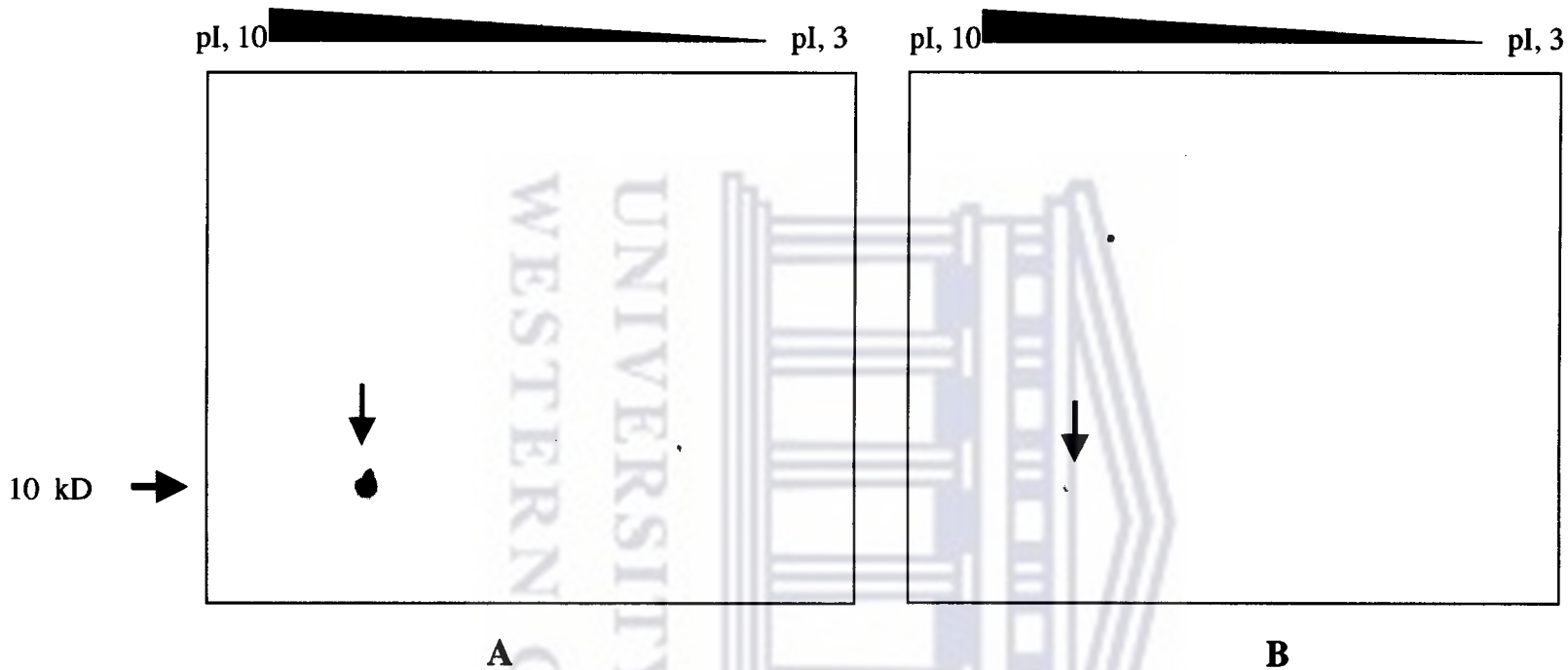

Figure 7.2. Western blot analysis comparing the expression of endozepine in the mitochondrial fractions of CHO22 and cerR1. Mitochondrial proteins were isolated from both CHO22 and cerR1 cells, electrophoresed on 2-D gels and after blot transfer, screened for the expression of endozepine using an anti-endozepine antibody. The red arrows point to the detection of a 10 kD protein with a pI close to 9. The expression level of this protein is significantly lower in the mutant cerR1 (**B**) compared to the parental CHO22 (**A**).

7.4. The subcellular localisation of endozepine by immunofluorescence.

CHO22 cells were cultured on cover slips as described in Section 2.30. When the cells reached confluence the medium was removed and replaced with medium containing 50 nM Mitotracker Green FM (Molecular Probes). The cells were fixed, permeabilised and stained (Section 2.30). The cells viewed using Zeiss Axioplan fluorescent microscope and images were captured using a Spot RT Digital camera (Figure 7.3).

In Figure 7.3-**A** blue indicates DAPI staining, green (Figure 7.3-**B**) indicates MitoTracker Green staining and red (Figure 7.3–**C**) indicates staining with Rhodamine and therefore also endozepine. Figure 7.3 shows that DAPI localised to the nucleus while MitoTracker Green specifically binds to and localise mitochondrial membranes. A comparison between the Figure 7.3-**B** (MitoTracker Green) and Figure 7.3-**C** (endozepine) reveals that endozepine co-localise with MitoTracker Green to the mitochondria.

7.5. Analysis of mitochondrial membrane potential changes using JC-1.

Recent studies showed that apoptosis induces changes in mitochondria and that these organelles play an active role in the apoptotic pathway (reviewed in Section 1.5). One of these mitochondrial changes is depolarisation of the mitochondrial inner membrane.

To investigate mitochondrial depolarisation in cerR1 cells, the cationic dye, JC-1 was used. Various cationic dyes such as $DiOC_6$ (3,3'-dihexyloxacarbocyanine iodide), rhodamine 123 and JC-1 have been used to evaluate mitochondrial membrane potential (Darzynkiewicz *et al.*, 1981; Johnson *et al.*, 1982; Cossarizza *et al.*, 1994). Mitochondrial depolarisation is an early apoptotic event and can be used to detect apoptosis.

JC-1 is a membrane permeable lipophilic cationic fluorochrome that can be used as an indicator of mitochondrial membrane potential (Salvioli *et al.*, 1997; Mancini *et al.*, 1997). This fluorochrome is taken up by charged mitochondria and its accumulation in the mitochondria is indicated by a fluorescence emission shift from 525 nm (green) to 590 nm (red) (Cossarizza *et al.*, 1994). In a monomeric form the fluorochrome has an emission wavelength of 525 nm and changes its emission wavelength to 590 nm as it forms aggregates. Mitochondrial depolarisation, and therefore the induction of apoptosis, is indicated by a decrease in the red/green fluorescence intensity ratio (i.e. a decrease in fluorochrome aggregation). This shift in fluorescence can be detected using the FL2 and FL1 channels on a conventional flow cytometer. JC-1 has been demonstrated to be significantly more specific for its use as an indicator of mitochondrial membrane potential during apoptosis than to $DiOC_6$ or rhodamine 123, because of possible changes in plasma membrane potential, which may interfere with the assessment of mitochondrial membrane potential changes (Salvioli *et al.*, 1997).

CHO22 and cerR1 cells were stained with JC-1 dye and analysed using a FACScan instrument (Section 2.29.7). Figure 7.4 shows density plots of the FL1 (530 nm) versus FL2 (585 nm) data whereas Figure 7.5 is showing overlaid histograms of the FL2 (585 nm) data for both cell lines at the different time points (0 min, 2 hrs, 3 hrs and 6 hrs). Figures 7.4-**A** and 7.4–**B** demonstrate that the fluorescence density plots of the untreated control cells (0 min) is the same for both cell lines. Even after 2 hr treatment (Figures 7.4-**C** and 7.4-**D**) with 60 μM C_2-ceramide the fluorescence density plots for the two cell lines still remains the same, although a fraction of the cells (in both cell lines) show a loss in red fluorescence (FL2) or a gain in green fluorescence (FL1). This is also illustrated in Figure 7.5, which represents an overlaid histogram of the changes in red fluorescence (FL2) for the two cell lines: CHO22 (Figure 7.5-**A**) and cerR1 (Figure 7.5-**B**). It is at the 3 hr time point (Figures 7.4-**E** and 7.4-**F**) where the fluorescence intensities between the two cell lines starts to reveal a difference. This is also illustrated in Figure 7.5-**A**, which shows that close to 90 % of the CHO22 cells demonstrates a significant loss in red fluorescence (FL2). In sharp contrast, Figure 7.5-**B** shows that only ~50 % of the cerR1 cells display a similar loss in red fluorescence (FL2). This suggests that there is a delay in mitochondrial depolarisation during the induction of apoptosis with C_2-ceramide in cerR1 cells. This is further illustrated at the 6 hr time point (Figure 7.5), which shows that the mitochondrial potential in CHO22 cells is increasing while the cerR1 cells are still approaching the stage where the cells reach minimal depolarisation as was observed in CHO22 cells at the 3 hr time point. This therefore suggests that there is at least a 3 hr delay or reduction in mitochondrial depolarisation in cerR1 cells.

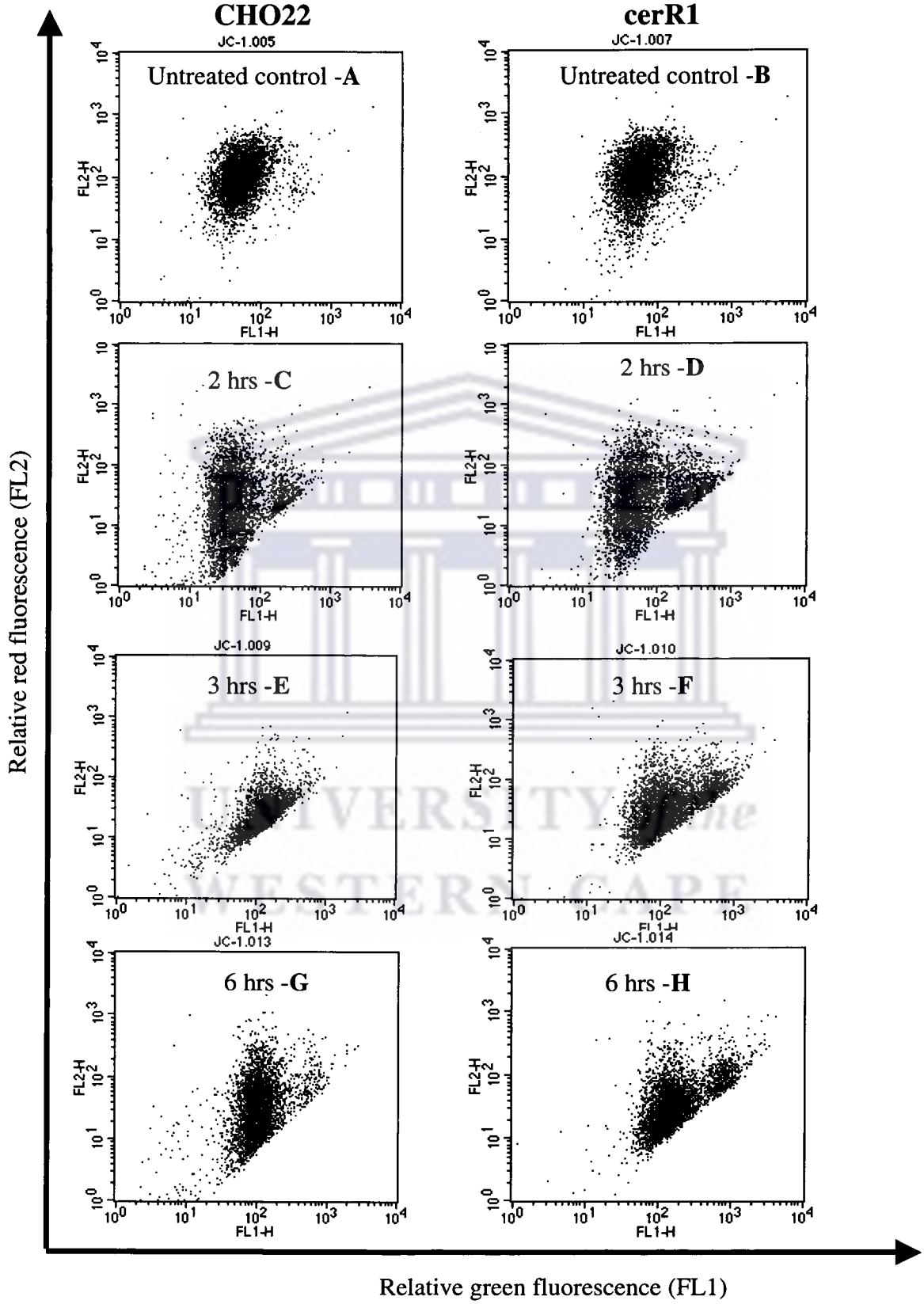

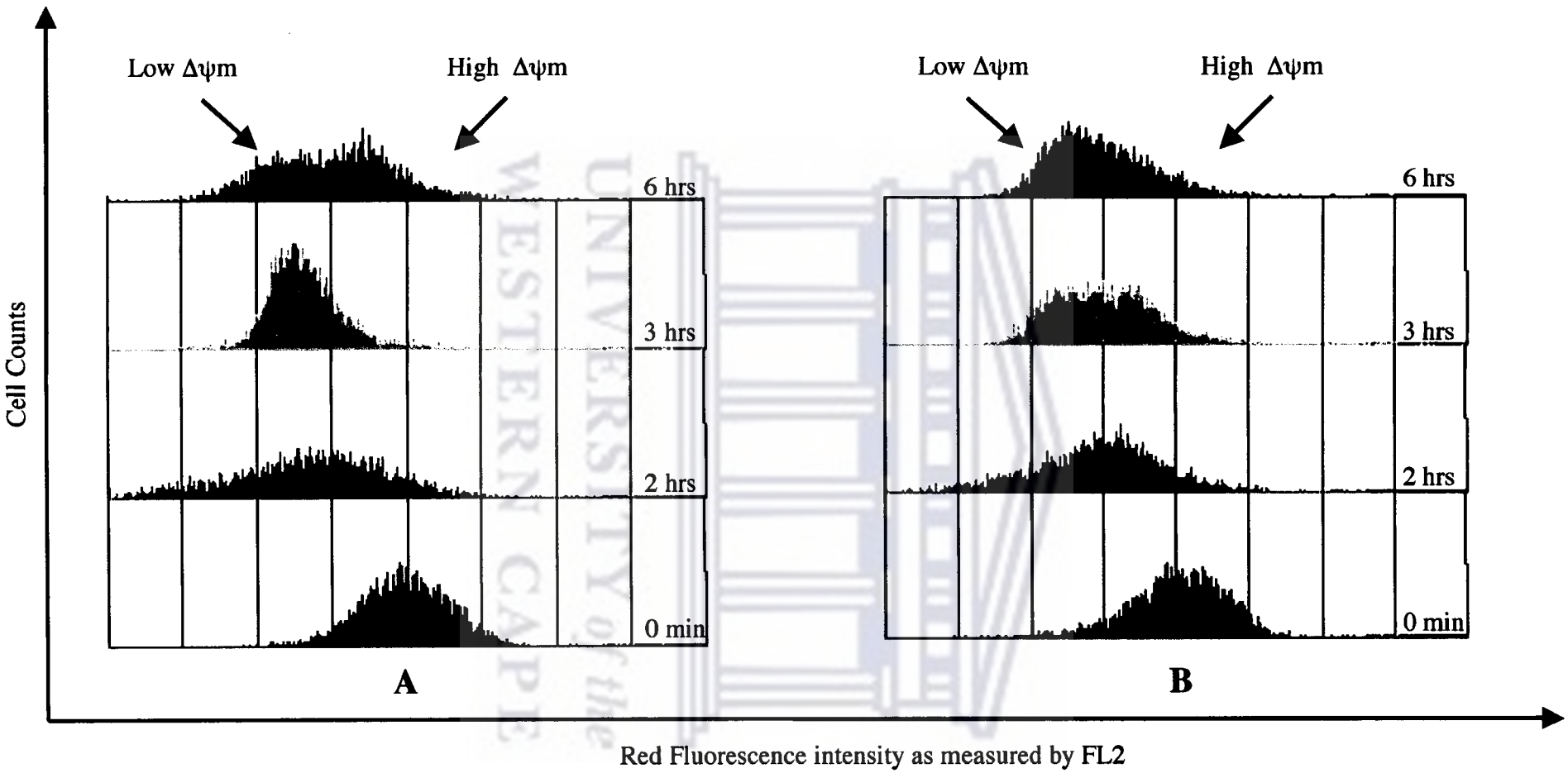

Figure 7.5. Overlaid histograms comparing changes in the mitochondrial membrane potential (Δψm) in CHO22 (**A**) and cerR1 (**B**) as measured by JC-1 staining and flow cytometric analysis. CHO22 and cerR1 cells were treated 60 μM C_2-ceramide and changes in red fluorescence was measured at 590 nm (FL2). The cells were monitored at time 0 min, 2 hrs, 3 hrs and 6 hrs.

7.6. **Summary.**

In this study two-dimensional gel electrophoresis was used to do a comparative analysis of the proteomes of the two related cell lines, CHO22 and cerR1. Since cerR1 was derived from CHO22, it is expected that the genetic make-up and therefore also the protein expression profile be the same. However, cerR1 has been transfected with the Moloney murine leukaemia retrovirus and it express a phenotype, resistance to C_2-ceramide-induced apoptosis, which is not expressed by CHO22. Depending on the expression levels of the genes involved, this phenotypic difference may be reflected by comparative two-dimensional gel electrophoresis.

Two-dimensional gel electrophoresis demonstrated that the protein expression profiles of CHO22 and cerR1 are very similar. Figure 7.1 shows that two proteins of about 20 kD with a pI of about 8 are differentially expressed between these two cell lines. The expression of these proteins appears to be significantly up regulated in the mutant cerR1. The characterisation of the mutation in cerR1 by inverse PCR and sequence analysis suggested that the expression of endozepine might have been affected by retroviral integration. The molecular weight of endozepine is 10 kD and the pI for this protein is 9. This eliminates the possibility that one of these proteins could be endozepine.

The inserted retrovirus contains two selectable marker genes: the neomycin resistance (*tk*-neo) and hygromycin B phosphotransferase ($Hygro^R$) genes. The *tk*-neo is constitutively expressed while the $Hygro^R$ will only be expressed if the

retroviral insertion is downstream of an active host promoter. It is therefore possible that these two proteins which are up regulated in the transfected mutant, cerR1 could represent these two selectable marker genes. However, the molecular weight of the *tk*-neo and Hygro^R proteins are 30 and 38 kD, respectively, which suggests that the up regulated proteins observed do not represent these retroviral genes. The identity of these proteins is not known yet, but these proteins could represent genes that are differentially expressed in the mutant cerR1 as a consequence of the promoter-trap insertional mutation. In Chapter 5 inverse PCR and sequence analysis identified endozepine as the gene that was knocked out in this mutant resulting in resistance to C_2-ceramide-induced apoptosis. Several lines of evidence (reviewed in Section 5.3.3) suggest that endozepine is a key component of the mitochondrial apoptotic pathway. The identity of these proteins may shed more light on the mechanism of the pathway or lead to the identification of other novel components of this pathway.

Two-dimensional gel electrophoresis and Coomassie staining did not show differential expression of any protein with the characteristics (size and pI) of endozepine. This could be a reflection of the low expression levels of this protein. It should also be noted that the resolution of two-dimensional gel electrophoresis of total cellular proteins is dependent on the size of the gel. In this study the proteins were electrophoresed on 8×10 cm PAGE gels. A cell expresses thousands of proteins at any one time. This complexity is not reflected in Figure 7.1, which is an indication that the proteins should be analysed on a larger gel in order to increase the resolution of two-dimensional gel electrophoresis. Increasing the

resolution of two-dimensional gels may demonstrate that more cellular proteins are differentially expressed. However, Western blot analysis (Figure 7.2) using an anti-endozepine antibody, showed reduced expression of this protein in cerR1, which can be attributed to retroviral integration into this gene.

There is evidence to suggest that endozepine/ACBP may associate with the PBR in mitochondrial membranes. This therefore means that this protein might be localised in the mitochondria. This was confirmed by immunofluorescent staining using the anti-endozepine antibody. MitoTracker Green FM was used as a stain for mitochondrial membranes, which showed that endozepine co-localised with MitoTracker Green FM in the mitochondria (Figure 7.3).

Several lines of evidence exist to suggest that endozepine is involved in the mitochondrial apoptotic pathway by facilitating mitochondrial permeability transition during apoptosis induced by C_2-ceramide. (1) Endozepine is a putative ligand to the PBR (Guidotti *et al.*, 1983; Garnier *et al.*, 1994). (2) The PBR and its ligands have been implicated in mitochondrial depolarisation and apoptosis (Hirsch *et al.*, 1998; Zamzami *et al.*, 1996; Xia *et al.*, 2000; Fennell *et al.*, 2001; Strohmeier *et al.*, 2002; Decaudin *et al.*, 2002). (3) Previous studies showed that endozepine is released from the mitochondria together with other pro-apoptotic proteins during mitochondrial permeability transition (Patterson *et al.*, 2000; Van Loo *et al.*, 2002). (4) This study shows that endozepine localises in the mitochondria. (5) This study shows that loss of endozepine results in resistance in apoptosis induced by C_2-ceramide. It therefore follows that if endozepine is

involved in MPTP opening that mitochondrial permeability transition in the mutant cerR1 should be aberrant since the expression of this protein in this mutant has been reduced by promoter-trap retroviral integration. To investigate this theory, both CHO22 and cerR1 cells were treated with C_2-ceramide and stained with JC-1 to assess changes mitochondrial potential. In accordance to the study by Waterhouse *et al.*, (2001) the mitochondrial potential decreased 2 hrs after treatment with ceramide and started to recover (mitochondrial potential was increasing) after 6 hrs (Figure 7.4 and 7.5). This trend was observed for both CHO22 and cerR1 cells, however, it is also clear that the decrease in mitochondrial potential in the mutant cerR1 is significantly reduced or slower compared to CHO22.

Mitochondrial depolarisation can be viewed as the rate limiting step regulating the opening of the mitochondrial permeability transition pore and the release of pro-apoptotic proteins such as cytochrome c, Smac/DIABLO and IAP. Once these proteins are released into the cytoplasm, the formation of the apoptosome and the consequent activation of caspase-9 and -3 will follow. This would imply that a block in mitochondrial depolarisation, as can be observed in cerR1, would prevent the release of cytochrome c, Smac/DIABLO and IAP. This will ultimately block the activation of caspase-3 and therefore also apoptosis.

CHAPTER 8: GENERAL DISCUSSION.

8.1. Introduction.

8.2. The identification of suitable apoptosis inducers and selection conditions for the selection of resistant mutants.

8.3. The generation and characterisation of apoptosis resistant promoter-trap mutants.

8.4. Characterisation of the mutations in cerR1 by inverse PCR.

8.5. The role of endozepine in ceramide-induced apoptosis.

8.6. Proposed model for the involvement endozepine/DBI in ceramide-induced apoptosis.

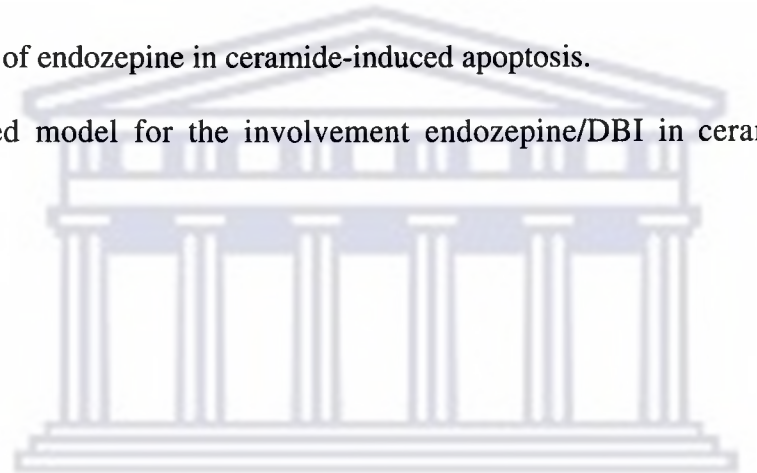

CHAPTER 8: GENERAL DISCUSSION.

8.1. Introduction.

The objectives of this research were to identify novel genes involved in apoptosis. The strategy involved the random inactivation of genes by promoter-trap mutagenesis, followed by the selection of mutants that were resistant to apoptosis. CHO22 cells were chosen as the target cell line for promoter-trapping, since these cells are pseudohaploid (Siminovitch, 1985). This implies that these cells express only one functional copy of a gene (although the mechanism is unknown) and that the chance of generating a complete knockout by a single retroviral integration event into the host genome is very high. Genes identified through the characterisation of such apoptosis resistant promoter-trap mutants can be classified into three categories: (1) genes known to be involved in apoptosis, (2) novel genes never characterised before and (3) known genes not previously been linked to apoptosis. This study identified a gene coding for an acyl-CoA binding protein called endozepine as a gene involved in apoptosis. Endozepine is not a novel gene, in fact a number of functions have been ascribed to this gene previously and therefore it falls into the third category of genes anticipated to be identified from this screen.

8.2. The identification of suitable apoptosis inducers and selection conditions for the selection of resistant mutants.

The activation of apoptosis involves the initiation of a number of intricate signalling pathways, which in some instances overlap with each other. The choice of pathway(s) is determined by the physiological status of the cell, the cell type, the developmental stage of the tissue and the nature of the apoptosis inducing stimulus. Numerous chemical substances can be used to mimic the action of physiological activators of apoptosis (Thompson, 1995).

The aim of this research was to select for mutants that are resistant to apoptosis induced under *in vitro* conditions and therefore the first objective was to identify suitable inducers of apoptosis. C_2-ceramide and camptothecin are known chemical inducers of apoptosis. These substances have been used in a number of *in vitro* studies to induce apoptosis in various cell lines (Smyth *et al.*, 1996; Tepper *et al.*, 1997; Dassonneville *et al.*, 2000). A major concern with these substances is their solubility. Both these compounds have low solubility's in water and therefore DMSO was used to dissolve these compounds. DMSO is also known to activate apoptosis at concentrations higher than 2 % in cultured cells (Lin *et al.*, 1995). To ensure that the effects of DMSO did not adversely affect the outcome of the selections for resistance to C_2-ceramide- or camptothecin-induced apoptosis, it was important to first identify the minimum and maximum concentrations of DMSO required to activate apoptosis in CHO22 cells. Since these compounds have the ability to be cytotoxic, it was important that the minimum concentration and exposure times be identified and used in the selection for apoptosis resistant

mutants. These experiments involved the titration of DMSO on CHO22 cells and studying the effect on the cells (Sections 3.4, 3.5 and 3.6). These experiments demonstrated that DMSO concentrations higher than 3 % induce morphological changes in CHO22 cells which can be associated with apoptosis and that a concentration of 0.1 % does not affect the cells. Experiments in this thesis used DMSO concentrations at 0.1 % or lower, thus ensuring that DMSO did not synergistically induce apoptosis together with ceramide or camptothecin.

Both C_2-ceramide and camptothecin were able to induce apoptosis in CHO22 cells. This was demonstrated (Sections 3.3 and 3.4) by biochemical changes in treated CHO22 cells, such as DNA fragmentation and positive staining with APOPercentage™ dye. Since the intention was use C_2-ceramide and camptothecin to select for mutants that are resistant to apoptosis, the next objective was to identify the appropriate concentrations of these compounds to be used in these selections experiments. If the stringency of the selection is not high enough, it will increase the possibility that false positive resistant mutants may occur. To achieve this level of stringency it was necessary to titrate the concentrations of both compounds on CHO22 cells and to identify the minimum concentration and the minimum exposure time required to achieve 100 % killing. These experiments demonstrated that a 72 hr selection period with 100 μM C_2-ceramide or a 24 hr selection period with 5 μg/ml camptothecin was the minimum level of exposure necessary to achieve 100 % killing.

8.3. The generation and characterisation of apoptosis resistant promoter-trap mutants.

Promoter-trap mutagenesis generated three somatic cell mutants that were resistant to apoptosis induced by C_2-ceramide. These cell lines: cerR1, cerR2 and cerR3 were generated by selection with C_2-ceramide. The characterisation of cerR1, cerR2 and cerR3 by inverse PCR demonstrated that these three clones originated from the same clone, since the sizes of the inverse PCR fragments produced by inverse PCR were the same for the three clones (Section 5.2.1).

The APOPercentage™ and LDH release assays were used to characterise the resistance of the cerR1 mutant to apoptosis induced by C_2-ceramide. Both assays demonstrated that the mutant, cerR1, is more resistant to apoptosis than the parental CHO22 cell line. On average both assays showed that the number of apoptotic cells is almost 50 % lower in the mutant cell line, cerR1 (Section 4.2).

8.4. Characterisation of the mutations in cerR1 by inverse PCR.

Inverse PCR is an extension of the conventional polymerase chain reaction that allows the amplification of unknown DNA sequences flanked by known sequences (Saiki *et al.*, 1985). This technique was used in this research to identify the genes inactivated by retroviral insertion. In a previous study (George, 1995) RACE (rapid amplification of cDNA ends) PCR was used to identify the unknown disrupted gene sequences. RACE PCR involves cDNA synthesis from mRNA using retroviral specific primers. The advantage of using RACE PCR is

that all the expected PCR products will be generated from expressed sequences and therefore only retroviral insertions into expressed sequences will be amplified and identified. In contrast inverse PCR products are generated from genomic DNA and may therefore also amplify genomic sequences at retroviral integrations into non-expressed genomic sequences. This implies that RACE PCR could potentially be more informative than inverse PCR. However complications with RACE PCR technology led to the development of the inverse PCR strategy, which was more successful in amplifying genomic sequences at retroviral integrations sites for the identification of unknown disrupted host gene sequences.

Inverse PCR analysis on cerR1 generated a total of five PCR amplification products demonstrating multiple retroviral insertion into this cell line (Section 5.2). One of these fragments corresponds to the expected size of the 3' end retroviral fragment, suggesting that the remaining four fragments were produced of the 5' end from the retrovirus and should therefore contain hamster genomic sequence. Sequence analysis of these fragments confirms that these four fragments are individual retroviral integration events, which is the consequence of four distinct retroviral insertions, which is most probably the result of multiple retroviral insertion. It is possible that high retroviral titres may be the cause of multiple retroviral insertion. The multiplicity of infection (moi) in a previous study (George, 1995) that aimed to generate mutants that were resistant cytotoxic T lymphocyte killing (CTL) was much higher (0.6) than the current study (0.01). In theory this means that in both these studies a single retroviral insertion per cell should be attained. However inverse PCR demonstrated that the mutants

generated in this study were generated by multiple retroviral insertion. Inverse PCR analysis on CTL resistant mutants generated in the previous study (George, 1995) also demonstrated multiple retroviral insertion (Skepu, Meyer, Rees; unpublished data). It is not clear why multiple retroviral insertion should occur even though the moi was quite low. One possible explanation could be variations in the CHO22 cells in terms of the expression of the Moloney murine leukaemia virus (MoMuLV) murine ecotropic receptor, which will make some CHO22 cells more susceptible to infection than others resulting in multiple infections.

The inverse PCR products were amplified from genomic DNA isolated from cerR1 was designated F1, F2, F3 and F4 (Section 5.2.3). The 5' end of these genomic DNA sequences all demonstrated the presence of the Moloney murine leukaemia virus. The sequence adjacent to the retrovirus was expected to contain host genomic DNA sequence. Retroviral integration can potentially affect the expression of any host genes in this region of the host genome either directly through the insertion event, or indirectly by affecting the chromatin organisation. Sequence analysis eliminated the F2, F3 and F4 retroviral insertions as possible integration events, which could have resulted in resistance to C_2-ceramide-induced apoptosis, since these sequences did not produce any significant matches against any known sequence in the databases in particular against fully annotated mouse, rat or human sequences (Section 5.2.3).

The F1 inverse PCR fragment showed retroviral integration into a region between two genes namely Gemin4 and endozepine (Section 5.2.4). Earlier sequence

analysis did not match Gemin4 as a possible candidate gene. This can be attributed to the incomplete status of sequence databases at that time. Gemin4 was therefore not considered as a possible candidate gene, instead endozepine was viewed as the only candidate gene. Recent developments in genome sequencing provided a more complete view of the genome and revealed Gemin4 as another possible candidate gene. Sequence analysis demonstrated that the retroviral insertion into Gemin4 is a promoter-trap event and that there is a high probability that this gene was knocked out. However, since the scope of this research did include this gene it is premature to speculate that Gemin4 was knocked out in cerR1. It is for these reasons that this study focused on endozepine as the gene that resulted in resistance to C_2-ceramide-induced apoptosis, which remains the more likely candidate gene for the phenotype observed in this study.

Western blot analysis demonstrated a ~90 % reduction in the expression of endozepine in the mutant cerR1 (Section 7.3). Although retroviral insertion into this gene did not achieve a complete knockout, it did result in greatly reduced expression of this gene. Based on the known functions of these genes, endozepine stands out as the most likely candidate to be involved in ceramide-induced apoptosis (Section 5.3). In spite of this, it is very likely that the F4 retroviral integration also affected the expression of Gemin4. However, this research did not investigate the expression of this gene in cerR1.

Two-dimensional gel electrophoresis also demonstrated differential protein expression between CHO22 and cerR1 cells. A comparison of their total protein

expression profiles is expectedly very similar, except for two proteins of about 20 kD, which is significantly up regulated in the mutant, cerR1. The identity of these two proteins is not known at this stage. Based on the sizes of these proteins, they appear not to be the retroviral selectable marker genes: neomycin resistance (*tk*NEO) or hygromycin B phosphotransferase ($Hygro^R$). This suggests that these proteins represent host genes, which are up regulated in the mutant due to retroviral integration and might even have a role to play in conferring resistance to C_2-ceramide-induced apoptosis. In this study proteins were analysed for the second dimension on a relatively small (8×10 cm) gel. As a consequence the resolution of single proteins was not very efficient. It is possible that more differentially expressed proteins may be identified by two-dimensional gel electrophoresis by increasing the size of the gel and therefore also the resolution.

Endozepine belongs to the acyl-CoA binding (ACBP) family (reviewed in Section 5.3). The ACBP family can be subdivided into at least five groups of ACBP based on sequence alignment. These subgroups include: 1-ACBP, t-ACBP, b-ACBP, m-ACBP and the membrane-associated ACBP. Endozepine belongs to the t-ACBP-isoform. This protein is predominantly expressed in the testes (Pusch *et al.*, 1996). The 1-ACBP-isoform appears to be involved in acyl-CoA metabolism and is crucial for cell survival. The b-ACBP-isoform is a brain-specific variant while the m-ACBP-isoform is a membrane-bound protein. Several functions including acyl-CoA metabolism, steroidogenesis, insulin secretion and GABA/benzodiazepine receptor modulation have been attributed to this protein family. Endozepine is predominantly expressed in the male germ cells of the testes of a wide range of

mammals with low level of expression in other tissues such as the ovary, uterus, adrenals and liver. In the testes the expression of endozepine coincides with spermatid elongation in post meiotic stages of male germ cell development (Pusch *et al.*, 1999). This tissue specific and developmentally regulated expression of this protein pointed towards a possible role in spermatid development. Another possibility is that endozepine might play a role in sperm metabolism since ACBP have been implicated in the transport of acyl-CoA to the mitochondria for energy metabolism (Faergeman *et al.*, 1997). Endozepine is expressed in a wide range of mammals, including rodents, carnivores and ruminants. This gene is conserved with a 54 % identity in amino acid sequence between these organisms. This suggests that there was a selective pressure on this gene during evolution and that the function of this gene must have been crucial for the survival of these organisms. Recent studies suggest that this gene has progressively been inactivated during the evolution of primates with no detectable expression in humans (Ivell *et al.*, 2000). Two transcripts on chromosomes 2 and 17 have been identified in human testes. Both have been inactivated by frame-shift mutations and insertions. It is not clear why a gene that has been retained in other species is not expressed in humans. One possible explanation could be that the other members of this gene-family are up regulated in humans, and since these proteins are structurally and functionally related, these isoforms could have taken over the function of endozepine in humans.

8.5. The role of endozepine in ceramide-induced apoptosis.

Ceramide is a sphingolipid second messenger signalling molecule that is involved in various signalling pathways. It has been demonstrated that C_2-ceramide, a synthetic analogue of ceramide, can mimic some of the physiological effects of endogenous ceramide. Apoptosis induced by C_2-ceramide can be associated with mitochondrial depolarisation, the release of cytochrome c and caspase-3 activation (Hearps *et al.*, 2002).

There are several lines of evidence to suggest that endozepine may play a possible role in the mitochondrial apoptotic pathway (Section 5.3.3). Endozepine has been described as a possible ligand to the peripheral benzodiazepine receptor (PBR), which forms part of the mitochondrial permeability transition pore (Guidotti *et al.*, 1983; Crompton, 1999; Casellas *et al.*, 2002). Ligands to the PBR have been shown to regulate apoptosis induced via the mitochondrial apoptotic pathway mediated through mitochondrial permeability transition. Two independent studies have shown that endozepine is amongst the proteins released from isolated mitochondria when mitochondrial permeability transition is induced (Patterson *et al.*, 2000; Van Loo *et al.*, 2002). In these studies mitochondrial permeability transition was induced by exposing the mitochondria either to mitochondrial permeability transition pore opening agent, attractyloside (Patterson *et al.*, 2000) or to tBID (Van Loo *et al.*, 2002). The identity of the released proteins were determined by mass spectrometry and in addition to known pro-apoptotic proteins such as cytochrome c and Smac/DIABLO, endozepine was also isolated. However these studies could not confirm whether endozepine also promoted

apoptosis. The current study presents evidence that implicates this protein in apoptosis, by showing that reduced expression of endozepine leads to resistance to apoptosis induced by C_2-ceramide.

At present there is no evidence to suggest that there is a direct interaction between endozepine and PBR. However, through competitive binding assays between DBI and diazepam (a benzodiazepine derivative, which acts as a ligand to PBR), it has been demonstrated that DBI may be an endogenous ligand to PBR, since DBI was able to displace diazepam from PBR (Guidotti *et al.*, 1983; Garnier *et al.*, 1994). The role of PBR ligands in regulating mitochondrial permeability transition is well documented (reviewed in Section 1.5.1.1). It has been demonstrated that these ligands could have both pro- and anti-apoptotic effects on cells. PK11195 has been shown to induce apoptosis in HL60 cells (Fennell *et al.*, 2001). While PK11195 did not activate apoptosis in thymocytes, it enhanced the pro-apoptotic activity of UV radiation, etoposide, doxorubicin, dexamethasone and ceramide (Hirsch *et al.*, 1998). A recent study also demonstrated that resistance of cancer cells to apoptosis induced by CD95 could be reversed when the cells are treated with the PBR ligands such as PK11195, Ro5-4864 and diazepam (Decaudin *et al.*, 2002). Apoptosis observed in cells treated with the substances was characterised by the release of cytochrome c and Smac/DIABLO from the mitochondria with a parallel increased caspase-3 activation.

Our current understanding of ceramide-induced apoptosis is still very limited. The downstream effects (such as cytochrome c release, mitochondrial permeability

and caspase-3 activation) of ceramide during apoptosis are well documented. The release of cytochrome c and the role of mitochondrial depolarisation in apoptosis is still a controversial issue in apoptosis biology. One view is that mitochondrial depolarisation results in the opening of the mitochondrial permeability transition pore, which results in mitochondrial swelling and ultimate lysis of the outer membrane with consequent release of cytochrome c and other pro-apoptotic proteins from the mitochondria (Petit *et al*, 1996). This will lead to the formation of the apoptosome and the activation of caspase-9. This model is supported by a large body of evidence, which suggest that ligands to the PBR (a component of the mitochondrial permeability transition pore) control mitochondrial depolarisation and apoptosis (Hirsch *et al.*, 1998; Chelli *et al.*, 2001; Fennell *et al.*, 2001; Strohmeier *et al.*, 2002). Recent studies present a different perspective based on data that demonstrates that cytochrome c release precedes mitochondrial depolarisation (Waterhouse *et al.*, 2001). These studies propose models for the mechanism based on the formation of pores in the mitochondrial membrane, which facilitate the release of cytochrome c (Section 1.3.1). However, evidence for the existence of such in structures in mitochondrial membranes is still lacking.

8.6. Proposed model for the involvement endozepine in ceramide-induced apoptosis.

This study presents evidence that a protein called endozepine facilitates mitochondrial depolarisation transition, and therefore also apoptosis, by

regulating mitochondrial depolarisation. As a consequence the data presented in this study lends support to the mitochondrial permeability transition pore model.

It has been proposed that endozepine/ACBP is a ligand to the PBR (Guidotti *et al.*, 1983; Garnier *et al.*, 1994). It has also been demonstrated that the PBR and its ligands play a role in mitochondrial depolarisation and apoptosis (Hirsch *et al.*, 1998; Zamzami *et al.*, 1996; Xia *et al.*, 2000; Fennell *et al.*, 2001; Strohmeier *et al.*, 2002; Decaudin *et al.*, 2002). At this stage it is not clear how ceramide, endozepine and the PBR interact with each other to bring about mitochondrial depolarisation. This research proposes that the interaction between these three components of the ceramide-induced apoptotic pathway triggers the opening of the mitochondrial permeability transition pore. This leads to mitochondrial depolarisation and consequent release of cytochrome c and other pro-apoptotic proteins. Four possible models can be proposed to explain the interaction between ceramide, endozepine and the PBR (Figure 8.1). The first possibility is that these three components form a trimeric complex as illustrated in Figure 8.1-**A**. The second possibility is that ceramide and endozepine forms a complex, which subsequently interacts with the PBR (Figure 8.1-**B**). Preliminary competitive binding assays (data not shown) between recombinant mouse endozepine, C_2-ceramide and agarose beads cross linked with acyl-CoA have demonstrated that endozepine might be a primary target for ceramide (Meyer, Onyemata, Pugh, Rees; unpublished data). These experiments showed evidence of a possible direct interaction between endozepine and C_2-ceramide. It also demonstrated the possibility that ceramide may bind to the acyl-CoA binding domain of endozepine

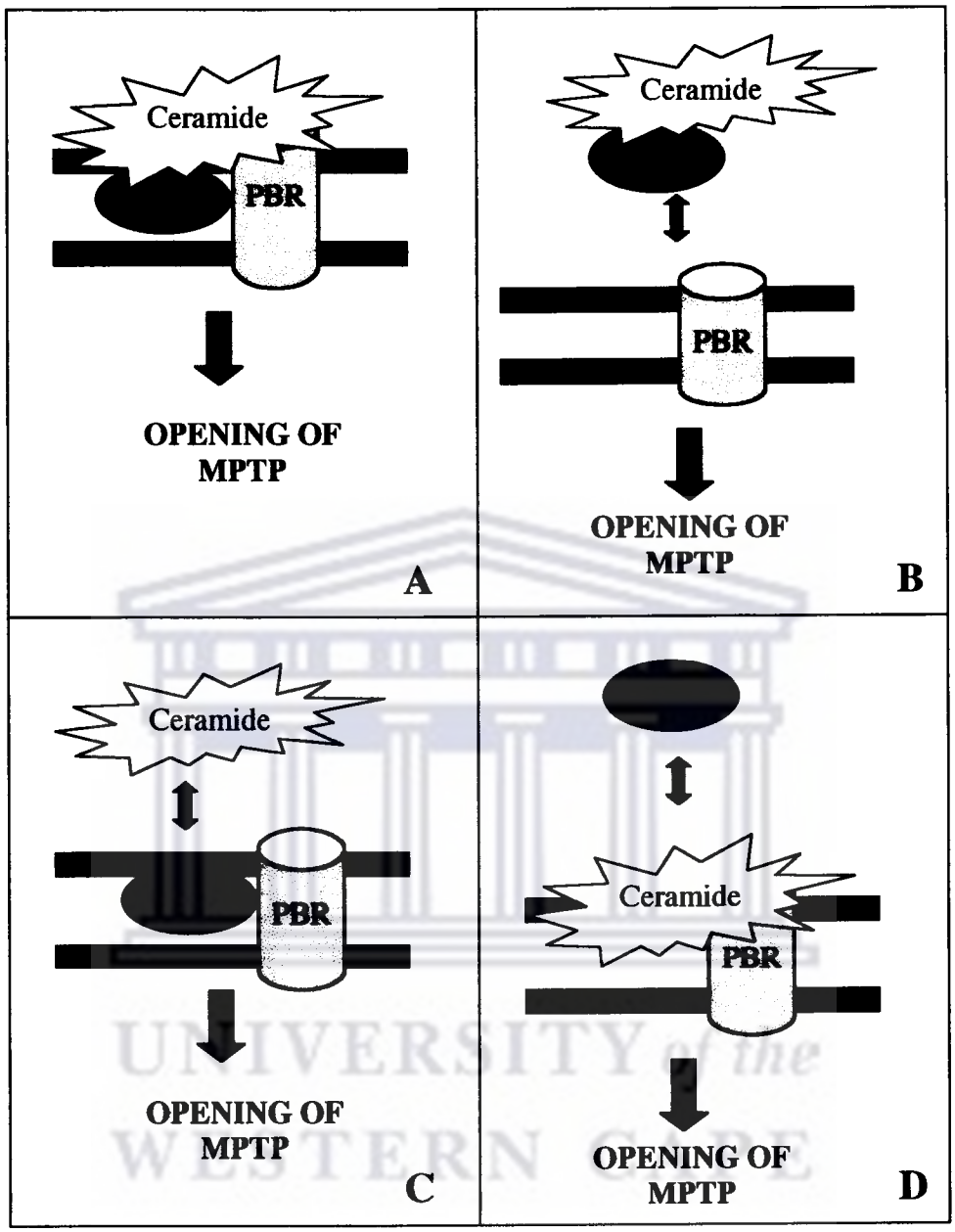

Figure 8.1. The four putative models describing the interaction between endozepine (ELP), PBR and ceramide resulting in mitochondrial permeability transition pore (MPTP) opening.

since C_2-ceramide was able to displace endozepine from agarose beads cross linked with acyl-CoA. However this data is not conclusive at this stage. A previous study (Blahos, 1995) demonstrated that a 10 kD unknown protein associates with PBR during the purification of the mitochondrial permeability transition pore. Endozepine has been described as a putative ligand to the PBR and it is also a 10 kD protein. It is tempting to speculate that this unknown protein might be endozepine. This would lend support to a third model (Figure 8.1-**C**), which proposes that endozepine and PBR forms a complex, which is activated by the binding of ceramide to this complex. The fourth model (Figure 8.1-**D**) proposes that ceramide first forms a complex with PBR before endozepine binds to it. It therefore follows that loss of endozepine expression will prevent the formation of the trimeric complex between ceramide, PBR and endozepine. Consequently loss of endozepine expression will block MPTP opening and therefore mitochondrial depolarisation and apoptosis.

The mitochondrial permeability transition pore model proposes that mitochondrial depolarisation will result in the opening of the mitochondrial permeability transition pore which will result in the release of cytochrome c and other pro-apoptotic proteins such as Apaf-1, Smac/DIABLO and AIF from the mitochondria Previous studies have already demonstrated that ligands to the PBR can activate mitochondrial depolarisation with the subsequent release of these proteins. Recent evidence also show that endozepine is amongst these proteins (Patterson *et al.*, 2000, Van Loo *et al.*, 2002). These studies did not demonstrate what the role of endozepine in apoptosis might be. However, with the new evidence at hand the

model illustrated in Figure 8.2 can be proposed for the involvement of endozepine in ceramide-induced apoptosis.

Using immunofluorescence microscopy this research showed that endozepine localises to the mitochondria (Section 7.4), which lends support to the suggestion that endozepine might be a ligand to PBR. This research also provides evidence that reduced expression of endozepine leads to resistance towards C_2-ceramide-induced apoptosis. This resistance to apoptosis is accompanied by a reduction in mitochondrial depolarisation. This implies that endozepine plays a role in the regulation of mitochondrial depolarisation and therefore also apoptosis. If endozepine is involved in the regulation of mitochondrial depolarisation and, then it would imply that loss of endozepine expression would delay or prevent mitochondrial depolarisation and therefore also the mitochondrial permeability transition, which in turn will inhibit cytochrome c release and subsequent caspase-3 activation. In line with this model this research demonstrated that mitochondrial depolarisation and caspase-3 activation were indeed reduced in the mutant cerR1 (Section 4.4). JC-1 staining of CHO22 and cerR1 cells treated with C_2-ceramide demonstrated reduced mitochondrial depolarisation in the mutant cells (Section 7.5).

Although the current data strongly favours the loss of endozepine expression as the reason for resistance of the mutant cerR1 to apoptosis induced by C_2-ceramide, the recent discovery of Gemin4 as another possible candidate gene should not be excluded. Therefore it can be concluded that this study has

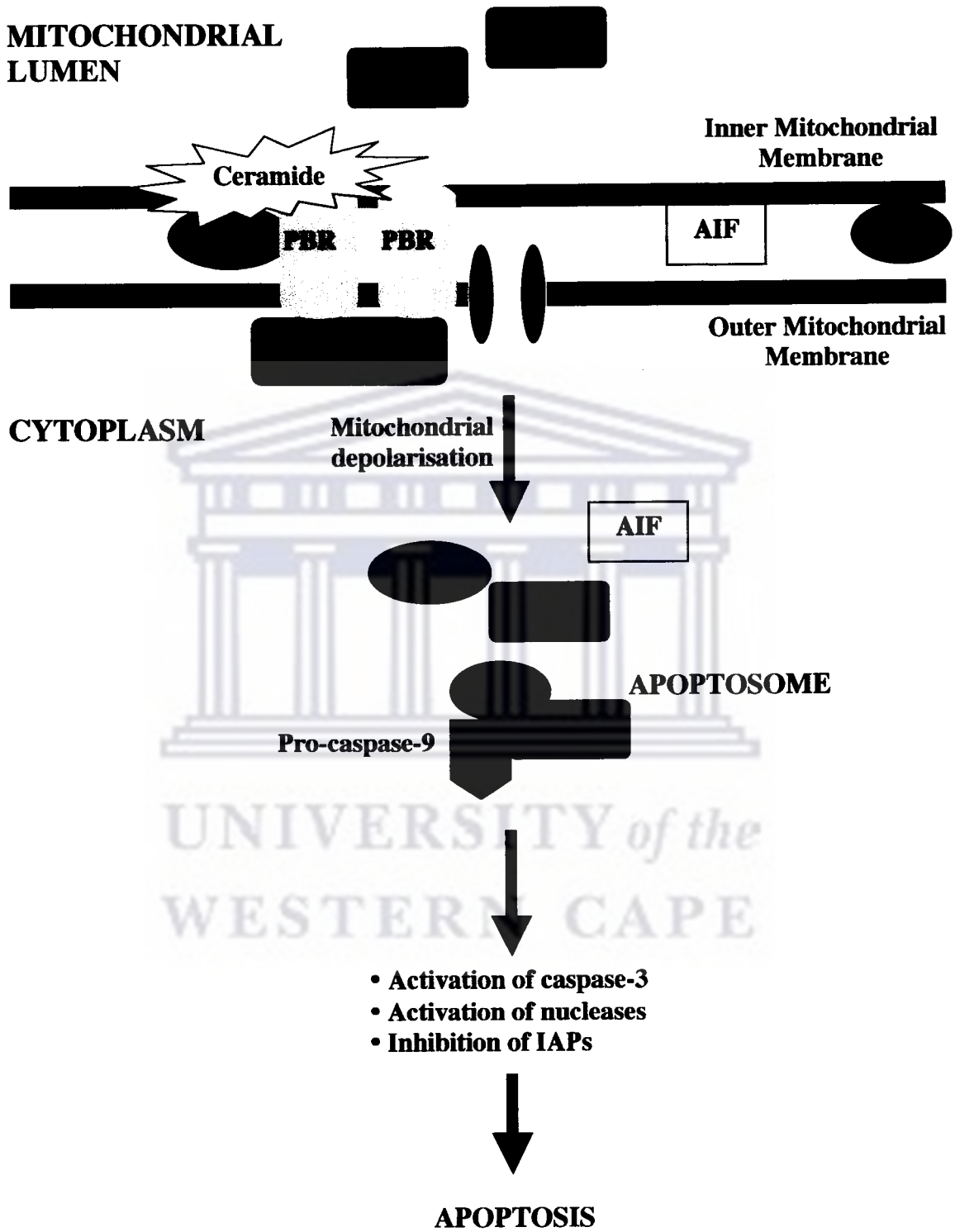

Figure 8.2. Proposed model for the involvement of endozepine (ELP) in ceramide-induced apoptosis.

identified two possible genes involved in ceramide-induced apoptosis. This study did not investigate Gemin4 as a possible candidate and therefore as a future prospect the expression and function of this gene should also be analysed. In spite that fact that the evidence points towards endozepine as the gene that is involved in ceramide-induced apoptosis, it is possible that Gemin4 could act in a synergistic or independent fashion with endozepine to activate apoptosis. It would be possible to verify the relationship between these two genes by complementing the mutant cerR1 with one of the two candidate genes. This can be achieved by either transfection of cells with a DNA plasmid containing the endozepine gene or transducing the cells with recombinant endozepine protein. Recent advances in protein transduction technology have made it possible to fuse proteins with the HIV-Tat protein transduction domain to generate a cell permeable Tat fusion protein which can be delivered into the intracellular environment of cells (Wadia and Dowdy, 2002). This strategy would address some of the shortcomings of the transfection technology discussed in Section 1.7. The complementation of the mutant cells with either the gene or protein that is responsible for the mutation should restore or increase sensitivity to apoptosis induced by C_2-ceramide and will therefore prove which one of the two possible genes is responsible for resistance to C_2-ceramide-induced apoptosis. Preliminary data which involved transducing parental CHO22 cells with Tat-GFP-endozepine recombinant protein shows that the transduced cells undergo cell death within 6 hrs after transduction. These results demonstrate that high levels of endozepine may activate apoptosis and therefore lend support to the view that loss of endozepine will result in

resistance to apoptosis. These experiments would form the basis for future research on this project.

The research described here demonstrated the successful use of promoter-trap mutagenesis to generate apoptosis resistant somatic cell clones. It also demonstrated that the use of the inverse PCR strategy is an improvement on the RACE PCR approach previously used to characterise promoter-trap mutants. This led to the identification of endozepine as a possible pro-apoptotic gene in the ceramide-induced apoptotic pathway. Although endozepine is not a novel gene this study provided a new target gene that could be exploited for the development of novel anti-cancer drugs. This research aimed to demonstrate that promoter-trap technology could be used to identify genes involved in ceramide-induced apoptosis. This was achieved through a small-scale trial experiment. This laid the basis for the expansion of this technology and has demonstrated the potential to generate much larger mutant cell libraries that could be used to identify novel pro-apoptotic genes, screen and identify novel anti-cancer drugs.

REFERENCES.

Adams JM, Cory S. Apoptosomes: engines for caspase activation. Curr Opin Cell Biol. 2002 Dec; 14 (6): 715-20.

Adams JM, Cory S. The Bcl-2 protein family: arbiters of cell survival. Science. 1998 Aug 28; 281 (5381): 1322-6.

Alam R, Gorska M. Genomic microarrays: arraying order in biological chaos? Am J Respir Cell Mol Biol. 2001 Oct; 25 (4): 405-8.

Albritton LM, Tseng L, Scadden D, Cunningham JM. A putative murine ecotropic retrovirus receptor gene encodes a multiple membrane-spanning protein and confers susceptibility to virus infection. Cell. 1989 May 19; 57 (4): 659-66.

Alnemri ES, Livingston DJ, Nicholson DW, Salvesen G, Thornberry NA, Wong WW, Yuan J. Human ICE/CED-3 protease nomenclature. Cell. 1996 Oct 18; 87 (2): 171.

Altschul SF, Gish W, Miller W, Myers EW, Lipman DJ. Basic local alignment search tool. J Mol Biol. 1990 Oct 5; 215 (3): 403-10.

Ameisen JC. The origin of programmed cell death. Science. 1996 May 31; 272 (5266): 1278-9.

Anjum R, Ali AM, Begum Z, Vanaja J, Khar A. Selective involvement of caspase-3 in ceramide induced apoptosis in AK-5 tumour cells. FEBS Lett. 1998 Nov 13; 439 (1-2): 81-4.

Aravind L, Dixit VM, Koonin EV. The domains of death: evolution of the apoptosis machinery. Trends Biochem Sci. 1999 Feb; 24 (2): 47-53.

Ashkenazi A, Dixit VM. Death receptors: signalling and modulation. Science. 1998 Aug 28; 281 (5381): 1305-8.

Ballou LR, Laulederkind SJ, Rosloniec EF, Raghow R. Ceramide signalling and the immune response. Biochim Biophys Acta. 1996 Jun 11; 1301 (3): 273-87.

Belloc F, Belaud-Rotureau MA, Lavignolle V, Bascans E, Braz-Pereira E, Durrieu F, Lacombe F. Flow cytometry detection of caspase-3 activation in pre-apoptotic leukaemia cells. Cytometry. 2000 Jun 1; 40 (2): 151-60.

Bellstedt DU, Human PA, Rowland GF, Van der Merwe KJ. Acid-treated, naked bacteria as immune carriers for protein antigens. J Immunol Methods. 1987 Apr 16; 98 (2): 249-55.

Benoist C, Mathis D. Cell death mediators in autoimmune diabetes-no shortage of suspects. Cell. 1997 Apr 4; 89 (1): 1-3.

Blahos J 2nd, Whalin ME, Krueger KE. Identification and purification of a 10-kilo Dalton protein associated with mitochondrial benzodiazepine receptors. J Biol Chem. 1995 Sep 1; 270 (35): 20285-91.

Boldin MP, Goncharov TM, Goltsev YV, Wallach D. Involvement of MACH, a novel MORT1/FADD-interacting protease, in Fas/APO-1- and TNF receptor-induced cell death. Cell. 1996 Jun 14; 85 (6): 803-15.

Borner C. The Bcl-2 protein family: sensors and checkpoints for life-or-death decisions. Mol Immunol. 2003 Jan; 39 (11): 615-47.

Bose R, Verheij M, Haimovitz-Friedman A, Scotto K, Fuks Z, Kolesnick R. Ceramide synthase mediates daunorubicin-induced apoptosis: an alternative mechanism for generating death signals. Cell. 1995 Aug 11; 82 (3): 405-14.

Boise LH, Gonzalez-Garcia M, Postema CE, Ding L, Lindsten T, Turka LA, Mao X, Nunez G, Thompson CB. Bcl-x, a Bcl-2-related gene that functions as a dominant regulator of apoptotic cell death. Cell. 1993 Aug 27; 74 (4): 597-608.

Brenner C, Cadiou H, Vieira HL, Zamzami N, Marzo I, Xie Z, Leber B, Andrews D, Duclohier H, Reed JC, Kroemer G. Bcl-2 and Bax regulate the channel activity of the mitochondrial adenine nucleotide translocator. Oncogene. 2000 Jan 20; 19 (3): 329-36.

Brojatsch J, Naughton J, Rolls MM, Zingler K, Young JA. CAR1, a TNFR-related protein, is a cellular receptor for cytopathic avian leucosis-sarcoma viruses and mediates apoptosis. Cell. 1996 Nov 29; 87 (5): 845-55.

Cai Z, Bettaieb A, Mahdani NE, Legres LG, Stancou R, Masliah J, Chouaib S. Alteration of the sphingomyelin/ceramide pathway is associated with resistance of human breast carcinoma MCF7 cells to tumour necrosis factor-alpha-mediated cytotoxicity. J Biol Chem. 1997 Mar 14; 272 (11): 6918-26.

Cande C, Cecconi F, Dessen P, Kroemer G. Apoptosis-inducing factor (AIF): key to the conserved caspase-independent pathways of cell death? J Cell Sci. 2002 Dec 15; 115 (Pt 24): 4727-34.

Carroll MC, Campbell RD, Bentley DR, Porter RR. A molecular map of the human major histocompatibility complex class III region linking complement genes C4, C2 and factor B. Nature. 1984 Jan 19-25; 307 (5948): 237-41.

Casellas P, Galiegue S, Basile AS. Peripheral benzodiazepine receptors and mitochondrial function. Neurochem Int. 2002 May; 40 (6): 475-86.

Cerretti DP, Kozlosky CJ, Mosley B, Nelson N, Van Ness K, Greenstreet TA, March CJ, Kronheim SR, Druck T, Cannizzaro LA. Molecular cloning of the interleukin-1 beta converting enzyme. Science. 1992 Apr 3; 256 (5053): 97-100.

Chang W, Hubbard SC, Friedel C, Ruley HE. Enrichment of insertional mutants following retrovirus gene-trap selection. Virology. 1993 Apr; 193 (2): 737-47.

Charroux B, Pellizzoni L, Perkinson RA, Yong J, Shevchenko A, Mann M, Dreyfuss G. Gemin4. A novel component of the SMN complex that is found in both gems and nucleoli. J Cell Biol. 2000 Mar 20; 148 (6): 1177-86.

Chelli B, Falleni A, Salvetti F, Gremigni V, Lucacchini A, Martini C. Peripheral-type benzodiazepine receptor ligands: mitochondrial permeability transition induction in rat cardiac tissue. Biochem Pharmacol. 2001 Mar 15; 61 (6): 695-705.

Cheng EH, Kirsch DG, Clem RJ, Ravi R, Kastan MB, Bedi A, Ueno K, Hardwick JM. Conversion of Bcl-2 to a Bax-like death effector by caspases. Science. 1997 Dec 12; 278 (5345): 1966-8.

Chicheportiche Y, Bourdon PR, Xu H, Hsu YM, Scott H, Hession C, Garcia I, Browning JL. TWEAK, a new secreted ligand in the tumour necrosis factor family that weakly induces apoptosis. J Biol Chem. 1997 Dec 19; 272 (51): 32401-10.

Chien CT, Bartel PL, Sternglanz R, Fields S. The two-hybrid system: a method to identify and clone genes for proteins that interact with a protein of interest. Proc Natl Acad Sci U S A. 1991 Nov 1; 88 (21): 9578-82.

Chinnaiyan AM, O'Rourke K, Lane BR, Dixit VM. Interaction of CED-4 with CED-3 and CED-9: a molecular framework for cell death. Science. 1997 Feb 21; 275 (5303): 1122-6.

Chinnaiyan AM, O'Rourke K, Tewari M, Dixit VM. FADD, a novel death domain-containing protein, interacts with the death domain of Fas and initiates apoptosis. Cell. 1995 May 19; 81 (4): 505-12.

Chinnaiyan AM, O'Rourke K, Yu GL, Lyons RH, Garg M, Duan DR, Xing L, Gentz R, Ni J, Dixit VM. Signal transduction by DR3, a death domain-containing receptor related to TNFR-1 and CD95. Science. 1996 Nov 8; 274 (5289): 990-2.

Cifone MG, De Maria R, Roncaioli P, Rippo MR, Azuma M, Lanier LL, Santoni A, Testi R. Apoptotic signalling through CD95 (Fas/Apo-1) activates an acidic sphingomyelinase. J Exp Med. 1994 Oct 1; 180 (4): 1547-52.

Clark JM. Novel non-templated nucleotide addition reactions catalysed by prokaryotic and eukaryotic DNA polymerases. Nucleic Acids Res. 1988 Oct 25; 16 (20): 9677-86.

Clem RJ, Fechheimer M, Miller LK. Prevention of apoptosis by a baculovirus gene during infection of insect cells. Science. 1991 Nov 29; 254 (5036): 1388-90.

Cohen GM. Caspases: the executioners of apoptosis. Biochem J. 1997 Aug 15; 326 (Pt 1): 1-1.

Cohen O, Feinstein E, Kimchi A. DAP-kinase is a Ca^{2+}/calmodulin-dependent, cytoskeletal-associated protein kinase, with cell death-inducing functions that depend on its catalytic activity. EMBO J. 1997 Mar 3; 16 (5): 998-1008.

Collins FS, Weissman SM. Directional cloning of DNA fragments at a large distance from an initial probe: a circularisation method. Proc Natl Acad Sci U S A. 1984 Nov; 81 (21): 6812-6.

Conradt B, Horvitz HR. The *C. elegans* protein EGL-1 is required for programmed cell death and interacts with the Bcl-2-like protein CED-9. Cell. 1998 May 15; 93 (4): 519-29.

Cordingley MG, Callahan PL, Sardana VV, Garsky VM, Colonno RJ. Substrate requirements of human rhinovirus 3C protease for peptide cleavage in vitro. J Biol Chem. 1990 Jun 5; 265 (16): 9062-5.

Cossarizza A, Kalashnikova G, Grassilli E, Chiappelli F, Salvioli S, Capri M, Barbieri D, Troiano L, Monti D, Franceschi C. Mitochondrial modifications during rat thymocyte apoptosis: a study at the single cell level. Exp Cell Res. 1994 Sep; 214 (1): 323-30.

Costa E, Corda MG, Guidotti A. On a brain polypeptide functioning as a putative effector for the recognition sites of benzodiazepine and beta-carboline derivatives. Neuropharmacology. 1983 Dec; 22 (12B): 1481-92.

Costa E, Guidotti A. Diazepam binding inhibitor (DBI): a peptide with multiple biological actions. Life Sci. 1991; 49 (5): 325-44.

Creagh EM, Martin SJ. Caspases: cellular demolition experts. Biochem Soc Trans. 2001 Nov; 29 (Pt 6): 696-702.

Crompton M, Ellinger H, Costi A. Inhibition by cyclosporin A of a Ca^{2+}-dependent pore in heart mitochondria activated by inorganic phosphate and oxidative stress. Biochem J. 1988 Oct 1; 255 (1): 357-60.

Darnell JE Jr, Kerr IM, Stark GR. Jak-STAT pathways and transcriptional activation in response to IFNs and other extracellular signalling proteins. Science. 1994 Jun 3; 264 (5164): 1415-21.

Darzynkiewicz Z, Staiano-Coico L, Melamed MR. Mitochondrial uptake of rhodamine 123 during lymphocyte stimulation. Proc Natl Acad Sci U S A. 1981 Apr; 78 (4): 2383-7.

Dassonneville L, Wattez N, Baldeyrou B, Mahieu C, Lansiaux A, Banaigs B, Bonnard I, Bailly C. Inhibition of topoisomerase II by the marine alkaloid ascididemin and induction of apoptosis in leukaemia cells. Biochem Pharmacol. 2000 Aug 15; 60 (4): 527-37.

de Mateos-Verchere JG, Leprince J, Tonon MC, Vaudry H, Costentin J. The octadecaneuropeptide [diazepam-binding inhibitor (33-50)] exerts potent anorexigenic effects in rodents. Eur J Pharmacol. 2001 Mar 2; 414 (2-3): 225-31.

Decaudin D, Castedo M, Nemati F, Beurdeley-Thomas A, De Pinieux G, Caron A, Pouillart P, Wijdenes J, Rouillard D, Kroemer G, Poupon MF. Peripheral benzodiazepine receptor ligands reverse apoptosis resistance of cancer cells *in vitro* and *in vivo*. Cancer Res. 2002 Mar 1; 62 (5): 1388-93.

Deiss LP, Kimchi A. A genetic tool used to identify thioredoxin as a mediator of a growth inhibitory signal. Science. 1991 Apr 5; 252 (5002): 117-20.

del Peso L, Gonzalez VM, Inohara N, Ellis RE, Nunez G. Disruption of the CED-9/CED-4 complex by EGL-1 is a critical step for programmed cell death in *C. elegans*. J Biol Chem. 2000 Sep 1; 275 (35): 27205-11.

Dobrowsky RT, Hannun YA. Ceramide stimulates a cytosolic protein phosphatase. J Biol Chem. 1992 Mar 15; 267 (8): 5048-51.

Ekert PG, Silke J, Hawkins CJ, Verhagen AM, Vaux DL. DIABLO promotes apoptosis by removing MIHA/XIAP from processed caspase-9. J Cell Biol. 2001 Feb 5; 152(3): 483-90.

Ellis RE, Yuan JY, Horvitz HR. Mechanisms and functions of cell death. Annu Rev Cell Biol. 1991; 7: 663-98.

Erlich H. 1989. "PCR technology" (Stockton Press), pp. 105-111, New York.

Fadok VA, Savill JS, Haslett C, Bratton DL, Doherty DE, Campbell PA, Henson PM. Different populations of macrophages use either the vitronectin receptor or the phosphatidylserine receptor to recognise and remove apoptotic cells. J Immunol. 1992 Dec 15; 149 (12): 4029-35.

Faergeman NJ, Knudsen J. Acyl-CoA binding protein is an essential protein in mammalian cell lines. Biochem J. 2002 Dec 15; 368 (Pt 3): 679-82.

Faergeman NJ, Knudsen J. Role of long-chain fatty acyl-CoA esters in the regulation of metabolism and in cell signalling. Biochem J. 1997 Apr 1; 323 (Pt 1): 1-12.

Fennell DA, Corbo M, Pallaska A, Cotter FE. Bcl-2 resistant mitochondrial toxicity mediated by the isoquinoline carboxamide PK11195 involves de novo generation of reactive oxygen species. Br J Cancer. 2001 May 18; 84 (10): 1397-404.

Ferrero P, Guidotti A, Conti-Tronconi B, Costa E. A brain octadecaneuropeptide generated by tryptic digestion of DBI (diazepam binding inhibitor) functions as a pro-

conflict ligand of benzodiazepine recognition sites. Neuropharmacology. 1984 Nov; 23 (11): 1359-62.

Fields S, Song O. A novel genetic system to detect protein-protein interactions. Nature. 1989 Jul 20; 340 (6230): 245-6.

Fiorani P, Bjornsti MA. Mechanisms of DNA topoisomerase I-induced cell killing in the yeast *S. cerevisiae*. Ann N Y Acad Sci. 2000; 922: 65-75.

Fishbein JD, Dobrowsky RT, Bielawska A, Garrett S, Hannun YA. Ceramide-mediated growth inhibition and CAPP are conserved in *Saccharomyces cerevisiae*. J Biol Chem. 1993 May 5; 268 (13): 9255-61.

Fire A, Xu S, Montgomery MK, Kostas SA, Driver SE, Mello CC. Potent and specific genetic interference by double-stranded RNA in *C. elegans*. Nature 1998 Feb 19; 391 (6669): 806-11.

Fischer H, Koenig U, Eckhart L, Tschachler E. Human caspase-12 has acquired deleterious mutations. Biochem Biophys Res Commun. 2002 May 3; 293 (2): 722-6.

Frankel W, Potter TA, Rosenberg N, Lenz J, Rajan TV. Retroviral insertional mutagenesis of a target allele in a heterozygous murine cell line. Proc Natl Acad Sci U S A. 1985 Oct; 82 (19): 6600-4.

Frohlich KU, Madeo F. Apoptosis in yeast: a new model for aging research. Exp Gerontol. 2001 Dec; 37 (1): 27-31.

Frohme M, Scharm B, Delius H, Knecht R, Hoheisel JD. Use of representational difference analysis and cDNA arrays for transcriptional profiling of tumour tissue. Ann N Y Acad Sci. 2000 Jun; 910: 85-104.

Gaigg B, Neergaard TB, Schneiter R, Hansen JK, Faergeman NJ, Jensen NA, Andersen JR, Friis J, Sandhoff R, Schroder HD, Knudsen J. Depletion of acyl-coenzyme A-binding protein affects sphingolipid synthesis and causes vesicle accumulation and membrane defects in *S. cerevisiae*. Mol Biol Cell. 2001 Apr; 12 (4): 1147-60.

Galat A. Peptidylproline cis-trans-isomerases: immunophilins. Eur J Biochem. 1993 Sep 15; 216 (3): 689-707.

Galiegue S, Jbilo O, Combes T, Bribes E, Carayon P, Le Fur G, Casellas P. Cloning and characterisation of PRAX-1. A new protein that specifically interacts with the peripheral benzodiazepine receptor. J Biol Chem. 1999 Jan 29; 274 (5): 2938-52.

Garnier M, Boujrad N, Ogwuegbu SO, Hudson JR Jr, Papadopoulos V. The polypeptide diazepam-binding inhibitor and a higher affinity mitochondrial peripheral-type benzodiazepine receptor sustain constitutive steroid genesis in the R2C Leydig tumour cell line. J Biol Chem. 1994 Sep 2; 269 (35): 22105-12.

George AE. 1995. A new method for isolating genes involved in the processing and presentation of antigens to cytotoxic T cells. (PhD Thesis). University of Oxford.

Goldstein JC, Waterhouse NJ, Juin P, Evan GI, Green DR. The coordinate release of cytochrome c during apoptosis is rapid, complete and kinetically invariant. Nat Cell Biol. 2000 Mar; 2 (3): 156-62.

Gorg A, Obermaier C, Boguth G, Harder A, Scheibe B, Wildgruber R, Weiss W. The current state of two-dimensional electrophoresis with immobilised pH gradients. Electrophoresis. 2000 Apr; 21 (6): 1037-53.

Gottlieb E, Van der Heiden MG, Thompson CB. Bcl-x_L prevents the initial decrease in mitochondrial membrane potential and subsequent reactive oxygen species

production during tumour necrosis factor alpha-induced apoptosis. Mol Cell Biol. 2000 Aug; 20 (15): 5680-9.

Grell M, Zimmermann G, Gottfried E, Chen CM, Grunwald U, Huang DC, Wu Lee YH, Durkop H, Engelmann H, Scheurich P, Wajant H, Strasser A. Induction of cell death by tumour necrosis factor (TNF) receptor 2, CD40 and CD30: a role for TNF-R1 activation by endogenous membrane-anchored TNF. EMBO J. 1999 Jun 1; 18 (11): 3034-43.

Gross A, McDonnell JM, Korsmeyer SJ. Bcl-2 family members and the mitochondria in apoptosis. Genes Dev. 1999 Aug 1; 13 (15): 1899-911.

Grosveld FG, Dahl HH, de Boer E, Flavell RA. Isolation of beta-globin-related genes from a human cosmid library. Gene. 1981 Apr; 13 (3): 227-37.

Guidotti A, Forchetti CM, Corda MG, Konkel D, Bennett CD, Costa E. Isolation, characterisation, and purification to homogeneity of an endogenous polypeptide with agonistic action on benzodiazepine receptors. Proc Natl Acad Sci U S A. 1983 Jun; 80 (11): 3531-5.

Gura T. New kind of cancer mutation found. Science. 1997 Aug 29; 277 (5330): 1201-2.

Hahne M, Rimoldi D, Schroter M, Romero P, Schreier M, French LE, Schneider P, Bornand T, Fontana A, Lienard D, Cerottini J, Tschopp J. Melanoma cell expression of Fas (Apo-1/CD95) ligand: implications for tumour immune escape. Science. 1996 Nov 22; 274 (5291): 1363-6.

Halestrap AP, Davidson AM. Inhibition of Ca^{2+}-induced large-amplitude swelling of liver and heart mitochondria by cyclosporin is probably caused by the inhibitor binding to mitochondrial-matrix peptidyl-prolyl cis-trans isomerase and preventing it interacting with the adenine nucleotide translocase. Biochem J. 1990 May 15; 268 (1): 153-60.

Halestrap AP, McStay GP, Clarke SJ. The permeability transition pore complex: another view. Biochimie. 2002 Feb-Mar; 84 (2-3): 153-66.

Hannun YA, Bell RM. Functions of sphingolipids and sphingolipid breakdown products in cellular regulation. Science. 1989 Jan 27; 243 (4890): 500-7.

Hannun YA, Luberto C. Ceramide in the eukaryotic stress response. Trends Cell Biol. 2000 Feb; 10 (2): 73-80.

Hannun YA. Functions of ceramide in coordinating cellular responses to stress. Science. 1996 Dec 13; 274 (5294): 1855-9.

Hearps AC, Burrows J, Connor CE, Woods GM, Lowenthal RM, Ragg SJ. Mitochondrial cytochrome c release precedes transmembrane depolarisation and caspase-3 activation during ceramide-induced apoptosis of Jurkat T cells. Apoptosis. 2002 Oct; 7 (5): 387-94.

Helene C, Toulme JJ. Specific regulation of gene expression by antisense, sense- and anti-gene nucleic acids. Biochim Biophys Acta. 1990 Jun 21; 1049 (2): 99-125.

Helledie T, Jorgensen C, Antonius M, Krogsdam AM, Kratchmarova I, Kristiansen K, Mandrup S. Role of adipocyte lipid-binding protein (ALBP) and acyl-coA binding protein (ACBP) in PPAR-mediated transactivation. Mol Cell Biochem. 2002 Oct; 239 (1-2): 157-64.

Hellerstein MK, McCune JM. T cell turnover in HIV-1 disease. Immunity. 1997 Nov; 7 (5): 583-9.

Hengartner MO, Horvitz HR. *C. elegans* cell survival gene *CED-9* encodes a functional homologue of the mammalian proto-oncogene *Bcl-2*. Cell. 1994 Feb 25; 76 (4): 665-76.

Hirsch T, Decaudin D, Susin SA, Marchetti P, Larochette N, Resche-Rigon M, Kroemer G. PK11195, a ligand of the mitochondrial benzodiazepine receptor,

facilitates the induction of apoptosis and reverses Bcl-2-mediated cytoprotection. Exp Cell Res. 1998 Jun 15; 241 (2): 426-34.

Hsu H, Xiong J, Goeddel DV. The TNF receptor 1-associated protein TRADD signals cell death and NF-kappa B activation. Cell. 1995 May 19; 81 (4): 495-504.

Huang B, Eberstadt M, Olejniczak ET, Meadows RP, Fesik SW. NMR structure and mutagenesis of the Fas (APO-1/CD95) death domain. Nature. 1996 Dec 19-26; 384 (6610): 638-41.

Hubbard SC, Walls L, Ruley HE, Muchmore EA. Generation of Chinese hamster ovary cell glycosylation mutants by retroviral insertional mutagenesis. Integration into a discrete locus generates mutants expressing high levels of N-glycolylneuraminic acid. J Biol Chem. 1994 Feb 4; 269 (5): 3717-24.

Ichas F, Jouaville LS, Mazat JP. Mitochondria are excitable organelles capable of generating and conveying electrical and calcium signals. Cell. 1997 Jun 27; 89 (7): 1145-53.

Ikawa S, Nakagawara A, Ikawa Y. p53 family genes: structural comparison, expression and mutation. Cell Death Differ. 1999 Dec; 6 (12): 1154-61.

Inbal B, Shani G, Cohen O, Kissil JL, Kimchi A. Death-associated protein kinase-related protein 1, a novel serine/threonine kinase involved in apoptosis. Mol Cell Biol. 2000 Feb; 20 (3): 1044-54.

Ivell R, Pusch W, Balvers M, Valentin M, Walther N, Weinbauer G. Progressive inactivation of the haploid expressed gene for the sperm-specific endozepine-like peptide (ELP) through primate evolution. Gene. 2000 Sep 19; 255 (2): 335-45.

Iwahashi H, Eguchi Y, Yasuhara N, Hanafusa T, Matsuzawa Y, Tsujimoto Y. Anti-apoptotic activity between Bcl-2 and SMN implicated in spinal muscular atrophy. Nature. 1997 Nov 27; 390 (6658): 413-7.

Jarvis WD, Fornari FA Jr, Browning JL, Gewirtz DA, Kolesnick RN, Grant S. Attenuation of ceramide-induced apoptosis by diglyceride in human myeloid leukaemia cells. J Biol Chem. 1994 Dec 16; 269 (50): 31685-92.

Johnson LV, Summerhayes IC, Chen LB. Decreased uptake and retention of rhodamine 123 by mitochondria in feline sarcoma virus-transformed mink cells. Cell. 1982 Jan; 28 (1): 7-14.

Joseph-Liauzun E, Delmas P, Shire D, Ferrara P. Topological analysis of the peripheral benzodiazepine receptor in yeast mitochondrial membranes supports a five-transmembrane structure. J Biol Chem. 1998 Jan 23; 273 (4): 2146-52.

Joyce DE, Gelbert L, Ciaccia A, DeHoff B, Grinnell BW. Gene expression profile of anti-thrombotic protein c defines new mechanisms modulating inflammation and apoptosis. J Biol Chem. 2001 Apr 6; 276 (14): 11199-203.

Katz Y, Eitan A, Gavish M. Increase in peripheral benzodiazepine binding sites in colonic adenocarcinoma. Oncology. 1990; 47 (2): 139-42.

Kerr JF, Wyllie AH, Currie AR. Apoptosis: a basic biological phenomenon with wide-ranging implications in tissue kinetics. Br J Cancer. 1972 Aug; 26 (4): 239-57.

Kimchi A. DAP genes: novel apoptotic genes isolated by a functional approach to gene cloning. Biochim Biophys Acta. 1998 Apr 17; 1377 (2): F13-33.

King W, Patel MD, Lobel LI, Goff SP, Nguyen-Huu MC. Insertion mutagenesis of embryonal carcinoma cells by retroviruses. Science. 1985 May 3; 228 (4699): 554-8.

Kischkel FC, Hellbardt S, Behrmann I, Germer M, Pawlita M, Krammer PH, Peter ME. Cytotoxicity-dependent APO-1 (Fas/CD95)-associated proteins form a death-

inducing signalling complex (DISC) with the receptor. EMBO J. 1995 Nov 15; 14 (22): 5579-88.

Kissil JL, Feinstein E, Cohen O, Jones PA, Tsai YC, Knowles MA, Eydmann ME, Kimchi A. DAP-kinase loss of expression in various carcinoma and B-cell lymphoma cell lines: possible implications for role as tumour suppressor gene. Oncogene. 1997 Jul 24; 15 (4): 403-7.

Kisseleva MV, Cao L, Majerus PW. Phosphoinositide-specific inositol polyphosphate 5-Phosphatase IV inhibits Akt/PKB phosphorylation and leads to apoptotic cell death. J. Biol. Chem. 2002 277 (8): 6266-6272.

Kitson J, Raven T, Jiang YP, Goeddel DV, Giles KM, Pun KT, Grinham CJ, Brown R, Farrow SN. A death-domain-containing receptor that mediates apoptosis. Nature. 1996 Nov 28; 384 (6607): 372-5.

Koch J, Gartner S, Li CM, Quintern LE, Bernardo K, Levran O, Schnabel D, Desnick RJ, Schuchman EH, Sandhoff K. Molecular cloning and characterisation of a full-length complementary DNA encoding human acid ceramidase. Identification of the first molecular lesion causing Farber disease. J Biol Chem. 1996 Dec 20; 271 (51): 33110-5.

Kohler C, Gahm A, Noma T, Nakazawa A, Orrenius S, Zhivotovsky B. Release of adenylate kinase 2 from the mitochondrial intermembrane space during apoptosis. FEBS Lett. 1999 Mar 19; 447 (1): 10-2.

Kolesnick R, Hannun YA. Ceramide and apoptosis. Trends Biochem Sci. 1999 Jun; 24 (6): 224-5.

Kolmer M, Pelto-Huikko M, Parvinen M, Hoog C, Alho H. The transcriptional and translational control of diazepam binding inhibitor expression in rat male germ-line cells. DNA Cell Biol. 1997 Jan; 16 (1): 59-72.

Koonin EV, Aravind L. Origin and evolution of eukaryotic apoptosis: the bacterial connection. Cell Death Differ. 2002 Apr; 9 (4): 394-404.

Kothakota S, Azuma T, Reinhard C, Klippel A, Tang J, Chu K, McGarry TJ, Kirschner MW, Koths K, Kwiatkowski DJ, Williams LT. Caspase-3-generated fragment of gelsolin: effector of morphological change in apoptosis. Science. 1997 Oct 10; 278 (5336): 294-8.

Kragelund BB, Knudsen J, Poulsen FM. Acyl-coenzyme A binding protein (ACBP). Biochim Biophys Acta. 1999 Nov 23; 1441 (2-3): 150-61.

Krajewski S, Krajewska M, Ellerby LM, Welsh K, Xie Z, Deveraux QL, Salvesen GS, Bredesen DE, Rosenthal RE, Fiskum G, Reed JC. Release of caspase-9 from mitochondria during neuronal apoptosis and cerebral ischaemia. Proc Natl Acad Sci U S A. 1999 May 11; 96 (10): 5752-7.

Kroemer G, Petit P, Zamzami N, Vayssiere JL, Mignotte B. The biochemistry of programmed cell death. FASEB J. 1995 Oct; 9 (13): 1277-87.

Kroemer G, Reed JC. Mitochondrial control of cell death. Nat Med. 2000 May; 6 (5): 513-9.

Kroemer G. The proto-oncogene Bcl-2 and its role in regulating apoptosis. Nat Med. 1997 Jun; 3 (6):614-20.

Laemmli UK. Cleavage of structural proteins during the assembly of the head of bacteriophage T4. Nature. 1970 Aug 15; 227 (259): 680-5.

Lampugnani MG, Pedenovi M, Niewiarowski A, Casali B, Donati MB, Corbascio GC, Marchisio PC. Effects of dimethyl sulphoxide (DMSO) on microfilament organisation, cellular adhesion, and growth of cultured mouse B16 melanoma cells. Exp Cell Res. 1987 Oct; 172 (2): 385-96.

Le Fur G, Perrier ML, Vaucher N, Imbault F, Flamier A, Benavides J, Uzan A, Renault C, Dubroeucq MC, Gueremy C. Peripheral benzodiazepine binding sites: effect of PK11195, 1-(2-chlorophenyl)-N-methyl-N- (1-methylpropyl)-3-isoquinolinecarboxamide. I. *In vitro* studies. Life Sci. 1983 Apr 18; 32 (16): 1839-47.

Lehtonen JY, Horiuchi M, Daviet L, Akishita M, Dzau VJ. Activation of the *de novo* biosynthesis of sphingolipids mediates angiotensin II type 2 receptor-induced apoptosis. J Biol Chem. 1999 Jun 11; 274 (24): 16901-6.

Levy-Strumpf N, Deiss LP, Berissi H, Kimchi A. DAP-5, a novel homologue of eukaryotic translation initiation factor 4G isolated as a putative modulator of gamma interferon-induced programmed cell death. Mol Cell Biol. 1997 Mar; 17 (3): 1615-25.

Li H, Zhu H, Xu CJ, Yuan J. Cleavage of BID by caspase-8 mediates the mitochondrial damage in the Fas pathway of apoptosis. Cell. 1998 Aug 21; 94 (4): 491-501.

Li P, Nijhawan D, Budihardjo I, Srinivasula SM, Ahmad M, Alnemri ES, Wang X. Cytochrome c and dATP-dependent formation of Apaf-1/caspase-9 complex initiates an apoptotic protease cascade. Cell. 1997 Nov 14; 91 (4): 479-89.

Liao WC, Haimovitz-Friedman A, Persaud RS, McLoughlin M, Ehleiter D, Zhang N, Gatei M, Lavin M, Kolesnick R, Fuks Z. Ataxia telangiectasia-mutated gene product inhibits DNA damage-induced apoptosis via ceramide synthase. J Biol Chem. 1999 Jun 18; 274 (25): 17908-17.

Lin CK, Kalunta CI, Chen FS, Nguyen TT, Kaptein JS, Lad PM. Dimethyl sulphoxide suppresses apoptosis in Burkitt's lymphoma cells. Exp Cell Res. 1995 Feb; 216 (2): 403-10.

Liu LF, Desai SD, Li TK, Mao Y, Sun M, Sim SP. Mechanism of action of camptothecin. Ann N Y Acad Sci. 2000; 922: 1-10.

Liu X, Kim CN, Yang J, Jemmerson R, Wang X. Induction of apoptotic program in cell-free extracts: requirement for dATP and cytochrome c. Cell. 1996 Jul 12; 86 (1): 147-57.

Maccioni HJ, Daniotti JL, Martina JA. Organisation of ganglioside synthesis in the Golgi apparatus. Biochim Biophys Acta. 1999 Feb 25; 1437 (2): 101-18.

MacFarlane M. TRAIL-induced signalling and apoptosis. Toxicol Lett. 2003 Apr 4; 139 (2-3): 89-97.

Malinin NL, Boldin MP, Kovalenko AV, Wallach D. MAP3K-related kinase involved in NF-kappa B induction by TNF, CD95 and IL-1. Nature. 1997 Feb 6; 385 (6616): 540-4.

Mancini M, Anderson BO, Caldwell E, Sedghinasab M, Paty PB, Hockenbery DM. Mitochondrial proliferation and paradoxical membrane depolarisation during terminal differentiation and apoptosis in a human colon carcinoma cell line. Cell Biol. 1997 Jul 28; 138 (2): 449-69.

Mao C, Xu R, Szulc ZM, Bielawska A, Galadari SH, Obeid LM. Cloning and characterisation of a novel human alkaline ceramidase. A mammalian enzyme that hydrolyses phytoceramide. J Biol Chem. 2001 Jul 13; 276 (28): 26577-88.

Martinon F, Holler N, Richard C, Tschopp J. Activation of a pro-apoptotic amplification loop through inhibition of NF-kappa B-dependent survival signals by caspase-mediated inactivation of RIP. FEBS Lett. 2000 Feb 25; 468 (2-3): 134-6.

Massaia M, Borrione P, Attisano C, Barral P, Beggiato E, Montacchini L, Bianchi A, Boccadoro M, Pileri A. Deregulated Fas and Bcl-2 expression leading to enhanced apoptosis in T cells of multiple myeloma patients. Blood. 1995 Jun 15; 85 (12): 3679-87.

Mathias S, Dressler KA, Kolesnick RN. Characterisation of a ceramide-activated protein kinase: stimulation by tumour necrosis factor alpha. Proc Natl Acad Sci U S A. 1991 Nov 15; 88 (22): 10009-13.

Mathias S, Pena LA, Kolesnick RN. Signal-transduction of stress via ceramide. Biochem J. 1998 Nov 1; 335 (Pt 3): 465-80.

McEnery MW, Snowman AM, Trifiletti RR, Snyder SH. Isolation of the mitochondrial benzodiazepine receptor: association with the voltage-dependent anion channel and the adenine nucleotide carrier. Proc Natl Acad Sci U S A. 1992 Apr 15; 89 (8): 3170-4.

Mengubas K, Riordan FA, Bravery CA, Lewin J, Owens DL, Mehta AB, Hoffbrand AV, Wickremasinghe RG. Ceramide-induced killing of normal and malignant human lymphocytes is by a non-apoptotic mechanism. Oncogene. 1999 Apr 15; 18 (15): 2499-506.

Mercurio F, Zhu H, Murray BW, Shevchenko A, Bennett BL, Li J, Young DB, Barbosa M, Mann M, Manning A, Rao A. IKK-1 and IKK-2: cytokine-activated Ikappa B kinases essential for NF-kappa B activation. Science. 1997 Oct 31; 278 (5339): 860-6.

Montgomery MK, Xu S, Fire A. RNA as a target of double-stranded RNA-mediated genetic interference in *C. elegans*. Proc Natl Acad Sci U S A. 1998 Dec 22; 95 (26): 15502-7.

Muchmore SW, Sattler M, Liang H, Meadows RP, Harlan JE, Yoon HS, Nettesheim D, Chang BS, Thompson CB, Wong SL, Ng SL, Fesik SW. X-ray and NMR structure of human Bcl-x_L, an inhibitor of programmed cell death. Nature. 1996 May 23; 381 (6580): 335-41.

Nagata S. Apoptosis by death factor. Cell. 1997 Feb 7; 88 (3): 355-65.

Natoli G, Costanzo A, Ianni A, Templeton DJ, Woodgett JR, Balsano C, Levrero M. Activation of SAPK/JNK by TNF receptor 1 through a non-cytotoxic TRAF2-dependent pathway. Science. 1997 Jan 10; 275 (5297): 200-3.

Nicholson DW. Caspase structure, proteolytic substrates, and function during apoptotic cell death. Cell Death Differ. 1999 Nov; 6 (11): 1028-42.

Nikolaev AY, Li M, Puskas N, Qin J, Gu W. Parc: a cytoplasmic anchor for p53. Cell. 2003 Jan 10; 112 (1): 29-40.

O' Farrell PH. High-resolution two-dimensional electrophoresis of proteins. J Biol Chem. 1975; 250: 4007-4021.

Obeid LM, Linardic CM, Karolak LA, Hannun YA. Programmed cell death induced by ceramide. Science. 1993 Mar 19; 259 (5102): 1769-71.

Olivera A, Spiegel S. Sphingosine kinase: a mediator of vital cellular functions. Prostaglandins. 2001 Apr; 64 (1-4): 123-134.

Osborne BA, Smith SW, McLaughlin KA, Grimm L, Kallinch T, Liu Z, Schwartz LM. Genes that regulate apoptosis in the mouse thymus. J Cell Biochem. 1996 Jan; 60 (1): 18-22.

Otterbach B, Stoffel W. Acid sphingomyelinase-deficient mice mimic the neurovisceral form of human lysosomal storage disease (Niemann-Pick disease). Cell. 1995 Jun 30; 81 (7): 1053-61.

Pan G, Ni J, Wei YF, Yu G, Gentz R, Dixit VM. An antagonist decoy receptor and a death domain-containing receptor for TRAIL. Science. 1997 Aug 8; 277 (5327): 815-8.

Pan G, Ni J, Yu G, Wei YF, Dixit VM. TRUNDD, a new member of the TRAIL receptor family that antagonises TRAIL signalling. FEBS Lett. 1998 Mar 6; 424 (1-2): 41-5.

Pan G, O'Rourke K, Chinnaiyan AM, Gentz R, Ebner R, Ni J, Dixit VM. The receptor for the cytotoxic ligand TRAIL. Science. 1997 Apr 4; 276 (5309): 111-3.

Parrish JZ, Xue D. Functional genomic analysis of apoptotic DNA degradation in *C. elegans*. Mol Cell. 2003 Apr; 11 (4): 987-96.

Patterson SD, Spahr CS, Daugas E, Susin SA, Irinopoulou T, Koehler C, Kroemer G. Mass spectrometric identification of proteins released from mitochondria undergoing permeability transition. Cell Death Differ. 2000 Feb; 7 (2): 137-44.

Perry DK, Hannun YA. The role of ceramide in cell signalling. Biochim Biophys Acta. 1998 Dec 8; 1436 (1-2): 233-43.

Peter ME, Heufelder AE, Hengartner MO. Advances in apoptosis research. Proc Natl Acad Sci U S A. 1997 Nov 25; 94 (24): 12736-7.

Petit PX, Susin SA, Zamzami N, Mignotte B, Kroemer G. Mitochondria and programmed cell death: back to the future. FEBS Lett. 1996 Oct 28; 396 (1): 7-13.

Petronilli V, Costantini P, Scorrano L, Colonna R, Passamonti S, Bernardi P. The voltage sensor of the mitochondrial permeability transition pore is tuned by the oxidation-reduction state of vicinal thiols. Increase of the gating potential by oxidants and its reversal by reducing agents. J Biol Chem. 1994 Jun 17; 269 (24): 16638-42.

Pitti RM, Marsters SA, Ruppert S, Donahue CJ, Moore A, Ashkenazi A. Induction of apoptosis by Apo-2 ligand, a new member of the tumour necrosis factor cytokine family. J Biol Chem. 1996 May 31; 271 (22): 12687-90.

Pusch W, Balvers M, Hunt N, Ivell RA novel endozepine-like peptide (ELP) is exclusively expressed in male germ cells. Mol Cell Endocrinol. 1996 Aug 30; 122 (1): 69-80.

Pusch W, Jahner D, Spiess AN, Ivell R. Rat endozepine-like peptide (ELP): cDNA cloning, genomic organisation and tissue-specific expression. Gene. 1999 Jul 22; 235 (1-2): 51-7.

Raff MC. Social controls on cell survival and cell death. Nature. 1992 Apr 2; 356 (6368): 397-400.

Rasmussen JT, Rosendal J, Knudsen J. Interaction of acyl-CoA binding protein (ACBP) on processes for which acyl-CoA is a substrate, product or inhibitor. Biochem J. 1993 Jun 15; 292 (Pt 3): 907-13.

Ray CA, Black RA, Kronheim SR, Greenstreet TA, Sleath PR, Salvesen GS, Pickup DJ. Viral inhibition of inflammation: cowpox virus encodes an inhibitor of the interleukin-1 beta converting enzyme. Cell. 1992 May 15; 69 (4): 597-604.

Reed JC. Apoptosis-regulating proteins as targets for drug discovery. Trends Mol Med. 2001 Jul; 7 (7): 314-9.

Reed JC. Cytochrome c: can't live with it-can't live without it. Cell. 1997 Nov 28; 91 (5): 559-62.

Reyes JG, Robayna IG, Delgado PS, Gonzalez IH, Aguiar JQ, Rosas FE, Fanjul LF, Galarreta CM. c-Jun is a downstream target for ceramide-activated protein phosphatase in A431 cells. J Biol Chem. 1996 Aug 30; 271 (35): 21375-80.

Saiki RK, Scharf S, Faloona F, Mullis KB, Horn GT, Erlich HA, Arnheim N. Enzymatic amplification of beta-globin genomic sequences and restriction site analysis for diagnosis of sickle cell anaemia. Science. 1985 Dec 20; 230 (4732): 1350-4.

Sakahira H, Enari M, Nagata S. Cleavage of CAD inhibitor in CAD activation and DNA degradation during apoptosis. Nature. 1998 Jan 1; 391 (6662): 96-9.

Salvioli S, Ardizzoni A, Franceschi C, Cossarizza A. JC-1, but not DiOC6 (3) or rhodamine 123, is a reliable fluorescent probe to assess delta psi changes in intact cells: implications for studies on mitochondrial functionality during apoptosis. FEBS Lett. 1997 Jul 7; 411 (1): 77-82.

Samali A, Cai J, Zhivotovsky B, Jones DP, Orrenius S. Presence of a pre-apoptotic complex of pro-caspase-3, Hsp60 and Hsp10 in the mitochondrial fraction of Jurkat cells. EMBO J. 1999 Apr 15; 18 (8): 2040-8.

Santana P, Pena LA, Haimovitz-Friedman A, Martin S, Green D, McLoughlin M, Cordon-Cardo C, Schuchman EH, Fuks Z, Kolesnick R. Acid sphingomyelinase-deficient human lymphoblasts and mice are defective in radiation-induced apoptosis. Cell. 1996 Jul 26; 86 (2): 189-99.

Sattler M, Liang H, Nettesheim D, Meadows RP, Harlan JE, Eberstadt M, Yoon HS, Shuker SB, Chang BS, Minn AJ, Thompson CB, Fesik SW. Structure of Bcl-x_L-Bak peptide complex: recognition between regulators of apoptosis. Science. 1997 Feb 14; 275 (5302): 983-6.

Scaffidi C, Fulda S, Srinivasan A, Friesen C, Li F, Tomaselli KJ, Debatin KM, Krammer PH, Peter ME. Two CD95 (APO-1/Fas) signalling pathways. EMBO J. 1998 Mar 16; 17 (6): 1675-87.

Scaffidi C, Schmitz I, Zha J, Korsmeyer SJ, Krammer PH, Peter ME. Differential modulation of apoptosis sensitivity in CD95 type I and type II cells. J Biol Chem. 1999 Aug 6; 274 (32): 22532-8.

Scheel-Toellner D, Wang K, Singh R, Majeed S, Raza K, Curnow SJ, Salmon M, Lord JM. The death-inducing signalling complex is recruited to lipid rafts in Fas-induced apoptosis. Biochem Biophys Res Commun. 2002 Oct 4; 297 (4): 876-9.

Schlesinger PH, Gross A, Yin XM, Yamamoto K, Saito M, Waksman G, Korsmeyer SJ. Comparison of the ion channel characteristics of pro-apoptotic BAX and anti-apoptotic Bcl-2. Proc Natl Acad Sci U S A. 1997 Oct 14; 94 (21): 11357-62.

Schnieke A, Harbers K, Jaenisch R. Embryonic lethal mutation in mice induced by retrovirus insertion into the alpha 1(I) collagen gene. Nature. 1983 Jul 28-Aug 3; 304 (5924): 315-20.

Screaton GR, Xu XN, Olsen AL, Cowper AE, Tan R, McMichael AJ, Bell JI. LARD: a new lymphoid-specific death domain containing receptor regulated by alternative pre-mRNA splicing. Proc Natl Acad Sci U S A. 1997 Apr 29; 94 (9): 4615-9.

Segui B, Bezombes C, Uro-Coste E, Medin JA, Andrieu-Abadie N, Auge N, Brouchet A, Laurent G, Salvayre R, Jaffrezou JP, Levade T. Stress-induced apoptosis is not mediated by endo-lysosomal ceramide. FASEB J. 2000 Jan; 14 (1): 36-47.

Selzner M, Bielawska A, Morse MA, Rudiger HA, Sindram D, Hannun YA, Clavien PA. Induction of apoptotic cell death and prevention of tumour growth by ceramide analogues in metastatic human colon cancer. Cancer Res. 2001 Feb 1; 61 (3): 1233-40.

Shani G, Henis-Korenblit S, Jona G, Gileadi O, Eisenstein M, Ziv T, Admon A, Kimchi A. Autophosphorylation restrains the apoptotic activity of DRP-1 kinase by controlling dimerisation and calmodulin binding. EMBO J. 2001 Mar 1; 20 (5): 1099-113.

Sheridan JP, Marsters SA, Pitti RM, Gurney A, Skubatch M, Baldwin D, Ramakrishnan L, Gray CL, Baker K, Wood WI, Goddard AD, Godowski P, Ashkenazi A. Control of TRAIL-induced apoptosis by a family of signalling and decoy receptors. Science. 1997 Aug 8; 277 (5327): 818-21.

Shimizu S, Ide T, Yanagida T, Tsujimoto Y. Electrophysiological study of a novel large pore formed by Bax and the voltage-dependent anion channel that is permeable to cytochrome c. J Biol Chem. 2000a Apr 21; 275 (16): 12321-5.

Shimizu S, Konishi A, Kodama T, Tsujimoto Y. BH4 domain of anti-apoptotic Bcl-2 family members closes voltage-dependent anion channel and inhibits apoptotic mitochondrial changes and cell death. Proc Natl Acad Sci U S A. 2000b Mar 28; 97 (7): 3100-5.

Shimizu S, Narita M, Tsujimoto Y. Bcl-2 family proteins regulate the release of apoptogenic cytochrome c by the mitochondrial channel VDAC. Nature. 1999 Jun 3; 399 (6735): 483-7.

Shohat G, Shani G, Eisenstein M, Kimchi A. The DAP-kinase family of proteins: study of a novel group of calcium-regulated death-promoting kinases. Biochim Biophys Acta. 2002 Nov 4; 1600 (1-2): 45-50.

Simivovitch L. 1985. Mechanisms of genetic variation in Chinese ovary cells. *In* "Molecular Cell Genetics" (M.M. Gottesman, Ed.), pp. 869-879, New York.

Slee EA, Harte MT, Kluck RM, Wolf BB, Casiano CA, Newmeyer DD, Wang HG, Reed JC, Nicholson DW, Alnemri ES, Green DR, Martin SJ. Ordering the cytochrome c-initiated caspase cascade: hierarchical activation of caspases-2, -3, -6, -7, -8, and -10 in a -9-dependent manner. J Cell Biol. 1999 Jan 25; 144 (2): 281-92.

Slobodyansky E, Guidotti A, Wambebe C, Berkovich A, Costa E. Isolation and characterisation of a rat brain triakontatetraneuropeptide, a posttranslational product of diazepam binding inhibitor: specific action at the Ro5-4864 recognition site. J Neurochem. 1989 Oct; 53 (4): 1276-84.

Smith CA, Farrah T, Goodwin RG. The TNF receptor super-family of cellular and viral proteins: activation, co-stimulation, and death. Cell. 1994 Mar 25; 76 (6): 959-62.

Smith DB, Johnson KS. Single-step purification of polypeptides expressed in *E. coli* as fusions with glutathione S-transferase. Gene. 1988 Jul 15; 67 (1): 31-40.

Smyth MJ, Perry DK, Zhang J, Poirier GG, Hannun YA, Obeid LM. prICE: a downstream target for ceramide-induced apoptosis and for the inhibitory action of Bcl-2. Biochem J. 1996 May 15; 316 (Pt 1): 25-8.

Spiegel S, Merrill AH Jr. Sphingolipid metabolism and cell growth regulation. FASEB J. 1996 Oct; 10 (12): 1388-97.

Srinivasula SM, Ahmad M, Ottilie S, Bullrich F, Banks S, Wang Y, Fernandes-Alnemri T, Croce CM, Litwack G, Tomaselli KJ, Armstrong RC, Alnemri ES.

FLAME-1, a novel FADD-like anti-apoptotic molecule that regulates Fas/TNFR1-induced apoptosis. J Biol Chem. 1997 Jul 25; 272 (30): 18542-5.

Stanger BZ, Leder P, Lee TH, Kim E, Seed B. RIP: a novel protein containing a death domain that interacts with Fas/APO-1 (CD95) in yeast and causes cell death. Cell. 1995 May 19; 81 (4): 513-23.

Stanley P, Chaney W. Control of carbohydrate processing: the lec1A CHO mutation results in partial loss of N-acetylglucosaminyltransferase I activity. Mol Cell Biol. 1985 Jun; 5 (6): 1204-11.

Stanley P. Selection of specific wheat germ agglutinin-resistant (WgaR) phenotypes from Chinese hamster ovary cell populations containing numerous lecR genotypes. Mol Cell Biol. 1981 Aug; 1 (8): 687-96.

Steinmetz M, Minard K, Horvath S, McNicholas J, Srelinger J, Wake C, Long E, Mach B, Hood L. A molecular map of the immune response region from the major histocompatibility complex of the mouse. Nature. 1982 Nov 4; 300 (5887): 35-42.

Steller H. Mechanisms and genes of cellular suicide. Science. 1995 Mar 10; 267 (5203): 1445-9.

Strasser A, Huang DC, Vaux DL. The role of the Bcl-2/CED-9 gene family in cancer and general implications of defects in cell death control for tumour genesis and resistance to chemotherapy. Biochim Biophys Acta. 1997 Oct 24; 1333 (2): F151-78.

Strasser A, Newton K. FADD/MORT1, a signal transducer that can promote cell death or cell growth. J Biochem Cell Biol. 1999 May; 3 (5): 533-7.

Strohmeier R, Roller M, Sanger N, Knecht R, Kuhl H. Modulation of tamoxifen-induced apoptosis by peripheral benzodiazepine receptor ligands in breast cancer cells. Biochem Pharmacol. 2002 Jul 1; 64 (1): 99-107.

Susin SA, Lorenzo HK, Zamzami N, Marzo I, Brenner C, Larochette N, Prevost MC, Alzari PM, Kroemer G. Mitochondrial release of caspase-2 and -9 during the apoptotic process. J Exp Med. 1999a Jan 18; 189 (2): 381-94.

Susin SA, Lorenzo HK, Zamzami N, Marzo I, Snow BE, Brothers GM, Mangion J, Jacotot E, Costantini P, Loeffler M, Larochette N, Goodlett DR, Aebersold R, Siderovski DP, Penninger JM, Kroemer G. Molecular characterisation of mitochondrial apoptosis-inducing factor. Nature. 1999b Feb 4; 397 (6718): 441-6.

Syapin PJ, Skolnick P. Characterisation of benzodiazepine binding sites in cultured cells of neural origin. J Neurochem. 1979 Mar; 32 (3): 1047-51.

Szekeres J, Pacsa AS, Pejtsik B. Measurement of lymphocyte cytotoxicity by assessing endogenous alkaline phosphatase activity of the target cells. J Immunol Methods. 1981; 40 (2): 151-4.

Takahashi A, Alnemri ES, Lazebnik YA, Fernandes-Alnemri T, Litwack G, Moir RD, Goldman RD, Poirier GG, Kaufmann SH, Earnshaw WC. Cleavage of lamin A by Mch2 alpha but not CPP32: multiple interleukin 1 beta-converting enzyme-related proteases with distinct substrate recognition properties are active in apoptosis. Proc Natl Acad Sci U S A. 1996 Aug 6; 93 (16): 8395-400.

Tani M, Okino N, Mitsutake S, Tanigawa T, Izu H, Ito M. Purification and characterisation of a neutral ceramidase from mouse liver. A single protein catalyses the reversible reaction in which ceramide is both hydrolysed and synthesized. J Biol Chem. 2000 Feb 4; 275 (5): 3462-8.

Tartaglia LA, Goeddel DV. Two TNF receptors. Immunol Today. 1992 May; 13 (5): 151-3.

Tepper AD, Cock JG, de Vries E, Borst J, van Blitterswijk WJ. CD95/Fas-induced ceramide formation proceeds with slow kinetics and is not blocked by caspase-3/CPP32 inhibition. J Biol Chem. 1997 Sep 26; 272 (39): 24308-12.

Thome M, Schneider P, Hofmann K, Fickenscher H, Meinl E, Neipel F, Mattmann C, Burns K, Bodmer JL, Schroter M, Scaffidi C, Krammer PH, Peter ME, Tschopp J. Viral FLICE-inhibitory proteins (FLIPs) prevent apoptosis induced by death receptors. Nature. 1997 Apr 3; 386 (6624): 517-21.

Thompson CB. Apoptosis in the pathogenesis and treatment of disease. Science. 1995 Mar 10; 267 (5203): 1456-62.

Thompson JD, Gibson TJ, Plewniak F, Jeanmougin F, Higgins DG. The CLUSTAL_X windows interface: flexible strategies for multiple sequence alignment aided by quality analysis-tools. Nucleic Acids Res. 1997 Dec 15; 25 (24): 4876-82.

Thornberry NA, Bull HG, Calaycay JR, Chapman KT, Howard AD, Kostura MJ, Miller DK, Molineaux SM, Weidner JR, Aunina J, Elliston KO, Ayala JM, Casano FJ, Chin J, Ding GJF, Egger LA, Gaffney EP, Limjuco G, Palyha OC, Raju SM, Rolando AM, Salley JP, Yamin TT, Lee TD, Shively JE, MacCoss M, Mumford RA, Schmidt JA and Tocci MJ. A novel heterodimeric cysteine protease is required for interleukin-1 beta processing in monocytes. Nature. 1992 Apr 30; 356 (6372): 768-74.

Ting AT, Pimentel-Muinos FX, Seed B. RIP mediates tumour necrosis factor receptor 1 activation of NF-kappaB but not Fas/APO-1-initiated apoptosis. EMBO J. 1996 Nov 15; 15 (22): 6189-96.

Tomassini B, Testi R. Mitochondria as sensors of sphingolipids. Biochimie. 2002 Feb-Mar; 84 (2-3): 123-9.

Tomei LD, Umansky SR. Apoptosis and the heart: a brief review. Ann N Y Acad Sci. 2001 Nov; 946:160-8.

Valentin M, Balvers M, Pusch W, Weinbauer GF, Knudsen J, Ivell R. Structure and expression of the mouse gene encoding the endozepine-like peptide from haploid male germ cells. Eur J Biochem. 2000 Sep; 267 (17): 5438-49.

Van de Craen M, Van Loo G, Pype S, Van Criekinge W, Van den brande I, Molemans F, Fiers W, Declercq W, Vandenabeele P. Identification of a new caspase homologue: caspase-14. Cell Death Differ. 1998 Oct; 5 (10): 838-46.

Van de Craen M, Vandenabeele P, Declercq W, Van den Brande I, Van Loo G, Molemans F, Schotte P, Van Criekinge W, Beyaert R, Fiers W. Characterisation of seven murine caspase family members. FEBS Lett. 1997 Feb 10; 403 (1): 61-9.

Van Loo G, Demol H, van Gurp M, Hoorelbeke B, Schotte P, Beyaert R, Zhivotovsky B, Gevaert K, Declercq W, Vandekerckhove J, Vandenabeele P. A matrix-assisted laser desorption ionisation post-source decay (MALDI-PSD) analysis of proteins released from isolated liver mitochondria treated with recombinant truncated Bid. Cell Death Differ. 2002 Mar; 9 (3): 301-8.

van Loo G, Schotte P, van Gurp M, Demol H, Hoorelbeke B, Gevaert K, Rodriguez I, Ruiz-Carrillo A, Vandekerckhove J, Declercq W, Beyaert R, Vandenabeele P. Endonuclease G: a mitochondrial protein released in apoptosis and involved in caspase-independent DNA degradation. Cell Death Differ. 2001 Dec; 8 (12): 1136-42.

Varmus H. Retroviruses. Science. 1988 Jun 10; 240 (4858): 1427-35.

Varmus HE, Quintrell N, Ortiz S. Retroviruses as mutagens: insertion and excision of a non-transforming provirus alter expression of a resident transforming provirus. Cell. 1981 Jul; 25 (1): 23-36.

Vaux DL, Cory S, Adams JM. Bcl-2 gene promotes haemopoietic cell survival and cooperates with c-Myc to immortalise pre-B cells. Nature. 1988 Sep 29; 335 (6189): 440-2.

Vaux DL, Haecker G, Strasser A. An evolutionary perspective on apoptosis. Cell. 1994 Mar 11; 76 (5): 777-9.

Vaux DL. CED-4-the third horseman of apoptosis. Cell. 1997 Aug 8; 90 (3): 389-90.

Venturini I, Alho H, Podkletnova I, Corsi L, Rybnikova E, Pellicci R, Baraldi M, Pelto-Huikko M, Helen P, Zeneroli ML. Increased expression of peripheral benzodiazepine receptors and diazepam binding inhibitor in human tumours sited in the liver. Life Sci. 1999; 65 (21): 2223-31.

Verhagen AM, Vaux DL. Cell death regulation by the mammalian IAP antagonist DIABLO/Smac. Apoptosis. 2002 Apr; 7 (2): 163-6.

von Melchner H, Ruley HE. Identification of cellular promoters by using a retrovirus promoter trap. J Virol. 1989 Aug; 63 (8): 3227-33.

Wadia JS, Dowdy SF. Protein transduction technology. Curr Opin Biotechnol. 2002 Feb; 13 (1): 52-6.

Wajant H. The Fas signalling pathway: more than a paradigm. Science. 2002 May 31; 296 (5573): 1635-6.

Walczak H, Degli-Esposti MA, Johnson RS, Smolak PJ, Waugh JY, Boiani N, Timour MS, Gerhart MJ, Schooley KA, Smith CA, Goodwin RG, Rauch CT. TRAIL-R2: a novel apoptosis-mediating receptor for TRAIL. EMBO J. 1997 Sep 1; 16 (17): 5386-97.

Walczak H, Krammer PH. The CD95 (APO-1/Fas) and the TRAIL (APO-2L) apoptosis systems. Exp Cell Res. 2000 Apr 10; 256 (1): 58-66.

Wallach D. Apoptosis. Placing death under control. Nature. 1997 Jul 10; 388 (6638): 123, 125-6.

Watson A, Mazumder A, Stewart M, Balasubramanian S. Technology for microarray analysis of gene expression. Curr Opin Biotechnol. 1998 Dec; 9 (6): 609-14.

Waterhouse NJ, Goldstein JC, von Ahsen O, Schuler M, Newmeyer DD, Green DR. Cytochrome c maintains mitochondrial transmembrane potential and ATP generation after outer mitochondrial membrane permeabilisation during the apoptotic process. J Cell Biol. 2001 Apr 16; 153 (2): 319-28.

Weber CH, Vincenz C. The death domain super family: a tale of two interfaces? Trends Biochem Sci. 2001 Aug; 26 (8): 475-81.

Williamson P, Schlegel RA. Transbilayer phospholipid movement and the clearance of apoptotic cells. Biochim Biophys Acta. 2002 Dec 30; 1585 (2-3): 53-63.

Wolf BB, Green DR. Suicidal tendencies: apoptotic cell death by caspase family proteinases. J Biol Chem. 1999 Jul 16; 274 (29): 20049-52.

Wu D, Wallen HD, Inohara N, Nunez G. Interaction and regulation of the *C. elegans* death protease CED-3 by CED-4 and CED-9. J Biol Chem. 1997 Aug 22; 272 (34): 21449-54.

Xia W, Spector S, Hardy L, Zhao S, Saluk A, Alemane L, Spector NL. Tumour selective G2/M cell cycle arrest and apoptosis of epithelial and haematological malignancies by BBL22, a benzazepine. Proc Natl Acad Sci U S A. 2000 Jun 20; 97 (13): 7494-9.

Xu J, Yeh CH, Chen S, He L, Sensi SL, Canzoniero LM, Choi DW, Hsu CY. Involvement of de novo ceramide biosynthesis in tumour necrosis factor-alpha/cyclohexamide-induced cerebral endothelial cell death. J Biol Chem. 1998 Jun 26; 273 (26): 16521-6.

Xue D, Horvitz HR. *C. elegans* CED-9 protein is a bi-functional cell-death inhibitor. Nature. 1997 Nov 20; 390 (6657): 305-8.

Yang X, Khosravi-Far R, Chang HY, Baltimore D. Daxx, a novel Fas-binding protein that activates JNK and apoptosis. Cell. 1997 Jun 27; 89 (7): 1067-76.

Yang Y, Fang S, Jensen JP, Weissman AM, Ashwell JD. Ubiquitin protein ligase activity of IAPs and their degradation in proteasomes in response to apoptotic stimuli. Science. 2000 May 5; 288 (5467): 874-7.

Yarmolinsky MB. Programmed cell death in bacterial populations. Science. 1995 Feb 10; 267 (5199): 836-7.

Ye X, Mehlen P, Rabizadeh S, VanArsdale T, Zhang H, Shin H, Wang JJ, Leo E, Zapata J, Hauser CA, Reed JC, Bredesen DE. TRAF family proteins interact with the common neurotrophin receptor and modulate apoptosis induction. J Biol Chem. 1999 Oct 15; 274 (42): 30202-8.

Yuan J, Shaham S, Ledoux S, Ellis HM, Horvitz HR. The *C. elegans* cell death gene CED-3 encodes a protein similar to mammalian interleukin-1 beta-converting enzyme. Cell. 1993 Nov 19; 75 (4): 641-52.

Zamore PD, Tuschl T, Sharp PA, Bartel DP. RNAi: double-stranded RNA directs the ATP-dependent cleavage of mRNA at 21 to 23 nucleotide intervals. Cell. 2000 Mar 31;101(1):25-33.

Zamzami N, Marchetti P, Castedo M, Hirsch T, Susin SA, Masse B, Kroemer G. Inhibitors of permeability transition interferes with the disruption of the mitochondrial transmembrane potential during apoptosis. FEBS Lett. 1996 Apr 8; 384 (1): 53-7.

Zamzami N, Susin SA, Marchetti P, Hirsch T, Gomez-Monterrey I, Castedo M, Kroemer G. Mitochondrial control of nuclear apoptosis. J Exp Med. 1996 Apr 1; 183 (4): 1533-44.

Zhang P, Liu B, Jenkins GM, Hannun YA, Obeid LM. Expression of neutral sphingomyelinase identifies a distinct pool of sphingomyelin involved in apoptosis. J Biol Chem. 1997 Apr 11; 272 (15): 9609-12.

Zimmermann KC, Bonzon C, Green DR. The machinery of programmed cell death. Pharmacol Ther. 2001 Oct; 92 (1): 57-70.

Zoratti M, Szabo I. The mitochondrial permeability transition. Biochim Biophys Acta. 1995 Jul 17; 1241 (2): 139-76.

Zornig M, Hueber A, Baum W, Evan G. Apoptosis regulators and their role in tumour genesis. Biochim Biophys Acta. 2001 Oct 1; 1551 (2): F1-37.

Zou H, Henzel WJ, Liu X, Lutschg A, Wang X. Apaf-1, a human protein homologous to *C. elegans* CED-4, participates in cytochrome c-dependent activation of caspase-3. Cell. 1997 Aug 8; 90 (3): 405-13.